Institut für Landtechnik

der Rheinischen Friedrich-Wilhelms-Universität Bonn

Study on the Response Time of Direct Injection Systems for Variable Rate Application of Herbicides

I n a u g u r a l - D i s s e r t a t i o n

zur

Erlangung des Grades

Doktor der Agrarwissenschaften

(Dr. agr.)

der

Hohen Landwirtschaftlichen Fakultät

der

Rheinischen Friedrich-Wilhelms-Universität

zu Bonn

vorgelegt am

20. Juli 2007

von

Ing. Peter Hlobeň

aus Prag, Tschechische Republik

Referent: Prof. Dr.-Ing. P. Schulze Lammers

Korreferent: Prof. Dr. G. Noga

Tag der mündlichen Prüfung: 18. September 2007

D 98

Bezugsquelle: Institut für Landtechnik
Rheinische Friedrich-Wilhelms-Universität
Nussallee 5
53115 Bonn

Diese Dissertation ist 2008 auf dem Hochschulschriftenserver der ULB Bonn
http://hss.ulb.uni-bonn.de/diss_online elektronisch publiziert.

Abstract

Study on the Response Time of Direct Injection Systems for Variable Rate Application of Herbicides

Progress in the technology of weed detection using cameras combined with image processing requires improvements in spray technology. Spraying systems of current design distribute herbicides uniformly across the field. Applying the chemical agents only at locations with weeds according to the indications of a weed treatment map (off-line application) or of a weed detection system (on-line application) will reduce costs significantly and contribute to environmentally friendly crop farming. Direct injection systems inject chemical agents into the hydraulic system of the sprayer in a manner that allows the rate and type of herbicide to be varied during field operation. In direct injection systems the herbicides and the water carrier are kept in separate tanks. The herbicides are metered into the carrier and mixed with it before being discharged through the nozzle. For on-line application, the distance between the point of injection and the nozzle has to be minimized. A disadvantage of current injection systems lies in long response times, i.e. the time until the required concentration of spray solution is reached at the nozzles. Application errors occur because the flow rate of the active ingredient at the nozzles is not adjusted rapidly enough to meet the herbicide requirement at a given location in the field.

This study presents results concerning the response time analysis of a direct injection system with two different locations of the injection point. The concentration development of a tracer as measured by a conductivity sensor was employed to determine lag and response times. The experiments were carried out with various carrier and tracer flow rates as well as different tubing sizes and tracer viscosities. In the case of injection of tracers into a boom section the response times were between 2.75 and 8.84 s. Under optimal conditions, the lag time can be reduced to less than 0.30 s by injecting the tracer close to a nozzle. At the regular operation speed of field sprayers (8 km/h ~ 2.2 m/s) the application rate can thus be adjusted in a distance of less than 1 m.

Kurzfassung

Untersuchung der Verzögerungszeit von Direkteinspritzsystemen für die teilflächenspezifische Ausbringung von Herbiziden

Fortschritte in der Unkrauterkennung mittels Kameras in Kombination mit Bildverarbeitungstechniken erfordern Verbesserungen der Applikationstechnik. Aktuelle Spritzsysteme verteilen die Herbizide gleichmäßig auf dem Feld. Die Beschränkung der Anwendung von Chemikalien auf Teilflächen mit Unkrautbesatz, der auf einer Unkrautkarte verzeichnet ist (offline-Ausbringung) oder von einem Unkrauterkennungssystem angezeigt wird (online-Ausbringung), würde die Kosten deutlich senken und einen Beitrag zu einem umweltfreundlichem Pflanzenbau leisten. In Direkteinspeisungssystemen werden die Chemikalien so in das hydraulische System der Spritze eingeleitet, dass sich Art und Menge des Herbizids während des Feldbetriebs verändern lassen. Herbizide und die Trägerflüssigkeit werden in getrennten Tanks aufbewahrt. Für die Applikation werden die Herbizide in die Trägerflüssigkeit eindosiert und darin vermischt, bevor sie durch die Düse ausgestoßen werden. Für die online-Ausbringung muss der Abstand zwischen dem Einspeisungsort und der Düse möglichst klein sein. Ein Nachteil aktuell verfügbarer Einspritzsysteme liegt in ihrer langen Reaktionszeit, d.h. der Zeit, die vergeht, bis die Spritzlösung an den Düsen die erforderliche Konzentration erreicht. Ausbringungsfehler sind darauf zurückzuführen, dass sich die Fließgeschwindigkeit des Wirkstoffs an den Düsen nicht schnell genug ändert, um an einer bestimmten Stelle auf dem Feld die erforderliche Herbizidmenge zur Verfügung zu stellen.

Diese Arbeit stellt die Ergebnisse von Reaktionszeitanalysen vor, die an einem Direkteinspeisungssystem mit zwei verschiedenen Einspeisungsorten durchgeführt wurden. Tot- und Reaktionszeiten wurden anhand des mit einem Leitfähigkeitssensor erfassten Konzentrationsverlaufs eines Indikators ermittelt. Die Versuche wurden mit verschiedenen Fließgeschwindigkeiten von Trägerflüssigkeit und Indikator sowie mit verschieden dimensionierten Rohrleitungen und mit Indikatorflüssigkeiten unterschiedlicher Viskosität durchgeführt. Bei Einspeisung des Indikators in eine Teilbreite lagen die Reaktionszeiten zwischen 2,75 und 8,84 s. Durch Einleiten des Indikators nahe an der Düse lässt sich die Totzeit unter optimalen Bedingungen auf weniger als 0,3 s verkürzen. So kann bei einer für Feldspritzen praxisüblichen Arbeitsgeschwindigkeit (8 km/h ~ 2,2 m/s) die Aufwandmenge innerhalb von weniger als einem Meter exakt angepasst werden.

Acknowledgements

I really appreciated all the contributions which the people at the Institute of Agricultural Engineering in Bonn and the members of DFG Research Training Group 772 (Precision Crop Protection) made to the successful completion of this study.

Particular thanks are due to my doctoral supervisor Prof. Dr.-Ing. Peter Schulze Lammers for his excellent suggestions and comments and his outstanding support throughout my studies in Bonn and during the writing of this dissertation. I also wish to extend many thanks to my second reviewer Prof. Dr. Georg Noga for his valuable comments and suggestions.

I am grateful to Dr. agr. Markus Sökefeld, Dr. agr. Oliver Schmittmann, Dr. Johannes Nieß and Ing. Jiri Vondricka for their support and valuable comments during the experimental phase. I would also like to thank all my colleagues in the workshop and the instrumentation section of the Institute for their excellent technical assistance with the experimental setup.

I am very grateful to the German Research Foundation (DFG) for its financial assistance throughout my studies.

Special thanks are due to my dear friend Tereza, to Frauke Beeken, Marianna Nemeth and to all my close friends for their sympathy and help. They created a pleasant environment for me in Bonn, and they are connected with a wonderful experience and memory.

Finally, I am deeply indebted to my parents for their love, understanding, patience and sacrifice throughout this period of my life. I dedicate this dissertation to them.

Mým rodičům

Table of Contents

List of Figures

List of Tables

Nomenclature

A	- ; l ha^{-1}; m^2	Absorbance; Application rate of spray mixture; Area
A_a	l ha^{-1}	Application rate of chemical
A_d	m^2	Area of discharge of the nozzle
c	mol l^{-1}	Concentration of a solution
c_a	ppm	Concentration of active ingredient in the tracer solution
c_i	mol cm^{-3}	Concentration of ions
c_m	ppm	Concentration of the mixture solution
CCD		Charge Coupled Device
C	-	Conductivity cell constant, Viscosity correction factor
C_d	-	Coefficient of discharge of the nozzle
CV	%	Coefficient of variation
d	m	Diameter; Distance between the electrodes; Cell width
d_i	m	Pipe, Hose diameter
d_3	m	Diameter of the check valve outlet
f	Hz	Frequency
G	S	Electrical conductance
GLR	-	Gray level reflectance
GLT	-	Gray level transmittance
I_0	lm	Initial intensity of the light
I_t	lm	Intensity of the transmitted light
I	A	Electrical current
IOD	-	Integrated optical density
ISOBUS		International Electronics Communications Standard
k	mm; -	Roughness coefficient; Nozzle coefficient
k_r	-	Relative roughness
K_v	l min^{-1}	K_v - value (flow factor)
K_{vs}	l min^{-1}	K_v – value at a nominal stroke *s* = 100 %
l	m	Length
l_i	m	Pipe, Tube length
l_s	m	Distance between centre of sensor and nozzle tip

n	-	Number of nozzles, Number of conduits
NaCl		Sodium chloride
p	Pa, bar; -	Pressure; Level of significance
p_c	Pa, bar	Carrier pressure
p_i	bar	Nozzle pressure
p_o	Pa	Cracking pressure of the check valve
p_z	Pa	Pressure losses
Δp	Pa, bar	Differential pressure
PWM		Pulse width modulation
Q	$l\ min^{-1}$	Flow rate
Q_a	$l\ min^{-1}$	Flow rate of chemical, Flow rate of tracer
Q_c	$l\ min^{-1}$	Flow rate of carrier
Q_s	$l\ min^{-1}$	Total flow rate for a section
Q_d	$l\ min^{-1}$	Nozzle flow rate
Q_t	$l\ min^{-1}$	Total flow rate of spray mixture
Q_i	$m^3\ s^{-1}$	Flow rate of the solution
Q_{an}	$l\ min^{-1}$	Tracer flow rate across the orifices
r	m	Radius of cylindrical layer
R	Ω, m	Electrical resistance, Tube radius
R_S	Ω	Sensor resistance
R_V	Ω	Resistor resistance
Re	-	Reynolds number
ROD	-	Relative optical density
s		Standard deviation
S	m	Area of the electrodes
t	s	Time
T	%	Transmittance of light
T_A	s	Acquisition time
T_{fall}	s	Fall time
T_{lag}	s	Lag time
T_p	N m	Pump torque
T_R	s	Total response time of the injection metering system

T_{rise}	s	Rise time
T_{RS}	s	Total response time of the application system
U	km h^{-1}, V	Forward speed, Electrical voltage
U_C	V	Conductivity sensor output voltage
U_D	V	Optical sensor output voltage
v	m s^{-1}	Fluid velocity
V_p	ml rev^{-1}	Pump displacement
W	m	Working width
W_t		Technical rating
$\bar{x}$		Sample mean
α	l mol^{-1} cm^{-1}	Molecules absorbing photons constant
β_1, β_2	K^{-1}	Thermal conductivity coefficients
ε	l mol^{-1} cm^{-1}	Molar extinction coefficient
ζ	-	Coefficient of minor (local losses)
η	Pa s	Dynamic viscosity
$\vartheta - \vartheta_0$	K	Thermal gradient
κ	S m^{-1}	Specific electric conductivity
λ	-	Coefficient of friction losses
Λ_m	S cm^2 mol^{-1}	Molar conductivity
ρ	kg m^{-3}	Density of liquid
ν	m^2 s^{-1}	Kinematic viscosity
τ	Pa	Shear stress
ω	rad s^{-1}	Angular velocity

1. Introduction

The application of plant protection agents plays an important role in current farm production. Rising chemical prices and over application in agricultural fields can contribute to increased production costs, thus limiting a company's profitability. Besides economical pressures there are also important ecological aspects of chemical application. Being related to food quality and environmental contamination, they call for a considerable reduction of the volume of active ingredients applied to agricultural fields. On the other hand, under application creates losses in yield and in the quality of crops due to weeds.

The traditional method of area spray application of herbicides with a constant chemical solution is adequate and efficient if the weed distribution in a larger field area is uniform in species composition. In many cases, e.g. in no-till planting, weed populations are not very uniform so that site-specific application of herbicides becomes preferable. This concept offers an opportunity to reduce agrochemicals without reducing their effectiveness.

Progress in the technology of weed detection by cameras combined with image processing implies the possibility of new advances in spray technology. Spraying systems of current design distribute herbicides uniformly across the field. In order to use the full advantages of site-specific weed control with herbicide application based on information about the distribution of weed species, it is necessary to use application technology with which it is possible to vary the application rate and type of herbicide rapidly.

One option is to employ sprayers with an integrated direct injection system. In injection sprayers, the herbicides and the carrier are kept separate from each other. According to the indications of a weed treatment map (off-line application) or of a weed analysis camera system (on-line application) (GERHARDS et al., 2001), the herbicides are metered into and mixed with the carrier immediately before entering the nozzles. This type of chemical injection system also offers logistical advantages over conventional sprayers because the chemical is not diluted earlier than required. Thus, such a system can provide a solution to problems such as the disposal of wash water and left-over tank mixtures or the exposure of applicators to concentrated pesticides during mixing and loading.

This study presents an overview of the current state of variable-rate application technology in combination with weed detection techniques as well as an analysis of the requirements and problems connected with direct herbicide injection. In the second part of the study, the design of a proposed direct injection system with different injection locations is described. A method for measuring the performance of injection metering systems was developed and used to assess the dynamic response characteristics of the proposed system.

1.1 Problem

A herbicide spray management system that accounts for variable weed distribution has three main components – weed mapping, treatment modelling and prescription delivery. Weed mapping involves the creation of grid models of the layout of agricultural fields in a computer database. The weed populations, detected for example by CCD cameras, are overlaid on these grids for decision analysis. In treatment modelling each individual image is analysed to identify the individual weed species by their shape, to establish the number of weeds in a block and to determine the level of weed concentration. These data determine a need for herbicide treatment, and are then transferred to a spray computer together with other decisions, such as the required delivery rate and type of chemical agent. Precise prescription delivery depends on the ability of the sprayer's control system to establish accurate field positioning relative to the grid and on the ability of the fluid delivery system to target the correct grid block with the required chemical solution.

The main task of this project is the prescription delivery of herbicides. This project takes advantage of information from the on-line weed detection analysis system and develops a direct injection system for site-specific application with a variable herbicide rate. The primary problem with injection systems is that there is always a transport lag in the system. The transport lag is the time it takes for the mixed solution to flow from the injection point to the spray nozzles. The transport lag is a function of the distance between the point of injection and the nozzles on the one hand and the velocity of the solution on the other. When a step change in the application rate is required, the transport lag will cause significant discrepancies between the desired and the actual application rate as the new concentration is travelling from the point of injection to the nozzles.

The injection concept is not a new one. It has been the subject of some research, and a few commercial systems have been developed. However, this technology has not yet achieved wide acceptance. Due to their long response times, current injection systems do not fulfil the requirements of on-line herbicide application. A characteristic of these systems is that the chemicals are injected centrally into the plumbing system before the sprayer boom. However, there are other inherent technical problems, some of which are discussed in this study. The proposed injection system which is described in this study is the outcome of research aimed at overcoming these problems.

1.2 Objectives

The main objective of this study is to develop, test and evaluate a laboratory model of a direct injection system which will meet the requirements of on-line variable rate herbicide application in combination with on-line weed detection.

In particular, the following objectives should be accomplished:

- Investigation of the technical issues and requirements of direct herbicide injection
- Proposal of the design of a metering injection system for online herbicide application
- Development of a laboratory test bench for experimental investigations of the response time of the metering system
- Development of a suitable method for measuring the performance of the injection metering system and use of this method in assessing the dynamic response characteristics of the proposed system
- Experimental investigation of parameters, which can affect the behaviour of the proposed metering injection system such as flow rates, system pressure and different physical properties of herbicides.

2. State of the Art

2.1 Site-specific Weed Control

Modern precision agriculture requires effective and efficient weed control methods for successful crop production. Weed control is primarily achieved by uniform herbicide application across an entire field. This traditional broadcast application of herbicides with a constant chemical solution is adequate and efficient only if a limited number of species is distributed evenly over a field area. The research relating to weed distribution which has been done over the last fifteen years indicates that the distribution of weeds within fields is not uniform and that weeds are usually spatially aggregated in "patches" (MORTENSEN et al., 1993; GERHARDS, 1997; LUTMAN and REW, 1997; MARSHALL, 1998).

Where the weed population is not uniform, site-specific application of herbicides becomes necessary to avoid under- or over-application in particular field areas. Excessive application causes an increase in production costs and environmental contamination, as well as having a negative influence on food quality. On the other hand, insufficient application creates losses in yield and crop quality due to weeds (STAFFORD and MILLER, 1993). This means that weeds are only sprayed where certain threshold values are exceeded (NORDMEYER and NIEMANN, 1997; GANZELMEIER, 2004). On weed infested areas, the treatment could be better tuned to the local weed conditions. In the ideal case, it means to adapt the weed treatment not only to the local weed species but also to the actual weed density, which is directly related to the potential yield damage of weeds (VRINDTS, 2000). For this purpose, weeds must be identified and treated with high spatial accuracy. Any system aiming to achieve spatially targeted pesticide application needs components to (MILLER, 2003):

a) detect, directly or indirectly, a parameter that is indicative of the need to apply a pesticide
   – a detection module
b) relate the detected parameter to the requirements of the application of a pesticide
   – a decision module
c) apply the pesticide in such way that the required dose is delivered to the defined target in such a form that the treatment is fully effective
   – an application module

As regards the weed detection module, which is a basic component of site-specific weed control, it is possible to differentiate between two approaches. The first one is a mapping approach (off-line). The detection of weeds, combined with a localisation system, e.g. Differential Global Positioning System (DGPS) and Geographic Information System (GIS), can result in a weed map (Fig. 2.1 a; b). The weed map can be used to plan local weed treatments in a treatment map. Tractor-mounted GPS units then enable application systems to target weed patches automatically in the field (CHRISTENSEN et al., 1999). In this concept, weed monitoring is carried out in a separate operation prior to the spraying operation. This approach is rather labour-intensive because it requires several manual or automated field inspections.

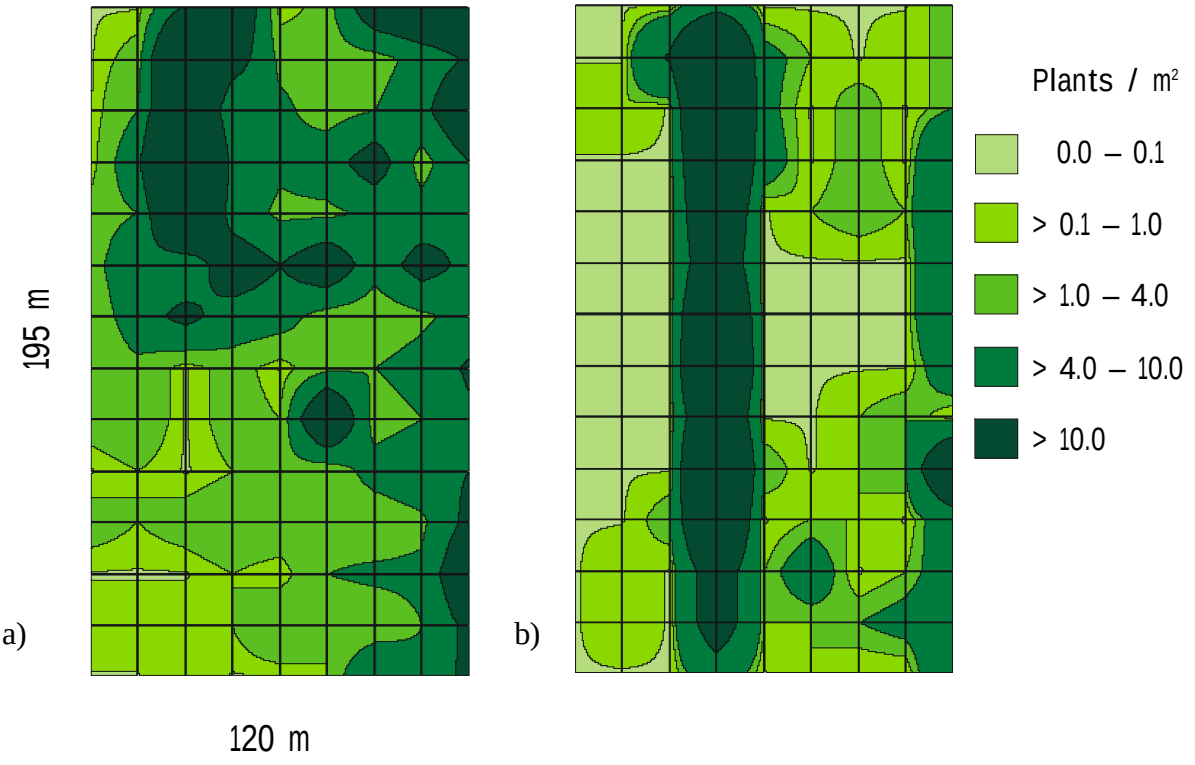

Figure 2. 8: Weed map documentation of heterogeneous weed distribution; a) Lamb's Quarters (Chenopodium album); b) grass weeds (indiscriminate); University of Bonn (SÖKEFELD et al., 1999)

The second approach is a real-time or on-line approach (Fig. 2.2). Weed detection and spraying are carried out sequentially in the same operation. On-line weed detection does not require a weed map for treatment setting, but recording the weed data in a map is useful for evaluating weed populations and treatments. The results of previous treatments can be read from such a weed map (NORDMEYER and NIEMANN, 1997; VRINDTS, 2000). The main advantage of this approach is the instantaneous detection and localization of weeds. This means that weeds are indicated at the point when information about infestation can be best utilized for a suitable treatment without delay. This is especially important at the time of post-emergence treatments, when weed control is vital to the condition and growth of the crop plants. Another advantage is the cost savings due to fewer machine passes.

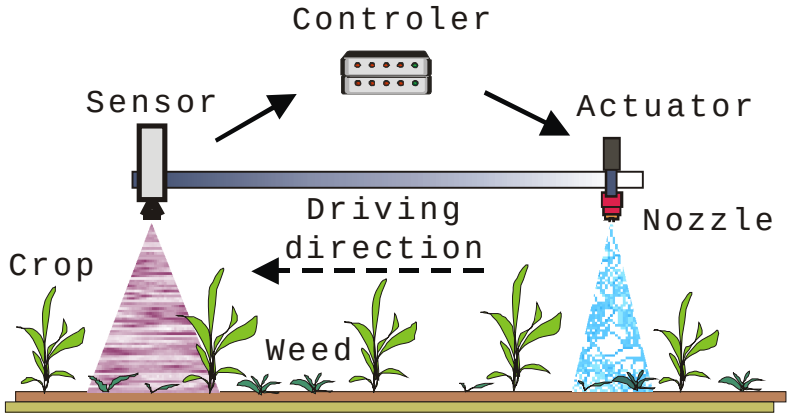

Figure 2. 9: Real-time concept of site-specific weed control

2.1.1 Spatial Distribution of Weeds

For treating weeds in a spatially selective way, it is necessary that the weeds be aggregated in distribution and that, if the spatial treatment is controlled by map, their distribution be relatively static (LUTMAN and REW, 1997). Several investigations on weed population have shown that weeds tend to be aggregated in distribution (NORDMEYER and NIEMANN, 1992; CARDINNA et al., 1995). Notably, weed grasses and perennial weeds such as blackgrass (*Alopecurus myosuroides*) or Canada thistle (*Cirsium arvense*) are known to grow in patches (BROWN et al., 1994; NORDMEYER et al., 1996). The reason for the growth of weeds in patches is that agricultural fields tend to be spatially heterogeneous with regard to soil characteristics, nutrients, topography and pest infestation (MORTENSEN and DIELEMAN, 1998).

Another important biological issue is the stability of weed patches. This is an important pre-requisite if the mapping approach is used for weed control. Very stable distributions need only to be mapped occasionally; rapidly changing distributions are either impossible to patch-spray or they require regular re-mapping (LUTMAN and REW, 1997). Weed patches remain stable from year to year, and relatively few new patches are formed because of the limited natural dispersion of weeds (BENNET and BROWN, 1998). Some cultivation techniques of, e.g. no-till planting, can cause new weed patches to form due to inappropriate cultivation of the seed banks in the soil. Also, although combine harvesters have the potential to move larger seeds over greater distances, their effects are influenced by the percentage of seed remaining on the parent plants at harvest (LUTMAN et al., 2002).

Table 2. 3: Herbicide savings by using site-specific weed control – mapping approach (adapted from AUTHORS' COLLECTIVE, 2001)

Year	Author	Crop	Herbicide saved (%)
1996	STAFFORD et al.	Corn	40-60
1997	NORDMEYER et al.	Winter barley (w. b.)	30-40
1997	GERHARDS et al.	Winter wheat (w. w.)	up to 21
1997	HEISEL et al.	Summer wheat	up to 41
1997	GREEN et al.	Ground pea	up to 70
1998	CHRISTENSEN and HEISEL	Winter wheat	41-51
1999	HEISEL et al.	Summer barley	up to 54
2001	TIMMERMANN et al.	Maize, sugar beet, w. w., w. b.	59

The concept of site-specific herbicide application offers the possibility of controlling weed patches with smaller amounts of agrochemicals without reducing the effectiveness of the chemicals (WARTENBERG, 1996). The economic side of site-specific weed control is still difficult to assess. One problem is the objective determination of the capital and labour costs of technology which is still under development. Such costs can only be estimated.

There have been a few examples of successful automated site-specific herbicide application by targeting weed patches on agricultural fields, mainly in cereal crops. However, due to differing test conditions the results are only partly comparable. In table 2.1, the percentage results of the herbicides savings resulting from the use of mapping systems are given for different crops. The amount of herbicide saved depends on the mapping system or approach used, on the actual weed occurrence at the date of monitoring, on the specific economical threshold for weed control measures and on dosing (AUTHORS' COLLECTIVE, 2001).

2.1.2 Automatic Weed Detection

For local weed treatment, local weed populations must be evaluated in the field. As mentioned above, there are two approaches (on and off -line) to site-specific weed control. The main component of these two approaches is a system for weed detection. This chapter will focus on automatic weed detection systems because they are the only ones that can be justified economically (AUTHORS' COLLECTIVE, 2001). The automatic weed detection systems discussed below include remote sensing systems, optoelectronic sensor systems and systems using digital image analysis.

Currently, remote sensing (satellite, aerial images or near-ground methods) plays only a minor role in site- specific weed control. It mainly provides spatial-spectral data that can be used to identify plant canopies. Important factors for recognition are the optical properties of different plant species (crop and weeds) and the spatial and spectral resolution of the remote sensing images. The resolution of satellite images is too low (~20-30 m depending on satellite) for the detection of weeds in the growth stage (LETTNER et al., 2001). Higher geometrical resolutions can be achieved with aerial photography.

Weed detection with optoelectronic sensors is based on spectral differences between soil and plants at red and near infra-red (NIR) wavelengths. Red light (600 - 700 nm) is strongly absorbed by chlorophyll, whereas NIR wavelengths are strongly reflected. This fact can be used to detect green plants and to distinguish them from the background in images.

A spot spraying system based on the information acquired by real-time reflectance sensors was developed for non-selective herbicides. Some commercial systems based on this principle are available for on-line weed detection, e.g. the Detectspray® system (FELTON and MCCLOY, 1992). If green vegetation is detected (vegetation index is high), a spray nozzle is quickly activated (on/off switched) by a solenoid valve.

Several research projects have investigated the possibility of using spectral analysis to detect and differentiate plants from weeds and to differentiate among different weed species. WANG et al. (2001) performed spectral analyses on stems and leaves of five crops and 30 weed species. Based on 4 wavelength bands, soil, plants and weed could be identified with a classification accuracy greater than 80 %. Spectral analysis would require less time for image processing.

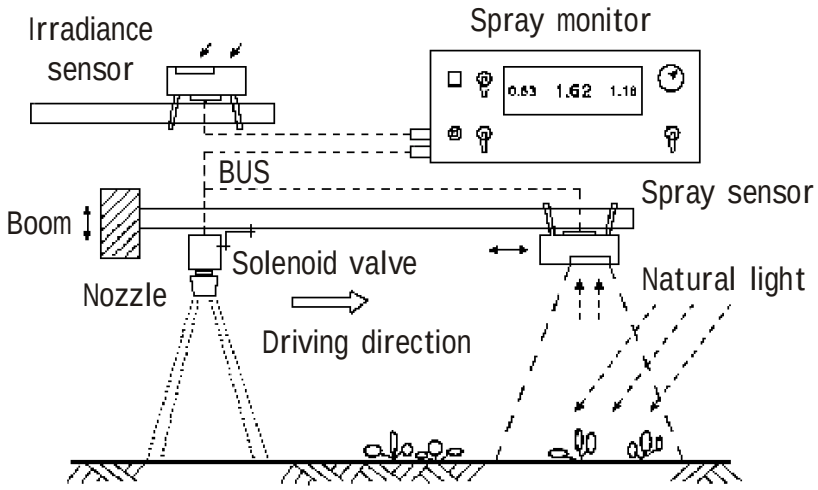

Figure 2. 10: Scheme of a weed-activated sprayer with an optical sensor - Detectspray® (HOLLSTEIN and BILLER, 1998)

A more sophisticated technique for identifying weeds and crops is image processing (LUTMAN and REW, 1997; TIAN et al., 1999; AUTHORS' COLLECTIVE, 2001; LUTMAN et al., 2002). The image analysis system enables the identification of plant species based on characteristic shapes, colours and texture features. The process consists of several steps. The first step is image acquisition by a suitable monitoring device, e.g. a CCD camera.

The second step is image pre-processing. This step can also be called 'separation' because the plants are separated from the background (soil). Separation can be carried out on the basis of visible colour differences or different reflection intensity in the NIR spectrum. The obtained data are then reduced, e.g. by contour extraction. In that way the processed images are prepared for the next step, which involves pattern recognition and weed classification. The shape, colour and texture properties are calculated and used to classify the plants into different crop and weed categories. This classification can also be used for creating weed distribution maps, and after calculation of the economic threshold it is also possible to create treatment maps directly.

An example of a successful system for real-time image acquisition is a system developed at the Institute of Agronomy in Bonn. The system works with three bi-spectral monochrome cameras mounted on a boom in front of a tractor with a distance of 3 m between the cameras. Each camera is equipped with a NIR band-pass filter (780-1150 nm) for scanning objects in two different wavelengths. The images are analysed automatically and on-line. A simple decision algorithm is used to switch on each boom section of the sprayer separately if a threshold for weed infestation has been exceeded. At a forward speed of 7 km h^{-1}, a set of three images was analysed approximately every two meters (AUTHORS' COLLECTIVE, 2001; GERHARDS et al., 2002).

An integral part of site-specific weed control is the prescription delivery of chemicals (application module). It depends on the ability of the sprayer's control system to establish accurate field positioning relative to the object (weed) and on the ability of the fluid delivery system to target the correct object with the required chemical solution.

In order to use the full advantages of site-specific herbicide application based on the real-time approach, it is necessary to use an application technology which is able to change the application rate and/or type of herbicide rapidly. It is possible to employ conventional sprayers with total flow control or sprayers with an integrated direct injection system.

2.2 Spatially Variable Application Technology

The spatially variable application of herbicides requires the use of systems with accurate dose control, high response speed, sufficient spatial resolution, and an ability to operate over a wide range of delivered dose rates with variable herbicide mixtures (MILLER et al., 1997).

A conventional sprayer is calibrated with respect to total nozzle flow rate Q_d (l min^{-1}), number of nozzles n (-), chemical concentration of the mixture solution in the tank c_m (-), boom working width W (m) and forward speed U (km h^{-1}) in order to apply a given chemical dosage per area A (l ha^{-1}) (VIDRINE et al., 1975; HUGHES and FROST, 1985; KIFFERLE and STAHLI, 2001). The relation between these variables is expressed in the following equation:

$$A = \frac{600 \cdot n \cdot Q_d \cdot c_m}{U \cdot W} \qquad (2.1)$$

There are several possible technologies for achieving a constant pesticide application rate, independent of forward speed. From the point of view of application rate control it is possible to classify the methods for spatially variable rate applications into three categories (STAFFORD and MILLER, 1993). The first one is total flow based control of the tank mix. The active ingredient is pre-mixed with the carrier in the tank; hence, the chemical concentration in the spray mixture during application is constant. The second method is chemical flow based control and the third is a combination of chemical and carrier flow control. A detailed classification of basic sprayer systems for spatially variable rate application is shown in figure 2.4.

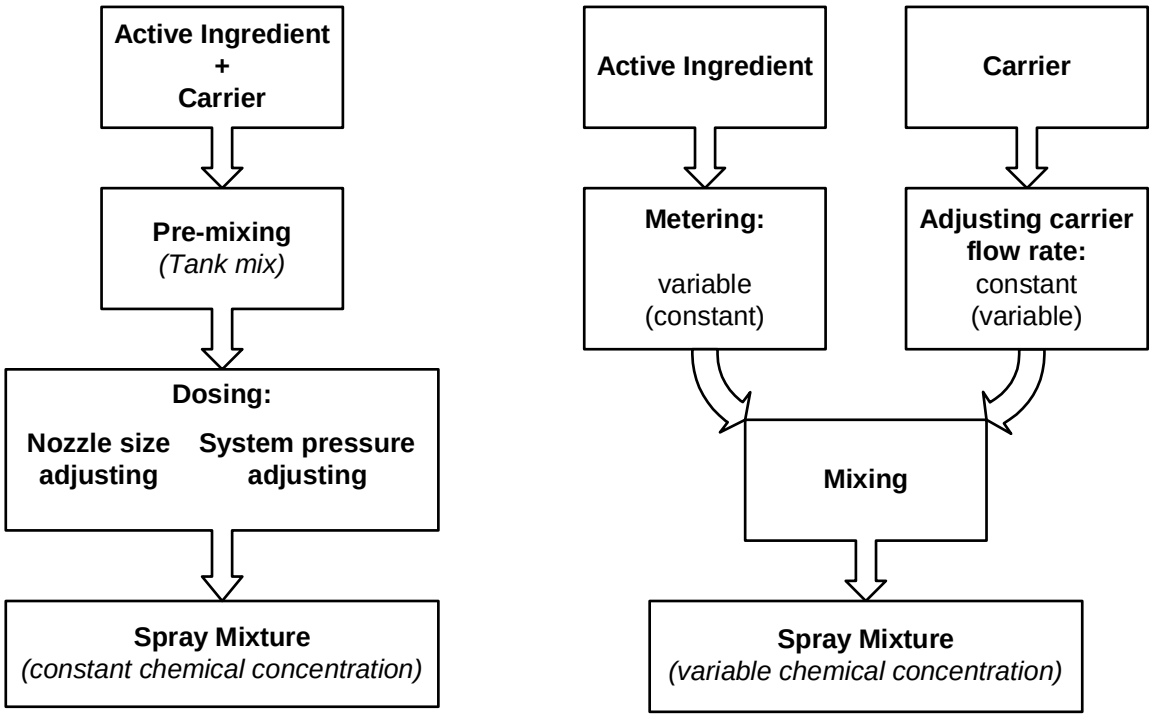

Figure 2. 11: Systems for controlling sprayer output for spatially variable rate herbicide application

2.2.1 Total Flow-Based Control Systems

The principle of this system is that the application rate is kept constant by varying the nozzle flow rate in direct proportion to the forward speed. The flow rate is regulated by adjusting the nozzle pressure (HUGHES and FROST, 1985; MILLER, 2003). The following are alternatives for varying the total flow (SCHMITT-OTT, 1974):

1. Varying the system pressure by:
   - direct pressure regulation
   - by-pass pressure control
   - eccentricity of the pump's rotor
   - pulse width modulated nozzles

2. Varying the nozzle diameter

The first approach and its technical solutions are limited, however, by the square root relationship (Equation 2.2) between pressure p_i and flow through a nozzle orifice Q_d so that doubling the flow rate requires a four-fold increase in pressure. Accordingly, the range of operating pressures is relatively narrow (VIDRINE et al. 1975; FROST, 1990; QIU et al., 1998; KIFFERLE and STAHLI, 2001). The coefficient k is an experimentally determined coefficient which depends on the type and size of the nozzle and liquid used.

$$Q_d = \frac{\sqrt{p_i}}{k} \tag{2.2}$$

Another limiting factor is the pressure range over which conventional pressure nozzles will provide a defined spray quality and volume distribution pattern (turn-down ratio). This means that the range of application rates that can be applied with a given size of conventional nozzle by changing the liquid pressure is limited to ±25 % of the nominal output (1.25:1) (PAICE et al. 2001). As the pressure drops below a specified level, the spray pattern becomes distorted and application uniformity is sacrificed. When nozzles are operated above the recommended pressure range, too many small droplets are generated. Because of these two limitations of the application rate range, traditional sprayers are not suitable for site-specific control strategies.

The second approach to controlling the sprayer output with a wider range of dose rates consists of using a twin-fluid nozzle with a dose rate range of 3:1 (PAICE et al., 2001) or a variable flow (swirl-type) nozzle with a range of 4:1 (KOO and KUHLMAN, 1993).

Variable-duration, pulsed spray emission technology was developed for flow rate control with conventional spray nozzles (GILES and COMINO, 1990). This is a relatively new variable rate application technology that is referred to as ‘pulse width modulation’ (PWM). It utilizes an electronically actuated solenoid valve coupled directly to the sprayer nozzle. An advantage of this technology over pressure-based systems is that the usable range of application rates available through one type of nozzle is greatly increased. Utilizing a duty cycle range (pulse width) of 10 to 100 % and the use of PWM nozzles would result in a flow control range of 10:1. To obtain this kind of flow control with a pressure-based system, the system pressure would have to vary 100:1. This is clearly out of the workable range for sprayer nozzles.

Not only can a wide range of flow control be obtained using a pulse width modulated sprayer system, it can also be changed relatively quickly. The nozzle valves' capability of changing the flow 10:1 has been given as less than one second (STONE et al., 1999).

Another approach to achieving a high turn ratio with common sprayers has been developed recently, e.g. in VarioSelect® or Patch Spray®. These systems involve the use of multiple nozzles in each nozzle location along a boom with the ability to pneumatically switch between output orifices and to adjust nozzle pressures (Fig. 2.5).

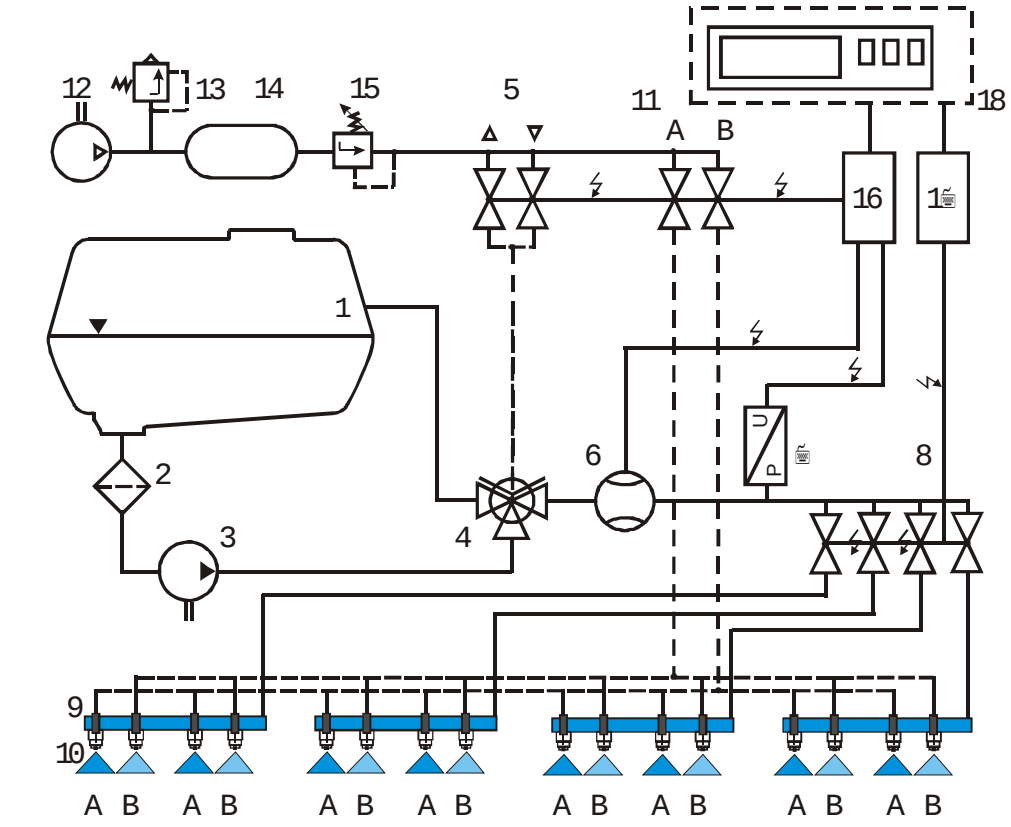

1 - Carrier tank
2 - Strainer
3 - Carrier pump
4 - Diaphragm control valve
5 - Air pressure reg. valves
6 - Flow meter
7 - Pressure transmitter
8 - Section valves
9 - Boom sections
10 - Nozzle valves
11 - Nozzle selection valves
12 - Air compressor
13 - Pressure relief valve
14 - Compressed air tank
15 - Pressure relief valve
16 - Junction box
17 - Job computer
18 - Board computer

Figure 2. 12: Scheme of the Patch Spray® system with arrangement of multiple nozzles (MICRON SPRAYERS, 2002)

By using different combinations of orifice sizes and pressures it is possible to achieve a turn-ratio of approximately 10:1. In this case the application rate ranges from 50 to 500 l ha^{-1} (MICRON SPRAYERS, 2002; BÖTTGER and LANGER, 2003; MILLER, 2003).

A reflectance-based system, Detectspray® (chapter 2.1.3) uses nozzles fitted with solenoid valves that open briefly to apply spray when the nozzles pass over green vegetation (ZHU et al., 1998). This system is commercially available along with another system, Weedseeker®, which is based on the same principle (NTECH INDUSTRIES, 2005).

The following two prototypes are examples of machine-vision-system guided sprayers. The first was developed and tested by TIAN et al. (1999). To create an intelligent sensing and spraying system, a real-time machine vision sensing system was integrated with an automatic herbicide sprayer. Multiple video images are used to cover the target area. For greater accuracy each individual spray nozzle is controlled separately. Instead of trying to identify each individual plant in the field, weed infestation zones (0.254 by 0.34 m) are detected. A system based on a similar principle was developed by GILLIS et al. (2002) for roadside herbicide application. The system uses a vertical boom with spray tips directed diagonally to the field surface. This road sprayer was later equipped with Raven SCS-750 injection modules.

A “triple-tank” system for variable application of three different chemical solutions was developed by the Institute of Agronomy in Bonn in cooperation with the spraying technology manufacturer Kverneland (OEBEL et al., 2004). This system was set up with three parallel nozzle supply lines; solenoid valves are used to switch between boom sections as instructed by the sprayer’s control unit. Each of the lines is connected to a tank with a spray mixture with an appropriate chemical concentration.

2.2.2 Direct Injection Metering Systems

The second, and fundamentally different, approach to variable-rate chemical application is the use of a direct injection system (Fig. 2.6). In direct injection systems the chemical concentrate and the water carrier are kept in separate tanks. The chemical concentrates are metered into the carrier and mixed with it before being discharged through the nozzle. This occurs only when needed according to changes in operating requirements, e.g. to apply higher application rate or different type of pesticide (LANDERS, 1998).

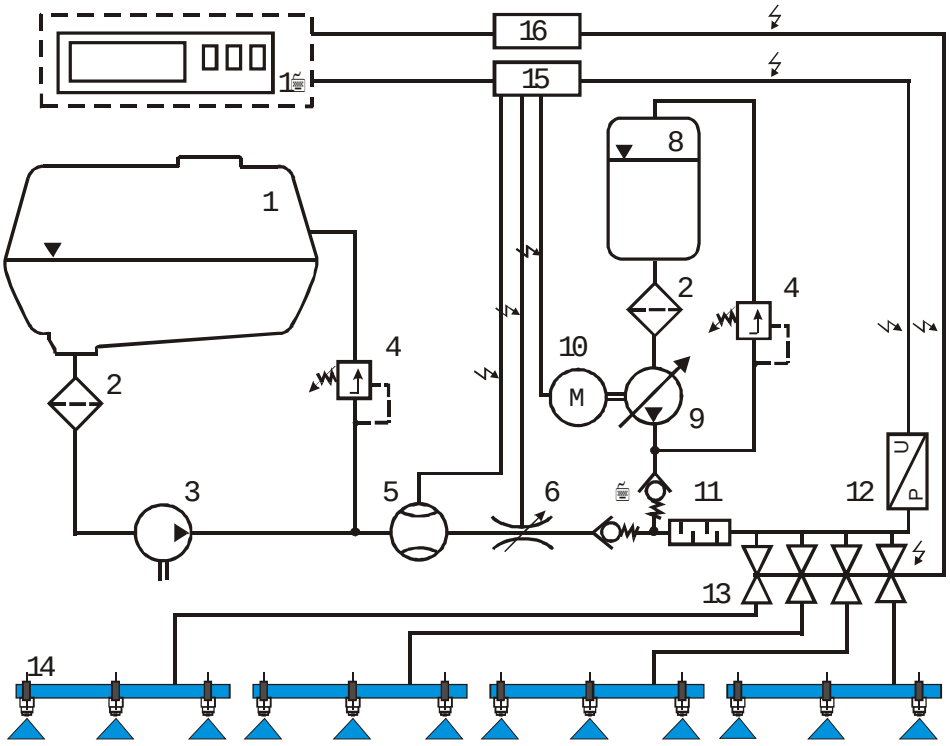

1 - Carrier tank
2 - Strainers
3 - Carrier pump
4 - Pressure relief valve
5 - Flow meter
6 - Pressure regulation valve
7 - Check valves
8 - Chemical tank
9 - Metering pump
10 - El. motor
11 - Mixer
12 - Pressure transmitter
13 - Section valves
14 - Boom sections
15 - Pressure relief valve
16 - Junction box
17 - Job computer
18 - Board computer

Figure 2. 13: Scheme of SCS-700 direct injection system (RAVEN INDUSTRIES, 2004)

Apart from the conventional application technology with total flow control, there are two more operational approaches to varying the application rate: it is also possible to regulate the active ingredient flow proportionally to the forward speed or to keep it at a constant level.

A control system of the sprayer should adjust the carrier and chemical flow rates proportionally to the forward speed in order to keep the application rate constant. However, the ratio of these two flow rates can vary during the specific chemical application as indicated by the weed treatment map. In figure 2.7, the next possible operational approaches are outlined.

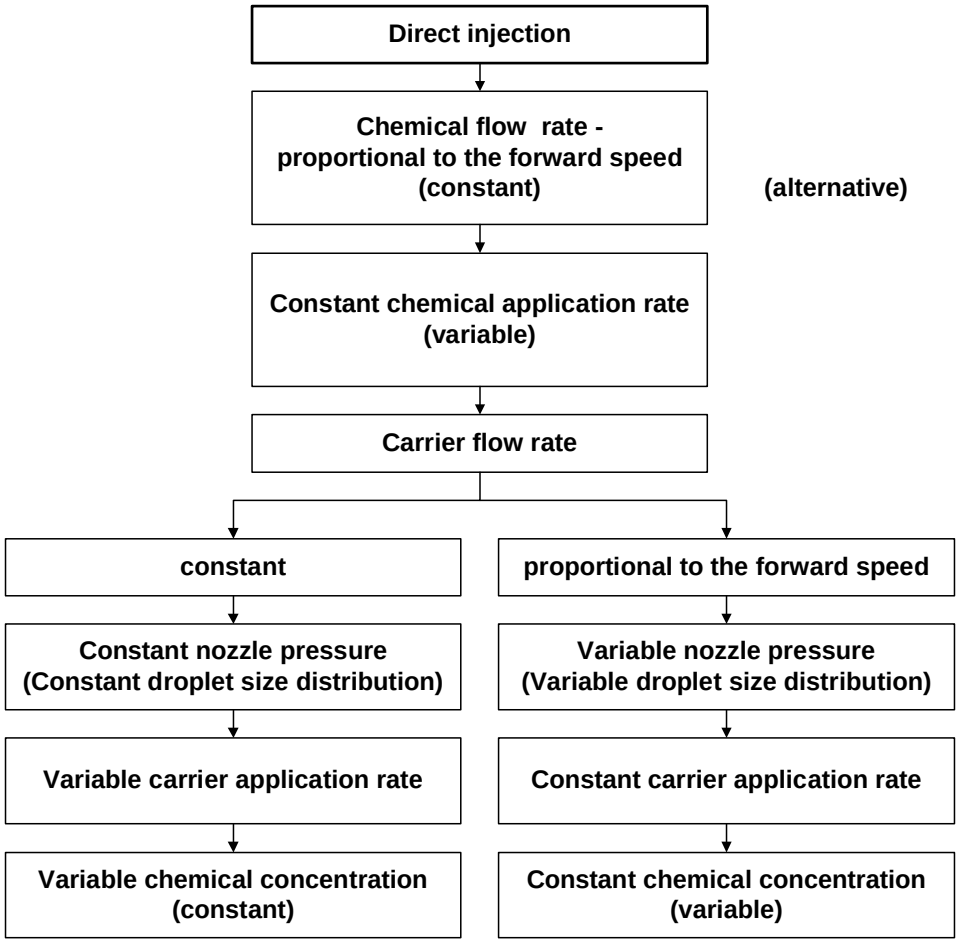

Figure 2. 14: Operational approaches to direct injection (alternative) (adapted from SCHMIDT, 1983)

The use of injection metering systems also has some advantages over conventional sprayers:

- in term of logistics, there are no disposal problems with wash water and left-over tank mixtures, and the exposition of operators to concentrated pesticides during mixing and loading is minimized (SUMNER et al., 2000)

- the main tank of the sprayer holds clean water only; there is no need to use a hydraulic circuit to agitate the spray mixture
- the components before the point of injection, e.g. carrier tank, pump and valves, do not need to be protected against aggressive chemicals
- the need to operate with a range of formulation volumes for a given dose and the requirement to use less than the full working width of the boom mean that the required turn-down ratio can be much greater than the 25:1 achieved with conventional pump designs (AUTHORS' COLLECTIVE, 2001)

2.3 Technical Approaches to Direct Injection

A conventional crop sprayer fitted with an injection system usually has one or more fluid mechanisms which dispense chemicals at a known rate at the junction of the chemical and carrier flows in the sprayer pipeline. Depending on the location of this injection point, it is possible to distinguish systems with injection upstream (at the suction) or downstream (at the discharge side) of the carrier pump. Behind the carrier pump, the chemical can be injected into all boom sections (centralised), into only one section (decentralised) or directly into individual nozzles (DNI) (see table 2.2).

Table 2. 4: Overview of basic technical variants of injection systems (c- continuous, d- discontinuous injection)

Point of Injection			
Suction side	Discharge side		
Central	Central	Decentral - Boom section	Local - Nozzle
Energy Transfer			
Hydrodynamic	Hydrostatic		Pneumatic
Hydrodynamic pumps **(c)** Eductors **(c)**	Hydrostatic pumps **(c/d)** Pressure injection **(c/d)** - syringes		Pressure injection **(c/d)**

Both of the above-mentioned approaches can deliver the active ingredient continuously or discontinuously. From the energy transfer point of view, the fluid mechanisms used in injection systems can be categorized into hydrodynamic (on suction side only), hydrostatic and pneumatic systems. The majority of direct injection systems use some form of hydrostatic pump to inject the pesticide into the pressure line after the main water pump. Alternatively, low pressure pumps, e.g. peristaltic pumps, meter pesticides into the suction side of the water pump to overcome high pressure and pulsation problems and to obtain a good mixture of pesticide and water in the main pump (LANDERS, 1993).

The fact that direct injection of plant protection agents is not new in the field of application technology is evidenced by previous theoretical and experimental works. For example, as early as 1970 GÖHLICH (1970) foreshadowed the idea of the direct injection of chemicals into the carrier by using a metering pump. He presented various possible techniques which could be used to keep the flow rate of the chemical proportional to the forward speed while keeping the carrier flow constant. SCHMITT-OTT (1974) continued the practical development of some direct injection techniques and considered solutions for controlling the application rate by the use of a control valve. No specific technical solutions were realized, however.

GEBHARDT et al. (1984) identified two injection strategies: (1) a positive-driven meter pump operated as an open-loop control system, and (2) a pump and a flow meter connected as a close-loop control system. The concentrated chemical was pumped from the container through a control valve regulated by a controller. Several types of injection system using hydrostatic pumps to meter chemicals into the carrier have also been proposed (GEBHARDT et al., 1984; CHI et al., 1989; ZHU et al., 1998). CHO et al. (1985) developed an experimental injection unit which used two pulse feeder diaphragm pumps to meter two chemicals simultaneously. WOMAC et al. (2002) used a carrier-driven (in-line) injection pump in an open-loop system. SCHMIDT (1983) described the possibility of varying the chemical application rate by means of an adjustment valve.

FROST (1990) proposed a hydrostatic metering system in which the carrier is pumped to the nozzles with a constant pressure. Some water is extracted from the lines feeding the nozzles and sent by the metering pump into the cylinder containing the chemical.

The water and the chemical are separated in the cylinder by a free piston or by a flexible membrane. A metered flow of a carrier displaces the chemical, which is injected into a mixing chamber where it is mixed with the carrier and delivered to the nozzles.

A hydrodynamic injection system based on the Venturi principle was constructed by SCHMIDT (1983). In this prototype the main carrier flow was split into two branches in which the water was mixed with the chemicals by means of a Venturi mixing nozzle. The mixture flow was then reconnected with the main carrier and the second mixture flow within the mixing chamber and delivered to the boom. The chemical was kept in a diaphragm tank and metered by means of the main carrier flow, which was regulated by a control valve or by varying the orifice size. Depending on the number of branches, this system allowed the simultaneous injection of two or more chemicals.

VIDRINE et al. (1975) constructed a sprayer prototype to evaluate the performance of an injection system providing a constant pesticide application rate. The prototype used a positive displacement pump to inject the chemicals into the spray boom. A hydro-pneumatic system delivered the carrier from a compressed tank at a constant flow rate. The chemical pump speed was directly proportional to the ground speed, while the hydro-pneumatic circuit was operated at a constant pressure. The junction of the chemical and carrier flows was located at the boom. Another pneumatic pressure system for an injection sprayer was developed by IMAG in the Netherlands: the chemical was compressed in the tank and metered into the carrier. The flow was adjusted according to the pressure difference between the water line and the chemical tank.

Combining both above-mentioned systems, a compressed air system was proposed by GHATE and PHATAK (1991). The system used compressed air to pressurize the chemical and water tanks. The pressurised chemical container forced the chemical into the mixing chamber. The water flow was dependent on the air pressure and the nozzle size, while the chemical flow was controlled by the air pressure and a needle valve in a flow meter. This system was further improved to achieve accurate pesticide application with respect to ground speed by using stepper motor-controlled air pressure regulators to vary the chemical flow rate (GHATE and PERRY, 1994).

The DOS-INTRO system, which uses a compressor to pressurise a stainless steel pesticide container, was developed by SCHÖNLEBER (PEISL and ESTLER, 1992). A solenoid valve controls the chemical flow rate. This system can inject up to three products.

Instead of injecting chemicals downstream of the pump and prior to the branching of the distribution lines carrying the solution to different boom sections, it is also possible to inject chemicals directly into the nozzles. Compared with the traditional and with the boom injection system, this system has the advantage of significantly reducing transport time. TOMPKINS et al. (1990) investigated a direct nozzle injection (DNI) system that used a metering pump for active ingredient flow control. Similarly, a direct injection prototypes, in which chemical concentrate were directly injected just upstream of each nozzle through a small metering orifice, was designed and evaluated by MILLER and SMITH (1992) and by ROCKWELL and AYERS (1996). In both systems, the discharge concentration through the nozzles varied with a variable differential pressure across the metering orifices. BENNET and BROWN (1997) developed a direct nozzle injection system consisting of a bank of linearly actuated pumps which were individually coupled with each nozzle.

2.4 The Use of Direct Injection Systems in Practice

Even though many different metering injection systems have been developed and experimentally tested, the real present state-of-the-art is represented only by commercially available technologies. Several recently developed injection systems which are currently commercially available are described below.

The Mid-West Technology direct injection system TASC 6600 from the USA is comprised of up to six individual tanks connected to peristaltic pumps. These pumps meter pesticide into an induction manifold pump where it combines with clean water before the carrier pump. For injection downstream of the carrier pump, the system can be equipped with a new positive displacement piston pump unit with a common flow rate ranging from 0.015 to 7 l min^{-1}. The pumps are driven by 12 V variable-speed electric motors and an electronic controller (MID-WEST TECHNOLOGY, 2005).

The Raven Industries injection module uses a variable-stroke piston pump which meters the chemical into the pressure side of the carrier line. The maximum operating pressure is 10 bar. There is an electronic console for controlling the speed of the pump, and the flow monitoring system is incorporated into the pump (RAVEN INDUSTRIES, 2004).

The German pump manufacturer MSR has developed, in conjunction with the pesticide manufacturer Ciba-Geigy, a system called Agroinject, which uses a proportional flow dosing pump driven by the water flow through the spray booms. Depending on the version, the dosing pump can combine up to four different liquids. The dosing pump sucks the plant protection agents from their original containers to avoid the operator having direct contact with the chemicals. Powdery plant protection agents must be dissolved before application (MSR DOSIERTECHNIK, 2004).

A system developed in the U.K. by the Micron Sprayers Company and based upon the Silsoe Research Institute (SRI) injection system comprises a syringe cylinder container which is used to extract chemicals from the original container and to meter them into the carrier. A metering pump is used to pressurize the plunger in the cylinder container, thus overcoming pump problems associated with pesticide viscosities. After evaluation by FROST (1990), the system is now in the commercial prototype stage (MICRON SPRAYERS, 2002).

Other systems are under development or their production is limited or has been stopped. Such systems include the Conduria GDE system, which uses a tractor-wheel controlled piston pump for the metering of chemicals at application rates ranging from 1 to 6 l ha^{-1} (LINDTNER, 1985); DOS Intro, a pneumatic system by the German farmer SCHÖNLEBER; Öko-log, a system by the German company Biotronic (PEISL and ESTLER, 1992). Lechler GmbH has patented a hydraulically driven micro-diaphragm pump coupled with a nozzle body (LECHLER, 2005).

The French sprayer manufacturer Tecnoma has investigated the use of a Dosatron injector/dilutor. The Vicon Injection System developed by a Dutch sprayer manufacturer, whose injection sprayer uses a novel dual pipe peristaltic pump, allows a wide variation in application rates thanks to the use of a combination of small and large bored pipes.

The Swedish AgriFutura Dose 2000/500 uses a hydraulically-driven piston pump to draw pesticide from 35 litre containers, delivering it into a mixing chamber situated between the water pressure regulating valve and the boom selection valves. The pump output can be controlled by means of a stepper motor and electronic controller (LANDERS, 1997; AUTHORS' COLLECTIVE, 2001).

2.5. Problems of Current Direct Injection Systems

Direct injection systems have been developed during the past decade to eliminate traditional application problems. The advantages of these systems include: elimination of wasted chemical, limited operator exposure, automatic on-the-go selection of herbicide application rates, and control of multiple injection modules with different herbicides (QIU et al., 1998). The current direct injection systems have two disadvantages. The first is that the dynamic characteristics of the sprayer are affected by the time required for the chemical to travel from the injection point to the spray tip. The second issue is the occurrence of non-uniform mixtures due to inadequate mixing of herbicides and carrier in the boom (TOMKINS et al., 1990; MILLER and SMITH, 1992; ZHU et al., 1998).

The time required for transporting and mixing the chemicals with the carrier depends on the location of the injection point and on the solution flow velocity. In the direct injection sprayers that are currently commercially available the central point of injection is located immediately downstream of the carrier pump, far away from the nozzle tips. This technical solution has a long response time, which causes significant discrepancies between desired and actual application rates while the new concentration travels from the injection point to the nozzles.

At present, the only injection system available on the German market to have been approved by the Federal Biological Research Centre for Agriculture and Forestry (BBA) is the Mid-tech LH Agro. Depending on application rate and boom length, its reaction time ranges from 10 to 40 seconds (PEISL and ESTLER, 1993; BBA, 2005). In relation to the target area such delays will cause great misapplications. For example, a sprayer equipped with an injection system with a response time of 30 s and a standard forward speed of 8 km h^{-1} will travel about 66 metres before the required concentration of solution in the nozzles is reached.

It is questionable if this can still be called site-specific application. These delays can be corrected using a forward regulation of the carrier and chemical flow rates by means of the valves and/or metering pumps. This type of injection system can only be used with the map based approach (off-line application).

TOMPKINS et al. (1990) studied boom flow characteristics of two direct injection systems with different injection positions: immediately upstream and downstream of the carrier pump. With the injection point upstream of the pump, approximately 3.5 m ahead of the boom, 26 s were required for the chemical concentration at the outermost spray tip to reach the equilibrium value. The maximum variation at this spray tip was 2.3 % of the time-average chemical concentration. For injection downstream of the pump, the chemical concentration equilibrium was reached in about 12 s with a maximum range of variation from 5 to 11 % of the average concentration, depending on the pump type. The previously described injection system by FROST (1990) was further developed and evaluated by STAFFORD and MILLER (1993). The minimum time delay of this system was 4.3 seconds.

A significant improvement can also be achieved by reducing the diameter of the nozzle supply lines. FROST (1990) described a method for minimizing lag time in boom injection systems by reducing the boom diameter. It was shown that the overall system delay could be reduced to less than 3.0 s for a practical plumbing arrangement on a typical machine. ZHU et al. (1998) proved that the lag time can be reduced by approximately 50 % when the boom diameter is reduced from 20 to 10 mm. Another option for reducing lag time is to place the point of injection immediately before each nozzle.

The direct nozzle injection systems mentioned in chapter 2.3 have very short response times. In a study by ROCKWELL and AYERS (1996) the average time constant was 2.5 seconds, while the average rise time was 3.8 seconds for a step input to the system. The term ‘time constant’ refers to the time until the system reaches 62.3 % of the step input to the system. The term ‘rise time’ refers to the time in which the system goes from 10 to 90 % of the step input to the system.

The second issue connected with direct injection concerns the uniform distribution of the chemical. Depending on the point of injection, transient time varies among several nozzles on a sprayer boom and thus affects the degree of uniformity of the distribution of the chemical. Non-uniformity of chemical application can also result from inadequate mixing of chemicals and carrier before discharge through a nozzle (TOMPKINS et al., 1990). In central or boom injection systems this problem is insignificant because the mixing of the carrier and the chemical takes longer than in direct nozzle injection systems. ROCKWELL and AYERS (1996) used the variation coefficient (CV) to evaluate the spray pattern, finding that the spray pattern of direct nozzle injection sprayers did not differ significantly from the spray pattern of tank mix systems.

WAY et al. (1992) simulated the chemical application accuracy of injection sprayers accelerating at 0.44 m s^{-2} from rest to constant speed. Comparisons were made between injection sprayers with conventional and modified plumbing systems on the one hand and conventional tank-mix sprayers without sprayer controllers on the other. The results revealed that the ratio of area receiving unacceptable chemical application rates to the total area sprayed was smaller with the tank-mix sprayer than with any injection sprayer.

To summarize previous studies: the performance of a direct injection system depends on many factors including spray tip size, system pressure, ground speed, injection position, and system configuration. The dynamic characteristics of direct injection systems are dominated by the time it takes for the chemical to travel from the injection point to the nozzle. Even though direct injection into the spray tip reduces lag time, the reduction is still not sufficient to fulfil the requirements of on-line herbicide application.

3. System Analysis and Design of Direct Injection System

In accordance with the objectives of this work – namely to design, construct and evaluate a model of a direct injection system with minimal response time – it is necessary to carry out an analysis of the problems which relate to this system. The first phase of the analysis will be dedicated to determining the requirements of on-line site-specific herbicide application using a sprayer with an integrated direct injection system. In the second phase the individual requirements will be considered and several possible technical solutions will be proposed. It is hoped that on this basis it will be possible to design an optimal injection system.

3.1 System Requirements

There is a range of possible solutions for the technical realization of the direct injection method. In considering the suitability of these solutions, it is first necessary to determine the requirements. In an ideal case, sprayers with a direct injection system should cover the whole operating range of common field sprayers currently available on the market. The most important factors and requirements can be divided into two groups. The first includes requirements which are relevant to the on-line approach to site specific herbicide application. The second group includes requirements which are related to injection metering systems only. The basic requirements are all listed below.

Requirements for on-line site-specific application:

- application rate of the carrier
- application rate of the chemical
- minimum total response time of the application system
- forward speed
- position of weed detection device (sensor)
- high spatial resolution of sprayer
- uniformity of mixture concentration across a working width (lateral distribution)
- application of several different herbicide/additive products according to weed population

Requirements for injection metering system:

- fast change of dose rates according to changes in operating parameters – minimum response time of injection system
- accurate metering of herbicides across the range of dose rates found in practice (flow rate of carrier/chemical)
- optimal number and position of injection points
- dimensioning of the injection system in accordance with the required nozzle/system pressure
- ability to deliver and inject a wide range of herbicides with varying physical properties
- good miscibility and solubility of herbicides with carrier (homogeneity of mixture)
- no or, if applicable, few herbicide / spray residues
- easy rinsing of chemical supply lines
- easy and safe handling of concentrate tanks
- capability of being fitted to most existing sprayers
- robust construction of the system and use of durable materials

Some of these requirements are interrelated and can therefore affect each other. The most important requirements that are the objects of this thesis are described in more detail in the following chapters.

3.1.1 Requirements for On-line Site-Specific Herbicide Application

3.1.1.1 Application rate

The amount of solution to be applied on the field is the basic decision factor which determines others requirements for spraying, e.g. forward speed, working width, flow rate of the carrier (pump capacity), nozzle size and working capacity (carrier tank). The next considerations about injection metering are based on the known equation for the application rate of the spray mixture (carrier and chemical):

$$A = \frac{600 \cdot Q_t}{U \cdot W} \tag{3.1}$$

where:

A = Application rate of spray mixture (l ha^{-1})
Q_t = Total flow rate of spray mixture (l min^{-1})
U = Forward speed of the machine (km h^{-1})
W = Working width (m)

Application rate of the carrier

The application rate of the carrier, deriving from the total application rate *A*, depends on the weed species, the growth stages of the crop plant and weeds, the type of chemical and its formulation, the weather condition, the type of sprayer and, if applicable, on other agronomic decisions, e.g. subsequent fertilization. The common range of application rates in crop farming is 100 to 400 l ha^{-1}. Application rates in this range ensure good wetting and have good biological effects. On the other hand, such application rates limit the working performance of the sprayer due to high carrier consumption (KIFFERLE and STAHLI, 2001). That means the need for often re-filling of the solution tank. On all sprayers on the market today, filling and rinsing account for nearly 25 % of each machine hour. However, economical pressures with regard to working performance have led to the development of new spraying technologies, e.g. air assisted nozzles (AUTHORS' COLLECTIVE, 2001). Such nozzles enable a significant reduction of the application rate (100 - 150 l ha^{-1}) by maintaining a constant spray quality (droplet size).

Application rate of chemicals

Different herbicides are applied at widely differing rates. The application rate is usually prescribed and depends on the type of active ingredient used, on its formulation, on application timing (pre-emergence, post-emergence and successive treatment), on the crop plants, on the weed species and on the degree of weed infestation. For liquid herbicide formulations, application rates of 0.1 l ha^{-1} and 5.0 l ha^{-1} are in common use. Table 9.1 in the appendix shows the most widely used herbicides and their application rates per hectare. The application rate of chemical A_a is given by equation (3.1), which is derived from (2.1):

$$A_a = \frac{600 \cdot Q_t \cdot c_m}{U \cdot W} \tag{3.2}$$

where:

A_a = Application rate of chemical (l ha^{-1})
Q_t = Total flow rate of spray mixture (l min^{-1})
c_m = Concentration of chemical in the spray mixture (-)
U = Forward speed of the machine (km h^{-1})
W = Working width (m)

The concentration of the chemical in the spray mixture c_m is then given by relations (3.3) and (3.4):

$$c_m = \frac{Q_a}{Q_T} \tag{3.3}$$

$$Q_t = Q_c + Q_a \tag{3.4}$$

where:

Q_a = Flow rate of chemical (l min^{-1})
Q_c = Flow rate of carrier (l min^{-1})

3.1.1.2 Total Response Time

A sprayer with an injection metering system combined with a weed detection system must be designed to fulfill the requirements of on-line herbicide application. The main limiting factor of on-line application is the total response time of the whole application system T_{RS}. This can be defined as the sum of the individual periods of time elapsing during each step of the on-line application process; see equation (3.5). In our case there are only two time components. The first component is acquisition time T_A, which is the minimum time required for the detection and recognition of the weeds. The second component of total response time T_{RS} is the response time of the injection metering system T_R, which is the time required for the change in concentration to become fully established at the spray nozzle.

$$T_{RS} = T_A + T_R \tag{3.5}$$

Acquisition time T_A depends on the type of weed (plant) detection system being used. For instance, with optoelectronic sensors for spectral analysis it is possible to achieve an acquisition time of about 2 ms (HOLSTEIN and BILLER, 1998). This kind of technology is much faster than image analysis with its high processing requirements, but it is not capable of distinguishing between crop plants and weeds. For example, the time required for analyzing three camera images and creating a decision about turning each boom section on or off is approximately 1 second using a 500 MHz board computer (GERHARDS et al., 2002). Chapter 3.1.2.1 will deal in detail with the response time of the injection system T_R.

3.1.1.3 Forward speed

The forward speed of the sprayer has a considerable impact on the accuracy of on-line application. This impact is both direct and indirect. A direct impact of the forward speed is evident in relation to the total response time T_{RS}. Weed detection and the activation of injection (valve opening) have to be virtually simultaneous so that the period between target detection and spraying is primarily determined by the forward speed of the sprayer. With a higher forward speed, the time limit available for one operation period decreases. In the extreme case, if the total response time is greater than the maximal time limit, there will be misapplications.

The forward speed has an indirect influence on the nozzle flow rate. Higher forward speeds require higher flow rates of carrier and chemicals. This is likely to have a positive influence on the transport time of the mixture in the nozzle supply lines, thus reducing the response time of the injection system (see chapter 3.1.2.1).

The forward speed varies according to the type of machine and the operating conditions. A range of 4 to 8 km h^{-1} would cover most spraying operations in Europe. However, improvements in spray boom and vehicle suspensions together with the need to optimize tramlines have meant that speeds in the order of 12 km h^{-1} are now common and some machines operate at even higher speeds. In on-line application, the forward speed of the sprayer is limited due to the duration of the scan cycles of the weed detection system. Weed detection systems using cameras and systems with optoelectronic sensors work with a maximum forward speed of 8 and 20 km h^{-1} respectively (OEBEL and GERHARDS, 2006; FELTON and MCCLOY, 1992).

3.1.1.4 Weed Detection Sensor Positioning

The position of the sensors, together with the forward speed, has a direct impact on application accuracy. Using Cartesian coordinates (x, y, z), the weed detection sensor can be positioned in relation to the travel direction and the soil surface. Fig. 3.1 shows the configuration of a sensor and a nozzle coordinated with the x-axis (longitudinally to the axis of travel), the y-axis (vertically to the ground and travel direction), and the z-axis (laterally to the axis of travel). From the point of view of application accuracy, the positioning of the sensor in the direction of travel (x-axis) is more important than the positioning in the other two directions, which is related to the spraying resolution. Between the sensor and the nozzles (spray boom), there is a constant distance l_s, which together with the forward speed of the machine U results in a certain time reserve necessary for the response of the whole system. The relation between these variables is:

$$T_{RS\,\max} \leq \frac{l_s}{U} \tag{3.6}$$

where:

T_{RSmax} = Maximum total response time of the application system (s)

l_s = Distance between centre of sensor and nozzle tip (m)

U = Forward speed (m s^{-1})

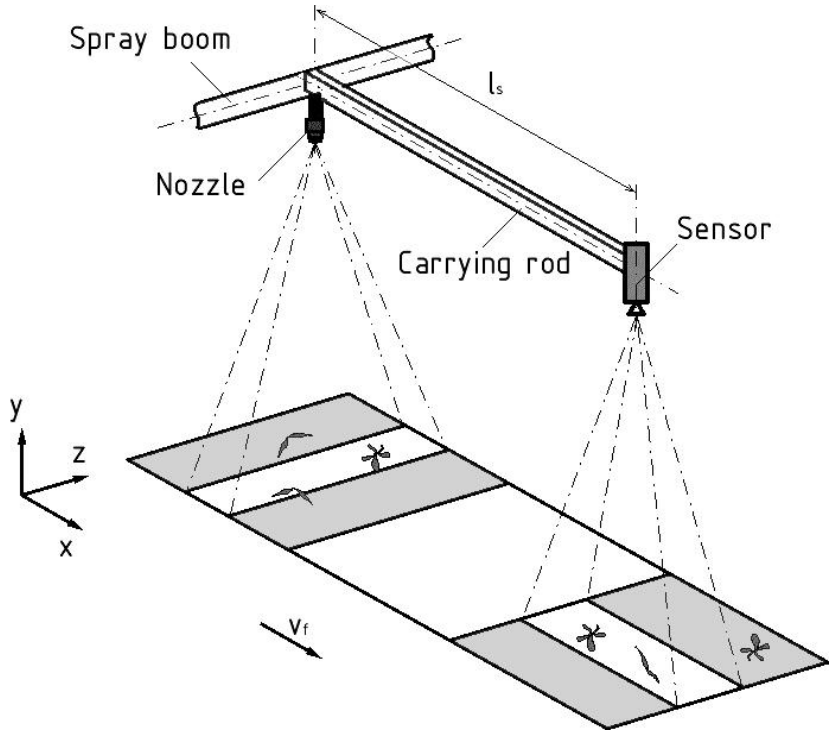

Figure 3. 9: Sensor positioning in direction of travel, S - sensor; N - nozzle (boom section)

If the weed detection sensor provides a trigger signal for a control unit of a single nozzle or spray boom section, it should be fitted as close to the nozzle as possible. The possibility of easy installation on existing sprayer booms by means of a rod would be optimal. However, this kind of arrangement requires that the rods have a certain minimum length, and simultaneously the required forward speed of the sprayer must not be exceeded. Thus, the response of the weed detection and injection system must be very fast. For example, assuming a forward speed of 8.0 km h^{-1} (2.22 m s^{-1}) and assuming that the maximum possible rod length for fitting on a sprayer boom is 1.0 m, then the time available for the response of the whole application system (T_{RS}) is 0.45 s. During this short period the system must provide information about the next application rate and adjust the required concentration at the nozzles.

3.1.1.5 Spatial Resolution of Liquid Deposition

In agricultural spraying, where discrete targets and non-targets are present in a localized area, a high spatial resolution of liquid deposition is essential for selective treatment. The economic value of patch spraying will increase as the minimum area that can be selectively treated decreases (AUDSLEY, 1993; WALLINGA et al., 1998). The spatial resolution of liquid deposition represents the sprayer performance required for reaching the minimum area that can be selectively treated with a prescribed application rate. Achieving high spatial resolution of liquid deposition from a moving source requires:

- brief high frequency emissions to reduce the minimum deposit length along the axis of travel
- individual control of emitters to reduce the minimum deposit width normal to the axis of travel (GILLES et al., 2004).

The first requirement represents the functional relation between the travel speed and the response time of the metering system, whereas the second requirement represents split-control of the carrier and chemicals flow rates over the whole length of the spray boom. Field sprayers are usually available with boom lengths from about 8 m to over 36 m. This will cause difficulties with weed detection systems that have a spatial resolution of 1 m or less. A suitable solution for current sprayers would be to distribute the control elements to individual boom sections with lengths of 3 m or 4.5 m. Then it would be possible to employ the boom section shut-off valves for brief control (opening and closing) of the carrier flow for each section. In an ideal case, the flow rate would be controlled separately by an elementary actuating units coupled with the individual nozzles. An example of this design is the already mentioned spot sprayer with electromagnetically controlled nozzle solenoid valves. The solenoid valves allow the opening of the nozzles for very short periods of 0.15 s. The area sprayed during one cycle is about 0.5 m (nozzle spacing) x 0.83 m (at the maximum operational speed of 20 km h^{-1} for this system) depending on the type of nozzle and the boom height.

A high spatial resolution of the weed detection system used is a prerequisite for the next consideration about the optimal arrangement of the actuators for flow rate control and, consequently, about the spatial resolution of the sprayer. The resolution of the weed detection system depends on the number and type of sensors used (scan frequency) and on the decision analysis about the maximum acceptable weed threshold. Fig. 3.2a shows the ratio of the area scanned by means of a weed sensor to the minimum area treated by one nozzle. In the next figures, two possible sensor positioning arrangements are shown. The first (Fig. 3.2b) is an extreme solution in which each nozzle is controlled separately by its own sensor. In the second arrangement (Fig. 3.2c) one sensor is used for the control of the whole boom section.

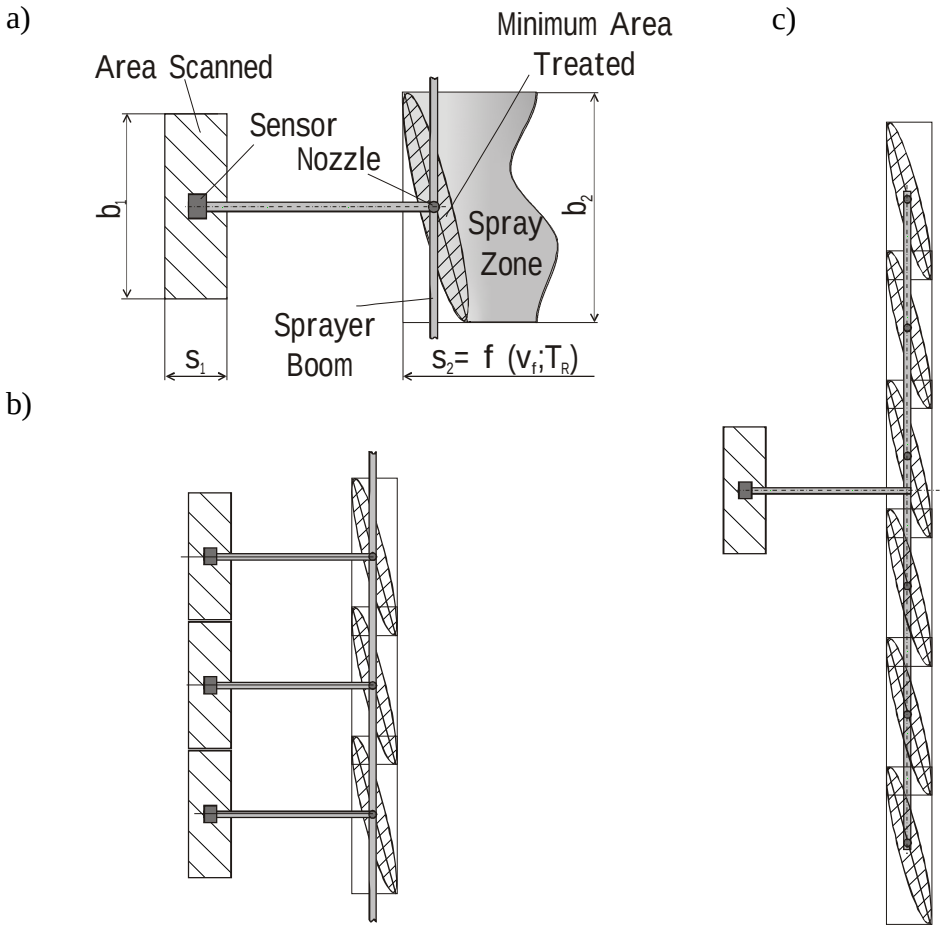

Figure 3. 10: Sensor and sprayer spatial resolution: a) ratio of scanned and treated areas; b) sensor - nozzle arrangement; c) sensor - boom section arrangement

The size of the mostly regular, square grids which are used for map-based site-specific herbicide application varies from a few square meters to 50 m^2 and depends on the width of the spray boom used. The new optoelectronic sensors and digital cameras with a high resolution were developed with the aim of detecting weed seedlings with a low distribution density. The optoelectronic system scans at a frequency of 300 Hz, which means that a new assessment is made every 1.85 cm at a forward speed of 20 km h^{-1}. The ground area scanned with each detector is nearly rectangular (approx. 0.2 x 0.6 m) if the sensor is mounted at a height of 0.5 m. This area approximates the coverage pattern of a flat fan nozzle operated at the same height.

The on-line approach presented by GERHARDS and CHRISTENSEN (2003) uses three bi-spectral digital cameras. The cameras were mounted on a spray boom at a height of 0.6 m, and the distance between the cameras was 3.0 m. The cameras with an intrinsic resolution of 636 x 480 pixels were triggered with an exposure time of 1/4000 s to get well-focused images of an area of approximately 0.02 m^2 (0.16 x 0.12 m) per image at a speed of 7-8 km h^{-1}. A set of three images was taken about every 2.0 m and stored on the on-board computer (OEBEL and GERHARDS, 2006). The spatial resolution (2.0 x 3.0 m) of this camera system achieves sufficient precision for the purpose of generating weed distribution maps (BACKES et al., 2005). Automatic control of the exposure time allows acquisition of 2 images per second at a forward speed of up to 10 km h^{-1}. Optionally, it is possible to extend the area scanned by each camera to 0.1 m^2.

Typical agricultural nozzles, e.g. flat fan nozzles, are unsuitable due to excessive flow rates and diverging spray patterns. One feature of diverging fan spray patterns is that the width of spray application depends on the distance from the nozzle to the target. There is also a variation in droplet velocity across the spray sheet. When high resolution deposition is required, variability in droplet size velocity in combination with the forward movement of the vehicle can alter the spray distribution. Furthermore, a high spray velocity is desirable as it allows higher spatial resolution in the deposits along the axis of travel.

3.1.1.6 Mixture Concentration Uniformity

Another requirement for on-line application with a direct injection system that needs to be evaluated is mixture concentration uniformity. Mixture concentration uniformity and spray deposit distribution in the lateral and longitudinal direction are the most important performance criteria for testing crop sprayer equipment. The concentration uniformity of a mixture depends on the amounts of chemical and carrier in the mix and on the mixing intensity. A homogeneous mixture is a prerequisite of uniform spray deposit distribution.

The maximal admissible coefficient of variation for the mixture concentration in a solution tank is 15 % (BBA, 2002). With common non-injection sprayers this would not be a problem since they are equipped with an agitation system which allows the pre-mixing of chemicals and carrier in the tank before application. Moreover, they also maintain the concentration rate at the required level during application.

Problems with non-uniform mixtures in injection systems usually relate to insufficient mixing of the chemicals. The degree of mixing of pesticide and carrier depends upon the time available, the degree of hydrodynamic turbulence and the design of the mixing chamber (if fitted). In the boom and nozzle injection systems, there is not enough time for complete mixing of chemical and carrier before discharge through a nozzle (TOMPKINS et al., 1990, ZHU et al., 1998). It would be probably necessary a static mixers or other mixing devices as a part of injection system and not rely on turbulence within the pipes because or momentary mixing at the nozzles. Another important role of an effective mixing system is to even out the pulses which may be caused by mechanical pumps. The formulation, polarity and the viscosity of chemicals have also an influence on the mixing process. Highly viscous herbicides tend to exhibit a large drag effect and may be difficult to mix with the carrier.

The spray deposit distribution in the lateral direction depends first of all on the nozzle types used, which must provide uniform distribution of the flow rate along the whole length of the boom. The spray deposit uniformity along the travel direction is affected by variable forward speed and pump pulsation.

The German Federal Biological Research Centre (BBA) has proposed a coefficient of variation of 7 % as a performance limit for the lateral spray deposit distribution for new sprayers. There are no prescribed limits for the longitudinal spray deposit distribution.

To determine the mixture uniformity at different positions along the boom sections, the samples of mixture solution flowed through nozzles at various nozzle positions are collected. The chemical concentration of these samples is then determined using the fluorescence or conductivity measurement methods. TOMPKINS (1990) investigated mixture uniformity in three injection systems with different injection positions: upstream and downstream of the carrier pump and in the individual nozzles. In a comparison of direct injection immediately upstream and downstream of the carrier pump, the chemical concentration variations at the nozzle were usually greater with downstream injection. The systems with a central injection point had maximum deviations from the average concentration of about 2.3 % and 11 % respectively. Direct injection of the chemical into the individual nozzles failed to achieve uniform chemical concentration from nozzle to nozzle. The concentrations deviated by 19.5 to 39 % from the average concentration. Another nozzle injection system has a maximum coefficient of variation of 16.3 %, which is a similar result (ROCKWELL and AYERS, 1996). ZHU et al. (1998) evaluated the mixture uniformity in the supply lines and of the spray patterns as a function of the Reynolds number. The measurement was done for a boom injection system. There was no statistically significant effect on the mean of the mixture concentrations measured from ten nozzles on the boom. The Reynolds number in the supply lines ranged from 1500 to 7000. The average coefficient of variation was 4.22 %. The mixture across the spray pattern of all nozzles showed uniform mixing, even if the mixture in the boom was not uniform. The average coefficient of variation was 1.31 %.

Moreover, there may be variations in the dosing of the chemical due to pulsation of the metering devices (e.g. metering pump, valve). This is also a significant factor affecting differences of spray deposit uniformity along the spray path. SUMNER et al. (2000) investigated a system using an injection pump. Injector pump frequencies above 300 rpm provide acceptable spray distribution along the nozzle path. The resulting coefficient of variation was less then 10 %.

3.1.2 Injection System Requirements

3.1.2.1 Response Time of the Injection System

The minimum response time of the injection system T_R is the most crucial factor when using this system for real time herbicide application. Sprayers that adjust the chemical injection according to different application requirements and/or travel velocities exhibit a time delay before the change in concentration becomes fully established at the spray nozzles. The response time of the complete system has two main components. The first one is related to the transport time between the injection point and the nozzles. The second component is the response characteristic of the injection metering system (PAICE et al., 1995).

The transport time is related to:

- fluid transportation time, also referred to as lag or dead time
- controller execution time

The response characteristic of the injection system is related to:

- turbulent mixing in the system
- the magnitude of concentration change
- metering device dynamics

Compared to other components of response time, the execution time of the controller is negligible. The microcontrollers used in the electronic control units provide single instruction cycle execution times of 0.5 μs (DARR, 2004). However, current CAN-based networks exhibit certain message latency. Simulations have shown that normal agricultural machinery configured with an ISO 11783 CAN bus can produce an average message latency of less than 6 ms with proper prioritization (HOFSTEE and GOENSE, 1999).

The dynamic response characteristics of the complete direct injection system are dominated by the transport time. Leaving the controller execution time delay out of consideration, the transport time is affected mainly by the volume of the chemical solution in the system from the injection point to the nozzle (pipe size) and by the flow rate of the solution. The lag time T_{lag} is calculated using the method derived from the continuity equation (FROST, 1990):

$$T_{lag} = \sum_{i=1}^{n} \frac{\pi l_i d_i^2}{4 Q_i} \tag{3.7}$$

where:

T_{lag} = Fluid transportation time required for the injected material to reach the nozzle (s)

Q_i = Flow rate of the solution ($m^3 s^{-1}$)

d_i = Pipe diameter (m)

l_i = Pipe length (m)

n = Number of conduits (-)

From equation 3.7, it possible to derive that pipe length and diameter have a significant impact on lag time. Therefore, it is desirable to ensure that these parameters will be minimized in the proposed system. Maximum acceptable line losses can be used to calculate the minimum pipe sizes. Thin pipes minimize not only the delay between the injection point and the nozzle, but they also reduce the quantities of residual diluted spray fluid in the pipe system. The flow rate of the solution also significantly affects the lag time. All delays are inversely proportional to the flow rate. According to equation 2.2, the flow rate is a function of nozzle size and system pressure.

Time response characteristics for dose step changes (e.g. concentration, flow rate) fundamentally affect the applicability of injection metering systems, but the results obtained depend greatly on the methodologies used. ROCKWELL and AYERS (1996) and PAICE et al. (1997) used two transient characteristics to evaluate the response time of a sprayer. The time constant of the system was the time required to reach 62.3 % of the step input while the rise time was the time required to go from 10 to 90 % of the step input.

The rise time was defined as the time it took for the concentration to change from 10 % of the mean value to within 10 % of the mean target value. SUDDUTH et al. (1995) used the three response time parameters delay time, dead time and rise time to determine the controller response. Delay time was defined as the time required for the output response of a step input to reach 50 % of its final value. Dead time was defined as the time required for the output response of a step input to reach 10 % of its final value. Rise time was defined as the time required for the output response of a step input to rise from 10 to 90 % of its final value. PECK and ROTH (1975) defined response time as the period from the instant the injection begins until the chemical concentration reaches 95 % of the equilibrium rate. The transient response and transportation time characteristics used for the evaluation of the proposed injection systems are shown in Fig. 3.3.

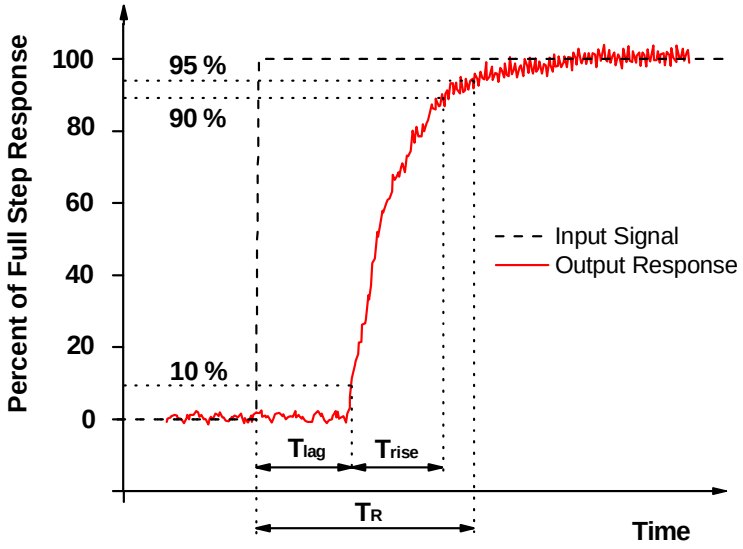

Figure 3. 11: Time response characteristics of injection systems

A 95 % concentration corresponds to the efficacy threshold i.e. the chemical concentration in the applied spray deposit necessary for satisfactory weed control (BENNETT and BROWN, 1997). Thus the transient characteristic from 0 to 95 % best characterizes the response time T_R. The rise/fall times are described by the transient curves rising from 10 to 90 % and falling from 90 to 10 % of the step input, respectively.

This transient characteristic most accurately describes the magnitude of the concentration change and the dynamics of the metering device. The time period from the onset of injection (change of chemical flow rate; 0 %) to the time when the mixture concentration at the nozzle (sensor) begins to change (10 %) describes the transport time T_{lag}.

3.1.2.2 The Injection Point

The length of the nozzle supply lines and the number of individual injection points may vary depending on the position of the injection point. This affects lag time, mixture uniformity, number of actuators and the volume of residual solution in the supply lines after application. According to equation 3.7, the length of the supply lines determines the lag time of the system. As we want to carry out on-line application, the distance between the injection point and the nozzle has to be minimized. The minimization of this distance necessitates the splitting of the injection point and consequently a greater number of actuators.

There are some technical requirements for actuators used in non-central injection systems. In the majority of systems the chemicals are injected centrally into the carrier line, somewhere between the sprayer carrier pump and the section manifolds, as shown in Fig. 3.4b. The chemical pump must therefore be able to inject the chemical at a pressure greater than the sprayer operating pressure. This necessitates the use of medium or high pressure pumps (required differential pressure is up to 20 bar). A constant delivery rate at higher pressures can be achieved by the use of positive displacement pumps (piston or gear pump).

In another design option, the injection point is located on the low-pressure side of the carrier pump; see Fig. 3.4a. This arrangement allows the injection system to operate at a low pressure. Accordingly, it is possible to use peristaltic pumps, which are operated at a maximum pressure of about 3 bar. The major advantage of these pumps is that the moving parts are not in contact with the supplied fluid medium so that it allows the precise metering of highly aggressive concentrated chemicals.

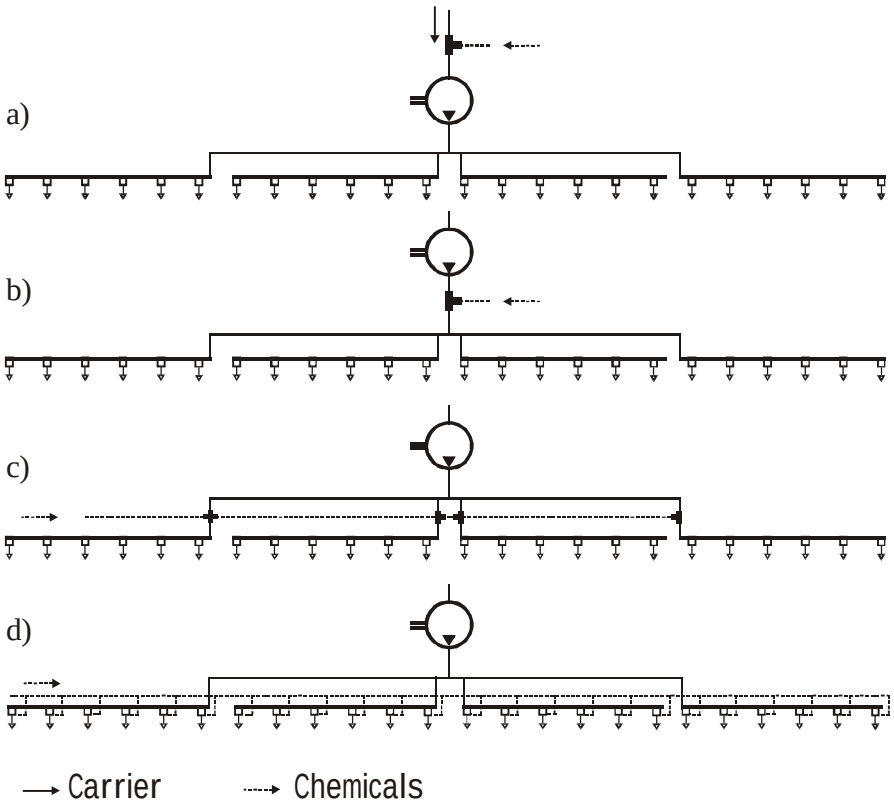

Figure 3. 12: Injection systems with different injection point arrangements: a) central, upstream of the carrier pump; b) central, downstream of the carrier pump; c) decentral, injection into boom section, d) decentral, injection into individual nozzles

A boom injection system is shown in Fig. 3.4c. This system configuration reduces the lag time and the residual volume of spray solution in the boom sections. The boom configuration allows decentralized flow rate control and thus more specific application. This requires more metering actuators to be mounted on the individual boom sections. In this specific case, it is necessary to employ one pump or valve for each boom section and chemical product applied.

In comparison with traditional systems and boom injection systems, direct nozzle injection (DNI) systems have the advantage of significantly reducing lag time. Nozzle injection (Fig. 3.4d) promises a very short lag time of less then 3 seconds (ROCKWELL and AYERS, 1996). However, this configuration has the disadvantage of inappropriate mixing of the carrier with the chemical in the nozzle. This problem is not significant in central injection systems due to the long transportation time available for mixing.

3.1.2.3 Control of Herbicide Flow Rate

Direct injection of concentrated pesticides into carrier supply lines can be effective only if the flow rate can be measured and controlled accurately. Essentially, there are two methods for the positive metering of concentrated pesticides. One method uses an open-loop control system. This system uses positives driven pumps and metering valves without positive feedback, and the output is assumed to be a function of the pump speed or of the differential pressure across the metering valve or orifices. Wear or changes in pumping characteristics would remain undetected in this open-loop system. The second method of metering uses a flow meter sensor as part of a closed-loop control system. The concentrated chemical is pumped from the container through a control valve that is regulated by a controller. One of the inputs to the controller is a feedback signal from the flow meter.

The wide range of physical properties of spray chemical formulations makes flow rate control difficult as many flow measurement techniques are affected by liquid density and viscosity and have to be calibrated for different liquids. The range of viscosities of spray chemicals is large and difficult to define since some pesticides are formulated as non-Newtonian suspension concentrates. These would make the calibration of many types of flow meter especially difficult (FROST, 1990). GEBHARDT et al. (1984) investigated the performance of a drag-body flow meter in an injection sprayer for five commercial pesticides with various densities and viscosities over a range of temperatures. On the basis of their test results they suggested that drag-body flow meters must be calibrated for each pesticide due to viscosity effects and that pesticide temperatures must be kept in a range within which the flow rate can be accurately controlled.

The range of flow rates that a chemical injection system would have to meter is determined primarily by the position of the injection point, but also by the application rate and the forward speed of the sprayer. The relation between these variables is described by equation 3.8 derived from equations 3.2 and 3.3:

$$Q_a = \frac{A_a \cdot U \cdot W}{600} \tag{3.8}$$

where:

Q_a = Flow rate of chemical (l min^{-1})

A_a = Application rate of chemical (l ha^{-1})

U = Forward speed of machine (km h^{-1})

W = Working width (m)

Taking the extremes of the application rate (0.1 – 5.0 l ha^{-1}) and forward speed (4.0 – 16.0 km h^{-1}) variables, the resulting range of the chemical flow rate would have to measure and control could be approximately 200:1. The flow rate is between 0.002 and 0.400 l min^{-1} for injection into a boom section with 6 nozzles and between 0.00033 and 0.0667 l min^{-1} for injection into an individual nozzle. This is a very large range compared to 10 or 20:1 covered by most types of flow meter. It could be reduced by fitting systems with different capacities to different machine sizes and by using more than one metering system on each machine, with each system accommodating a portion of the overall flow range. The minimum required range for each of *n* systems with adjacent flow rate ranges would then be given by the following equation (FROST, 1990):

$$\frac{Q_{max}}{Q_{min}} = \left(\frac{A_{max}}{A_{min}} \cdot \frac{U_{max}}{U_{min}} \right)^{\frac{1}{n}} \tag{3.9}$$

where:

$Q_{min;\ max}$ = Flow rate of chemical (l min^{-1})

$A_{min;\ max}$ = Application rate of chemical (l ha^{-1})

$U_{min;\ max}$ = Forward speed of machine (km h^{-1})

This relationship provides no overlap between adjacent flow rate ranges and assumes that more than one system may be used during a particular spraying operation. This is undesirable because it does not take changes in forward speed into account. The required flow might exceed the capacity of the system, which would then have to be switched off so that an adjacent, larger system would have to be switched on. If systems with overlapping flow rate ranges were used, a single system could be selected for each application.

In conventional spraying practice the required dose rate for a given chemical does not usually change during application. It may therefore be possible to regard it as a constant during application and to use the variable flow rate from the metering system only for changes in forward speed. However, in site-specific herbicide application this is not feasible because of the varying flow rates of the carrier and/or the chemicals. Accordingly, it will be necessary to rely only on open-loop metering control and to reduce strongly the required range of dose rates and the variations in forward speed. Another argument for open-loop control is the response time of the injection system in combination with the frequency of dose rate changes. To reach the required chemical concentration promptly, the flow control actuator must be placed near the nozzles. This solution requires the use of active (valves, pumps) or passive (metering orifices) flow regulators with calibrated flow characteristics.

3.1.2.4 System Pressure and Plumbing Sizing

The system pressure is significant for the injection and mixing of the herbicides with the carrier at a mixing point. The pressure in the carrier lines must be lower than the outgoing pressure from the chemical metering pump/valve. Conventional spraying machines are designed so that the pressures at the nozzles are approximately equal, rendering the nozzle outputs uniform. Depending on the nozzle size and the required application rate and spray quality, the nozzle (system) pressure ranges from 1 to 8 bar. In common practice, the pressure at the flat fan nozzles does not exceed 4 bar due to spray drift.

The pressure drop between the pump and the nozzles must be kept as low as possible in order to reduce the pressure that the pump is required to develop. The spray liquid usually passes from the pump to a manifold, where it is distributed to a number of separate pipes/hoses, each feeding several nozzles in turn. Pressure drops in the plumbing are caused by friction losses in straight pipes and by minor (local) losses. With booms with a minimized pipe diameter, such pressure losses may cause the discharge rates (lateral distribution) to vary from nozzle to nozzle. The aim of minimizing pipe diameters is to reduce the lag time T_{lag}.

Friction losses are determined by the flow rate, the density and the viscosity of the liquid and by pipe sizing (length, diameter) and roughness. The pressure loss along a straight hose is calculated using Weisbach’s equation:

$$p_z = \lambda \frac{l}{d} \frac{\rho v^2}{2} \tag{3.10}$$

where:

p_z = Pressure loss (Pa)

l = Pipe length (m)

d = Pipe diameter (m)

ρ = Density of the liquid (kg m^{-3})

v = Fluid velocity (m s^{-1})

λ = Coefficient of friction losses (-)

Approximations for the friction coefficient λ in circular section tubes are as follows (ULRYCH, 2001):

- for laminar flow ($Re \leq 2300$)

$$\lambda = \frac{64}{Re} \tag{3.11}$$

- for non-developed turbulent flow ($Re > 2300$ and $Re < 500/k_r$)

$$\lambda = \left[-2 \log \left(0.27 \frac{k}{d} + \left(\frac{6.81}{Re} \right)^{0.9} \right) \right]^{-2} \tag{3.12}$$

- for fully developed turbulent flow ($Re > 2300$ and $Re > 500/k_r$)

$$\lambda = \left(2 \log \frac{d}{k} + 1.14 \right)^{-2} \tag{3.13}$$

where:

Re = Reynolds number of flow in the individual hoses (-)

k = Roughness coefficient (mm)

k_r = Relative roughness ($k_r = k/d$), (-)

The Reynolds number of the flow is given as:

$$\mathrm{Re} = \frac{v\, d}{\upsilon} \tag{3.14}$$

where:

ν = Kinematic viscosity of the fluid ($m^2\ s^{-1}$)

Minor losses are caused by changes in flow direction and pipe diameter (e.g. tee fittings at the boom manifold or regulation members). Minor pressure losses can generally be computed using the following formula (ULRYCH, 2001):

$$p_z = \zeta \frac{\rho\, v^2}{2} \tag{3.15}$$

where:

ζ = Coefficient of minor losses (-)

The coefficient of minor losses ζ depends on the geometry of the fitting parts used; it is usually provided by the manufacturer, or empirical values for different cases are listed in published tables (KRIZ, 1994). For the minimization of lag time it is only necessary to consider the minor pressure losses in tee junctions and the losses due to abrupt reductions in pipe/hose diameter.

The ζ value for the tee junction in a tee configuration of nozzles was assumed to be 1.25. This single value was obtained using an empirically derived relation for ζ, with the assumption that the flow was divided equally at the junction. Another method of determining minor losses is to calculate the pressure losses using equation 3.10 and to substitute the real pipe length l with an equivalent length (l_{eq} = 60 mm) (PACIGA, 1990).

Pressure losses due to a diameter change in a straight hose can be calculated using the following equation (ULRYCH, 2001):

$$p_z = 0.5 \left(1 - \frac{A_i}{A_{(i-1)}}\right)^2 \frac{\rho\, v^2}{2} \tag{3.16}$$

where:

A_i, = Area of hose at section i of the pipe (m^2)

A_{i-1} = Area of hose at section i-1 of the pip

3.1.2.5 Physical Properties of Pesticides to Be Applied

Apart from the requirements related to the injection metering system, there are some requirements on the physical properties of the chemicals to be injected which must be considered. One of these requirements is the ability of the system to operate with different chemical formulations. The possible formulations of spray chemicals available on the market today cover a wide spectrum. Emulsifiable concentrates (EC), soluble (liquid) concentrates (SL), suspension concentrates (SC) as well as wettable powders (WP) and water dispersible powders and granulates (SP, WG) are the most common formulations. The three latter examples (SP, WP and WG) are not usable for direct injection without appropriate pre-mixing with water. KUHLMAN et al. (1986) recommended chemical dilution of the injected materials in order to increase the flow rates in the chemical lines to the nozzles, thus improving the flow uniformity among the nozzles.

There is a wide range of physical and chemical properties of liquid formulations affecting flow rate control, response time, the quality of the mixture and the choice of components (construction materials). Specific gravity and dynamic viscosity are two of the most significant physical properties of pesticides. These two factors affect the Reynolds number and hence most flow-rate measuring techniques, which need to be calibrated for each different liquid. CHI et al. (1989) reported that the equation for calibration of flow rate could be either a single linear or quadratic relationship, depending on the degree of liquid viscosity of injected chemicals. GEBHARDT et al. (1984) presented results showing that the response of a flow meter can be directly linked to the chemical used and that with some flow meters and chemicals the accuracy can only be achieved by controlling the temperature of the pesticide. COCHRAN et al. (1987) found fluctuations up to 50 % in viscosity over ambient temperature ranges when testing some chemicals.

Dynamic viscosity η depends primarily on temperature. Fig. 3.5 shows two examples of this relation for different concentrations of an aqueous glycerine solution. Glycerine and glycerol-based polyethylene derivates are additives commonly used in many different pesticide formulations.

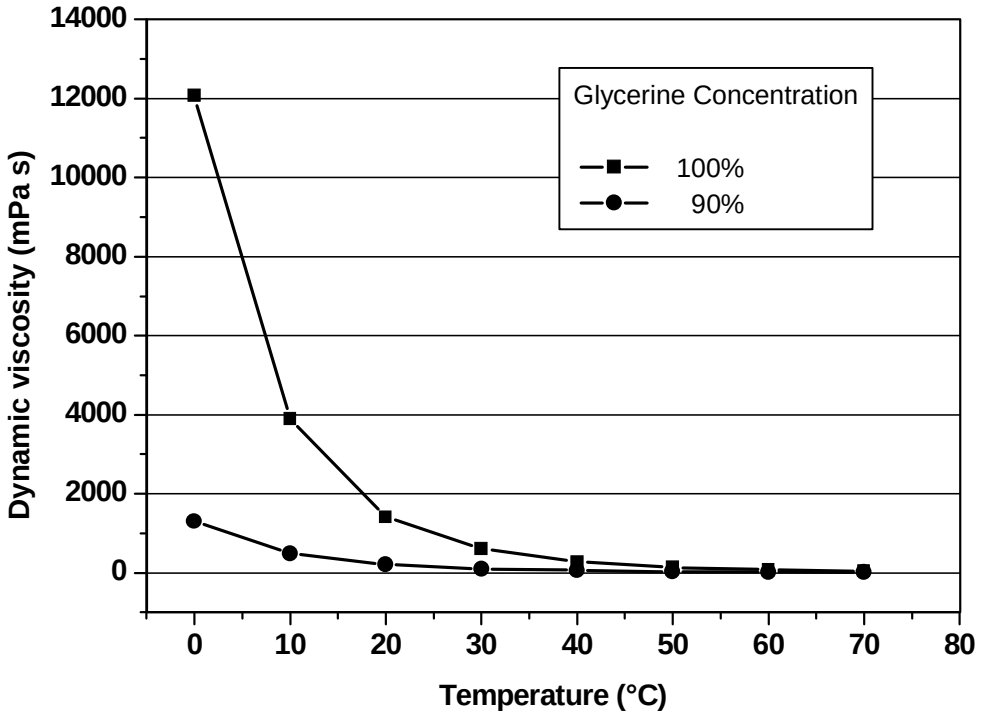

Figure 3. 13: Relationship between viscosity and temperature for solutions with different glycerine concentrations (adapted from STREETER, 1961)

Commercial liquid pesticide formulations have a wide range of viscosities, varying from below 1 mPa s to about 1000 mPa s. The viscosities of most common liquid pesticide formulations are below 100 mPa s (ZHU et al., 1998). From the data in table 3.1 it is evident that the viscosity ranges of pesticide products, are large and that they sometimes overlap. The viscosity range is in principle independent of the type of indication for which a product is used. Fungicidal, insecticidal and herbicidal ECs have the same viscosity range, which differs from that of SCs. In general, viscosity is a specific property of a product, and in the case of SCs it can vary between different batches of the same product (SCHWIEDOP, 2002).

Table 3. 3: *Range of dynamic viscosity* (BAYER A.G.; measured according to OECD method 114)

Formulation	Dynamic viscosity, (mPa s)
SCs (water based)	81.3 -185
ECs (solvent based)	13.6 -77.2
EWs (water emulsion)	Is either in the range of ECs or in the range of SCs, depending on the type of stabilisation chosen.

Compared with water, which is used as a solvent for solid formulations (WPs, WGs), pesticide agents also have significantly different liquid densities, with approximate specific gravity ranges of 0.6 to 1.5 g cm^{-3} (MC, 1996). Detailed information about the viscosity and density of common herbicide products is given in table 9.1 in appendix. The data were obtained from the relevant product specification sheets.

Some of the solvents used in pesticide formulations attack many of the materials and regulation parts of the sprayer that come into contact with the liquid. For example, organic solvents attack plastics and rubber. Moreover, some chemicals have a tendency to form crystals when they become dry, which can affect the performance of tanks, moving parts, seals and flow meters. AMSDEM and SOUTHCOMBE (1977) discussed the problems associated with chemical and physicochemical attack and noted that the severity of attack declines if the pesticide is diluted; however, over a longer period of time the cumulative effect can still be devastating.

A way of solving some of the problems associated with the pumping of pesticides, such as chemical attack and wear of moving parts, is to use suitable construction materials. SCHMITT (1983) evaluated the effect of chemicals on different elastomers. 40-day surveillance tests showed that only two commonly used elastomers, EPDM and FPN (known as Viton®), are resistant to swelling. Tests of similar duration were carried out with seals used for gear pump heads and sprockets. The use of corrosion-resistant steals from class number 1.4571 upwards was recommended highly.

Another way to reduce the negative impact of pure chemicals is to rinse all plumbing with clear water after application or to use an air pressure source to inject the pesticide.

3.1.2.6 Logistical Requirements

Logistical requirements relate mostly to the handling of concentrated chemicals during the whole spraying operation. After application there are concentrated pesticides left in the chemical tank and in the supply lines. Such residues can be under certain conditions stored and re-used later without risk of contamination. The design of a simple hydraulic system for the rinsing of the chemical lines of an injection-type sprayer must therefore be considered as well.

The traditional packaging of pesticides has been one of the barriers to the success of direct injection sprayers. The use of small 5 to 10 litres containers requires decanting into larger vessels. The minimal required volume of the chemical container depends on the application rates of the carrier and the herbicides and on the content of the carrier tank. If only average application rates (carrier $\approx$ 300 l ha^{-1}; herbicide $\approx$ 1.5 l ha^{-1}) are taken into account, then a chemical tank with a minimum volume of 15 litres is required for a sprayer with a carrier tank with 3000 litres. However, this relation is only valid for a single filling operation. For a sprayer that is filled with carrier several times during application it would be suitable to use a larger chemical tank. The development of closed transfer systems (e.g. Agro Super LINK, Bayer CropScience) has helped to simplify the handling of concentrates. Refillable containers (FELBER, 1993) along with water dispersible granules and other novel techniques of packaging are some of the ways forward.

Further concentrate and solution residues remain in the conveyor mechanism, e.g. in the chemical pumps or in the hydraulic accumulator, and in the supply lines. It is possible to transport residues of pure concentrate from the pipes (dead volume) back to the original container by means of three-way valves and reverse operation of the chemical pump or with the aid of a pneumatic system. The empty pipes/hoses can afterwards be rinsed with clear water. The remaining herbicide-carrier solution downstream of the injection point can be rinsed and then sprayed out on the field. One of the main purposes of direct injection systems is to reduce the amount of spray solution residues.

The volume of the spray solution in the lines depends on the position of the injection point (pipe length) and on the pipe diameter. Residue quantities are easy to estimate; Fig. 3.6 shows calculated volumes for different inner diameter and lengths.

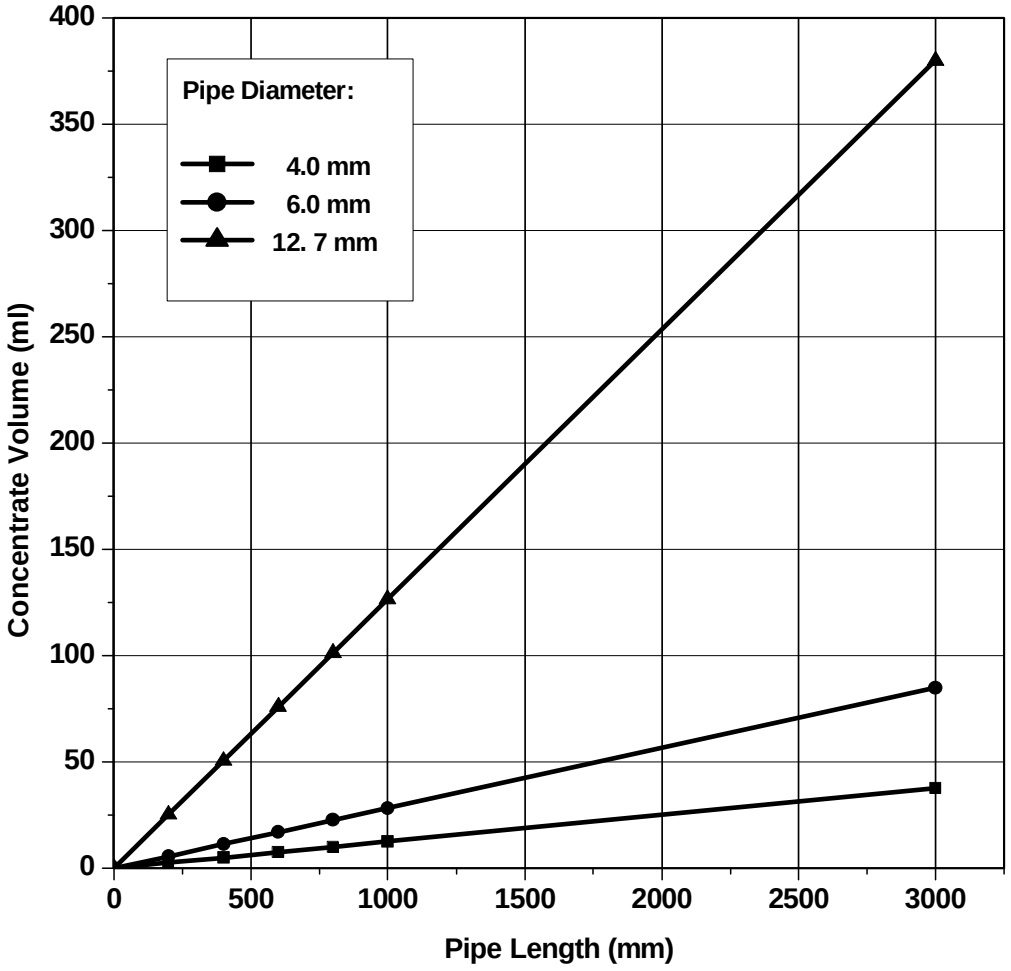

Figure 3. 14: Volume of concentrated residues in pipes with different inner diameters

It is evident that a system in which the concentrates are injected directly into the nozzles will have minimal spray residues in comparison with an injection system with a central injection point. On the other hand, nozzle injection requires the longest chemical supply lines. However, after emptying they need not be rinsed with as large a volume of water as is required for rinsing central injection systems.

3.2 The Proposed Direct Injection Systems

In the second phase, the individual requirements will be considered and several possible technical solutions will be proposed. As the result of a selection process an optimal technical design of a chemical injection system is expected. Figure 3.7 shows an example of a sprayer with integrated boom injection and weed detection systems. This design is based on a standard sprayer without chemical ejector, solution mixing system, solution tank rinsing and agitation system. The chemical line is parallel to the carrier (water) line up until the point of injection where both lines meet. The point of injection can be positioned arbitrarily depending on the application requirements. The weed detection sensors are mounted in driving direction directly on the sprayer boom in front of the nozzles. A 2.5 m long six-nozzle boom was chosen because it provides sufficient lateral resolution for the precision field grid.

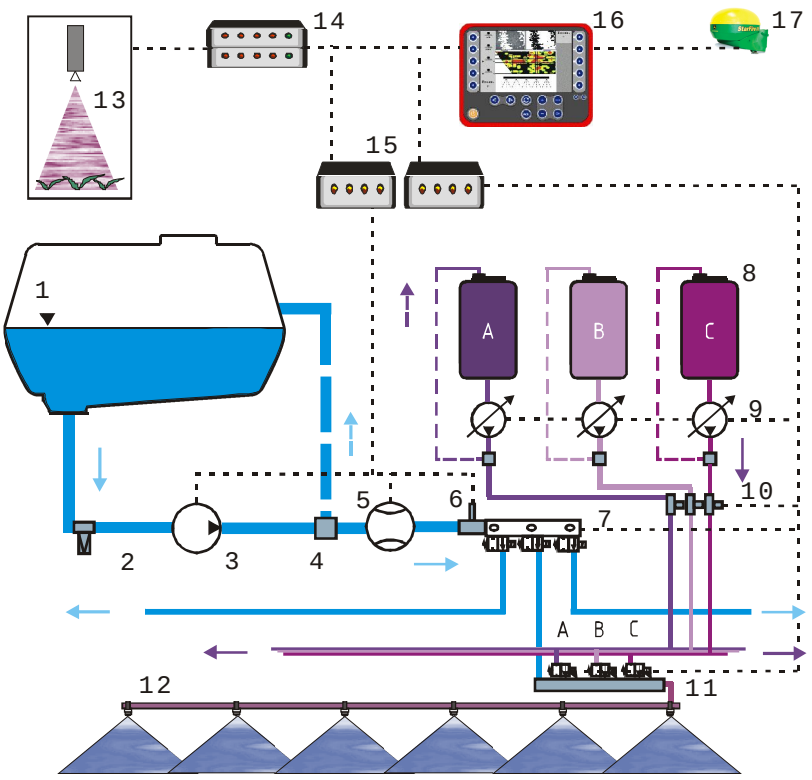

1 - Carrier tank
2 - Strainer
3 - Carrier pump
4 - By-pass valve
5 - Flow meter
6 - Pressure transmitter
7 - Section valves
8 - Chemical tanks
9 - Chemical pumps
10 - Pressure transmitters
11 - Proportional valves
12 - Boom Section
13 - Weed Sensor
14 - Sprayer computer
15 - Electronic power modules
16 - Display
17 - GPS receiver
18 - Board computer

Figure 3. 15: Scheme of a sprayer with direct injection system – a boom injection variant

Weed detection sensors (CCD cameras) are connected to a sprayer computer which controls all functions of the sprayer, e.g. carrier flow rate/pressure ratio, chemical flow rate/pressure ratio, speed, application rate and active section. The system can deliver and inject up to three different chemical products.

The crucial component of this system is the flow rate regulator. The selection of this control element has the greatest impact on the complete system. In principle, there are three control elements that can be used to control the chemical flow rate in the proposed design: a proportional control valve, a metering pump and a Venturi eductor. All systems mentioned have their relative merits, but some have major disadvantages. There are a few basic criteria, which integrate the defined requirements on the injection systems. The criteria can be used for an assessment of technical solutions for the flow rate regulators. The following assessment criteria were chosen:

- quality of control
- response time
- variations in flow rate and pressure
- construction volume
- mixture homogeneity
- ability to dose a wide range of herbicides
- dosing of multiple products
- reliability
- robustness
- acquisition costs

The use of solenoid valves with pulse width modulation makes it possible to control the chemical flow proportionally to the input control signal (voltage, current). The use of proportional valves makes it possible to achieve very accurate and sensitive regulation of the flow rate without any pulsations. The valves enable good coverage of a wide flow rate range while maintaining the required operational pressure range. This feature is defined as volume/pressure variation. The prompt reaction of the valves reduces the response time of the metering system to a minimum.

Another significant advantage of the valves is that they can be easily mounted anywhere throughout the boom length because of their compact size. Moreover, they can be adjusted easily into a set of valves for injecting multiple chemical products. The acquisition costs are generally lower than for a positive displacement pump. The rinsing and purging of pure chemicals from the nozzle supply lines is easily achieved by adjusting the valve into the open position. A disadvantage of the valves is the dependence of the regulated flow on the physical properties (viscosity, density) of the fluids flowing through the valve. The valves must be calibrated for each viscosity group of chemicals.

This negative feature can be eliminated by using a positive displacement metering pump. The constant stroke of the pump ensures a constant volume of injected chemicals without regard to their properties. However, it is just these strokes that cause pulsations which negatively affect the homogeneity (quality) of the mixture. It is generally possible to achieve a very good variation of flow rates and pressures by varying the rotational speed or stroke frequency of the pump. The pump response to a control signal and the successive achievement of a required pressure is slower than in solenoid valves. Moreover, the construction volume is normally larger than that of valves. For multiple-product dosing and for the positioning of pumps along the boom width, special pumps must be used (developed). The acquisition costs for a special injection pump without a drive-train can be very high in comparison with valves.

A distinctive feature of Venturi eductors is that the chemical flow rate depends on the carrier flow rate. The injection (ejection) of chemicals into the carrier at a required ratio is possible only under certain conditions which are given by the Venturi principle. In fact, this feature very much reduces the possible range of flow rates and hence the usability of this system in the injection of chemicals in common practice. The Venturi eductors does not maintain steady flow with daily or seasonal temperature changes and is unacceptable for accurate injection of chemicals with high viscosity. However, the construction volume is optimal for positioning eductors at each nozzle and for multiple-product dosing. As the system does not include any moving parts, it can be classified as relatively reliable. The response time of the system depends on the response of the carrier delivery system, which is generally very slow in comparison with the two systems mentioned above.

3.2.1 Assessment of Concept Variants of the Metering System

A list of assessment criteria was used to help make a decision about the selection of the most suitable flow rate regulation element. In table 3.2 the most relevant criteria are listed and assessed in accordance with the four-level VDI 2225 scale (VDI, 1998). A variant with the highest W_t technical rating is considered as the most suitable solution.

Table 3. 4: Assessment criteria for tracer flow rate control element

ASSESSMENT CRITERIA LIST - Tracer Flow Rate Control								
AIM: Objective selection of a control element for tracer flow rate control in direct injection systems.								
VDI 2225 Value Scale. Grades range from 0 to 4. **0 = unsatisfactory, 1 = barely satisfactory, 2 = satisfactory, 3 = good, 4 = very good**								
the weighting factor "g" is used if assessment criteria are not equal for all variants. **0 ≤ g ≤ 1**								
Concept Variants			**Proportional valve**		**Positive displacement metering pump**		**Venturi eductor**	
No.	**Criteria**	**g**	**P**	**P*g**	**P**	**P*g**	**P**	**P*g**
1	Quality of control (dosing accuracy)	1	3	3	4	4	2	2
2	Reaction time	1	4	4	3	3	2	2
3	Variation of flow rate and pressure	1	3	3	4	4	1	1
4	Construction volume	1	4	4	3	3	4	4
5	Mixture homogeneity	1	3	3	2	2	3	3
6	Ability to dose a wide range of herbicides (viscosity)	1	2	2	4	4	1	1
7	Multiple-product dosing	1	4	4	2	2	2	2
8	System rinsing	1	4	4	3	3	2	2
9	Reliability	1	3	3	3	3	3	3
10	Robustness	1	3	3	3	3	2	2
11	Costs	1	3	3	2	2	3	3
Max. Point No. P_{max} = 44		Σ		36		33		25
Technical Rating W_t				0.82		0.75		0.57
Rank				**1**		**2**		**3**

After assessment of the technical variants, a proportional valve was selected for flow rate control in the proposed direct injection system. This decision offers many different technical variants as regards minimal response times and good spatial resolutions of the sprayer. The following three configurations with different injection points were developed with the objective of experimentally determining the effect of the number of nozzles, of the size of the spray boom section and of the viscosity of the chemical on the response time of the proposed systems:

1. Boom injection system
2. Nozzle injection system
    a) with central flow control for a set of nozzles
    b) with flow control for individual nozzles

The boom injection system described in chapter 3.1.2.2 was proposed with the aim of reducing the number of valves used for flow rate control. Another motivation for utilizing that system was the spatial resolution of the weed detection cameras, which is about 3 m. An alternative to injection at one point in the boom section is to inject the herbicides into the carrier at each nozzle. Such a direct nozzle injection system requires additional plumbing to deliver the active ingredient to each nozzle. Two nozzle injection systems were proposed. The first system uses one control valve only for each section. This system has a common rail for a set of nozzles in a section. The chemical is injected immediately upstream of each nozzle through small metering orifices. The metering orifices were used to distribute the chemical flow equally into each nozzle. The third proposed system uses a proportional valve for each individual nozzle. All three configurations are described in detail in the methodological part of this study.

3.2.2 Lag Time Minimization Procedure

The plumbing design of boom sprayers with boom injection plays an important role in determining the lag times for changes in chemical concentration at the spray tip. To reduce the system lag time, the possibility of altering the on-boom hose diameters from the centre of a boom section to the furthest spray nozzle was considered in the analysis.

A computer program was written to enable the lag time to be minimized for a boom section with a given width, nozzle spacing, nozzle discharge coefficient, system pressure and maximum allowable differences between flow rates at different nozzles. In order to achieve a restriction to solutions that would be easy to realize, only a given set of hose diameters was considered. Possible plumbing arrangements were restricted to the symmetrical tee configuration illustrated in figure 3.8.

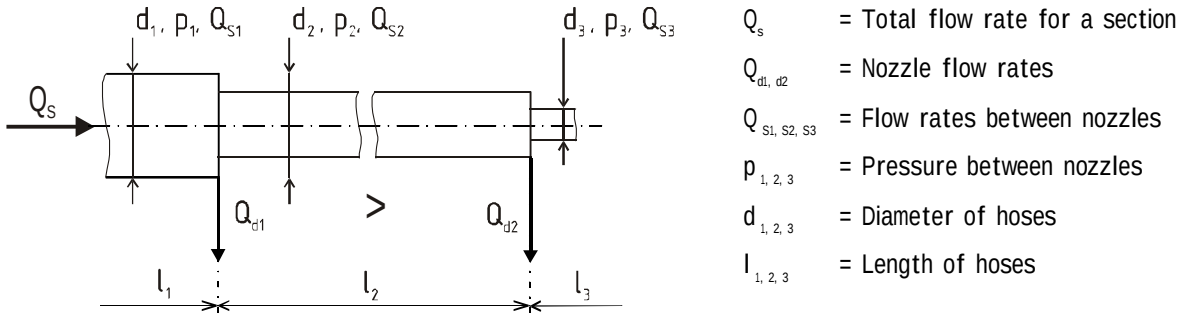

Figure 3. 16: Reducing of boom pipe diameter

The pressure losses along a straight hose were calculated according to the equation 3.10. Equations 3.15 and 3.16 were used to calculate minor pressure losses due to abrupt contractions in a hose pipe, for example from d_1 to d_2 in figure 3.8. The time lag minimization procedure was started by ascribing a pressure nozzle furthest form the point of injection in the centre of the boom section. The output of the nozzle was calculated from equation 2.2 ($Q_d = p_i^{0.5} / k$), where the coefficient k is calculated as follows (SARKER, 1997; WOZNIAK, 2003):

$$\frac{1}{k} = C_d \; A_d \; \sqrt{\frac{2}{\rho}} \tag{3.17}$$

where:

C_d = Coefficient of discharge of the nozzle

A_d = Area of discharge of the nozzle (m^2)

ρ = Density of liquid (kg m^{-3})

Various plumbing configurations with three different spray nozzle sizes (XR80015, XR8003, and XR8005, Spraying Systems Company), three system pressures (1.0, 3.0, and 5.0 bar) and four different hose diameters (4.0, 6.0, 8.0 and 12.7 mm) were considered. The program computed flow rate errors, pressure losses, and delay times for each spray tip. Based on the results, and the requirement that the spray tip discharge rate varies less than 5%, the most suitable plumbing configuration for reducing the time delay was selected.

4. Material and Methods

4.1 Materials Used to Simulate Herbicides

In assessing the effect of herbicide viscosity on response time and mixture uniformity, it is favourable to use substitute liquids such as oil or other highly viscous substances. Water-soluble glycerine can easily be mixed into solutions with the required viscosity grades. As the quality of the provided glycerine concentration products differs from batch to batch, it is necessary to measure the viscosity of the test solutions first. Ten glycerine solutions with different concentrations (ranging from 60 to 99 %) were obtained by mixing 99 % glycerine (Gustav Heess GmbH, Stuttgart) with tap water. Glycerine is a highly viscous liquid, and the viscosity of glycerine and glycerine solutions changes dramatically with changes in temperature (STREETER, 1961). The viscosity of the injection solution had to be measured at constant temperatures in order to maintain same conditions during the response time measurements.

4.1.1 Viscosity Measurements

Various types of viscometers can be used to measure the viscosity of Newtonian fluids. Glycerine solutions show Newtonian behaviour (MOTZIGEMBA et al., 2002). Viscosity can be measured by means of capillary, rotational, rolling and drawing ball viscometers. In this study, the viscosities of glycerine solutions at a constant temperature of 20 °C were measured using a Haake RotoVisco 1 (Thermo Electron Corp.) rotational rheometer. The viscometer consists of an inner and outer cylinder (double gap cylinder system DG 43). It uses a highly sensitive torque measuring system to ensure rapid response to changes in torque (Thermo Electron Corp. - user manual).

The sample solution was poured into the temperature-regulated interchangeable measuring cup (inner cylinder) covered by the outer cylinder. The outer cylinder was driven by a speed-controlled motor incorporated in the measuring head. The speed was controlled by an electric module which generated 50 fixed speeds in a geometric progression between 10^2 and 10^{-2} revolutions per minute.

The measuring principle is based on the determination of the shear stress τ by sensing the torque *T(r)* which is exerted on a cylindrical layer of liquid between the two cylinders at accurately defined speeds resulting from rotation of the measuring cylinder. The viscosity of Newtonian liquids is calculated on the basis of the shear rate (using torque and device constants) and the velocity gradient (dω/dx) using the following formula (GUYON et al., 2001):

$$\eta = \frac{\tau}{r\frac{d\omega}{dx}} \tag{4.1}$$

where:

η	=	Dynamic viscosity (Pa s)
τ	=	Shear stress (Pa)
r	=	Radius of cylindrical layer (m)
ω	=	Angular velocity (rad s^{-1})

The device constants were integrated in the measurement software RheoWin™ provided by the viscometer's manufacturer. Share stress τ (Pa), gradient speed (1/s), temperature T (°C) and dynamic viscosity η (Pa s) were recorded by means of this software.

For the calculation of the Reynolds number and for other flow dynamic calculations, e.g. of pressure losses, it is necessary to determine the kinematic viscosity of the test solutions. The kinematic viscosity is given by the following formula:

$$\nu = \frac{\eta}{\rho} \tag{4.2}$$

where:

ν	=	Kinematic viscosity (m^2 s^{-1})
η	=	Dynamic viscosity (Pa s)
ρ	=	Liquid density (m^3 kg^{-1})

The densities of the tested glycerine solutions were determined by weighing exact volumes of the solutions. The exact metering of the volumes was effected with a glass pycnometer with a volume of 50 ml.

4.2 Laboratory Model of Direct Injection System

A test bench was assembled to study the accuracy and time response of the proposed direct injection systems. A schematic of the test bench is shown in figure 4.1. The objective was to design a variable system that can be used with various technical configurations of the injection system. The test bench was constructed for one boom section only, with the aim of simulating the minimum working range of a regular field sprayer.

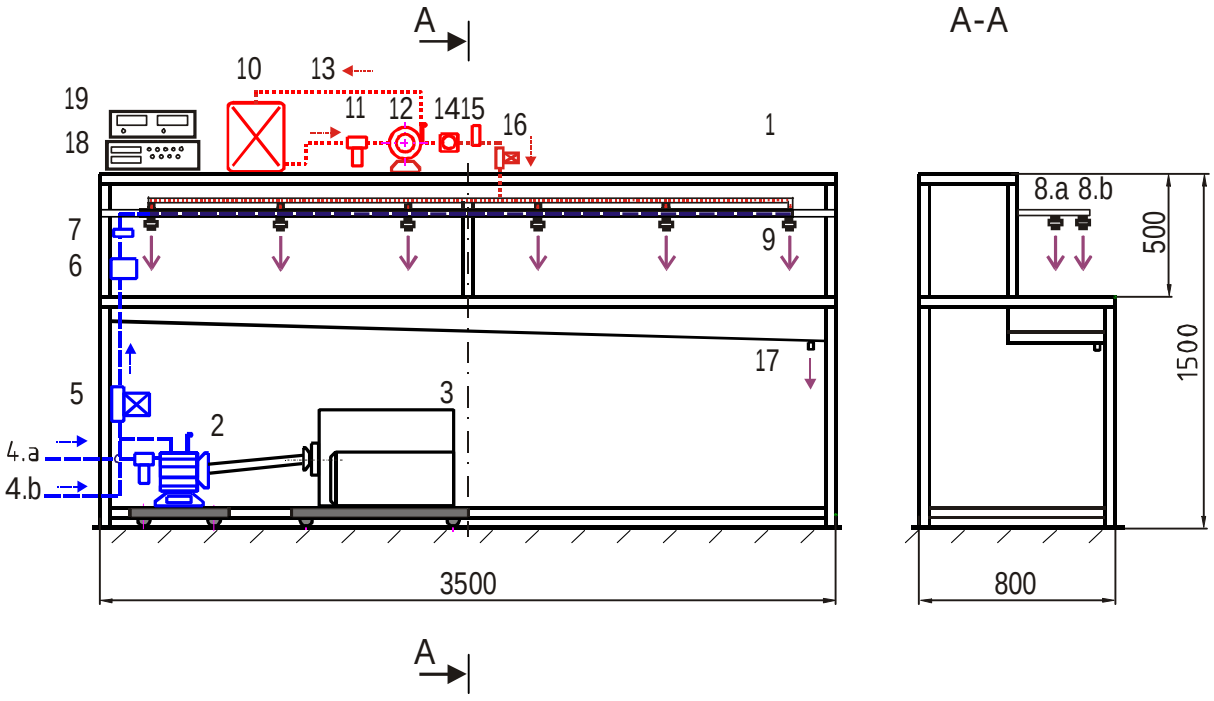

1 - Frame
2 - Carrier pump with strainer
3 - Electric motor
4 - Carrier supply
a - from the tank
b - from the water tap
5 - Pressure regulation valve
6 - Flow meter
7 - Pressure transmitter
8 - Boom assembly
a - Boom injection
b - injection into nozzles
9 - Nozzles
10 - Tracer tank
11 - Strainer
12 - Delivery pump
13 - Bypass line
14 - Flow meter
15 - Pressure transmitter
16 - Injection valve
17 - Outlet solution drain

Figure 4. 28: Test bench

At the injection point, the test bench is divided into two parts. The first one, upstream of the injection point, is the basic supply system, which includes one carrier line and one tracer line. These two parallel supply lines are joined together at the injection point. The second part of the test bench is the mixing line downstream of the injection point, where the solution of carrier and tracer is mixed. The mixing line compounded from a boom, tee junctions, spray nozzles and additional supply lines is adjustable depending on the injection system and/or the injection position being tested. As it was already mentioned (see chapter 3.2.1) three injection systems with different injection points were investigated:

1. Boom injection system
2. Nozzle injection system
    a) with central flow control for a set of nozzles
    b) with flow control for individual nozzles

A schematic diagram of the basic hydraulic supply system of the injection system implemented in the test bench is shown in figure 4.2. The hydraulic system was designed as an open circuit with an aim to avoid a back-contamination of the clear carrier by already used solution of tracer and carrier. The hydraulic system can deliver and mix only one carrier and one tracer at a time. Tap water was used as carrier in all experiments. Instead of mostly toxic chemical protection agents, different basic solutions were used as tracers. Depending on the type of test and the instrumentation used, salt, colorant or aqueous glycerine solutions were used as tracers.

In principle, the carrier supply line is identical to the supply lines of standard sprayers. An AR 120bp (Annovi-Reverberi) sprayer diaphragm pump (3) coupled with a 5.5 kW AC motor supplied the carrier flow from a carrier tank (1) through a strainer (2) with a 50 mesh. Then the carrier flowed through tubing with a 12.7 mm inside diameter to a manifold and to a 3 m long boom section (14). A UCM pressure relief valve (Annovi-Reverberi) (4) in the carrier line was coupled with the manifold. The carrier flow rate was set by selecting nozzles (15) and adjusting a two-way pressure regulation valve (5) in conjunction with a pressure relief valve (4).

A 38410-EM-05-1/2 (Spraying System Co.) magnetic-induction flow meter (6) was installed vertically, to avoid air bubbles, on the pressure side of the carrier pump before a pressure sensor (7) in order to obtain accurate readings of the carrier flow in the system. The static pressure in the carrier line was measured with a PTMv (Armaturenbau GmbH) absolute pressure transmitter. The pressure at the nozzles is normally determined as the relative (gauge) pressure, meaning the sensor was calibrated so that the resultant pressure value was relative to ambient atmospheric pressure.

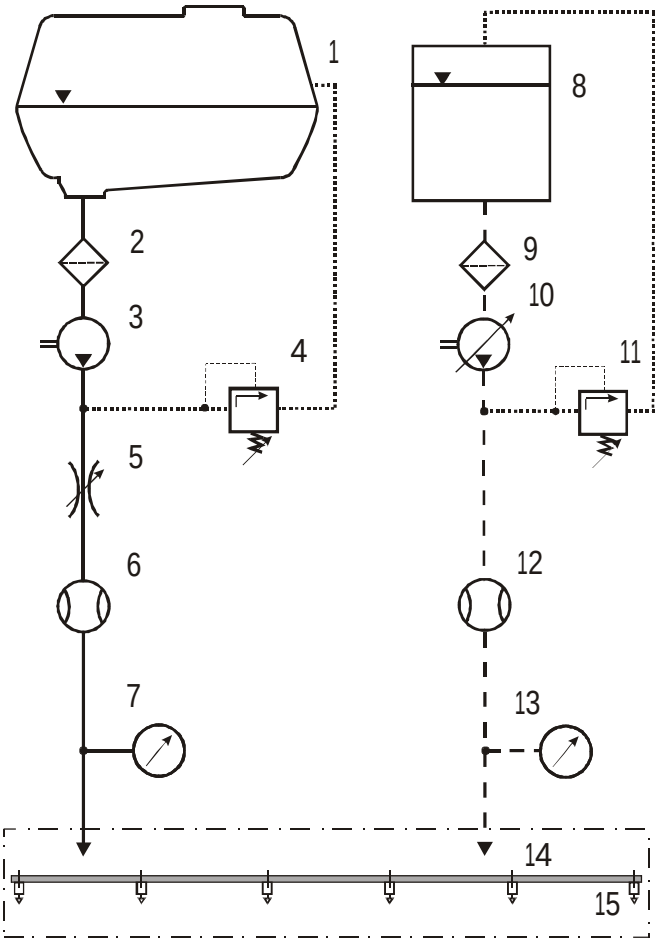

1 - Carrier tank
2 - Strainer
3 - Carrier pump
4 - Pressure relief valve
5 - Pressure regulation valve
6 - Flow meter
7 - Pressure transmitter
8 - Tracer tank
9 - Strainer
10 - Delivery pump
11 - Pressure relief valve
12 - Flow meter
13 - Pressure transmitter
14 - Boom assembly
15 - Nozzles

Figure 4. 29: Basic hydraulic supply circuit of the test bench

The tracer delivery line, which is parallel to the carrier line, begins at the tracer tank (8). A chemical pump (10) coupled with a strainer filter (9) (50 mesh) on the suction side and a pressure relief valve (11) on the pressure side supply the tracer from the tank to the injection point. Two types of chemical pumps with different performances were used and tested for the injection systems. The first one was a P- Series PDS.38PPPV1 (Tuthill Co.) metering gear pump with a 12 V DC motor driven by a laboratory power supply. The second one was an AR 202 (Annovi-Reverberi) diaphragm pump coupled with a 0.45 kW AC motor. Both pumps had their own pressure relief valves, through which the rejected volume of active ingredient was directed into the by-pass.

Two measurement methods, one direct and one indirect, were used for the determination of tracer flow rates. The first method used an FCH-PP (B.I.O – TECH) wheel flow meter based on Hall effect sensing (12). The second method used a DDS 332 (SIKA Dr. Seibert & Kühn GmbH & Co.) pressure transmitter to measure the differential pressure across a capillary tube. This method can be used to measure small volumes of active ingredient at the high frequency (1 kHz) needed for real-time measurements. A custom capillary flow meter was used because of the specific requirements of response time measuring. The development and calibration of the capillary flow meter will be described in chapter 4.2.3.4. The use of these two flow sensors depends on the kind of measurement carried out and the injection system configuration to be tested.

The tracer flow rate was regulated by means of a type 6022 00-A00 8 NC (Bürkert GmbH) 2/2-way proportional solenoid control valve. This type of valve was used for all three configurations. The pressure in the tracer line was measured with a DMU (Paul Rüster & Co. GmbH) pressure transmitter (13) similar to the one used in the carrier line. Additionally, two analogue pressure gauges with measurement ranges from 0 to 10 bar were used for the visual control of pressure and pressure drops in different positions of the carrier and tracer line. The positions of the pressure sensors and the regulation valve in the tracer line also depend on the kind of measurement carried out and the injection system configuration to be tested.

4.2.1 Boom Injection System Test Assembly

In contrast to injection systems with a central injection point for all boom sections upstream or downstream of the carrier pump, the boom injection configuration is a decentralized system. The hydraulic system supplied the tracer to the injection point in the middle of the boom section (tee configuration) and/or at the end of the boom section (straight configuration). For the test bench tee configuration was chosen (Fig. 4.3a).

a)

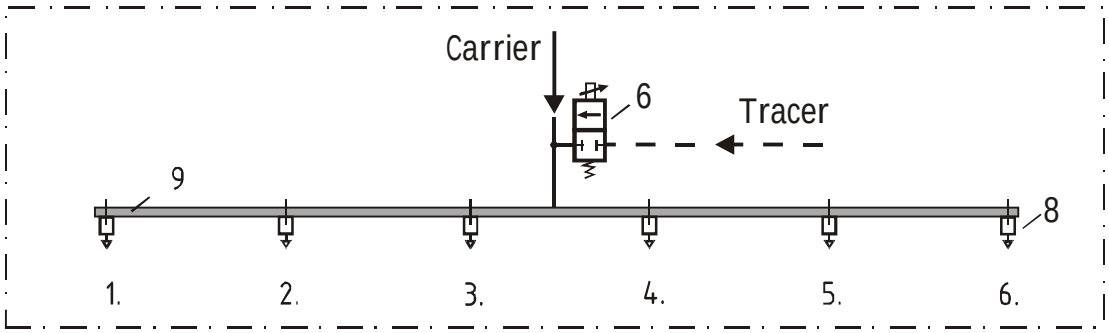

b)

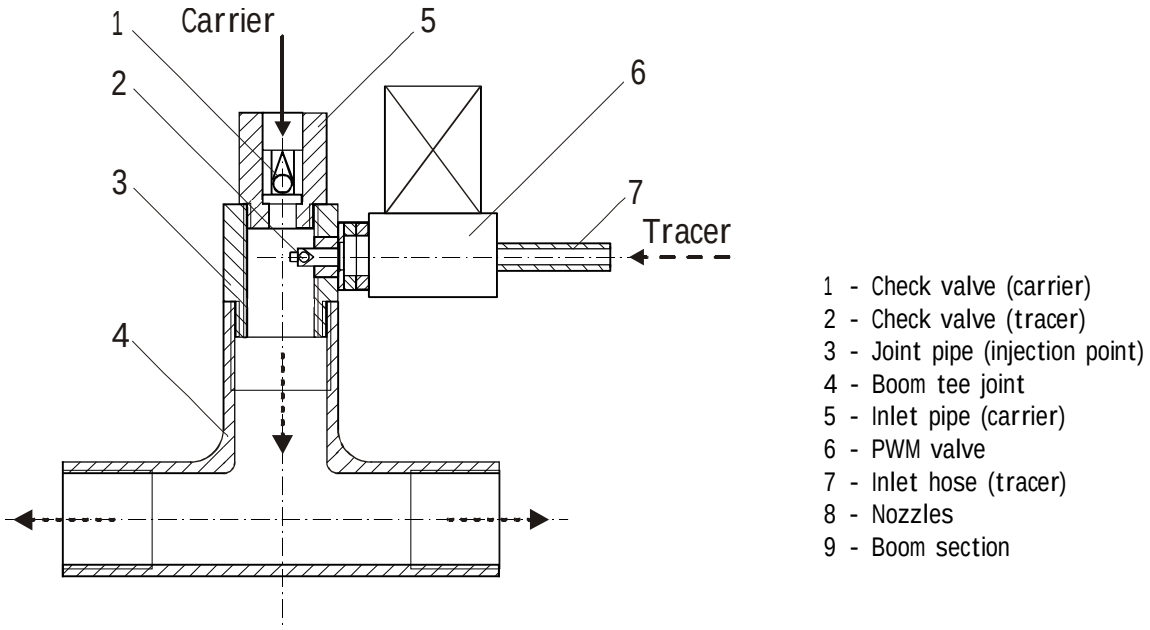

Figure 4. 30: Direct injection system with injection for one boom section (tee configuration)

The carrier and tracer lines were connected by means of one tee joint (4) to the 2.5 m long sprayer boom pipe (9) with 6 nozzles (8) spaced 50 cm apart. The nozzles had an 8079-PP-50 (Spraying System Co.) check valve strainer in the standard nozzle body. The same check valve (1) was used in the carrier inlet of the tee junction (5). For the tracer supply line a C 855 UF (LEE GmbH) check valve (2) with a cracking pressure of 0.14 bar was chosen. These two valves were built into the inlets of the tee junction in order to avoid unwanted ingression and mixing of both liquids before the beginning of injection. To ensure appropriate mixing of tracer and water, a Quadro® 8.8 x 8 (Sulzer GmbH) static mixer was placed in the joint pipe between the injection point and the bottom of the tee (not displayed in figure 4.3b).

The tracer flow was controlled directly by means of a proportional valve mounted immediately upstream of the tee junction as shown in figure 4.3 b. The wheel flow meter was employed for the calibration of the proportional valve. For the monitoring of the flow rate by means of response time measurements, the capillary flow meter was used in combination with the wheel flow meter. The pressure in the tracer supply line was sensed with a pressure transmitter positioned upstream of the proportional valve.

According to the results of the lag time minimization procedure described in chapter 3.2.2, various boom plumbing configurations with three different hose inner diameters of 6.0, 8.0 and 12.7 mm respectively were tested. The dimensions of the plumbing configuration are shown in figure 4.4.

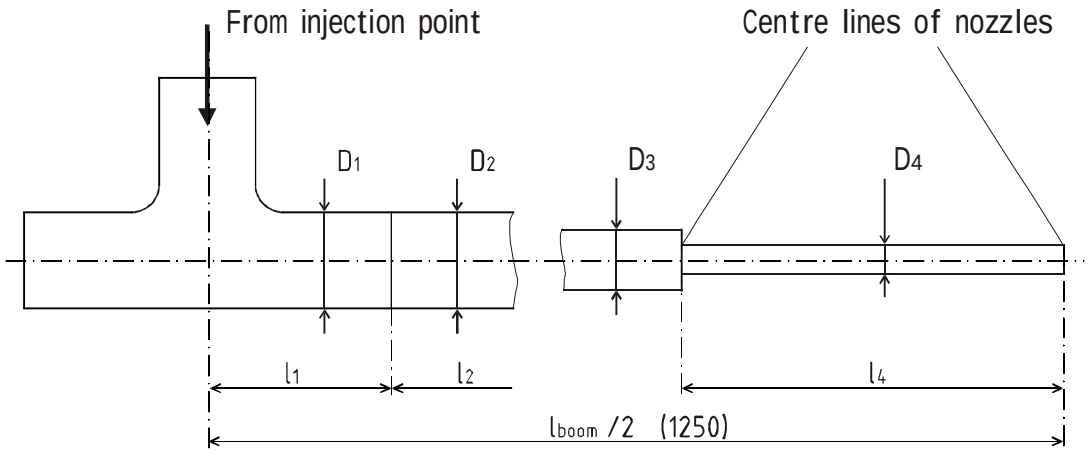

Figure 4. 31: Dimensions of tee configuration

The nozzle bodies were connected with hoses by means of reduction hose shank adapters. The distance between the nozzles l_4 was 500 mm. The hose length from the boom centre to the first nozzle (l_1 + l_2) was 250 mm. Two tees with different IDs (hose inner diameters) of 8.0 and 12.7 mm were used in the centre of the boom. The following plumbing configurations were constructed (IDs are listed in order from the d_1 to d_4): 12.7 - 12.7 - 12.7 - 12.7; 8.0 - 8.0 - 8.0 - 8.0 and 8.0 - 8.0 - 6.0 - 6.0.

4.2.2 Direct Nozzle Injection Test Assembly

Two configurations of the direct nozzle injection (DNI) system were set up and tested. One was for injection into a whole set of nozzles (Fig. 4.5a), and another was for injection into an individual nozzle (Fig. 4.6a). The main difference between these two configurations is the distance between the nozzle and the tracer flow regulation valve. In the first configuration, only one central regulation valve was used for the whole set of nozzles on the test boom section. The outermost nozzle was positioned 1.5 m from the centre of the boom. In the second configuration, the valve outlet was coupled to the spray nozzle body. Thereby, the dead volume of tracer in the supply tubes was minimized and, hence, the change in concentration at the nozzle could be reached quickly.

4.2.2.1 Injection into a Set of Nozzles

A six-nozzle DNI spray boom was constructed as shown in figure 4.5a, with each nozzle conforming to the arrangement shown in figure 4.5b. The tees (12) were made of a plastic tube and a branch connected together by using a nut (4). The nut was fitted with a small C 558 UF (Lee GmbH) check valve (3). This valve has the same cracking pressure, namely 0.14 bar, as the check valve used in the boom injection system. The check valve prevented any mixed fluids from travelling in the wrong direction back to the tracer line. The tee junctions were connected to the 2.5 m long spray boom pipe (1) of a test bench (straight configuration) by means of a 25775-NYB (Spraying System Co.) nozzle body on the inlet of each tee. Each of these nozzle bodies contains an 8079-PP-50 (Spraying System Co.) nozzle check valve strainer (2). The branch of each tee consisted of a housing cap (10) containing a flow regulator (metering orifice) (11) and a rubber sealing (9) held in position with a hollow screw (8). The screw was connected with a tracer supply hose (7).

Six such nozzle assemblies were installed on the boom at intervals of 50 cm and connected by means of a hose with an inner diameter of 4.0 mm. The tracer was injected immediately upstream of the nozzle through the metering orifice and the check valve. The distance between the injection point and the nozzle outlet was 58 mm. CP 4916-8; -10; -12; -16; and -20 (Spraying System Co.) flow regulators were used as orifice plates.

a)

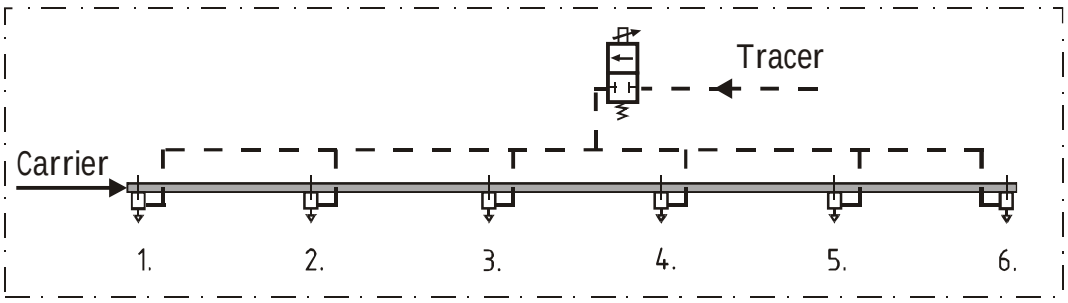

b)

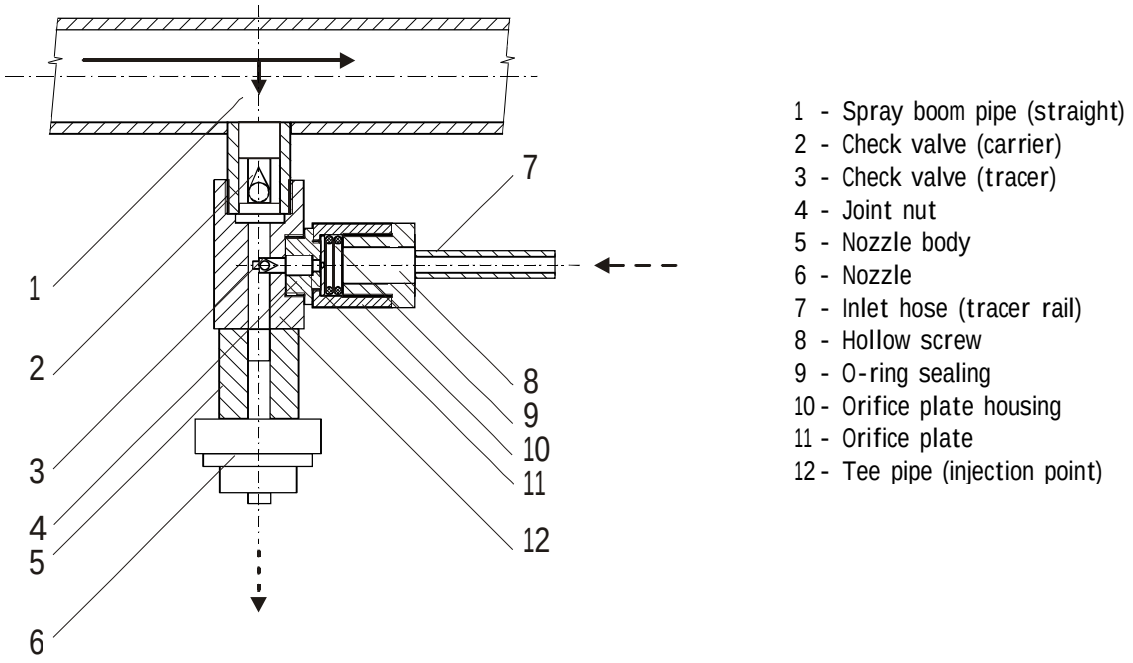

Figure 4. 32: Direct nozzle injection system with injection into a set of nozzles

Six similar orifices were selected for installation in the nozzle injection system to provide uniform flow rates along the boom. The proportional regulation valve was used to control the differential pressure across the orifice plates and, hence, to obtain varying spray nozzle discharge concentrations.

Before use in the injection system, the orifice plates were calibrated and tested with regard to flow performance at differential pressures from 0.5 to 5.0 bar (see chapter 4.2.3.3). During the calibration tests the injection pressure was monitored by two pressure sensors before and behind the proportional regulation valve. During the response time measurements only one pressure sensor was placed before the inlet of the valve in order to avoid unnecessary dead volume in the tracer supply line. Both flow meters were placed before the regulation valve and used only in the calibration tests.

4.2.2.2 Injection into Individual Nozzles

The system of injection into individual nozzles is shown in figure 4.6 a. The proportional regulation valves were placed immediately upstream of the tee branch. For injection into the individual nozzles the same tee nozzle injection systems as the ones described in the previous chapter were used. The branch of the tee arrangement connected with the inlet of the tracer line (6) was designed so that a proportional regulation valve (7) can be mounted directly on the orifice plate housing (8). This arrangement is shown in figure 4.6b. The tracer flow rate was controlled by means of orifice plates and a proportional regulation valve in the same way as in the system with injection into a set of nozzles. The capillary flow meter in combination with the wheel flow meter was used for monitoring the flow rate during the response time measurements. The flow meters and the pressure sensor were placed before the regulation valve only for the calibration tests. For the response time measurements one proportional regulation valve was used in three different positions, i.e. in the first, third and fifth nozzle position on the boom.

a)

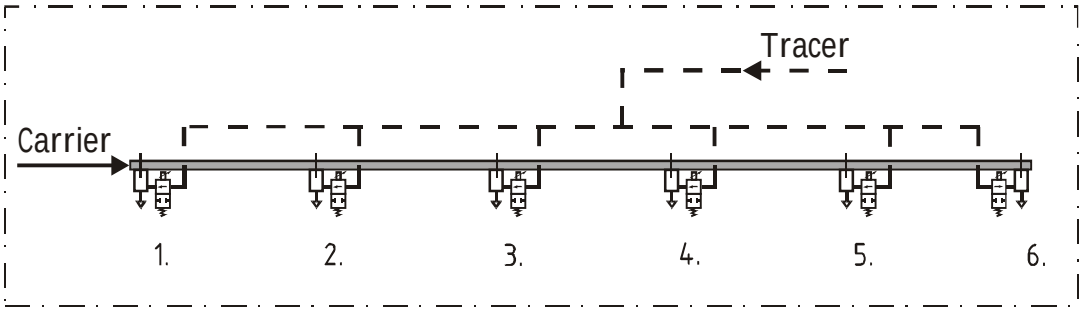

b)

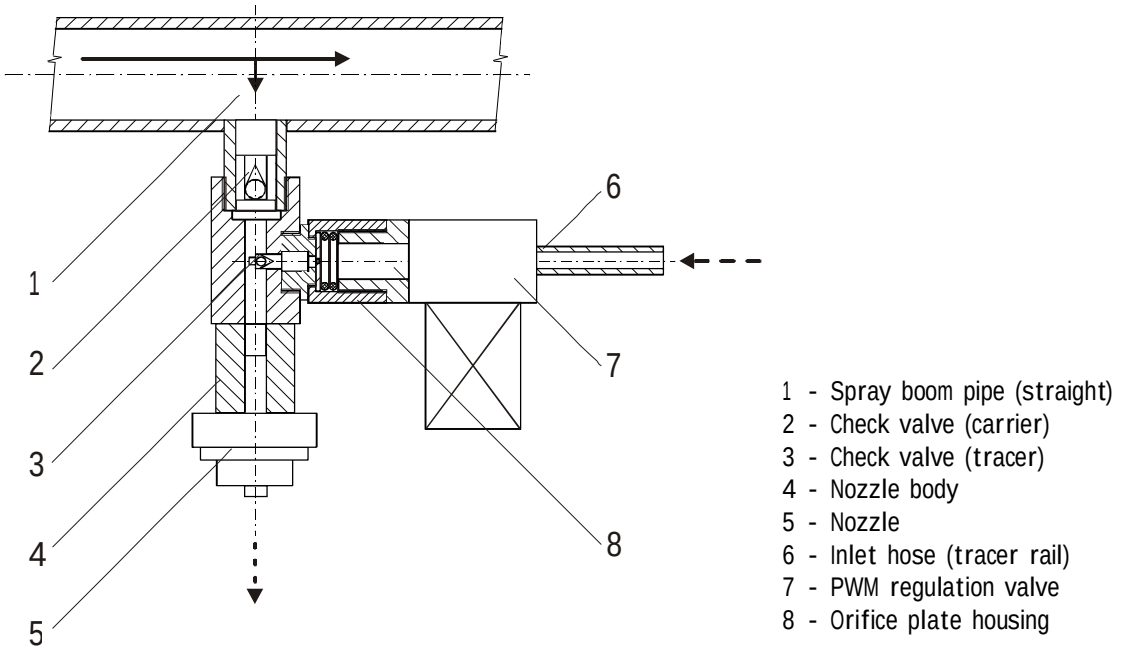

Figure 4. 33: Direct nozzle injection system with injection into an individual nozzle

4.2.3 System Components

For the required application rate (mixing ratio between carrier and tracer) to be reached, the carrier and tracer flow rates must be controlled and monitored accurately. The main flow regulation components of the injection system, i.e. the tracer supply pumps, the regulation valve, the metering plates, the spray nozzles and the control and measurement system will be described in the following chapters along with the calibration procedures for all flow regulators.

In addition, a capillary flow meter was developed and calibrated for the monitoring of the tracer flow rate. The capillary flow meter was used for response time measurements, as well as, for the calibration of the proportional valve.

The technical specifications of all components and of the measurement instrumentation used for the response time measurements are given in tables 9.2 and 9.3 in the appendix.

4.2.3.1 Tracer Supply Pump

Two pumps were tested and used for the delivery of the tracer to the injection point. The first pump was a P series PDS.38PPPV1 (Tuthill Co.) positive displacement gear pump. The second pump was an AR 202 SP (Annovi-Reverberi) two-diaphragm pump. This pump has a higher delivery capacity then the first one. The effect of different pumping capacities on response time was studied.

The gear pump was originally designed as an accurate metering pump for dosing aggressive chemicals and highly viscose fluids. The pump is self-priming and designed for a range of viscose fluids from 0.3 to 1000 mPa s. The pump was coupled with a 12 V DC motor driven by a laboratory power supply. The maximum nominal pump revolutions were 4000 min^{-1}; combined with the small volume of 0.38 ml delivered per revolution, it provides an almost pulseless flow and a maximum delivery rate of 1.445 l min^{-1}, which covers the required range of delivery flow rates for one boom section.

The pump was calibrated by monitoring its revolutions by means of an optical counter.
The differential pressure was determined by means of a pressure sensor (4). A pressure relief valve (3) was used only for filling the pump; during calibration it was closed. The flow rate of the tracer (water 20° C) was measured by means of a wheel flow meter (6) placed behind a pressure regulation valve (5). In parallel, the flow rate was measured by the weighing of samples on digital scale. The samples were collected during a sampling period of 1 minute. Average flow rates were calculated on the basis of ten iterations. The test setup, which was used for the calibration of both pumps, is shown in figure 4.7.

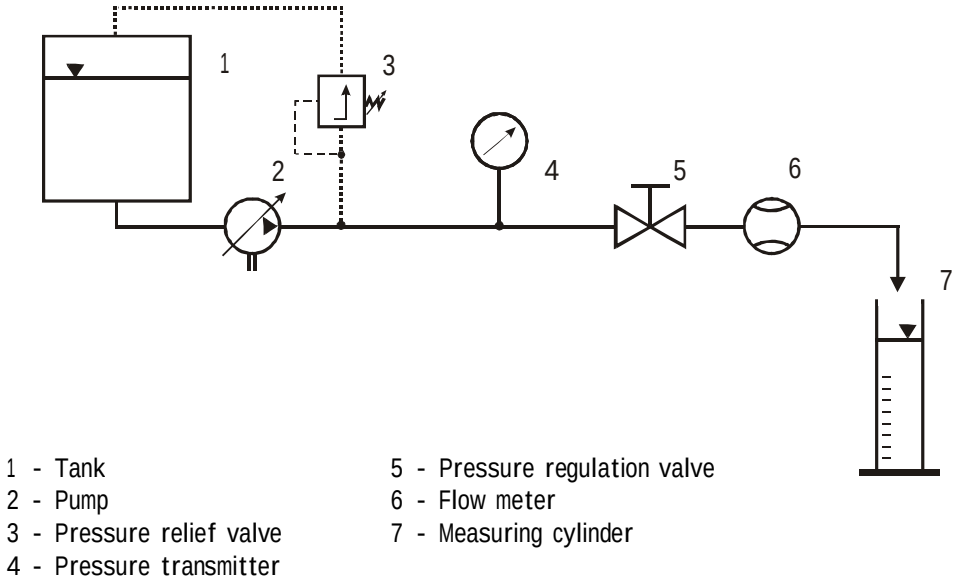

Figure 4. 34: Test setup for pump calibration

The AR 202 SP (Annovi-Reverberi) semi-hydraulic two-diaphragm pump is a small sprayer pump used mainly for the application of chemicals in the garden. The pump was coupled with an external electromotor through a cardan shaft. Its nominal revolutions were in a range form 450 to 650 min^{-1}. With a maximum delivery pressure of 25 bar, the pump has a maximum delivery rate of 19.9 l min^{-1}. The pump was calibrated by monitoring its revolutions by means of a revolution counter coupled with the electromotor shaft. The flow rate was measured by means of a magnetic-induction flow meter (which was also used for the measurement of the carrier flow rate).

For a comparison of the dynamics of both pumps the ratio between pump displacement V_p and revolutions can be used. The volume per revolution delivered by the diaphragm pump was 32.0 ml rev^{-1} at a pump speed of 450 rev min^{-1} and a differential pressure of 0 bar. The gear pump is able to deliver about 0.36 ml rev^{-1} at the same differential pressure and at a higher pump speed of 3500 rev min^{-1}. The theoretical pump torque acting inside the pump and generating the pressure on the fluid in the piping system was calculated as follows for a differential pressure of 10 bar and at the above mentioned number of revolutions:

$$T_p = \frac{\Delta p \, Vp}{2 \cdot \pi} \tag{4.3}$$

where:

T_p = Pump torque (N m)

V_p = Pump displacement (ml rev^{-1})

Δp = Pressure differential across the pump (MPa)

The resulting pump torques are 4.14 N m for the diaphragm pump and 0.057 N m for the gear pump. The fluid power produced by the diaphragm pump is 0.2 kW, which is almost ten times that of the small gear pump (0.019 kW). These values allow the conclusion that the diaphragm pump is more powerful and has better dynamic properties which enable it to achieve a steeper increase of pressure and hence its faster compensation in the pipe lines after the beginning of pumping or injection.

4.2.3.2 Proportional Regulation Valve

A type 6022 00-A00 8 NC, (Bürkert GmbH) 2/2-way direct-acting proportional solenoid control valve (Fig. 4.8) was used to control the tracer flow in all three direct injection configurations. This proportional solenoid valve consists of a basic valve and a plug-on electronic control unit (type 1049). The valve is controlled by a standard input signal of 0-10 V which is converted into a pulse width modulation (PWM) signal by means of control electronics. The opening of the valve can be continuously varied using the PWM signal. The valve has a relatively short setting time of 50 ms when opening form 10 to 90 %. The maximum allowed system pressure for this valve is 16 bar.

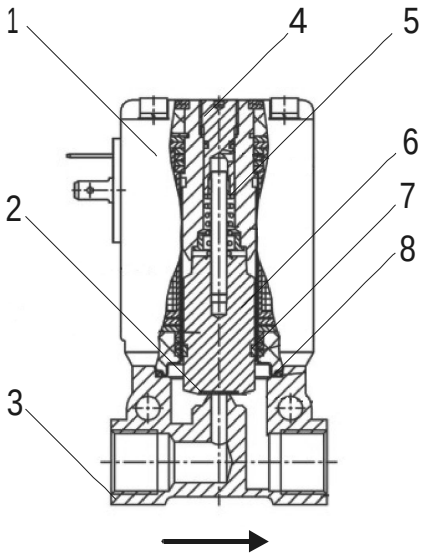

1 - Coil
2 - Plunger
3 - Valve body
4 - Stopper with adjusting screw
5 - Return spring
6 - Plunger
7 - Glide ring
8 - O-ring

Figure 4. 35: Proportional solenoid control valve (adapted from BÜRKERT GmbH)

For the rating and selection of the control valve, the flow factor K_v must be calculated for actual operating data (flow rate, differential pressure) and liquid's parameters. A distinction must be made between the maximum load $K_{v\ max}$ (maximum quantity Q_{max}, minimum differential pressure Δp_{min}) and the minimum load $K_{v\ min}$ (Q_{min}, Δp_{max}). K_v is a reference variable that is defined as the quantity Q in $m^3\ h^{-1}$ of cold water (+5 to +30 °C) flowing through the valve at a differential pressure of 1 bar at stroke s. The K_v value for liquids is calculated as follows:

$$K_v = Q\sqrt{\frac{\rho}{\Delta p_{12} \cdot 1000}} \tag{4.4}$$

where:

Q = Volumetric flow rate ($m^3\ h^{-1}$)

ρ = Density of the liquid ($kg\ m^{-3}$)

Δp_{12} = Pressure differential at the valve (bar)

For liquids with viscosities greater than 22 cSt, K_v is modified according to the following formula:

$$K_{vx} = K_v \cdot C \tag{4.5}$$

where C is the viscosity correction factor calculated by means of the formula:

$$C = \frac{\upsilon\sqrt{K_v}}{200 \cdot Q} + 1 \tag{4.6}$$

where:

K_v = Flow factor (l min^{-1})

ν = Kinematic viscosity of liquid (m^2 s^{-1})

Q = Volumetric flow rate (l min^{-1})

After calculation of the K_v (K_{vx}) values, the K_{vs} value must be determined so that a suitable valve can be selected from the manufacturer's catalogue. K_{vs} is the quantity at stroke *s* = 100 % (valve fully open, control signal =10 V) and is defined as the 1.25-fold of $K_{v\,max}$.

For the maximum required chemical flow rate for one boom section (300 ml min^{-1}) is the resulting K_{vs} value for water 0.018 m^3 h^{-1}. For viscose liquids (aqueous glycerine solution) with a maximum required viscosity of 162 cSt (≈200 mPa s) and a density of 1.2 kg m^{-3} the K_{vs} value is 0.045 m^3 h^{-1}. However, for most response time measurements with highly viscose solutions the maximum flow rate will not be required. Higher flow rates can be provided at higher differential pressures (>1 bar). Because of these two facts, the valve was selected for water-salt solutions only. The K_{vs} value of the selected valve is 0.020 m^3 h^{-1}. An appropriate valve for this K_{vs} value has a nominal orifice diameter of 0.8 mm.

The valve characteristics can be determined on the basis of the tracer flow rate and the pressure difference across the valve. These two parameters were measured with the test setup shown in figure 4.9. The valves (3 and 7) were used to set differential pressures in a range from 0.5 to 5 bar. The tracer flow rates (water and aqueous glycerine solutions with dynamic viscosities of 60, 109 and 219 mPa s at 20° C) were measured with the wheel flow meter (8). In parallel, the flow rates were measured by weighing the samples with the digital scale.

The samples were collected during a period of 1 minute. The average flow rates were calculated on the basis of four iterations.

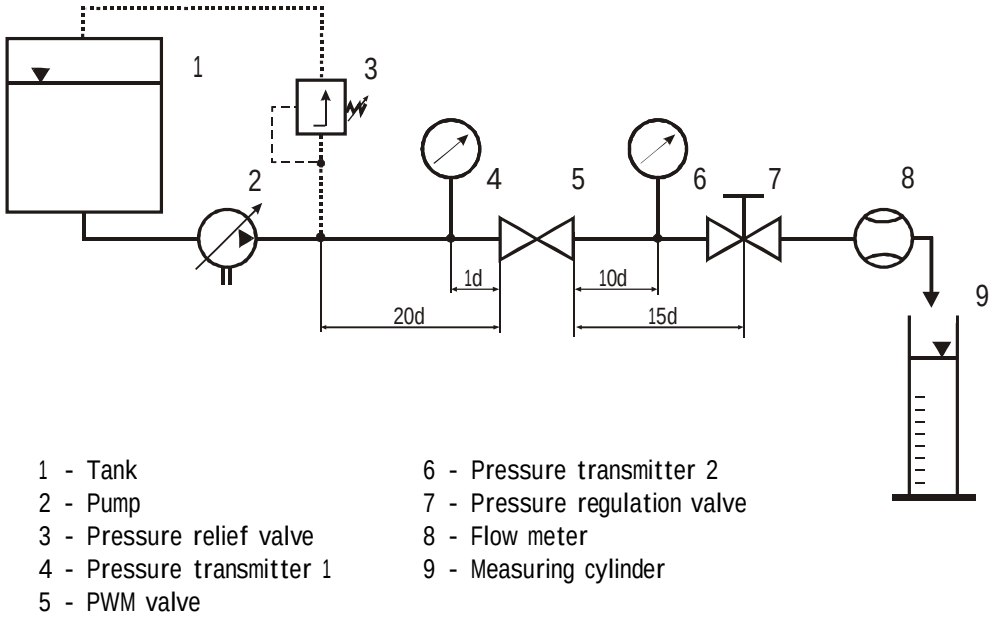

Figure 4. 36: Test setup for proportional regulation valve calibration and K_v value determination according to VDI-VDE 2173 standard (VDI/VDE, 1962)

The measurements of flow rate characteristics described above are valid only for a single valve. If a particular amount of tracer is to be injected into the carrier, the resulting pressure drop, e.g. in the check valve, as well as friction pressure losses in the supply lines must also be taken in account.

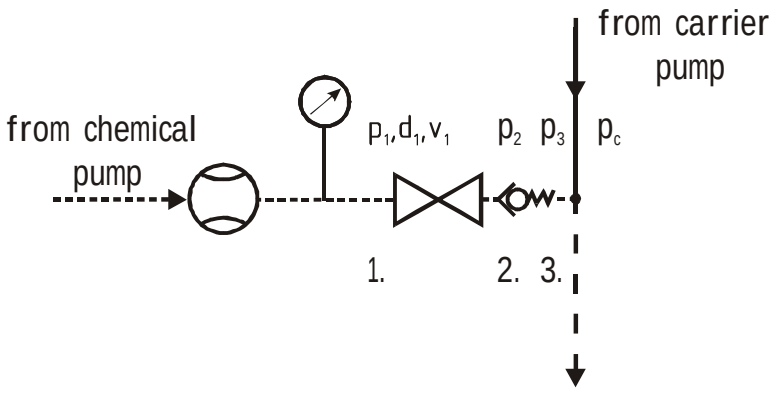

Figure 4. 37: Test model of the boom injection system used for proportional valve calibration

For a simplified model of a boom injection system (see Fig. 4.10) the relation between tracer flow rate Q_a and differential pressure Δp_{1c} can be determined experimentally or mathematically by using Bernoulli's equation:

$$Q_a = \frac{\pi d_3^{\,2}}{4}\sqrt{\frac{2}{\rho}\left(p_1 - p_C - p_z\right) + v_1^2} \tag{4.7}$$

where:

d_3 = Diameter of the check valve outlet (m)

v_1 = Fluid velocity at point 1 (m s^{-1})

p_1 = Pressure at point 1 (Pa)

p_c = Pressure in the carrier line (Pa)

p_z = Pressure losses between points 1 and 3 (Pa)

The pressure loss is the sum of the local and friction losses in the pipe lines:

$$p_z = \rho\ \frac{v_1^{\,2}}{2}\left(\zeta_{12} + \zeta_{23} + \zeta_{3C} + \sum \lambda_i \frac{l_i}{d_i}\right) + p_o \tag{4.8}$$

where:

ζ_{12} = Minor losses coefficient for the proportional valve

ζ_{23} = Minor losses coefficient for the check valve

ζ_{3C} = Minor losses coefficient for the tee junction

λi = Friction coefficient (Pa); (for laminar flow $\lambda = 64/R_e$)

d_i = Pipe diameter (m)

l_i = Pipe length (m)

p_o = Cracking pressure of the check valve (Pa)

In general, the results depend strongly on the relative pipe lengths, the friction coefficient and the pressure drops in the check valve and in the tee junction. As ζ and λ can only be determined very roughly, the tracer flow rate characteristics for the complete boom injection system including the check valve and the plumbing must be investigated experimentally.

The corresponding tests were carried out with water and glycerine solutions at three degrees of viscosity. In the tests the system (carrier) pressure p_c was set by degrees from 1 to 6 bar and maintained constant. The pressure in the tracer line before the regulation valve p_1 was set to 7.5 bar. The valve was then opened by degrees from 0 to 10 V and then closed again in the same way. The flow rates were measured by the wheel flow meter placed before the regulation valve. The control voltage signals for the response time measurements were determined from the resulting flow rate characteristics.

4.2.3.3 Orifice Plates

CP 4916-8; -10; -12; -16; and -20 flow regulators were used to ensure the uniform distribution of tracer along the boom in the system developed for injection into a set of six nozzles. The orifice plates tested (see Fig. 4.11) had holes with diameters of 0.203 mm (0.008 in), 0.254, 0.305, 0.406 and 0.508 mm, respectively. Before use in the direct nozzle injection system, the orifice plates were calibrated for flow performance at differential pressures from 0.5 to 5.0 bar.

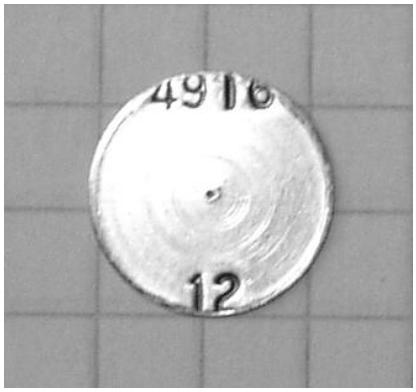

Figure 4. 38: 4616-12 (Spraying System Co.) metering plate modified for the nozzle injection assembly

There are two approaches how to control the flow rate of tracer through orifice plates. The first is to control p_2 by means of a proportional valve and hence directly control the differential pressure across the orifices Δp_{2c}. The method of controlling p_2 by means of a proportional valve is partially described in the previous chapter. Generally speaking, the pressure p_2 depends on the pressure drop characteristic of the regulation valve used.

However, for the response time measurements the second approach was used, i.e. simple manual pressure regulation. The pressure p_2 was set manually by means of the pressure relief valve coupled with the tracer pump while the proportional valve was fully open. The proportional valve was used only to open and close the tracer line (on/off). A simplified model of the nozzle injection system with injection into a set of six nozzles is shown in figure 4.12.

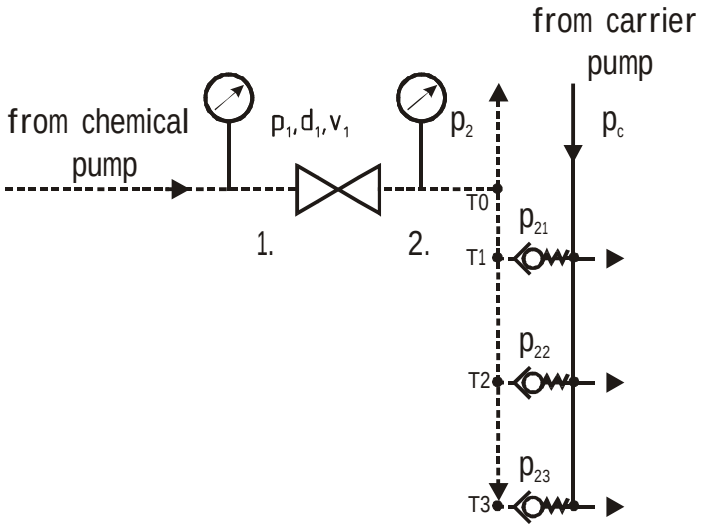

Figure 4. 39: Test model of nozzle injection system with injection into a set of six nozzles used for orifice plate calibration

The relation between the tracer flow rate across the orifices Q_{an} and the differential pressure Δp_{2C} can be determined for each nozzle position:

$$Q_{an} = \frac{\pi {d_2}^2}{4} \sqrt{\frac{2}{\rho}\left(p_2 - p_c - p_{zn}\right) + v_2^2} \tag{4.9}$$

where:

d_2 = Pipe diameter at point 2 (m)

v_2 = Fluid velocity at point 2 (m s^{-1})

p_2 = Pressure at point 2 (Pa)

p_c = Pressure in the carrier line (Pa)

p_{zn} = Pressure losses between point 2 and injection point n (Pa)

The pressure losses are the sum of the local and friction losses in the plumbing and were calculated according to the following equation:

$$p_{zn} = \left(\sum_{i=0}^{i=n} \rho \frac{v_i^2}{2} \zeta_{T_i} \right) + \rho \frac{v_i^2}{2} \zeta_{D_i} + \left(\sum_{i=1}^{i=n} \rho \frac{v_i^2}{2} \lambda_i \frac{l_i}{d_i} \right) + p_{o_i} \tag{4.10}$$

where:

ζ_{Ti} = Minor losses coefficient for the tee junction with a proportional valve

ζ_{Di} = Minor losses coefficient for an orifice plate

λi = Friction coefficient (Pa)

d_i = Pipe diameter (m)

l_i = Pipe length (m)

v_i = Fluid velocity (m s^{-1})

p_{oi} = Cracking pressure of the check valve (Pa)

The range of tracer flow rates for one nozzle is determined by the required chemical application rate and operational speed. The required flow rate range is between 1.67 and 50 ml min^{-1}. The minimum flow rate achievable with one orifice plate at a minimum feasible differential pressure depends mainly on the viscosity of the injected liquid. This can be a serious issue because of the limited dimensions of the orifices. The tracer flow rate characteristic $Q_a = f(\Delta p_{2c})$ was measured for all used orifice plates and for all test liquids.

In addition to the $Q_a = f(\Delta p_{2c})$ characteristics, the flow rate uniformity along the boom was studied for pure water and for the three aqueous glycerine solutions. These measurements were carried out by measuring the flow rates among the individual nozzles. Relying on this method it is possible to determinate indirectly the mixture uniformity along the spray boom. The flow rates were determined by measuring the weight of tracer samples collected from each orifice plate in the sprayer boom over sampling periods of 1 minute. The coefficient of variation (CV) was used to evaluate flow rate uniformity and was found using the following equation:

$$CV = \frac{s}{\bar{x}} 100 \tag{4.11}$$

where:

CV = Coefficient of variation (%)

s = Sample standard deviation

$\bar{x}$ = Sample mean

4.2.3.4 Differential Pressure Flow Meter

A differential pressure flow meter was designed and assembled to monitor rapid changes in flow rate of the injection metering system. For satisfactory on-line measurements of response time it is necessary to obtain at least 10 values per second at a high frequency. Each of the values should be averaged from 100 impulses, which necessitates a frequency f = 1000 Hz. The problem inherent in flow rate measurements is related to the limited number of impulses provided by common flow meters per measured unit (1.0 litre) as well as to very low tracer flow rates. For example, the wheel flow meter, used during the valve calibration measurements, provides 2350 impulses l^{-1}, and the minimal required tracer flow rate is 10 ml min^{-1}. The resulting measurement frequency is then only f = 0.39 Hz. Therefore, another measuring principle or a different type of signal must be used for dynamic measurements. One possibility is to employ an analogue signal provided by a pressure sensor which senses the differential pressure across a cylindrical tube; this pressure is proportional to the square of the flow rate through it. This method is based on the Hagen-Poiseuille law, which is valid for laminar flows (Re<2300) in capillary tubes:

$$Q = \frac{\partial V}{\partial t} = \frac{\pi R^4}{8 \eta l} \Delta p \tag{4.11}$$

where:

Q = Stationary laminar flow ($m^3 s^{-1}$)

η = Pressure in the carrier line (Pa)

R = Tube radius (m)

l = Tube length (m)

η = Dynamic viscosity of the liquid (Pa s)

Using this equation it is possible to theoretically determine the appropriate size of capillary tubes for different viscosities measured and for different flow rate ranges. The results for water and a 90 % glycerine solution are shown in table 4.1. A limiting factor was the Reynolds number, which should be kept under 2300. For the differential pressure measurements a differential pressure transmitter (7) with a measuring range form 0 to 0.3 bar was used. The schematic of the capillary flow meter and the calibration arrangement are shown in figure 4.13.

Table 4. 2: Capillary tube dimensioning

Liquid	**Viscosity at 20 °C (mPa s)**	**Flow rate range Q_a (ml min^{-1})**	**Capillary radius R (mm)**	**Capillary length l (m)**	**Reynolds n. at max. Q_a (-)**	**Differential pressure Δp (mbar)**
Water	1.0	10 - 200	1.0	1.0	2122.1	84.9
		200 - 300	1.35	1.0	2357.5	38.3
90 % Aq.-Glycerine	219	10 - 150	2.0	0.3	4.7	250.7
		150 - 300	2.0	0.1	9.3	167.1

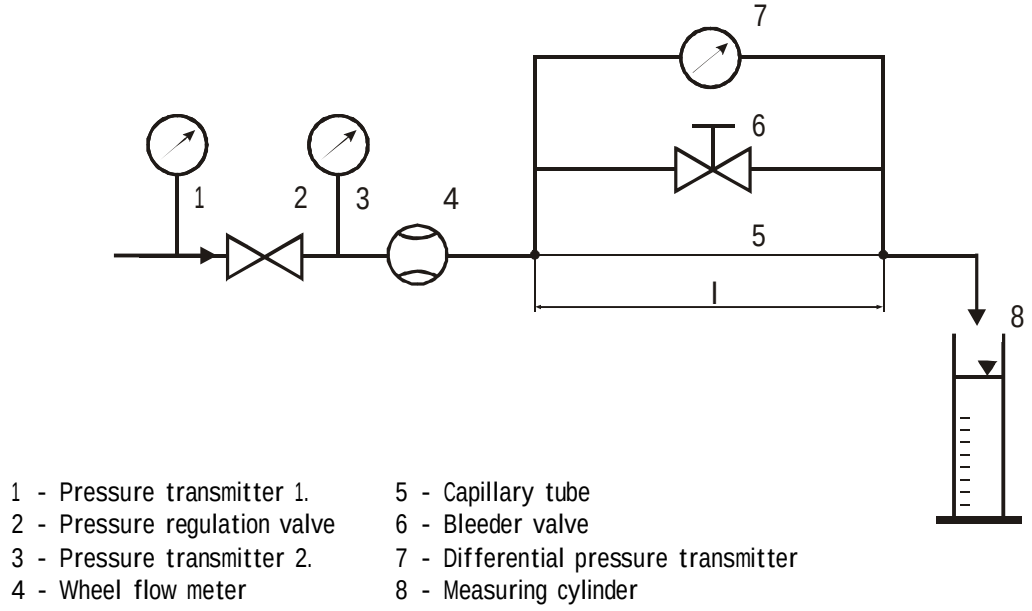

Figure 4. 40: Schematic of differential pressure capillary flow meter in calibration arrangement

The flow meter was calibrated by collecting liquids in a measuring cylinder placed on a digital scale. The flow rate was calculated by measuring the time required to collect a certain amount of liquid with a stopwatch. Parallel to this manual measurement, the flow rate was also measured with a wheel flow meter (4). Whereas the flow meter was calibrated with water, the flow of other fluids with different viscosities and densities could not be accurately measured because the flow meter registered differential pressure and was thus affected by differences in fluid density and viscosity. Therefore, volumetric calibration with liquids other than water was necessary.

4.2.3.5 Spray Nozzles

Regular XR 80015 and 8005 (Spraying Systems Co.) flat fan nozzles were used to maintain the carrier flow rate constant during the response time measurements. The nozzles were calibrated before each set of response time measurements. The required nozzle flow rate range (300 - 2500 ml min^{-1}) was controlled with a pressure regulation valve. The system pressure was set by degrees to 1, 3 and 5 bar. The flow rates trough the spray nozzles were determined by recording the amount of pressurized water that exited the nozzle. The samples were collected during a period 120 s and weighted.

The dynamic calibration procedure was replicated six times for each of the three boom pipe diameter configurations (12.7-12.7-12.7-12.7, 8-8-8-8 and 8-8-6-6 mm). An aim of these measurements was to verify the theoretical calculation of reduction of the boom pipe diameter described in chapter 3.2.2. The maximum allowable variation between the nozzle outputs was determined to be 5 %.

4.2.3.6 Instrumentation - Control and Measurement System

A common 32-bit electronic measurement card DagBoard/2000 (IO-Tech, Inc.) was used for the measurements of physical quantities such as pressure, flow rate and concentration and for valve control. The card has 16 analogue inputs and 2 output channels, 40 digital I/O channels and 6 counters. The measurement frequency used depended on the kind of measurement being performed. The calibration measurements were performed at 10 and 100 Hz. A frequency of 1000 Hz was used for the dynamic response time measurements. The card was installed in a PC and connected with an electronic box via three parallel slots.

The sensors and valves were supplied with the required voltages, and the input and output signals were amplified according to card specifications. The schema of the sensor connections in the electronic box is shown in figure 9.1 in the appendix.

LabView® software was used to write a program for controlling the measurement card via a PC interface. The main page of the resulting application is shown in figure 4.14.

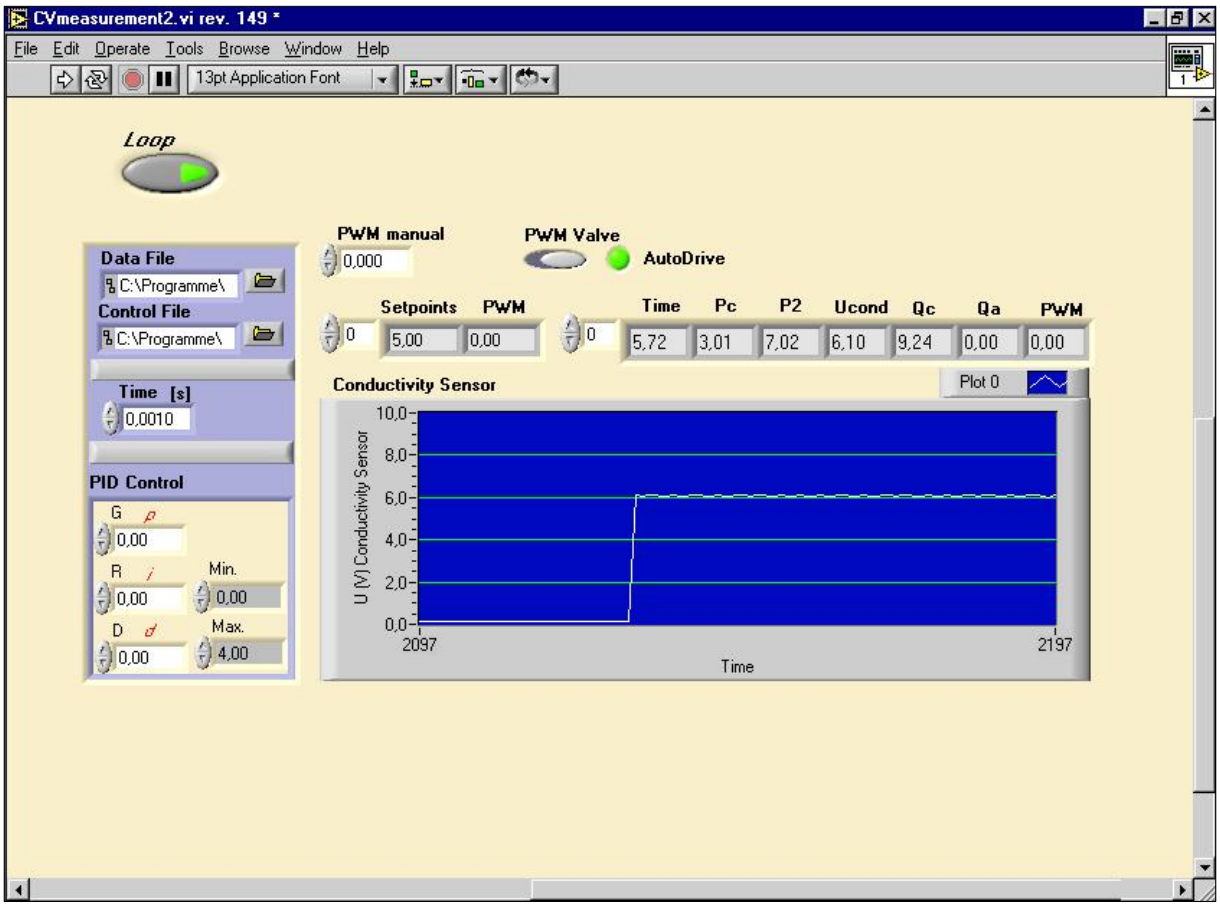

Figure 4. 41: Template of software application used for response time measurements and for monitoring the physical quantities of the injection system

4.3 Chemical Concentration Measurements

Monitoring the most important factors such as dose accuracy, mixture uniformity across the boom and response time characteristics, requires accurate on-line methods for measuring mixture concentrations. Several sampling methods, e.g. colorimetry, fluorometry, spectrophotometry (KOO et al., 1987, PESINA et al., 2002, SUI et al., 2003) and conductivity measurements (TOMKINS et al., 1990, ANTUNIASSI et al. 1997), have been used to measure mixture concentrations in nozzle supply lines (ZHU et al., 1997). Some of these sampling methods have obvious disadvantages: they require considerable time and labour for sample analysis, the physical properties of herbicide substitutes are limited, or calibration is too difficult.

A conductivity method and an optical method based on spectrophotometry were developed for the on-line measuring of mixture concentrations. As described by PAICE (1997), the conductivity method is based on electrical conductivity measurements to estimate the salt concentration of the injected solution. Both methods are very sensitive and allow measuring a wide range of concentrations of different substances. There is no need for special or complex assembled devices. From these reasons they are so often used in common practice. These two methods were also used for the immediate determination of time response characteristics and mixture uniformity of laboratory models of injection metering systems. In addition, another optical (densitometric) method using a CCD camera was tested for determining the mixture uniformity of spray solution.

4.3.1 Methods and Sensors Used for the Concentration Measurements

4.3.1.1 Conductivity Method

The fundamental principle of the sensor system developed here is the measuring of the electrical resistance of a fluid element (spray solution) emitted from the mixing point immediately before entering the nozzle. The hypothesis is that the relationship between the instantaneous resistance of the emitted fluid element and the concentration of an electrically conductive fluid injected into a relatively resistive carrier fluid could be an accurate and precise method for quantifying the injection event. Electrical conductivity is usually measured by means of two isolated electrodes which are in direct contact with the medium.

An alternating-current voltage is applied to the electrodes in order to prevent electrolysis. The applied voltage generates a current that depends on the resistance of the medium (Ohm's law $U=RI$). Electrical resistance R (Ω) is the reciprocal of electrical conductance G (S) (BRDLICKA, 1982):

$$R = \frac{1}{G} \tag{4.12}$$

Electrical conductance is inversely related to the distance between the electrodes d and continually proportional to the area of the electrodes S and the specific electric conductivity κ (S m^{-1}), which is mathematically represented by:

$$G = \kappa \frac{S}{d} \tag{4.13}$$

The geometry of a measuring cell (area S and distance d) is defined by the quotient C:

$$C = \frac{d}{S} \tag{4.14}$$

The conductivity of a solution is calculated on the basis of this known cell constant C and by measuring the current generated. The cell constant is designed in relation to the measuring range of the sensor. The specific electrical conductivity of a solution is a measure of its ability to conduct electrical current and it depends on the molar conductivity of its ions Λ_m and its concentration of ions c_i:

$$\kappa = \Lambda_m \cdot c_i \tag{4.15}$$

Specific electrical conductivity increases with increasing concentration. For a given electrolyte, the molar conductivity of ions Λ_m is constant. For a solution of sodium chloride (NaCl), which was used as tracer, the resulting value of molar conductivity is 126.45 S cm^2 mol^{-1} (ATKINS, 2002).

Additionally, electrical conductivity is a function of temperature. For low concentrated solutions the relationship between conductivity and temperature is represented by the following equation:

$$\kappa_{\vartheta} = \kappa_{\vartheta_0}\left[1 + \beta_1(\vartheta - \vartheta_0) + \beta_2(\vartheta - \vartheta_0)^2\right] \tag{4.16}$$

where:

β_1, β_2 = Thermal conductivity coefficients (e.g. for a NaCl solution at 20° C $\beta_1 = 0.0226\ K^{-1}$, $\beta_2 = 0.085\ 10^{-2}\ K^{-2}$)

$\kappa_{\vartheta}, \kappa_{\vartheta_0}$ = Conductivity at temperatures ϑ and ϑ_0 ($S\ m^{-1}$)

$\vartheta - \vartheta_0$ = Thermal gradient (K)

As the second square term is insignificant at lower temperature intervals, it is possible to simplify the equation and calculate the relation without that parameter. The values of the thermal conductivity coefficients β_1 and $\beta 2$ decrease rapidly as the temperature of the electrolyte ϑ increases. The conductivity of diluted solutions increases with increasing temperatures by a rate of 1 to 5 % per degree Celsius (NIEBUHR and LINDER, 1994). Therefore, it is necessary to compensate the temperature dependence by means of an integrated thermistor or by keeping the temperature of the solution constant.

4.3.1.2 Conductivity Sensor

The sensor system is comprised of two elements: a pair of brass electrodes in contact with the emitted fluid jet, and an electronic circuit for determining the electrical resistance of the fluid element. The conductivity sensor is shown in figure 4.15. The measuring cell (ELWA GmbH) was chosen for its suitable housing parameters and its constant C = 0.1. The sensor housing was fabricated from a polyethylene rod with a ¼" inner and outer pipe thread. The distance between the electrodes was about 1.3 mm, and the cross-sectional area of one electrode was 13.0 mm^2. The sensor was mounted between nozzle body and nozzle cup. The reference distance between the centre of the electrodes and the nozzle tip was 40 mm, and the volume necessary to fill the sensor up to electrode level was 0.48 ml.

a)

b)

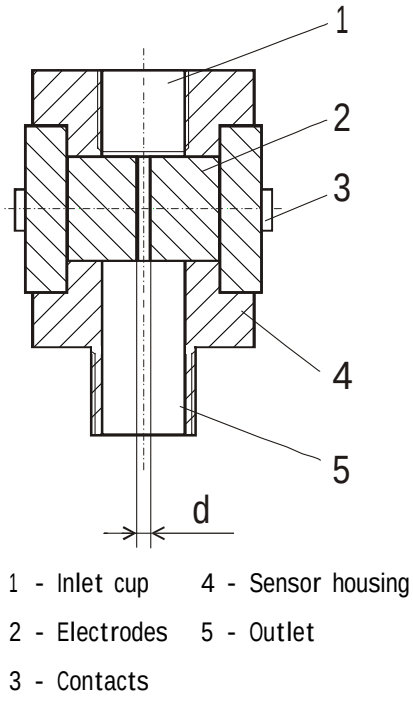

Figure 4. 42: Conductivity sensor; a) sensor as a part of the nozzle body for calibration and response time measurement; b) sensor cross-section

The sensor was connected with an electronic circuit board which was placed in a measurement box. The electronic circuit is shown schematically in figure 4.16, a detailed connection plan is shown in the appendix, figure 9.2. An astable multivibrator (pulse generator) and a driver circuit supply the conductivity sensor with a symmetrical rectangular voltage of 1.28 kHz and 12 volts peak to peak. This is to prevent electrolysis, and it directly provides a DC voltage after rectifying. The sensor causes the output voltage U_C to break down according to the conductivity of the spray mixture.

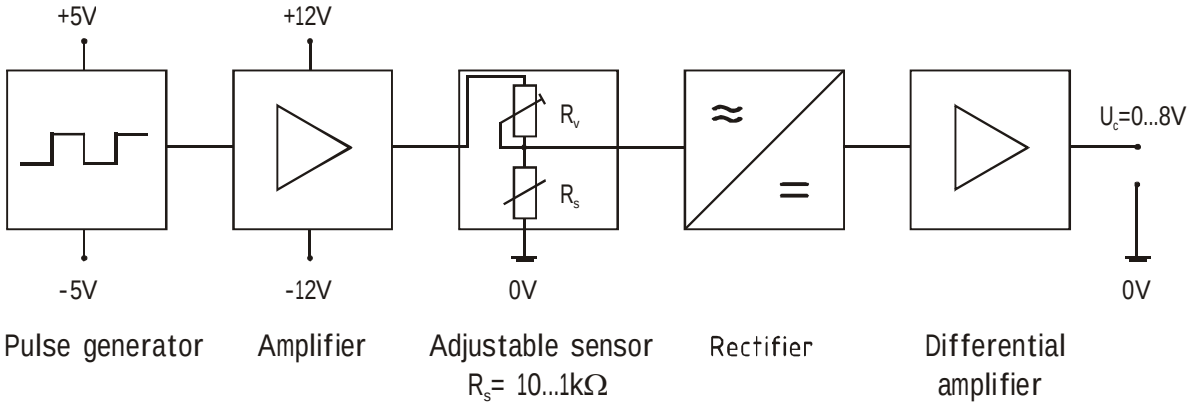

Figure 4. 43: Scheme of the conductivity sensor electronic circuit

The measurement range of the sensor can be adjusted by means of the resistor R_V. The magnitude of resistance R_V was calculated for the maximum and minimum value of resistance (R_{Smin}; R_{Smax}) of the medium measured. The minimum value of resistance measured was calculated for a water-NaCl solution at a maximum concentration of 0.1 mol of NaCl per 1 litre (≈ 5.84 g l^{-1}) by using formulas 5.1, 5.2 and 5.4. For the sensor with a cell constant C = 0.1 the result was R_{Smin} = 7.9 Ω (10 Ω). The maximum value of resistance measured R_{Smax} was calculated in the same way as the minimum value. However, in this case the resistance was calculated for a minimal (zero) concentration of NaCl. Mathematically, the resulting value is $R_{Smax} = \infty$. For the practical resistance measurements the maximum value was defined as 1 kΩ.

4.3.1.3 Light Transmittance Method

The second concentration measurement method is based on sensing the transmittance of light by means of a photodiode. Transmittance can be defined as the amount of light that penetrates a solution. Transmittance T (%) can be expressed as the ratio of the intensity of the transmitted light I_t (lm) to the initial intensity of the light beam I_0 (lm) as expressed by formula 4.17 and figure 4.18 (BRDLICKA, 1982):

$$T = \frac{I_t}{I_0} \tag{4.17}$$

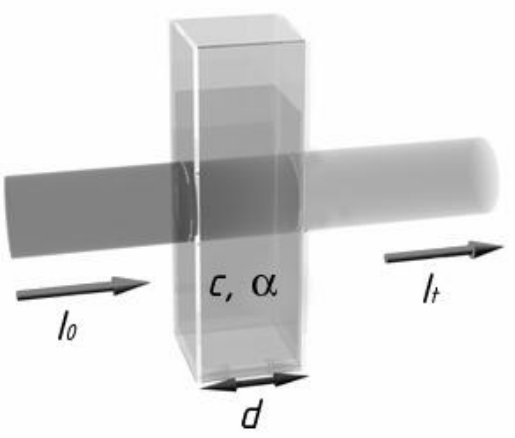

Figure 4. 44: Transmittance method - measurement principle

The transmittance of a homogeneous fluid element is determined by its width *d* and the concentration of the solution *c*. By increasing the pathway that the light must travel through the sample, the number of molecules that will interact with the light is increased; in effect, the apparent concentration will be increased. Secondly, the concentration of molecules in the solution affects the transmittance as each molecule can absorb light. As the number of molecules in the solution increases, the number of photons absorbed in the process also increases and the transmittance decreases. The relation between these parameters is:

$$T = e^{-\alpha dc} \tag{4.18}$$

where:

T = Transmittance of light (-)

α = A constant which takes into account the specific properties of molecules absorbing photons (l mol^{-1} cm^{-1})

d = Fluid element (sample) width (cm)

c = Concentration of the solution (mol l^{-1})

From the equations 4.17 and 4.18, an equation for absorbance can be obtained (Beer's law):

$$A = -\lg T = \lg \frac{1}{T} = \lg(e)\alpha dc = \varepsilon dc \tag{4.19}$$

where:

A = Absorbance (-)

ε = Molar extinction coefficient (l mol^{-1} cm^{-1})

d = Cell width (cm)

c = Concentration of the solution (mol l^{-1})

The quantity ε is the molar extinction coefficient (molar absorptivity). This coefficient represents the fact that molecules absorb light at different efficiencies and at different energies. Therefore, the transmittance is dependent on the specific molecule in the solution and on the wavelength of the light passing through the sample.

4.3.1.4 Light Transmittance Measurement Device

The first considerations in designing a transmittance measurement device must be the choice of a suitable colour solution to be used as a tracer and the choice of a suitable source of monochromatic light with an appropriate wavelength. Food colorants were selected as an active ingredient in water solutions because they are non-toxic, non-polluting, highly soluble, stable for long time and relatively inexpensive. All these features are favourable for carrying out laboratory tests and sample analyses. The three colorants Azorubine (E122), Brilliant Black (E161) and Brilliant Blue (E 133) were used for preliminary absorbance measurements. The measurements were carried out with a spectrophotometer in order to determine the absorption peaks of the tested colorants. The colorants were diluted in water at a basic concentration of 50 mg l^{-1}. The results are shown in figure 4.18. The E161 black colorant has an absorption peak around 570 nm in the region of the yellow-green spectrum zone (500 – 590 nm). The course of the absorbance curve indicates that the black colorant would be the most suitable tracer for transmittance tests. A green LED with an emission band of 565±5 nm was used as the source of monochromatic light for the tests.

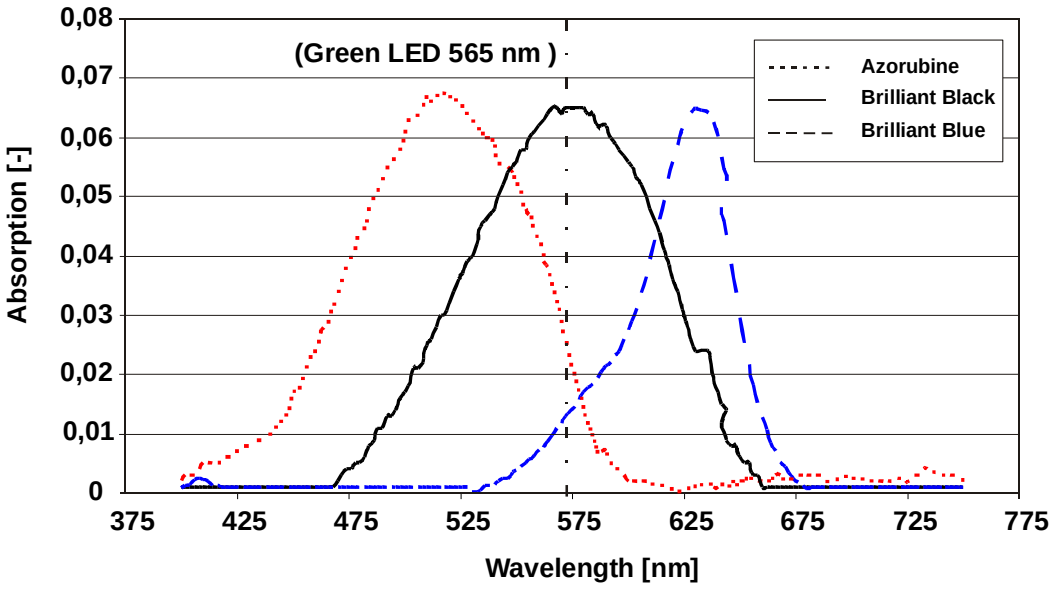

Figure 4. 45: Absorbance measurement for water-colorant solutions

Based on these considerations, an experimental device was set up. Inside of this device was a LED which emits green light through a coloured solution, flowing through an in-line sight glass cell, towards a receiving photodiode with an integrated linear feedback amplifier. There is linear correlation between the photocurrent and the voltage-current characteristic of the photodiode (NIEBUHR and LINDNER, 1994). The photocurrent flows in reverse direction and depends on the intensity of the incident light, which is a parameter of the voltage-current characteristic curve. The LED, the photodiode and the sight glasses were placed inside a plastic housing as shown in figure 4.19.

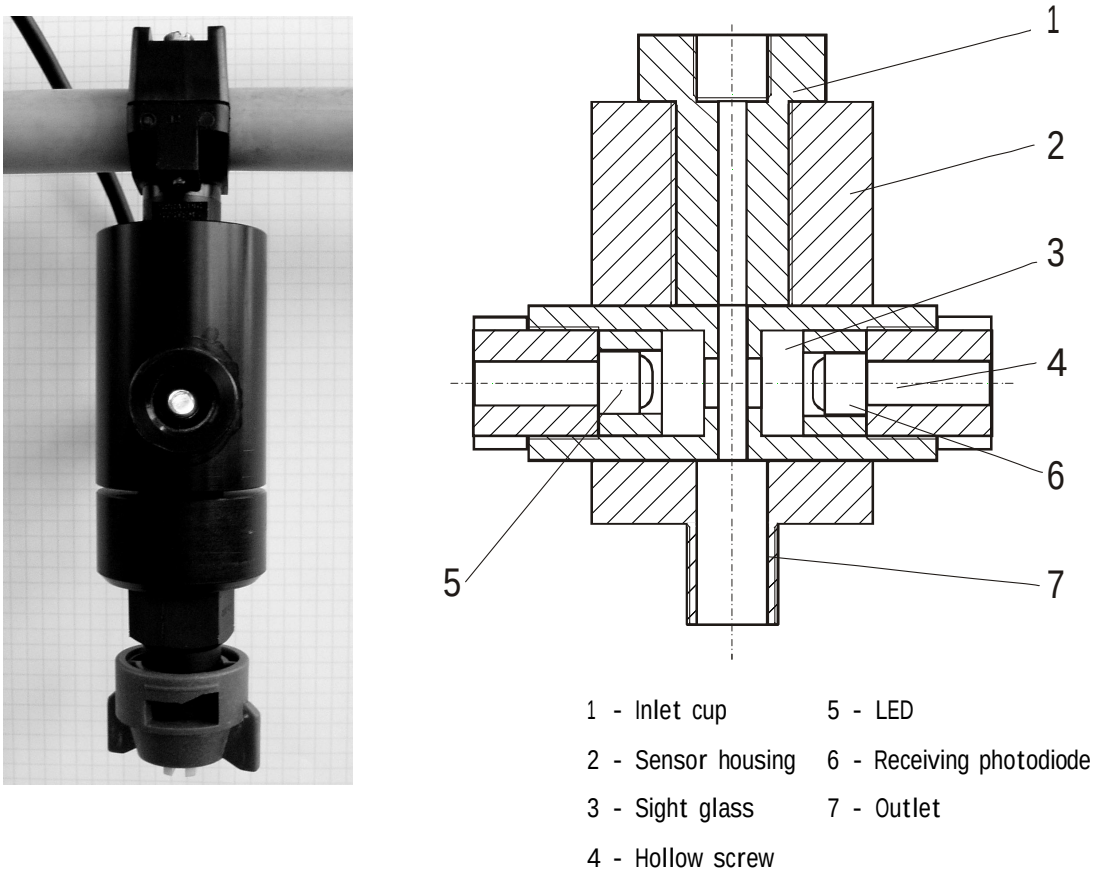

Figure 4. 46: Transmittance sensor; a) sensor as part of a nozzle body for calibration and response time measurements; b) sensor cross-section

The width of the fluid element between the sight glasses was 8 mm, and the distance between the LED and photodiode was 18 mm. The volume necessary to fill the sensor up to diode level was 1.74 ml. A suitable electronic circuit provided the required stabilized symmetric output voltage supply.

The photodiode was powered with a constant bias voltage in reverse direction. The output voltage produced by the photodiode U_D in the range from 0 to 4V was digitised and recorded by means of the measurement card. The electrical circuit is shown schematically in figure 4.20, the detailed connection plan is shown in the appendix, figure 9.3.

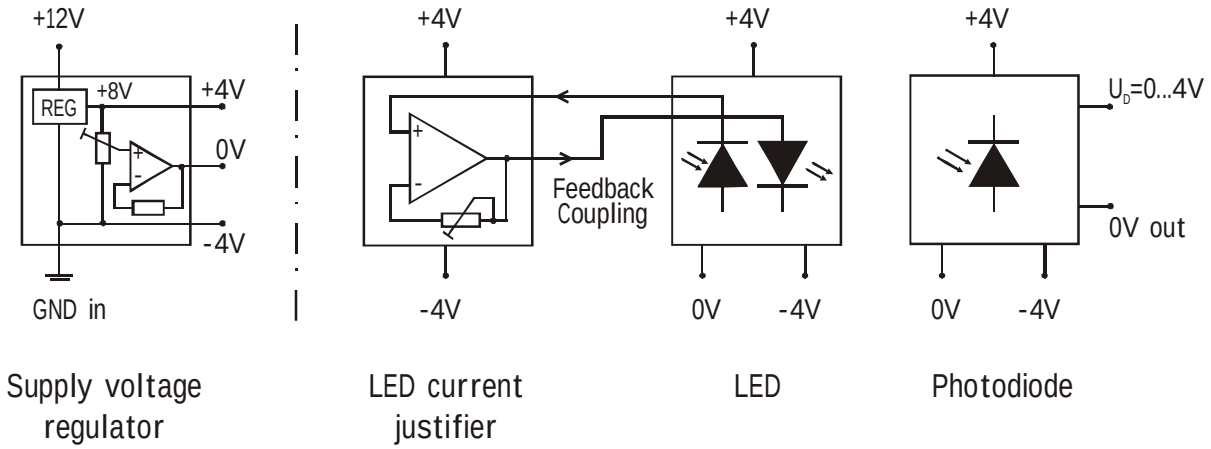

Figure 4. 47: Scheme of the transmittance sensor's electronic circuit

4.3.1.5 Densitometry Method

As an alternative to the two methods mentioned above, the densitometry method proved its suitability for determining mixture concentrations. Densitometry is the quantitative measuring of the absorbance (optical density, OD) of incident light by a substance. In principle, this method is identical with the light transmittace method. According to Beer's law (equation 4.19), the concetration of the coloured sample is proportional to absorbance. The logarithmic absorbance scale, and net integral of density values for an object in an image, is the proper measure for use in quantitation. In other words, it is possible to use a scaling system, for e.g. pixels in a graphic image, which has a one-to-one correspondence to the concentration of a mixture. Sample concentrations can be determined using optical, electronic, and – as in this study – computer-based imagine techniques. One of the standard methods for determining the density of an object or a point on an image is to measure its optical density values by means of a CCD camera. With a CCD camera, the OD values are measured indirectly. The camera and frame grabber pixel values are linear with respect to transmission (T).

Incident light induces a voltage in the CCD sensor. Light below the sensitivity threshold of the sensor induces a voltage that cannot be discriminated from internally generated noise. Light that is too bright will saturate the sensor. Between these extremes is a range of incident illumination that will affect the voltage output of the sensor in a usable fashion. This is the dynamic range of the sensor. The dynamic range must be broken up (digitized) into discrete steps. Imaging systems contain a digitizer which digitizes the sensor's voltage output range into discrete levels. Each of these levels corresponds to a shade of grey in the image. Although 8-bit (256 grey levels) density resolution is by far the most common, some imaging systems work with greater bit densities. High bit densities are critical when using scanning imagers, imaging plate readers, and cooled CCD cameras. Most of these instruments provide up to 16-bit (65536 grey levels) digital data in order to take advantage of broad dynamic range of the camera.

If the amount of incident illumination can be precisely quantified, it is possible to measure both incident and transmitted illumination in grey levels and to calculate an optical density ratio as described in equation 5.8. Measurements of incident illumination are possible in systems that pass a beam of coherent or highly collimated light over the specimen (scanning densitometers). However, incident illumination measurements are not practicable in camera-based systems, which illuminate the specimen with diffuse light. Camera-based image analyzers start with uncalibrated grey levels. These can be used directly, or they can be converted to uncalibrated transmittance or density values. Gray level transmittance or reflectance (GLT or GLR) can be measured as follows:

$$GLT\ (GLR) = \frac{observed\ grey\ levels}{maximum\ \ possible\ number\ of\ \ grey\ levels} \tag{4.20}$$

Gray level transmittance or reflectance increases with increasing brightness. Therefore, GLT is usually converted to relative optical density (ROD) as follows:

$$ROD = \lg \frac{1}{GLT} \tag{4.21}$$

In using GLT or ROD, specimen density values are referenced to the dynamic range of the imaging system and not to any external reference. Therefore, a GLT or ROD value tells very little about the optical density which would be measured by a densitometer (IMAGING RESEARCH, 2007).

Quantitative densitometry is performed by calibrating to a set of concentration standards before reading density values in the unit of calibration. A good density calibration provides a ratio scale (a scale with fixed 0 point and equal step intervals) and allows the reading of density values in units of concentration. In the light transmittance method the entire sensor area is integrated to yield a single voltage. This voltage is compared with the calibration curve to yield a single concentration value. This is termed the integrated optical density (IOD) of the specimen. In an imaging system, this is equivalent to taking the mean grey level values of all the pixels in a sample window and then converting this single mean grey level value to a concentration:

$$IOD = \frac{\sum pixel\ \ grey\, level\ values}{number\ of\ \ pixels} \tag{4.22}$$

The IOD value was chosen as the most suitable parameter for calibrating the camera system.

4.3.1.6 CCD Camera Measurement Device

The measurement system is comprised of an 8-bit CCD camera with a 1024(H) x 1024(V) resolution which takes monochromatic pictures of a coloured mixture in a glass cuvette. The cuvette was placed before a light desk as shown in figure 4.21. The calibration measurements were performed in a screened optical laboratory to guarantee constant light conditions.

A histogram function for image analysis in the Adobe Photoshop™ software was used to acquire IOD values; see figure 4.22b. The number of pixels evaluated was 10 000, which corresponds to the marked sampling area of the investigated image in figure 4.22a.

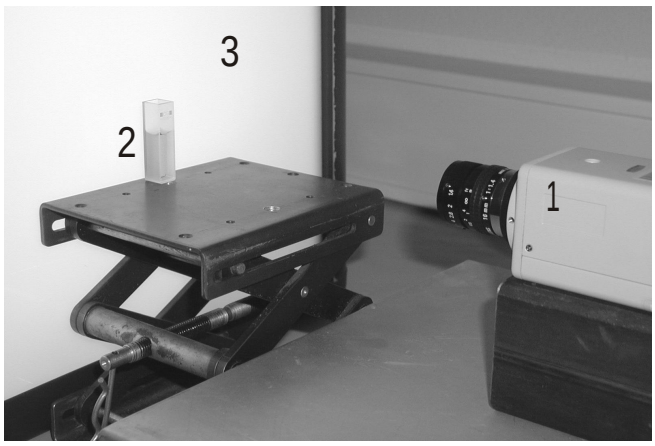

1 - CCD camera
2 - Cuvette with a sample
3 - Light desk

Figure 4. 48: Arrangement for concentration measurement by means of a CCD camera

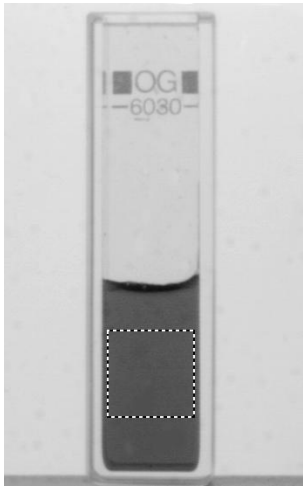

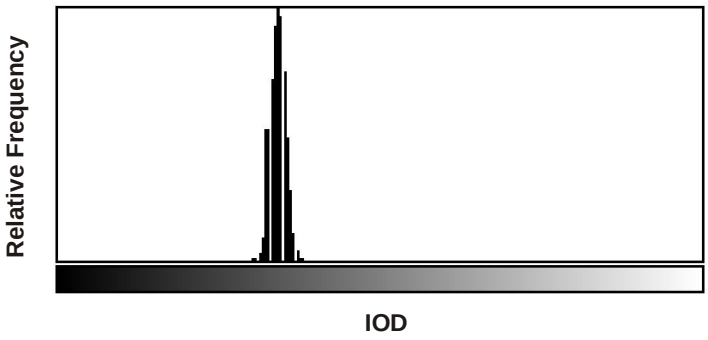

a) b)

Figure 4. 49: Evaluation of optical density; a) image sampling area; b) histogram

4.3.2 Calibration of the Sensors

At first, a preliminary static calibration of all three sensors was performed in order to verify the practicability of the methods for on-line measurements of mixture concentrations and in order to determine the concentration measurement range of the sensors. Samples with known tracer concentrations were placed in the measurement device by means of a pipette. These results of the static measurements were used as reference values for comparison with the results of the second (dynamic) part of the calibration.

The densitometry method using the CCD camera required only static trials. Examples of the samples in the cuvettes are shown in figure 4.23. An E133 Brilliant Blue colorant (Ringe & Kuhlmann, Hamburg, Germany) diluted in water at a basic concentration of 7.5 g l^{-1} (7500 ppm) was used. Each cuvette with a known concentration was captured 3 times by means of the camera.

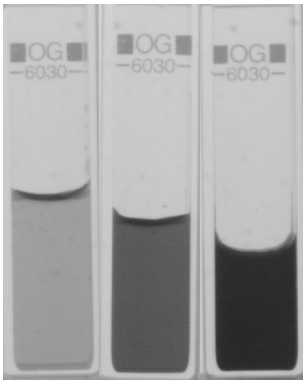

a) b) c)

Figure 4. 50: CCD camera static calibration - measured samples with different concentrations a) 15; b) 220; c) 3750 ppm

Dynamic calibration was performed for the conductivity sensor and the light transmittance sensor only, and it was performed under the same test conditions. The sensors were calibrated by performing five measurements of 30 s output voltage averages. The output voltages were recorded by the measurement card while known concentrations of solution were discharged through the three straight stream spray nozzles used in the study. During the dynamic calibration the flow rates of carrier and tracer were kept constant.

For the conductivity method, sodium chloride (NaCl) diluted in water at a basic concentration of 20 g l^{-1} (20 000 ppm) was used as tracer. The calibration solutions were prepared using finely ground chemically pure NaCl (Dr. Paul Lohmann GmbH, Emmerthal, Germany). During calibration and also during the response time measurements with the conductivity sensor, the temperatures of the carrier and the tracer were kept constant at 20 ± 0.5 °C. This was achieved by using a 500 l sprayer tank as a reservoir for tap water and by using a cooler system with a thermostat for the salt solutions.

E161 black food colorant (Ringe & Kuhlmann, Hamburg, Germany) diluted in water at a basic concentration of 50 mg l^{-1} (50 ppm) was used as tracer in the light transmittance tests.

4.3.2.1 Dynamic Calibration Test Assembly

Both the conductivity and the light transmittance sensors were installed at three different nozzle positions (1, 3 and 5) on the spray boom in turn; see figure 4.24. The spray boom was part of the test bench. The assembly for sensor calibration was set up similar to the nozzle injection system configuration described in chapter 4.2.2.2. The measuring cells were placed between a nozzle body T-junction (injection point) and the nozzle. The tracers were loaded into a 10 l tank of the injection system as substitutes for the liquid herbicide formulations. A metering gear pump was used to deliver the tracer to the injection point at the nozzle body. The tracer flow rate was measured with a wheel flow meter. The relative pressure in the active ingredient tubes was measured by a pressure transmitter placed before the proportional valve.

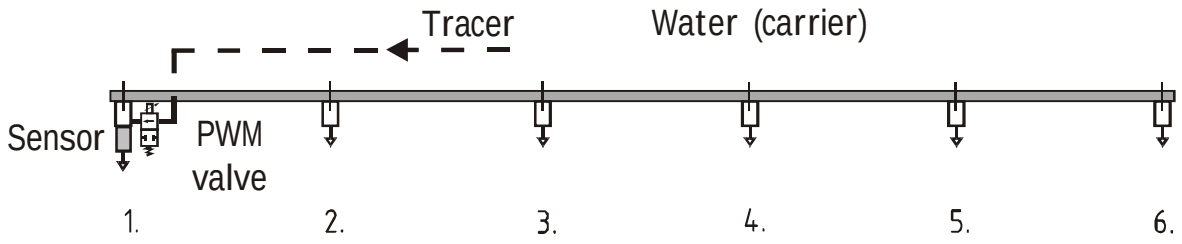

Figure 4. 51: Positioning of the sensors during the dynamic calibration measurements

4.3.2.2 Steady-State Flow-Rate Control

XR 80015, 8003 and 8005 flat fan nozzles were used to maintain the carrier flow rate constant. The flow rates through the spray nozzles were determined by the same calibration procedure as was used for nozzle calibration (see chapter 4.2.3.5). The maximum and minimum carrier flow rates were in the same range as in nozzle calibration. The range of carrier flow rates Q_c extended from 344.5 to 2502.9 ml min^{-1}. The calibrated Q_c values were used to calculate spray concentrations.

The concentration of the measured spray solution was controlled by means of a proportional valve. The steady-state flow rate ranged from 0 to 520 ml min^{-1}, depending on the differential pressure and the proportional valve input signal. The input signal was increased in 0.5 V steps from 0 to 10 V and then decreased from 10 to 0 V.

The duration of each step was 30 s. This time period was identical with the time required by the sensor for measuring spray concentration. An example of the measurement record from the calibration of the optical sensor is shown in figure 4.25.

The following quantities were recorded at a frequency of 100 Hz: system (carrier) pressure, pressure in the tracer line before the proportional valve, flow rates of carrier and tracer, proportional valve control signal and output signal from the sensor.

The mean values of the measured tracer flow rate, the carrier flow rates and the concentrations of active ingredient in the basic solution were used to calculate the mixture concentration c_m:

$$c_m = c_a \frac{Q_a}{(Q_a + Q_c)} \tag{4.22}$$

where:

c_m = Concentration of the mixture (ppm)

c_a = Concentration of active ingredient in the tracer solution (ppm)

Q_a = Tracer flow rate (ml min^{-1})

Q_c = Carrier flow rate (ml min^{-1})

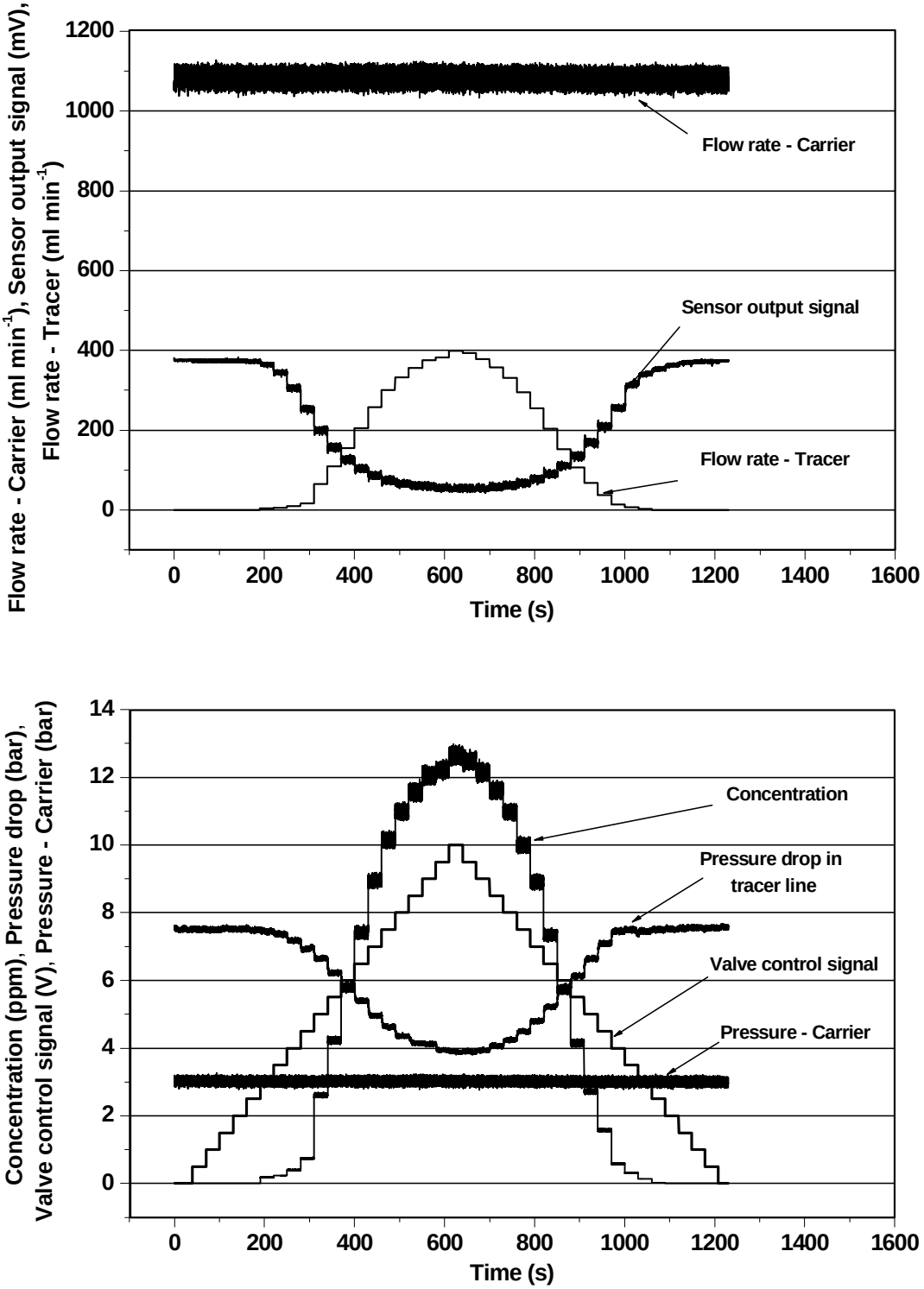

Figure 4. 52: Dynamic calibration - measurement record

4.4 System Response Time Measurements

The objective of these tests was to carry out dynamic response time measurements (transient characteristics), which were needed to assess the applicability of the tested injection systems. For variable-rate herbicide application the input to the injection controller has to undergo a step change, e.g. as the sprayer moves from a mapped area with one application rate to an adjacent area with a different rate.

The response time of the injection system tested was defined as the period from the instant the injection was initiated to the instant the tracer application rate (concentration) reaches 95 % of the equilibrium rate (100 %). The required equilibrium values of the concentration specific for each combination of carrier and tracer flow rate were determined by means of the previous calibration of the conductivity sensor (see chapter 4.3.2). The calibration data obtained for the conductivity sensor (see Fig. 5.20) were re-plotted to obtain an inverse function c = f (U_c) (see Fig. 4.26). The power function 4.23 was used to calculate the resulting concentration, which was then compared with the desired one.

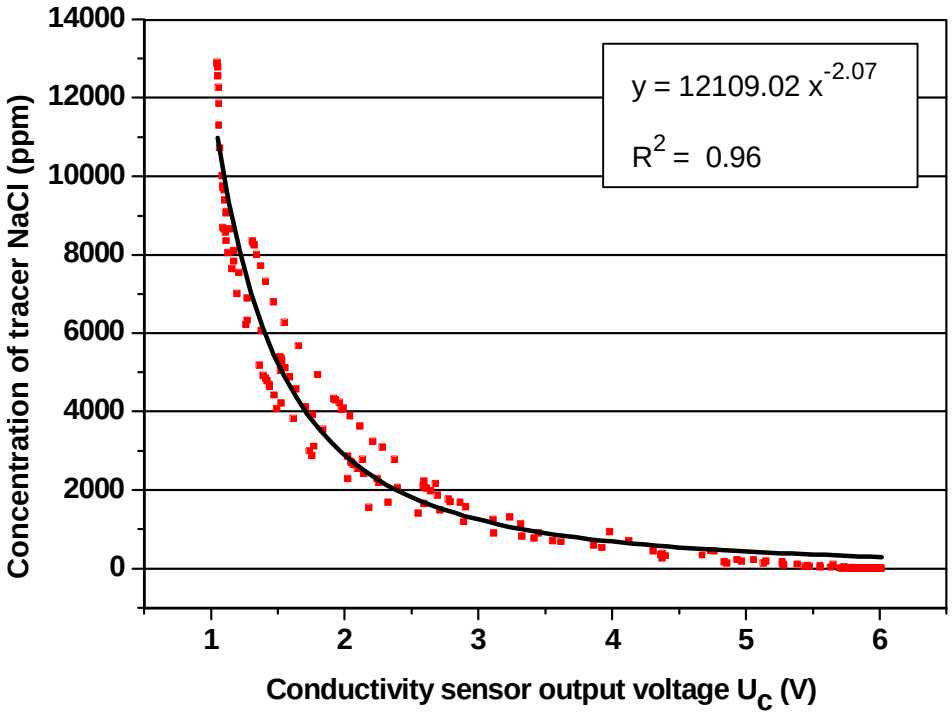

Figure 4. 53: Concentration as a function of conductivity output voltage

$$U_C = 12109.02\ x^{-2.07} \tag{4.23}$$

On the basis of the total response times T_R (0 - 95 %) measured for each injection system, the following parameters were evaluated: lag time T_{lag}, rise time T_{rise} and fall time T_{fall}. The lag time (0 - 10 %) was defined as the time elapsing between the beginning of the flow rate (control signal) change to the instant when the mixture concentration at the nozzle (sensor) starts to change. The rise time was defined as the time required for the output response to a step input to rise from 10 to 90 % of its final value. The fall time was recorded and evaluated together with both previous response time parameters. The fall time was defined as the time required for the output response to a step input to fall from 90 to 10 % of its final value.

Response times at the nozzle were measured using a flow-through conductivity cell for all three direct injection configurations. As tracer the same concentrated NaCl solution (20 000 ppm) was used as for the conductivity sensor calibration. The ranges of the carrier and tracer low rates, the nozzles and the system pressures were selected depending on the parameters to be measured. Five channels of analogue data were recorded during the measurements: the conductivity sensor output voltage, the system pressure, the pressure and flow rate of the tracer and the control signal from the system controller to the proportional valve driver (0 - 10 V). The scan frequency was 1000 Hz.

Data collection for all dynamic tests began with the system in steady state; the timing of the step inputs can be seen in figure 4.27, which shows the conductiometric results of one test with the conductivity sensor. The desired target concentration application rate in figure 4.27 shows the level of concentration which the injection system was expected to achieve. After 5 seconds the data acquisition system simulated a step change in the application rate and opened the control valve. The duration of the first step period was 5 seconds, whereupon the control valve closed fully. The duration of each of the following three steps was 10 s. This method produced four response times for an opening valve and four for a closing valve. The test was replicated three times for each parameter or effect studied. Thus, the total number of results obtained for each time parameter T_R, T_{lag}, T_{rise} and T_{fall} is 12.

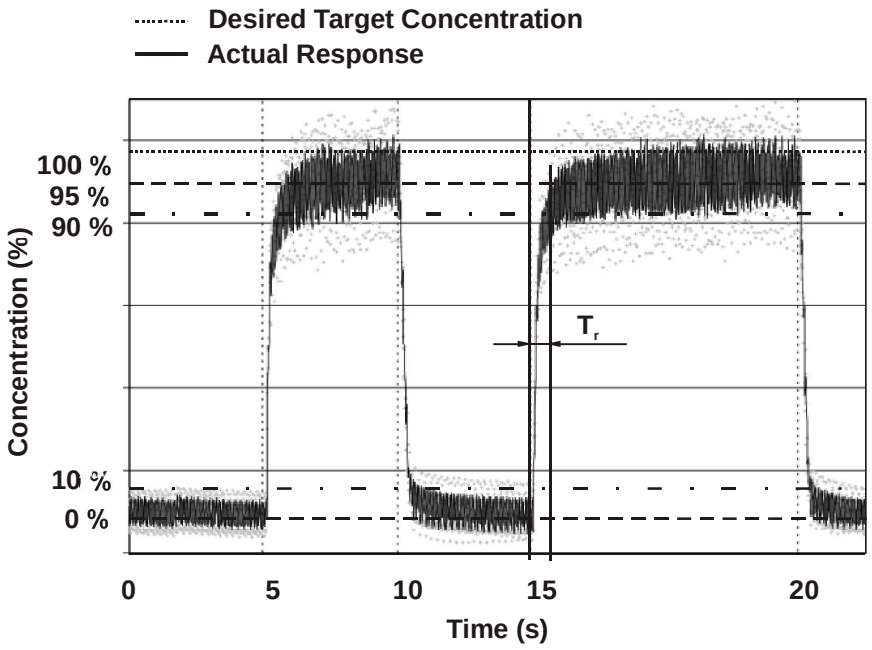

Figure 4. 54: Concentration as a function of time for injection systems

The mean and standard deviation values from these data were used for statistical analysis using the one-way ANOVA and post hoc Tukey's test at a significance level of p = 0.05 with the aim of finding significant differences between two or more group means. The Tukey's test is a post hoc test designed to perform a pairwise comparison of means in order to locate significant differences.

4.4.1 Boom Injection System Measurements

In the measurements of the lag and response times of the boom injection system the gear pump was used to deliver the tracer to the injection point. The proportional regulation valve was used only to open and close the tracer supply line. The control signal of the proportional valve ranged from 0 to 10 V. The following parameters and their effects on the response time parameters were studied:

- Boom pipe diameter
- Boom pipe length
- Carrier flow rate
- Tracer flow rate
- Dynamic viscosity of the tracer

4.4.1.1 Effect of Boom Pipe Diameter

Three configurations of spray booms with inner diameters of 6.0, 8.0 and 12.7 mm were used in the test in order to investigate the influence of different boom diameters on the lag and response times. For the measurements the conductivity sensor was located at the outermost nozzles 1 and 6 (see figure 4.3a). The system pressure was maintained constant at 3.0 bar, which yielded carrier flow rates of Q_c = 590 and 1970 ml min^{-1} when using XR 80015 and XR 8005 nozzles, respectively. For these two measurements the tracer flow rate was maintained constant at 385 ml min^{-1} by means of the PWM valve.

4.4.1.2 Effect of Boom Pipe Length

The effect of the boom pipe length, or rather the distance between the injection point and the nozzles, on lag and response time was studied for two boom pipe configurations with inner diameters of 6.0 and 12.7 mm. The responses of these boom injection systems were measured at all nozzle positions. The carrier flow rate Q_c was maintained constant in a nominal range from 340 to 2540 ml min^{-1}. The tracer flow rate in a range from 270 to 525 ml min^{-1} was determined by the differential pressure and the control valve characteristics. The results were compared with the theoretical estimates obtained from the lag time minimization procedure (see chapter 3.2.2).

4.4.1.3 Effect of Carrier Flow Rate

The influence of the carrier flow rate is related to the concentration of the monitored solution. By combining different spray nozzle sizes (XR 80015, XR 8005) and system pressures (1.0 and 3.0 bar), the carrier flow rate Q_c was set to 340, 590, 1140 and 1970 ml min^{-1}. The tracer flow rate Q_a was maintained constant at 385 and at 525 ml min^{-1}. The lag and response times were measured at the outermost nozzles 1 and 6 of the 6.0 mm boom configuration.

4.4.1.4 Effect of Tracer Flow Rate

The effect of tracer flow rate on lag and response time was studied at constant nominal carrier flow rates of 1140 and 1970 ml min^{-1}. The tracer flow rate varied between 60 and 385 ml min^{-1}. The lag and response times were measured at the outermost nozzles (1 and 6) of the 6.0 mm boom configuration. The rise/fall times, described by the transient curve rising from 10 to 90 % and falling from 90 to 10 % of the step input, respectively, were evaluated together with the response times.

4.4.1.5 Effect of Viscosity

The effect of different tracer viscosities on lag and response times was investigated for a range of three simulated pesticides (water and two aqueous glycerine solutions). The viscosities of the tracers used in the tests were 1, 109 and 219 mPa s. The tracer flow rate Q_a was maintained constant at 60 and 180 ml min^{-1}. For the tracer flow rate Q_a = 180 ml min^{-1}, tests were performed only with water and with tracer with a dynamic viscosity of 109 mPa s. The carrier flow rate through the outermost nozzles Q_c was maintained constant at 1970 ml min^{-1} for both concentrations tested. The lag and response times were measured at the outermost nozzles (1 and 6) of the 6.0 mm boom configuration. The rise and fall times were also evaluated.

4.4.2 Direct Nozzle Injection System Measurements

The lag and response times of both direct nozzle injection systems (injection into a set of six nozzles and injection into individual nozzles) were measured under similar test conditions. Both nozzle injection systems used the diaphragm and the gear pump to deliver the tracer to the injection point; the aim was to investigate the effect of the pump on the dynamic response of the system.

In the system with injection to a set of six nozzles, the control valve was used centrally for all nozzles on the boom pipe. The valve controlled the differential pressure across the metering orifices. The control signal of the valve ranged from 0 to 10 V. The lag and response times were measured at the different nozzles depending on what effect was being investigated. The following parameters and their effects on the response time parameters were studied:

- Metering orifice size
- Chemical rail length
- Carrier flow rate
- Tracer flow rate
- Dynamic viscosity of the tracer

In the system with direct injection into individual nozzles (see Fig. 4.6 a, b) the step change tests were performed only for one nozzle. The studied effects and parameters for that system were:

- Carrier flow rate
- Tracer flow rate
- Dynamic viscosity of the tracer

4.4.2.1 Effect of Metering Orifice Size

For direct injection into a set of six nozzles, the effect of the size of the metering orifice on the response of the system was studied using the rise and fall times. Three different metering orifices of the sizes 4916- 08, 10 and 12 were tested. The carrier flow rate was maintained constant at 340 and 1970 ml min^{-1}, respectively. While the tracer flow rate was set to 10 and 45 ml min^{-1}. The maximum flow rate achieved with the 4916- 08 orifice plate at a differential pressure of 5.0 bar was 45 ml min^{-1}. The diaphragm pump was used for tracer delivery. The rise and fall times were obtained from measurements at the outermost nozzles (N1, N6).

4.4.2.2 Effect of Tracer Rail Length

The effect of the length of the rail used for supplying a tracer (chemical) into several nozzles was studied only for the system with injection into a set of six nozzles. The effect of the length of the rail on lag and response time was studied at three nozzle locations (N1, N3 and N5). Response times were obtained both for the gear pump and the diaphragm pump. Lag and response times were measured for two different carrier flow rates of Q_c = 1140 and 1970 ml min^{-1}. The tracer flow rate Q_a was maintained constant at 10 and 30 ml min^{-1}.

4.4.2.3 Effect of Carrier Flow Rate

The effect of the flow rate of a carrier on lag and response time was measured at the outermost nozzles (N1, N6) for both nozzle injection systems. Measurements were also obtained for both tracer delivery pumps. The carrier flow rate Q_c was stepwise adjusted at 340, 1140, 1970 and 2540 ml min^{-1}, respectively. The tracer flow rate Q_a was maintained at a constant level of 10 ml min^{-1}.

4.4.2.4 Effect of Tracer Flow Rate

The effect of the flow rate (concentration) of a tracer on lag and response times was studied at the outermost nozzles (N1, N6). The tests were performed for nozzle injection system using the diaphragm pump as well as for the system using the gear pump. The carrier flow rate was maintained constant at 1140 and 1970 ml min^{-1}. The tracer flow rates were set to 10, 30 and 50 ml min^{-1}, which provided a range of spray solution concentrations from 101 to 840 ppm of NaCl per nozzle.

4.4.2.5 Effect of Viscosity

Lag and response times for a range of viscous aqueous glycerine solutions were obtained for both nozzle injection systems under the same measurement conditions. The dynamic viscosity of the tracers used was 1 mPa s for water and 60 and 219 mPa s for the aqueous glycerine solutions. The times were measured only for the injection system using the gear pump at the outermost nozzles (N1, N6). The tracer flow rate Q_a was maintained constant at 10 and 30 ml min^{-1} by a CP 4916-10 metering orifice. The carrier flow rate Q_c through the outer nozzles was maintained constant at 1970 ml min^{-1} for both tracer concentrations.

5. Results

5.1 Viscosity of Glycerine Solutions

Figure 7.1 shows the relationship between the solution concentrations and dynamic viscosities of the tested aqueous glycerine solutions as measured by means of a rotational viscometer at a constant liquid temperature of 20° C. The resulting curve is compared with reference values from chemical tables (GUSTAV HEESS, 2002). It was found that the measured viscosities of the glycerine solutions corresponded to the reference values. The viscosities increased rapidly at glycerine concentration above 80%.

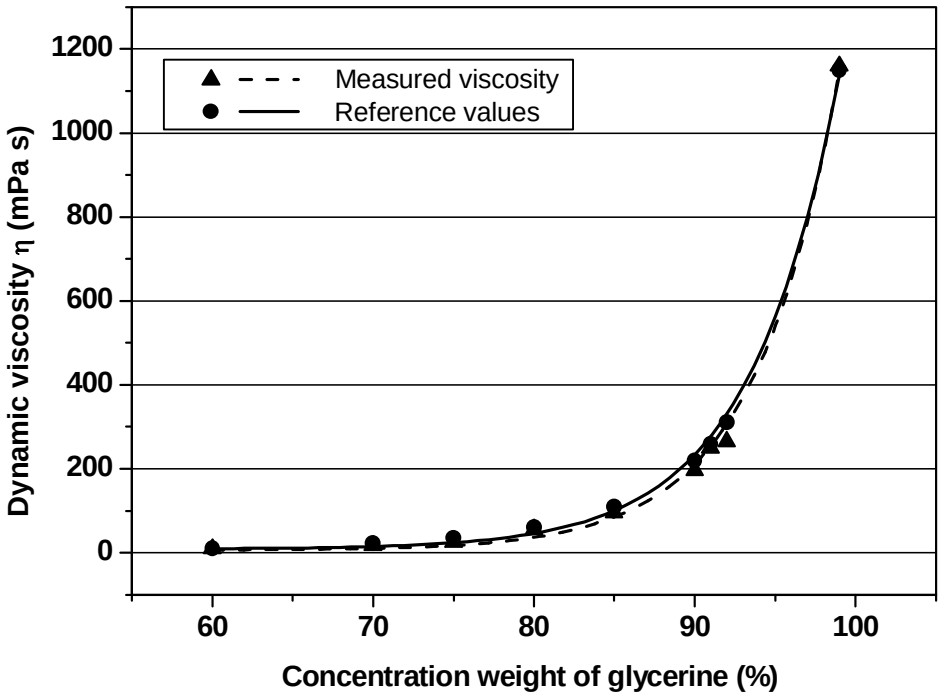

Figure 5. 50: Dynamic viscosities of aqueous glycerine solutions with different concentrations; measured at 20° C constant liquid temperature

As regards the range of viscosities of the most widely used herbicide products, tap water (~1 mPa s) and three aqueous glycerine solutions with the following concentrations: 80 % (60.1 mPa s), 85 % (109 mPa s) and 90 % (219 mPa s) were selected for tests. The aim of the tests is to investigate the influence of liquid viscosity on response time and to determine the flow characteristics of the flow regulators used.

The density values of the tested glycerine solutions measured with a pycnometer are listed in table 5.1 together with both types of viscosity.

Table 5. 3: Resulting viscosity values and densities of tested aqueous glycerine solutions

Concentration weight [%] glycerine	Dynamic viscosity measured at 20°C (mPa s)	Dynamic viscosity - reference values 20°C (mPa s)	Density [g/cm^3]	Kinematic viscosity (mm^2/s)
60	9.6	10.8	1.151	8. 4
70	17.4	22.5	1.178	14.8
75	25.7	35.5	1.192	21.6
80	56.1	60.1	1.205	46.5
85	95.3	109	1.219	78.2
90	197.4	219	1.232	160.2
91	249.4	259	1.235	202.0
92	265.9	310	1.237	214.9
99	1160.0	1150	1.255	924.0

Source of dynamic viscosity reference values: GUSTAV HEESS, 2002

5.2 Calibration of Flow Regulation Components

5.2.1 Flow Characteristics of Tracer Supply Pump

The delivery characteristics of the gear pump are shown in figure 5.2. The maximum flow rate of 1.38 l min^{-1} was achieved at 0 bar differential pressure, and the maximum achieved revolutions were 3820 min^{-1}. The maximum standard deviation (SD) of the flow rate was 0.006 l min^{-1}. The maximum differential (delivery) pressure was 9 bar.

The delivery characteristics of the diaphragm pump are shown in figure 5.3. The average flow rate resulting from four iterations corresponds to the nominal values specified in the pump's data sheet. The maximum standard deviation was 0.26 at a maximum flow rate of 20 l min^{-1}. The high fluctuations in the flow rates were due to pump pulsation at lower differential pressures, which were adjusted by a pressure relief valve. The revolutions have no significant effect on the standard deviation.

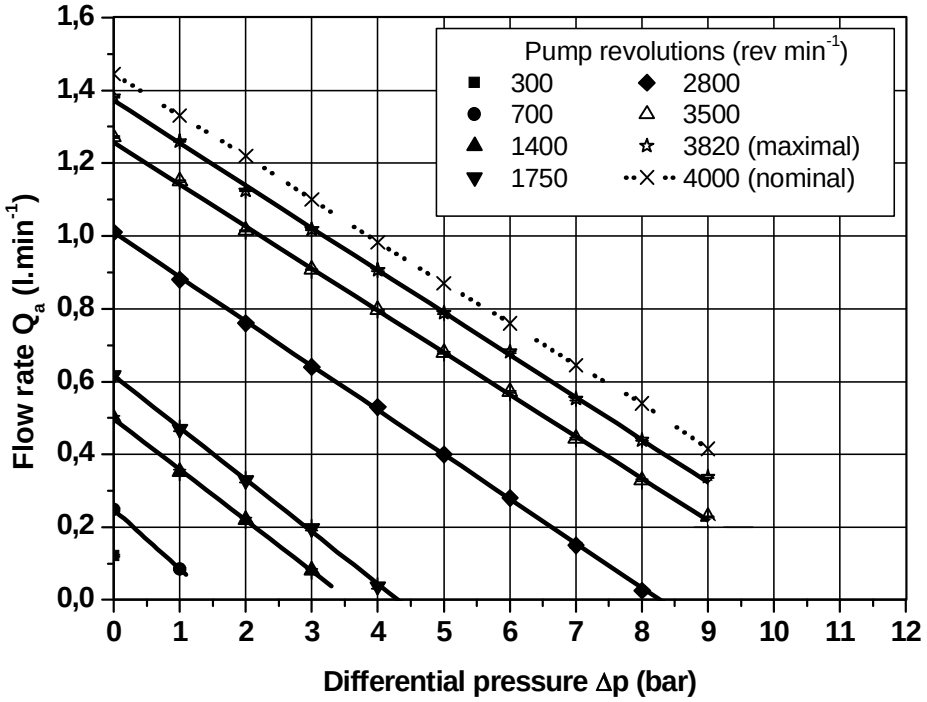

Figure 5. 51. Delivery characteristics of the metering gear pump, P-series (Tuthill Co.)

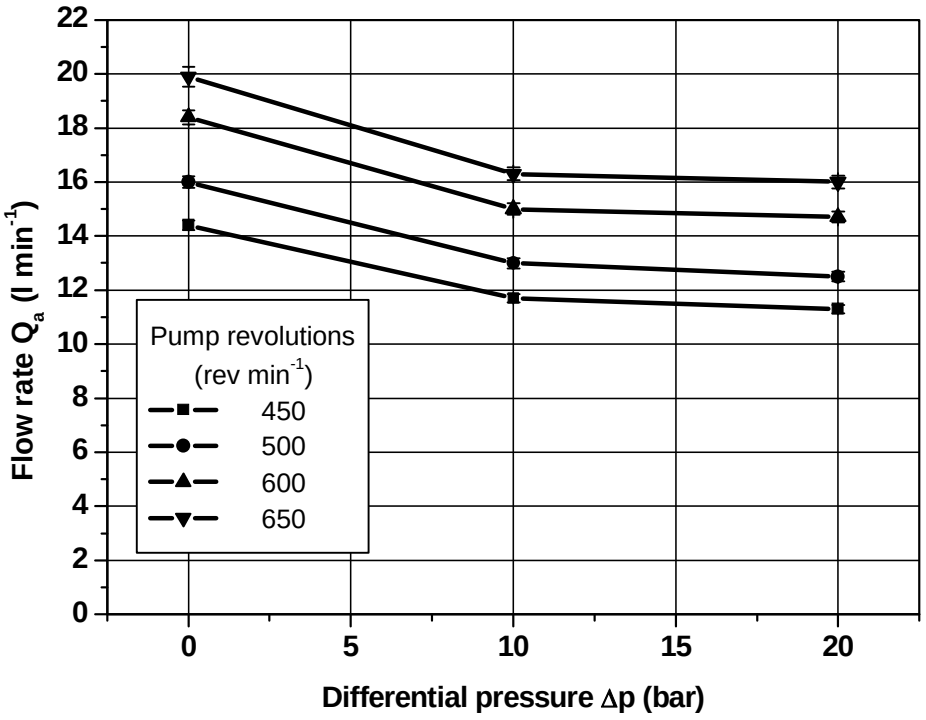

Figure 5. 52. Delivery characteristics of the two-diaphragm pump, AR 202 SP (Annovi-Reverberi)

5.2.2 Proportional Regulation Valve Characteristics

The obtained proportional valve characteristic is plotted in figure 5.4 together with the nominal curve. The valve has an almost linear characteristic. There were some deviations from the nominal curve beyond the allowed range defined in the valve specification data sheet. Such errors were probably caused by the low sensitivity of the valve's actuators to the control signal in the lower range (from 0 to 5 V), which is evinced by the fact that the measured curve is steeper. Moreover, the average maximal flow rate measured was 392.8 ml min^{-1}, which is about 30 % higher than the nominal value. Such a deviation can be accepted with regard to the required flow rates and valve size (small orifice diameter). The discrepancy between the performance curves measured by the opening and closing of the valve was identical to the discrepancy between the nominal curves.

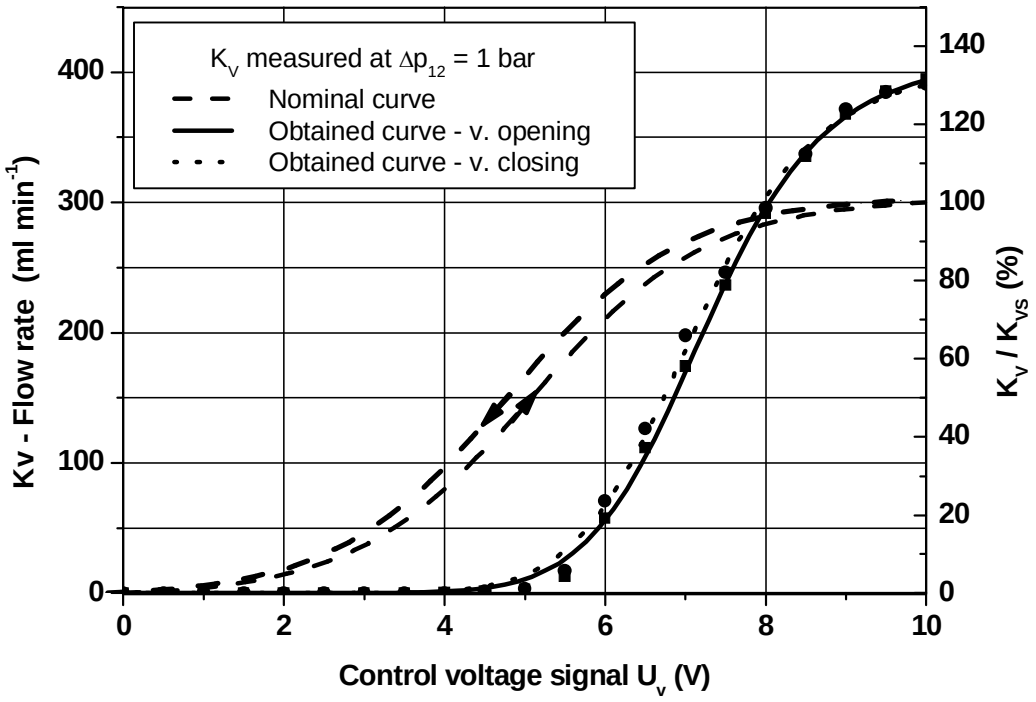

Figure 5. 53: Proportional regulation valve characteristic (type 6022 00-A00 8 NC) in comparison with the nominal curves

The performance curves of the tested valve for water and aqueous glycerine solution (viscosity = 219 mPa s) at various differential pressures Δp_{12} are plotted in figures 5.5 and 5.6, respectively.

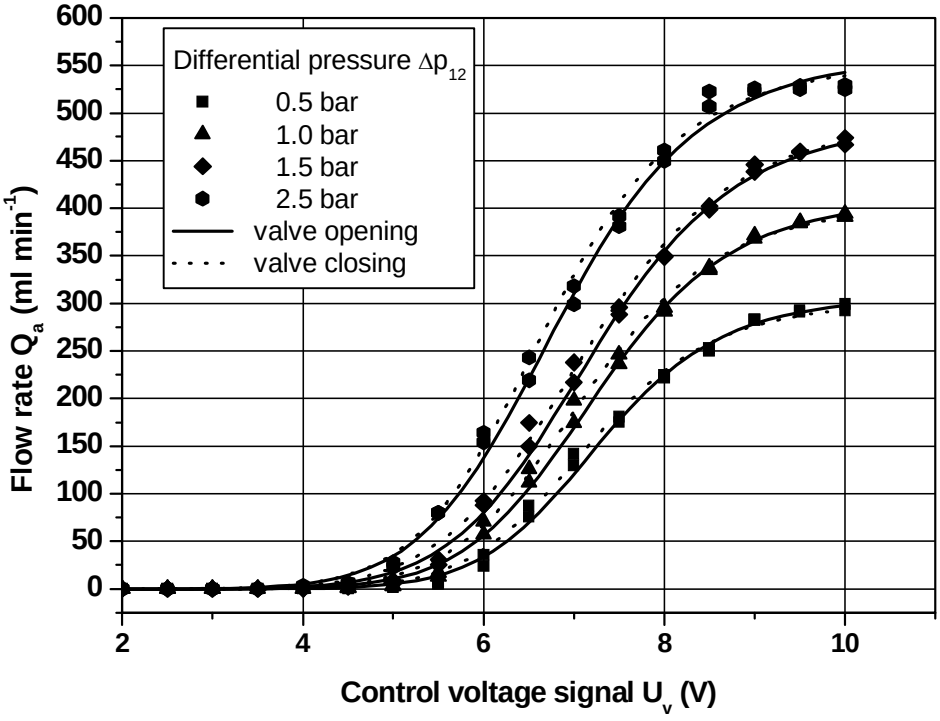

Figure 5. 54: Performance curves of the investigated valve at various differential pressures (for water)

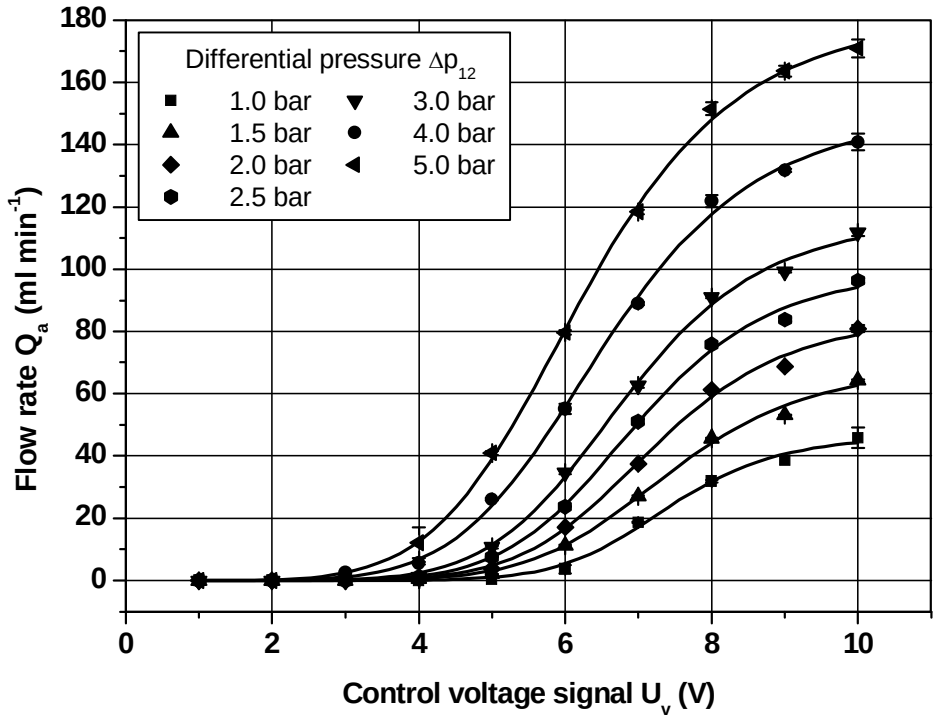

Figure 5. 55: Performance curves of the investigated valve at various differential pressures (for aqueous glycerine solution with a dynamic viscosity of 219 mPa s)

As is evident in the graphs, the maximum flow rate was obtained at maximum differential pressure and at maximum valve stroke (10 V). For water the differential pressure was set by degrees from 0.5 to 2.5 bar. The maximum flow rate of 525.0 ml min^{-1} with a standard deviation of 4.32 was obtained at 2.5 bar. For the glycerine solutions the differential pressure was set by degrees from 0.5 to 5.0 bar. In this case, the flow rate was significantly lower. The maximum flow rate of 170.9 ml min^{-1} was obtained at 5.0 bar. The maximal standard deviation was 2.87.

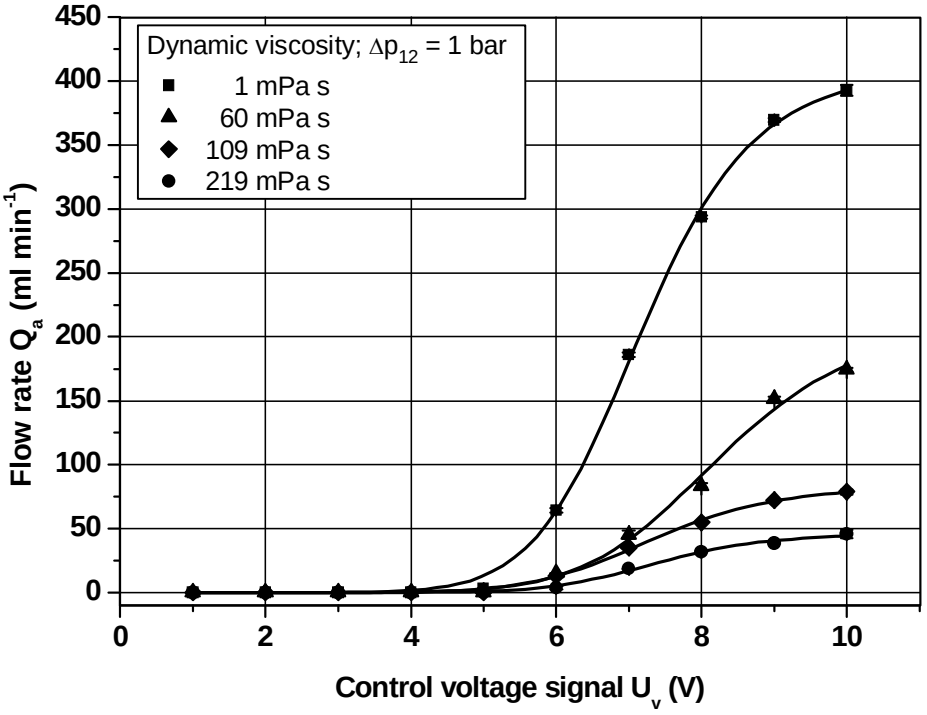

Figure 5. 56: *Performance curves of the investigated valve for liquids with different dynamic viscosities (water and aqueous glycerine solutions with 60, 109 and 219 mPa s; Δp_{12} = 1bar)*

A comparison of the performance curves for various test liquids at a differential pressure of 1 bar is presented in figure 5.7. For all liquids tested, the standard deviations were highest at the maximal flow rates. At 4.1 ml min^{-1} the error was largest for water, whereas the maximal standard deviations for aqueous glycerine solutions with dynamic viscosities of 60, 109 and 219 mPa s were 3.26, 2.06 and 3.28, respectively.

For controlling the tracer flow rate, the voltage-flow rate characteristic must be determined mathematically for each calibration curve. The sigmoidal curves can be defined by the Logistic function:

$$Q_a = \frac{A_1 - A_2}{1 + \left(\frac{U_v}{U_0}\right)^b} + A_2 \tag{5.1}$$

where:

Q_a = Tracer flow rate (l min^{-1})

U_v = Control voltage (V)

U_0, A_1, A_2, b = Parameters

The resulting flow rate characteristics for the complete boom injection system at a constant carrier pressure are shown in figure 5.8. The tracer flow rate characteristics are reciprocal to those obtained from differential pressure measurements (Fig. 5.5). The curves can be defined using the same Logistic function (4.5) as was used for the differential pressure characteristics.

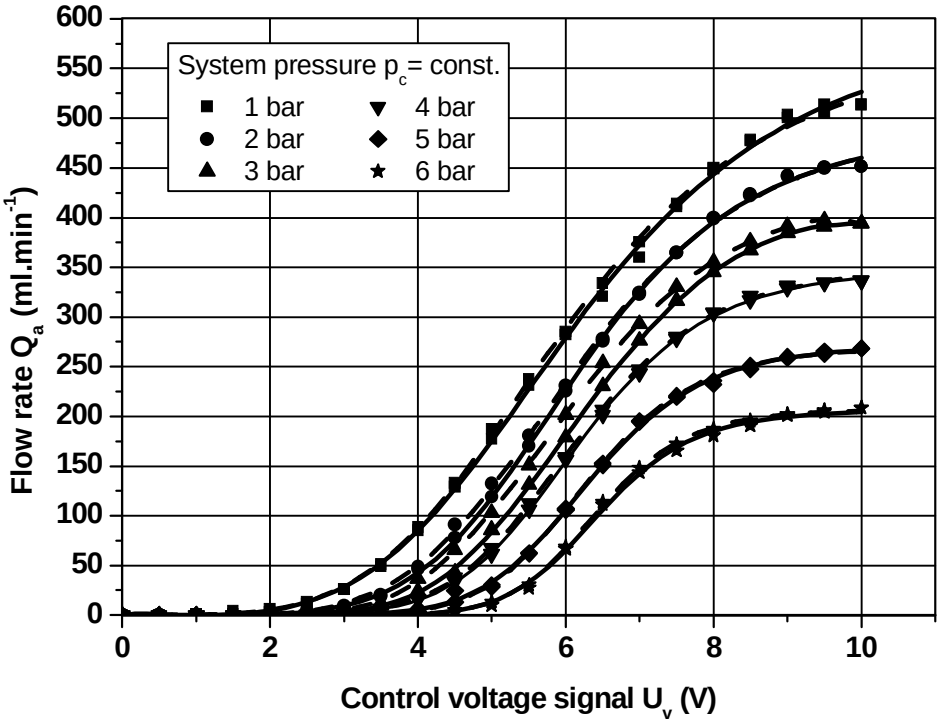

Figure 5. 57: Performance curves of investigated valve for water at constant carrier pressure

The flow rate characteristics are comparable to the differential pressure characteristics with determining differential pressure from figure 5.9, where $\Delta p_{1c} = p_c - p_1$, or directly from figure 9.4 in the appendix. The average flow rates were reduced slightly by 15 ml min^{-1} due to the pressure drop in the check valve Δp_{23}. The largest error (SD) was being 3.8 ml min^{-1}. The pressure drop Δp_{23} ranged from 0.14 to 0.33 bar, depending on the actual flow rate.

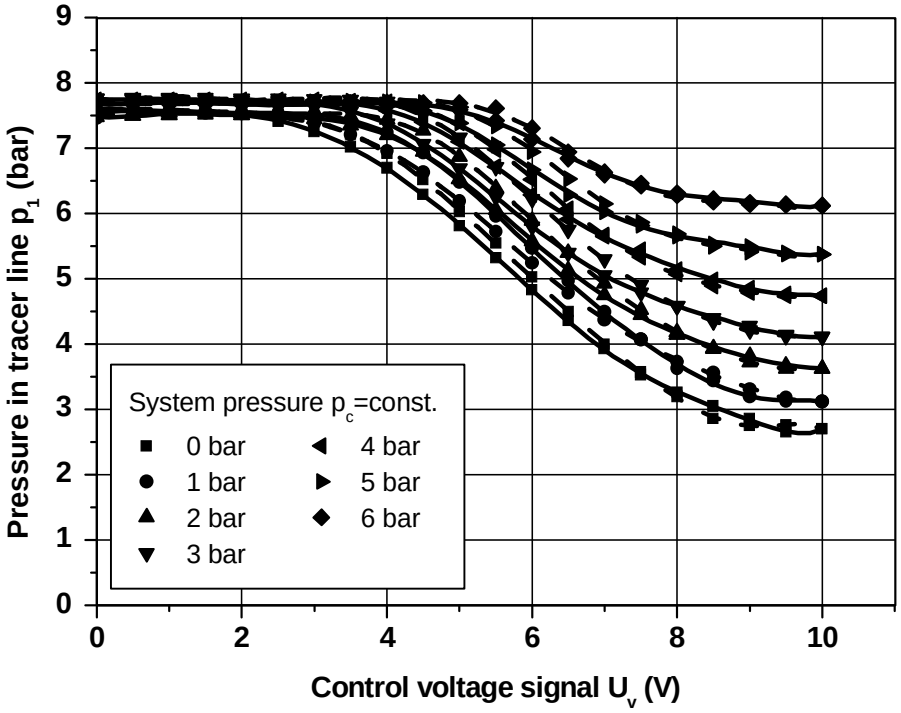

Figure 5. 58: Course of pressure p_1 in the tracer line at valve opening (measured at constant system pressure p_c)

5.2.3 Calibration of Orifice Plates

The minimum flow rate of water 13.0 ml min^{-1} was obtained with using the smallest orifice 4916-08 at 0.5 bar differential pressure as shown in figure 5.10. The maximal flow rate measured was 44.8 ml min^{-1} at 5.0 bar differential pressure. After four measurement iterations, the maximum standard deviation was 1.84 ml min^{-1}. The general relation between the flow rate and the differential pressure across the orifices and liquids tested is described by a polynomial square function.

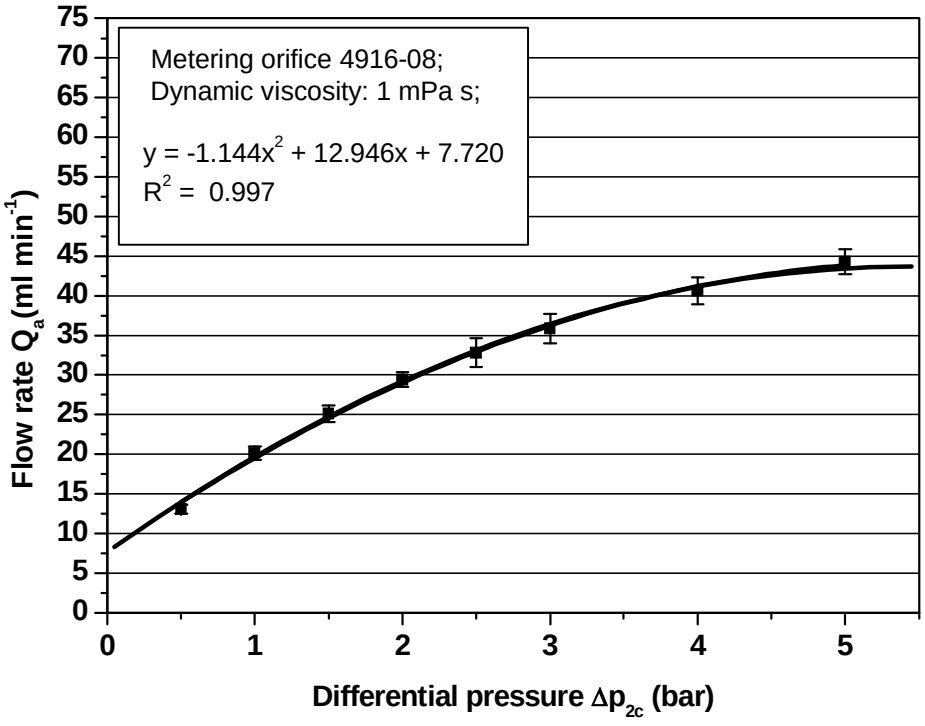

Figure 5. 59: CP4916-08 metering orifice performance across the range of differential pressures; measured for pure water

The effect of the fluid viscosity on the orifice flow rate is shown in figures 5.11 and 5.12. With increasing viscosity, the orifice flow rate decreases significantly. The minimum orifice flow rate measured for orifice size 10 and an aqueous glycerine solution with a dynamic viscosity of 219 mPa s was 3.86 ml min^{-1}, with a standard deviation error of 0.97 ml min^{-1}. This is almost 6.5 times less compared with flow rates measured for pure water. The results of the calibration measurements show that it is almost impossible to cover the whole range of flow rates with one orifice size. The ratio between maximum and minimum flow rate depends on the given orifice size, the range of differential pressures and on the viscosity. If liquids with different viscosities within the same pressure range are compared, the flow rate ratio changes significantly. For example, for orifice size 10 (see Fig. 5.11) the ratio for water can be determined to be 1:3. For the more viscous solutions with $\eta \sim 60$, 109 and 219 mPa s the ratios were higher, with 1:4, 1:6 and 1:7 respectively. The flow rate characteristics for orifice sizes 16 and 20 are shown in figures 9.5 and 9.6 in the appendix.

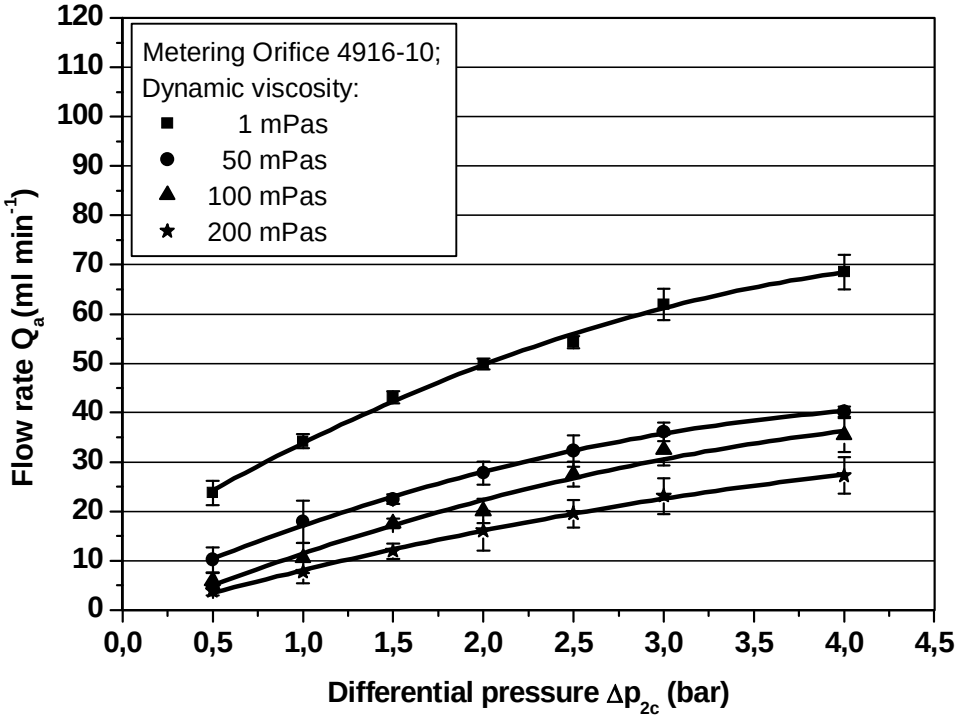

Figure 5. 60: CP4916-10 orifice plate performance across a range of differential pressures and dynamic viscosities

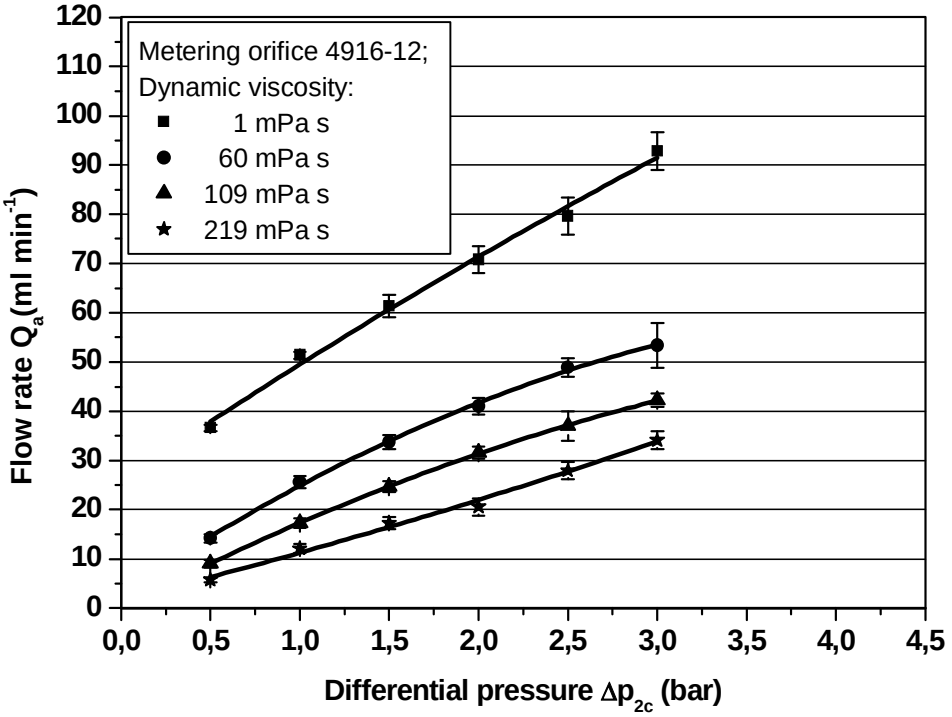

Figure 5. 61: CP4916-12 orifice plate performance across a range of differential pressures and dynamic viscosities

The resulting flow rate uniformity values along the boom are presented in the following figures. In figure 5.13 are showed the flow rates of pure water flowing through a set of orifice plates with sizes 8, 16 and 20 are shown. During the measurements the differential pressure Δp_{23} was kept constant at 1 bar. The flow rate sample patterns obtained were very uniform. The largest CV was 12.41 % for orifice size 20. Sample pattern uniformity values with a CV less than 10 to 12 % can generally be considered as very good. Patterns with CVs greater than 15 % are unacceptable.

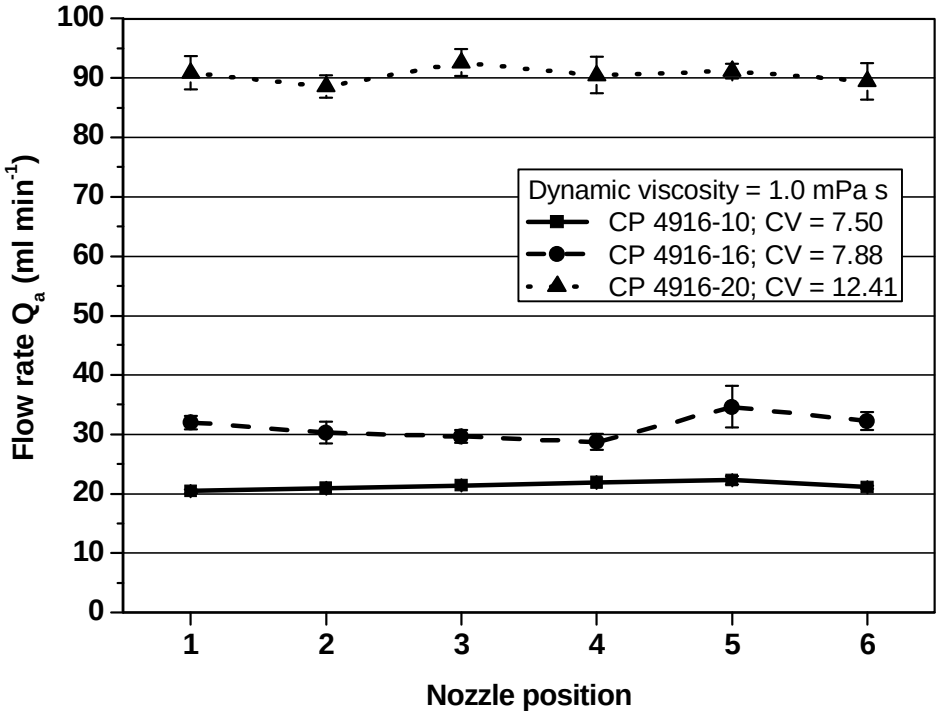

Figure 5. 62: Boom performance for set of six orifice plates; measured for pure water at Δp_{2C} =1bar

For purposes of comparison, the same measurements were performed with aqueous glycerine solutions. The results are shown in figure 5.14 and 9.7 in the appendix. From the graphs it is evident that there are significant differences among the flow rates across the bigger orifices if highly viscous fluids are injected. The largest CV value of about 21.61 % was determined for orifice size 20 and a 90 % glycerine concentration (η = 219 mPa s). This value is not acceptable for uniform herbicide application. A flow rate deficiency through the outer orifice plates (no. 1 and 6.) was caused partially by a pressure drop in the tubes, when the viscous liquids were tested. Another possibility is that the performance of the pump was marginally too low for the desired process conditions.

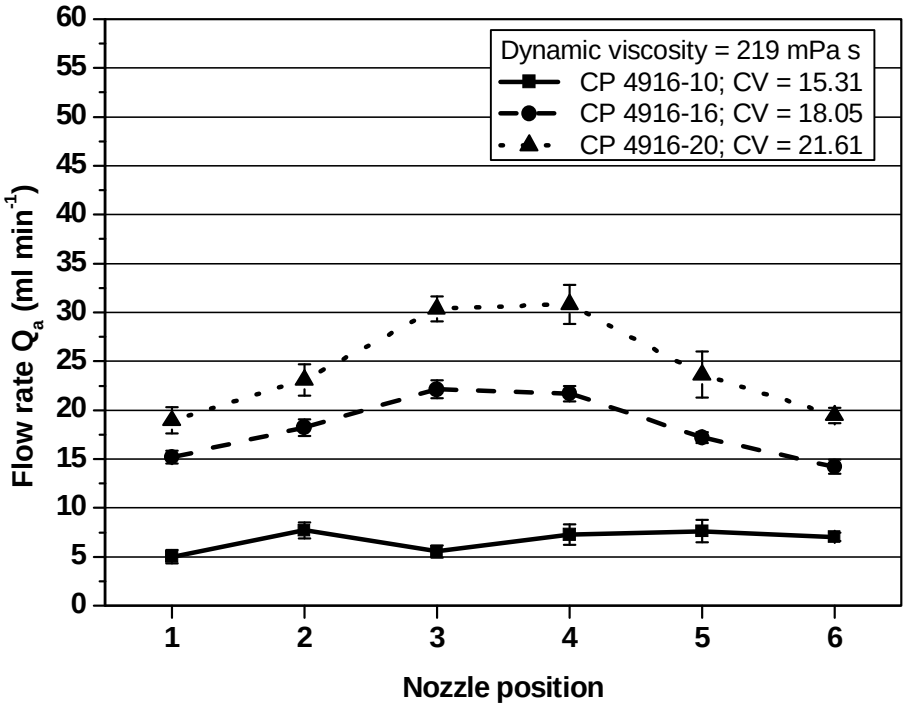

Figure 5. 63: Boom performance for set of six orifice plates; measured for aqueous glycerine solution (219 mPa s) at Δp_{2C} =1bar

For a better overview of the effect of viscosity on the flow rate, flow rates of water and two aqueous glycerine solutions through the CP4916-12 orifice plates at 1 bar differential pressure are compared in figure 5.15. The largest coefficient of variation value of about 8.01 % was found for the aqueous glycerine solution with a dynamic viscosity η = 219 mPa s. For water the CV was about 1.31 %.

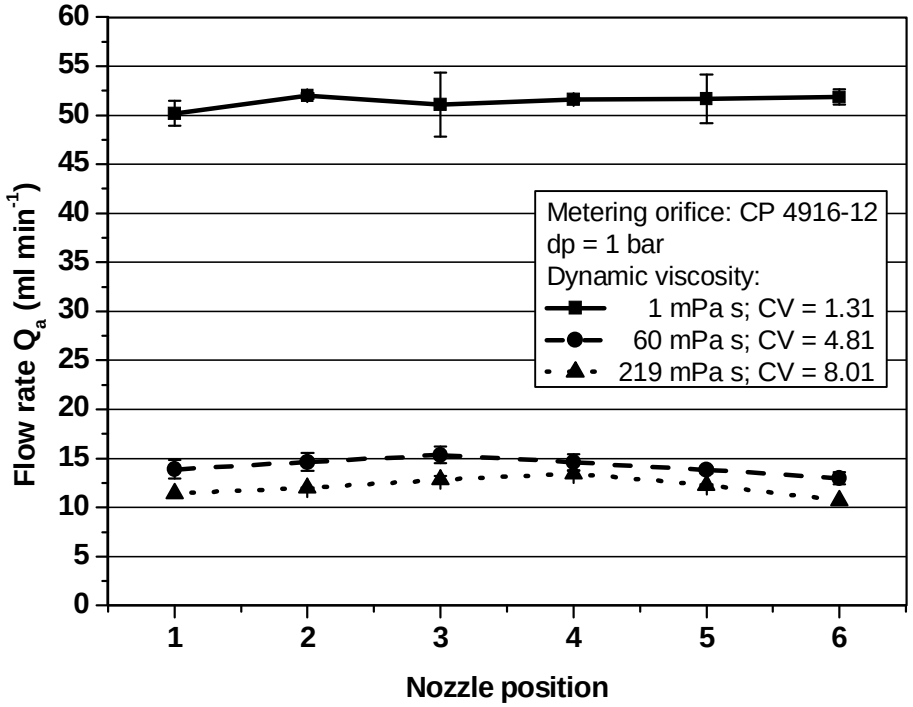

Figure 5. 64: Boom performance for set of six orifice plates C4916-12; measured for pure water and aqueous glycerine solutions (60 and 219 mPa s) at Δp_{2C} =1bar

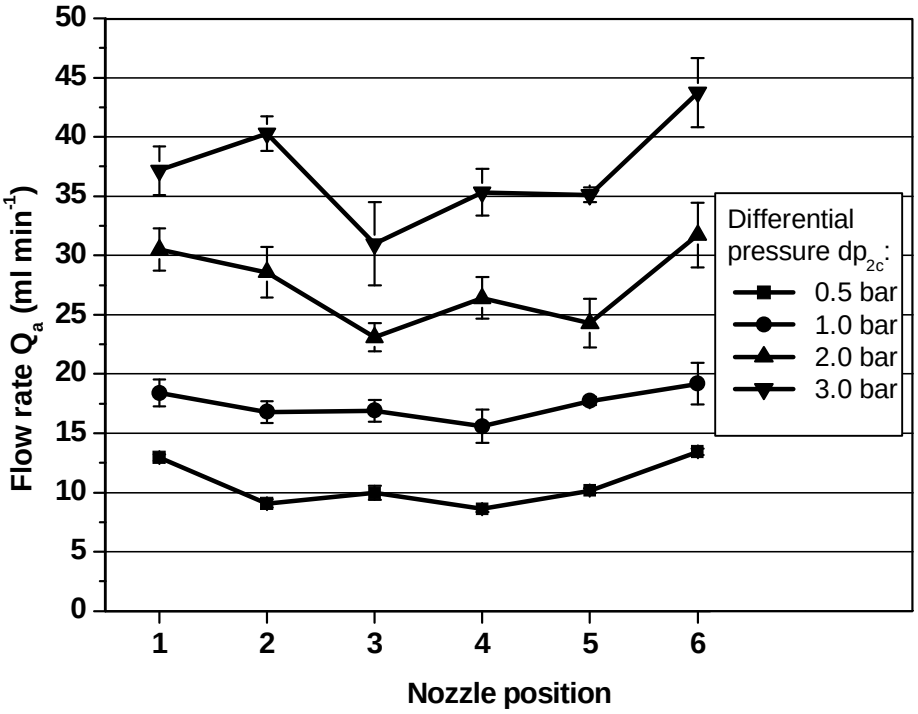

Figure 5. 65: Boom performance for set of six C4916-10 orifice plates across a range of differential pressures Δp_{2C}; measured for aqueous glycerine solution (60 mPa s)

Figure 5.16 shows the flow rates of an aqueous glycerine solution with a dynamic viscosity of about 60 mPa s measured for the CP4916-10 orifice plates at various differential pressures. The variations in flow rate among the orifices were higher at higher differential pressures. These non-uniformities may be due to the fact that the gear pump was performing at maximum load. The CVs for all events measured did not exceed 15 %; for differential pressures of 0.5, 1.0, 2.0 and 3.0 the CVs were 8.9, 7.5, 12.5 and 11.97 % respectively. The slightly higher variation in flow rates among the orifices evinces similar characteristic as the characteristic obtained for water, which is shown in figure 9.8 in the appendix.

5.2.4 Calibration of Differential Pressure Flow Meter

The signal from the differential pressure sensor was calibrated to provide data in ml min^{-1}. The accuracy of the flow meter was found to be within ± 2.5 % of the measured flow. An example of the calibration results is shown in figure 5.17.

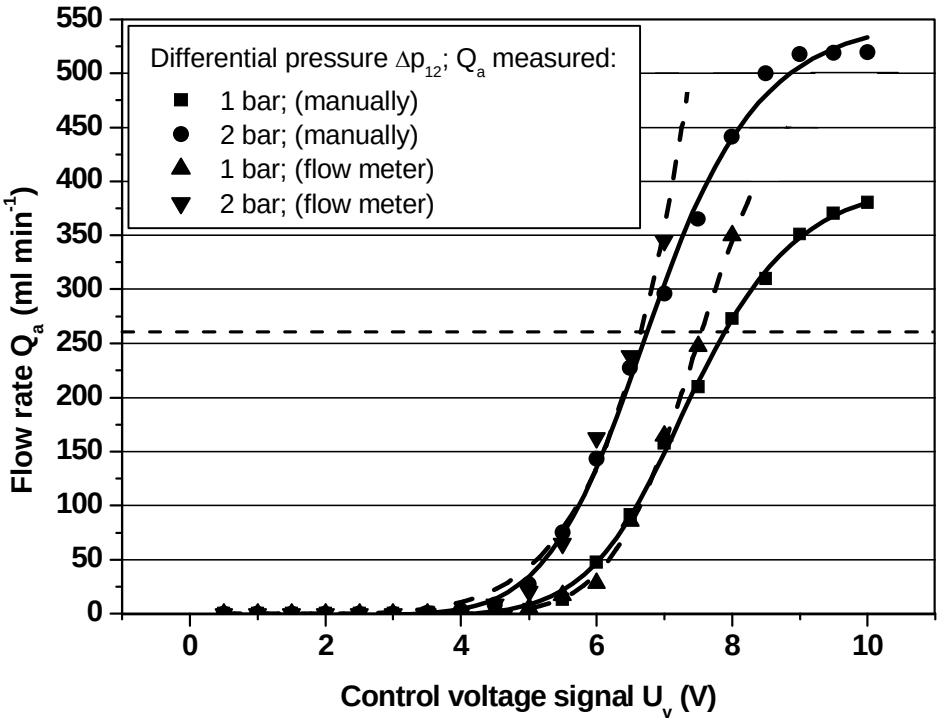

Figure 5. 66: Calibration of differential pressure flow meter; measured for water, R = 1.35 mm

From the calibration curves obtained by measuring the flow rate of water with a capillary (R = 1.35 mm), at various differential pressures across the proportional valve, it is evident that the flow meter can measure a maximum flow rate of 260 ml min^{-1}. It cannot be used to measure higher flow rates because of an error that is probably caused by non-laminar flow in the capillary.

5.2.5 Calibration of Spray Nozzles

In figure 5.18 the calibrated average flow rates and standard deviations of numbered nozzles are compared for boom pipe diameter configurations of 12.7-12.7-12.7-12.7 and 8-8-6-6 mm. The results are also listed in the appendix in tables 9.4 and 9.6 together with the results obtained for the 8-8-8-8 mm boom pipe diameter configuration. The results are also compared with the nominal flow rates of the nozzles (appendix, table 9.5).

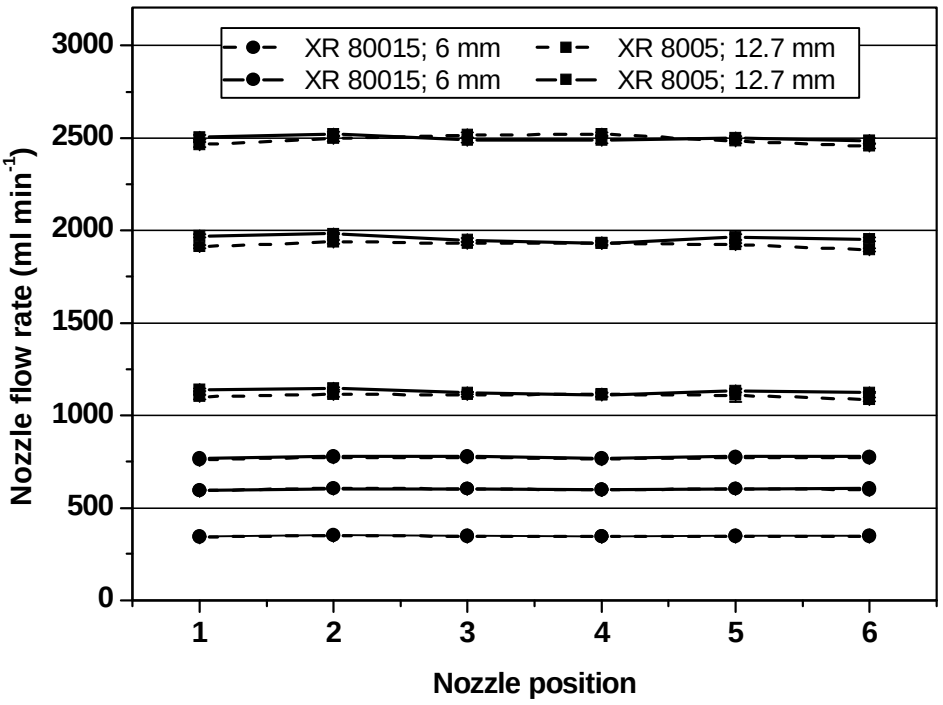

Figure 5. 67: Nozzle flow rate calibration

The minimum carrier flow rate of about 340 ml min^{-1} was obtained with XR 80015 nozzles at a system pressure of 1 bar. The maximum flow rate of approximately 2500 ml min^{-1} was achieved with XR 8005 nozzles at a system pressure of 5 bar. The maximum standard error obtained for one nozzle was 19.6 ml min^{-1}.

The uniformity of the nozzle flow rate along the boom was determined by the coefficient of variation. The maximal CV value obtained was 1.09 % for the smallest boom pipe diameter configuration 8-8-6-6 mm. In figure 5.19 the flow rates of XR 8005 nozzles at a system pressure of 5 bar are compared for all three boom configurations. It can be seen from figure that there is a flow rate drop in the outer nozzles because of the reduction in the pipe diameter. However, the maximum allowable nozzle output variation of 5 % was not exceeded.

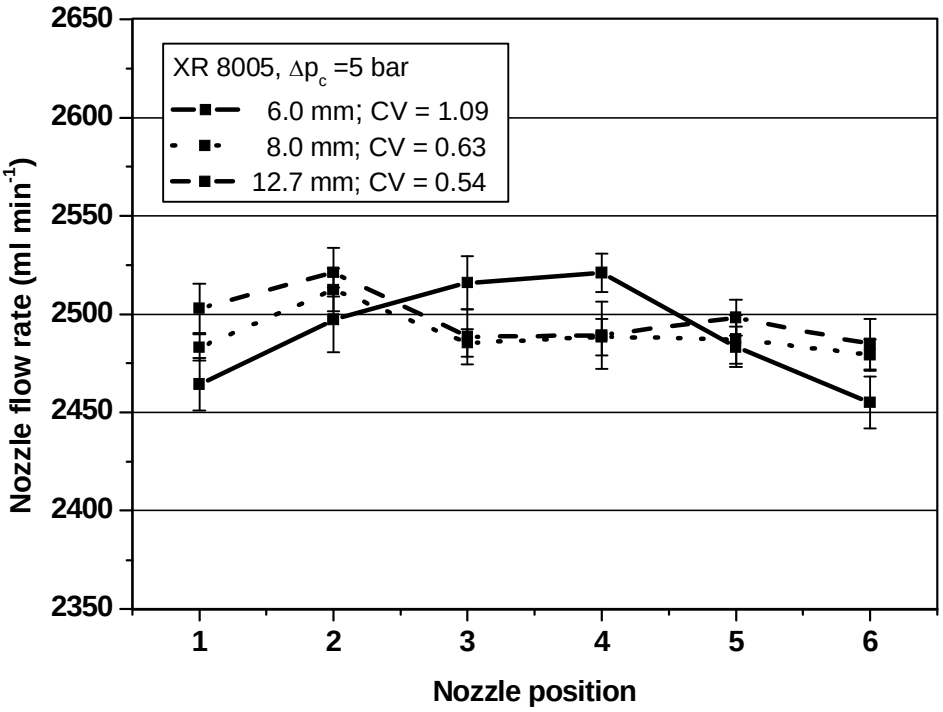

Figure 5. 68: Comparison of different boom pipe diameter configurations

5.3 Calibration of Chemical Concentration Measurements

5.3.1 Nozzle Flow Rate

In table 5.2 the nominal flow rates in nozzles used at nominal pressures are compared with the calibrated average flow rate values of the nozzles (at position 1, 3 and 5). The measured standard deviation tends to increase with increase of the nozzle flow rate.

Table 5. 4: Nominal and calibrated nozzle flow rates

Nozzle size	System pressure (bar)	Nominal flow rate (ml min^{-1})	Calibrated nozzle flow rate					
			Nozzle 1 (ml min^{-1})	SD (-)	Nozzle 3 (ml min^{-1})	SD (-)	Nozzle 5 (ml min^{-1})	SD (-)
XR 80015	1	340	344.5	0.7	349.6	0.7	348.7	1.5
	3	590	595.5	2.2	603.5	4.6	602.8	3.3
	5	760	766.6	4.6	779.4	8.7	776.1	4.1
XR 8003	1	680	515.2	2.7	511.8	3.8	496.5	4.5
	3	1180	1072.0	5.9	1069.9	8.7	1103.0	7.8
	5	1520	1529.0	6.4	1495.3	7.1	1438.4	6.5
XR 8005	1	1140	1138.5	6.0	1121.2	7.0	1133.1	9.1
	3	1970	1969.7	7.9	1947.6	10.8	1963.6	13.6
	5	2540	2502.9	12.6	2488.6	14.0	2498.3	9.3

5.3.2 Conductivity Sensor Calibration

The calibration curve (Fig. 5.20) for the relationship between the conductivity sensor output voltage U_C [V] and concentration c [ppm] was obtained experimentally. The resulting calibration equation for the calibration solution used was:

$$U_C = 1.05 + 2.84e^{(-\frac{c}{2796.7})} + 2.0e^{(-\frac{c}{503.2})} \tag{5.2}$$

The results from the conductance method showed an exponential relation between electric resistance, which depends on the concentrations of salt mixture ranging from 0 to 13000 ppm, and output voltage U_C [V]. The mean output voltages ranged from 1 to 6 V with maximum SD values of 0.35. The quality and especially the temperature of the water used as carrier have an influence on the electrical conductivity of the mixture. If the temperature is not kept constant there is a shift in the calibration curve.

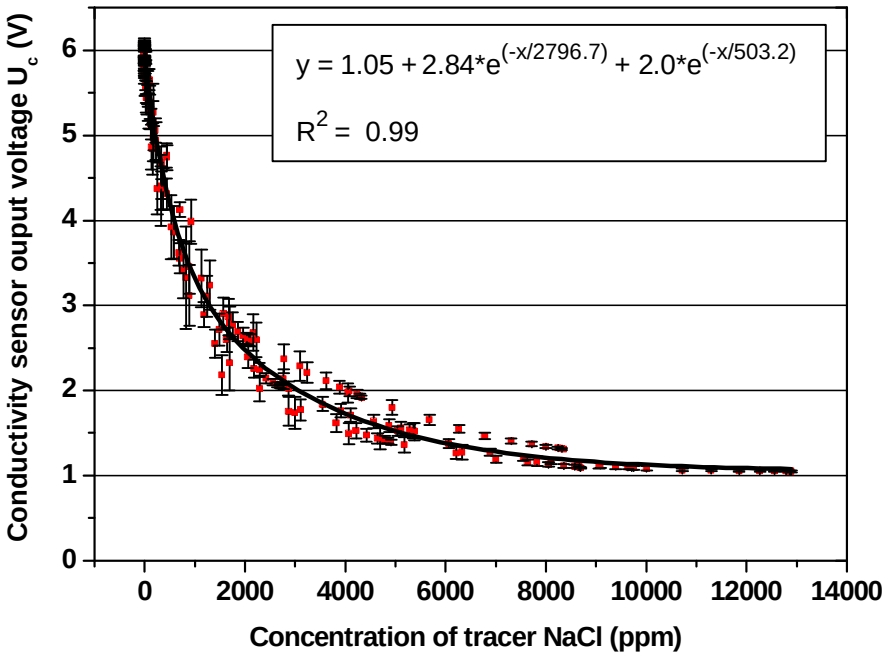

Figure 5. 69: Conductivity sensor calibration curve

5.3.3 Light Transmittance Sensor Calibration

As is evident in the calibration curve of the light transmittance sensor (Fig. 5.21), the relation between the output voltage from the photodiode U_D [mV] and the mixture concentration is an exponential function. The calibration curve has the same decreasing course as the curve obtained by the conductivity method. The resulting calibration equation for the calibration solution used was:

$$U_D = 8.95 + 364.13e^{(-\frac{c}{6.37})} \tag{5.3}$$

The colorant concentrations ranged from 0 to 32.5 ppm. The mean output voltage value was lowest at 11.6 mV when the mixture concentration was highest. The highest mean output voltage value 379.7 mV was obtained at zero concentration of tracer in the solution. The standard deviation values were in the range of 0.28 to 19.6. The occurrence of otherwise negligible air bubbles in the nozzle supply lines had an influence on the intensity of light transmission through the cell. In combination with dose pulsation it can cause excessive deviations of the output voltage.

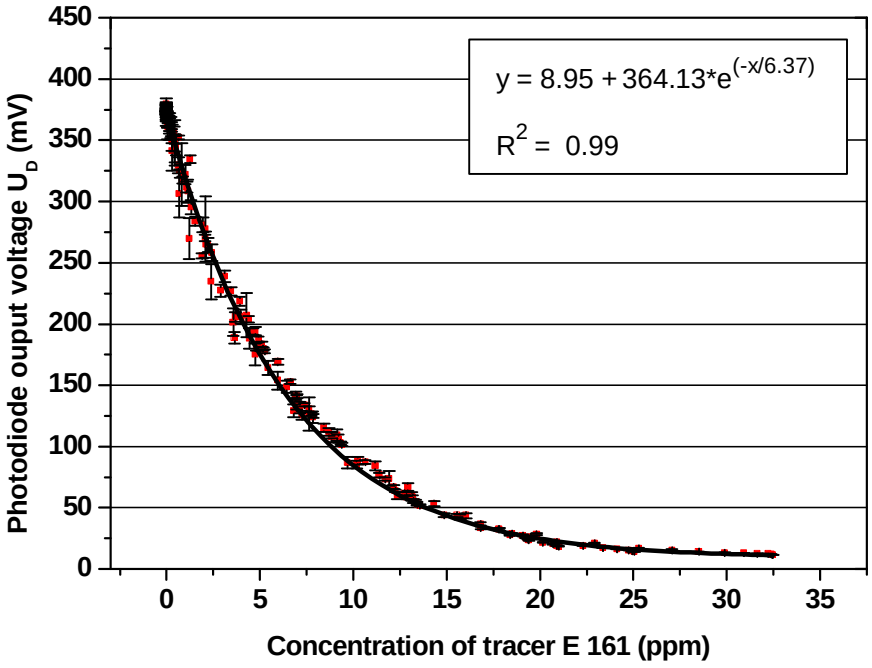

Figure 5. 70: Light transmittance sensor calibration curve

5.3.4 CCD Camera Calibration

For the CCD camera method static calibration was performed, and the concentrations of the colorant were higher than in the light transmittance method. These trials resulted in a calibration curve of the device (figure 5.22) which is based on the average values of samples of known concentrations ranging from 0 to 3750 ppm of E133. There is an exponential decay relation between the mixture concentrations *c* and the mean value of grey levels *(IOD)* of monochromatic images obtained with the camera (equation 5.4):

$$IOD = 45.83 + 276.65e^{\left(-\frac{c}{329.26}\right)} + 54.26e^{\left(-\frac{c}{47.91}\right)} \tag{5.4}$$

Even if, the most common sources of error (dirty cuvettes, poorly mixed solutions, poor pipetting techniques and inadequate light sources) were minimized the standard deviation values within three replications were in the range of 0.43 to 2.94. Additionally, the standard deviation from the mean value of each image can be obtained by means of image analysis software.

This SD value provides information about the mixture uniformity of the solution in the cuvette. The standard deviations related to mixture uniformity were in the range of 1.39 to 2.57.

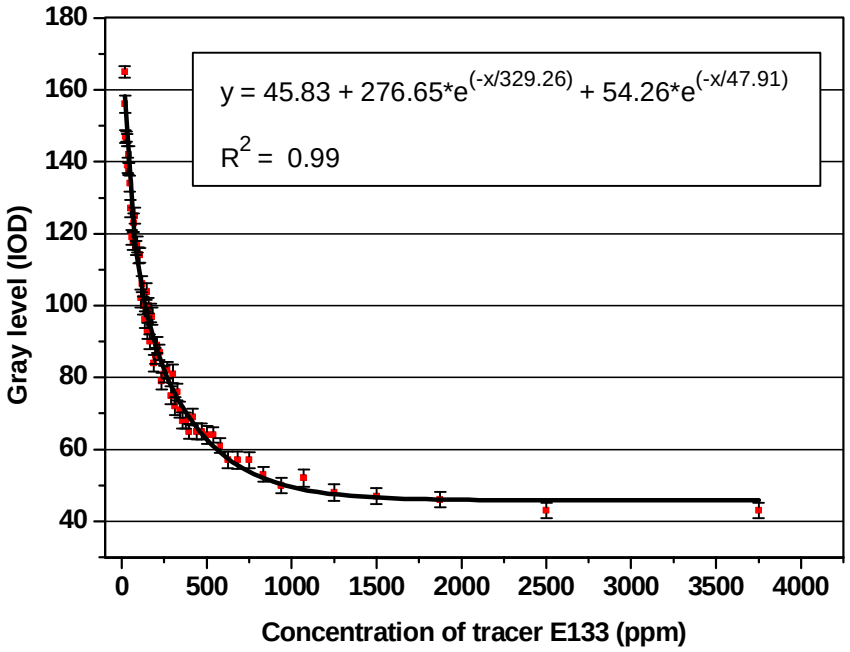

Figure 5. 71: CCD camera calibration curve

5.4 Results of Response Time Measurements

The dynamic response results presented in the following chapters do not cover the whole range of measurements that were carried out. The selected results describe the different effects related to the response time of the metering system in an exemplary way.

5.4.1 Response Times of Boom Injection System

5.4.1.1 Effect of Boom Pipe Diameter

Figures 5.23 and 5.24 illustrate the effect of the boom pipe diameter on the lag and response time. The average results, obtained at outermost nozzles (N1 and N6), are summarized for three different boom pipe inner diameters. The system pressure was 3.0 bar, which gives carrier flow rates of Q_c = 590 and 1970 ml min^{-1} when using XR 80015 and XR 8005 nozzles, respectively. The tracer flow rate was maintained constant at 385 ml min^{-1} for these two measurements.

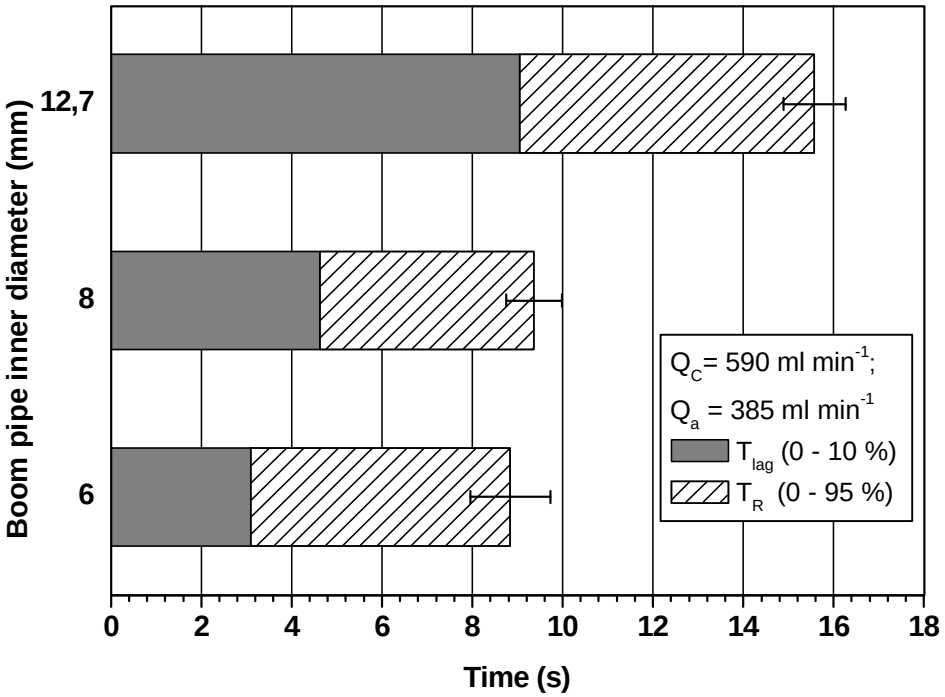

Figure 5. 72: Lag and response times for different boom pipe diameters; Q_c = 590 ml min^{-1}

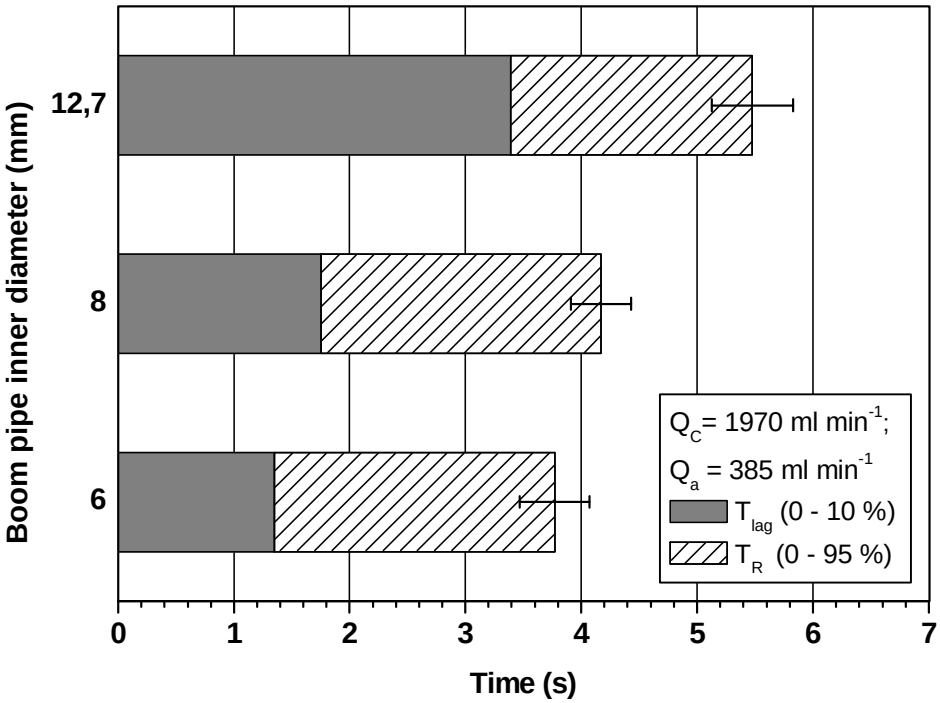

Figure 5. 73: Lag and response times for different boom pipe diameters; Q_c = 1970 ml min^{-1}

The graphs indicate that reducing the boom pipe diameter greatly reduced the lag time and hence the response time. The shortest lag times T_{lag} were obtained at an inner pipe diameter of ID = 6.0 mm (8-8-6-6 boom configuration). Depending on the carrier flow rate, the minimum lag times were 3.10 s for Q_c = 590 ml min^{-1} and 1.35 s for Q_c = 1970 ml min^{-1}. In these two cases, the resulting response times T_R were 8.84 s with a maximum standard deviation of 0.89 s and 3.93 s with a maximum SD of 0.35 s, respectively. When the spray solution flowed through the boom pipe with ID = 12.7 mm, the time required before the required level of concentration was reached was approximately double the time required for the boom pipe with ID = 6.0 mm. The longest response time T_R of 15.58 s (SD = 0.69 s) was measured when the carrier flow rate was at its minimum of 590 ml min^{-1}. This response time includes a transport lag time T_{lag} of 9.05 s.

5.4.1.2 Effect of Boom Pipe Length

The effect of the boom pipe length on the lag and response time was studied for the two boom pipe diameter configurations 8-8-6-6 and 12.7-12.7-12.7-12.7 mm. The responses of these boom injection systems were measured at each nozzle position. Figure 5.25 shows the theoretical and measured average lag times as a function of nozzle position for the 8-8-6-6 boom pipe diameter configuration.

The times in the figure were measured at all nozzles on the boom with a pipe diameter of 6 mm at carrier flow rate Q_c = 340; 1140 and 1970 ml min^{-1}. The values for the centre of the boom were interpolated. Figure 5.25 shows that the lag times increased with the distance from the injection point. The values of T_{lag} on the outermost nozzle increased as the number of active nozzles increased.

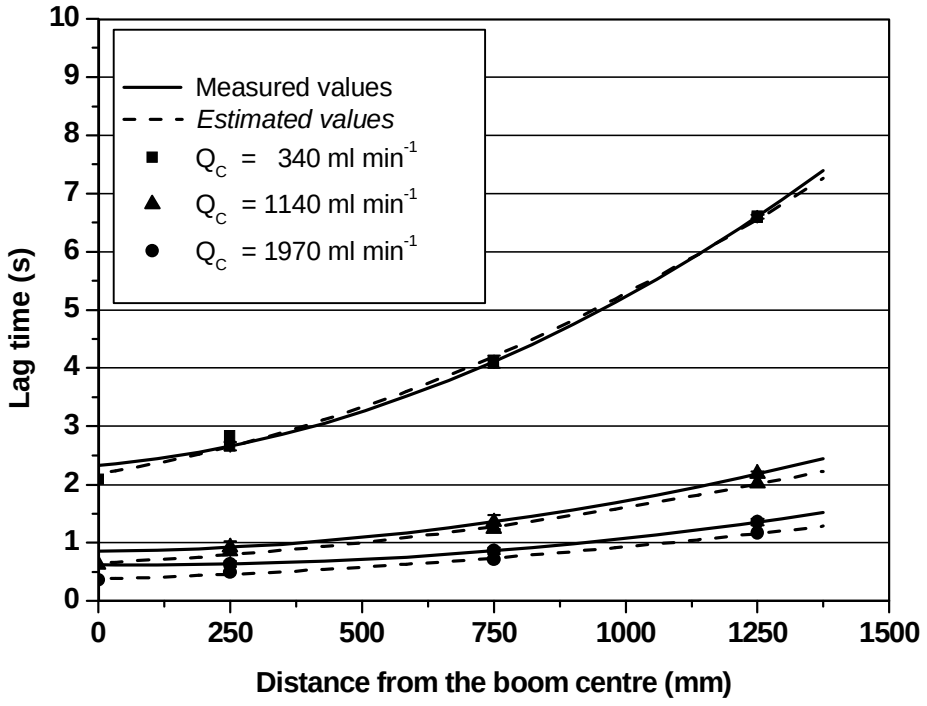

Figure 5. 74: Lag times for different carrier flow rates measured at different distances from the boom centre (nozzle positions)

The longest lag time of 6.480 s was measured at the outermost nozzle and at Q_c = 340 ml min^{-1}. The transport lag time was significantly lower for Q_c = 1140 and 1970 ml min^{-1} because of the increased carrier flow rate.

According to estimates using the algorithm for determining theoretical lag time, the lag time for the outermost XR 8005 nozzles should have been about 1.12 s because the flow rate in the XR 8005 nozzles (1970 ml min^{-1}) was approximately 5.8 times that measured in the XR 80015 nozzles (340 ml min^{-1}). However, the T_{lag} values measured at Q_c = 1140 and 1970 ml min^{-1} along the whole boom were higher than the estimated values (T_{lag} = 2.18 and 1.36 s, respectively). The difference of approximately 0.2 s was caused partly by a measurement error and partly by the use of an inappropriate local loss coefficient for the lag time calculation.

The other results obtained for Q_c = 340 ml min^{-1} were identical with the theoretically estimated values. Quadratic functions describing the relationship between the lag time and the distance from the boom centre, which were obtained from the lag time measurements at different nozzle positions, are compared with the estimated functions in appendix in table 9.7.

In figures 5.26 and 5.27 the lag and response times for two boom pipe configurations (6.0 and 12.7 mm) at the maximal tested nozzle flow rate Q_c = 2540 ml min^{-1} are shown. The graph in figure 5.26 shows how, in the 12.7 mm boom pipe configuration, the lag time T_{lag} (0-10 %) as a component of the total time T_R increased with the distance from the injection point while the rise time (10-90 %) as a component of the response time remained constant for each nozzle position. The average rise time value was 1.72 s. This characteristic was different for the 6.0 mm boom pipe configuration, where the rise time measured at the last nozzles exceeds the lag time. The rise time increased with the distance from the injection point in the same way as the lag time. The minimum lag obtained in this configuration was approximately 0.56 s at nozzles N3 and N4. The maximum lag time measured was approximately 1.18 s at nozzles N1 and N6. The minimum and maximum response times were 1.36 and 2.79 s respectively. The maximum standard deviation was 0.21 s. The results from the corresponding measurements are shown in appendix in table 9.8.

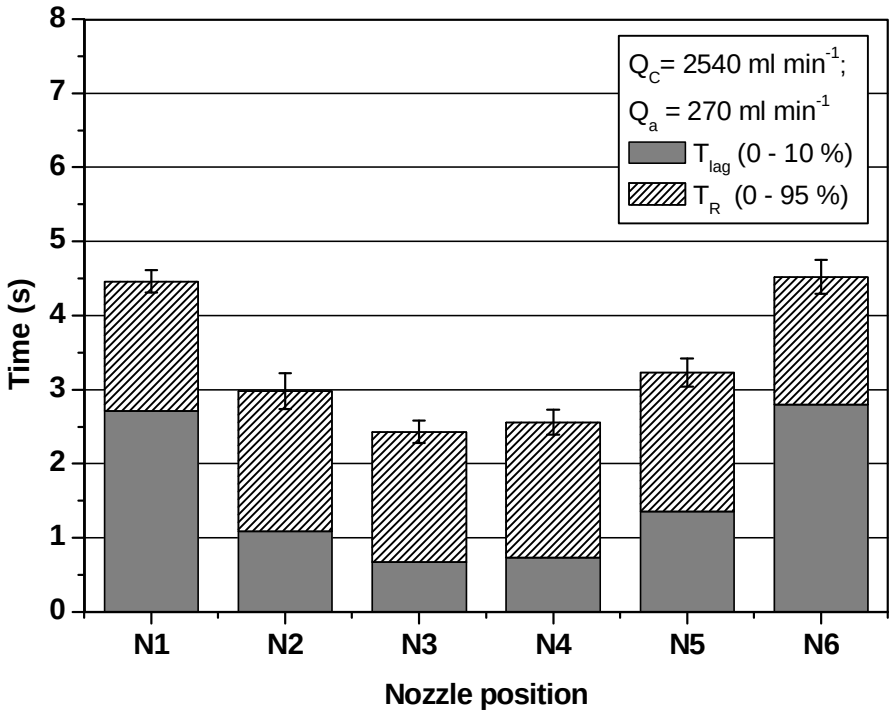

Figure 5. 75: Lag and response times measured at different nozzle positions (boom pipe ID = 12.7 mm)

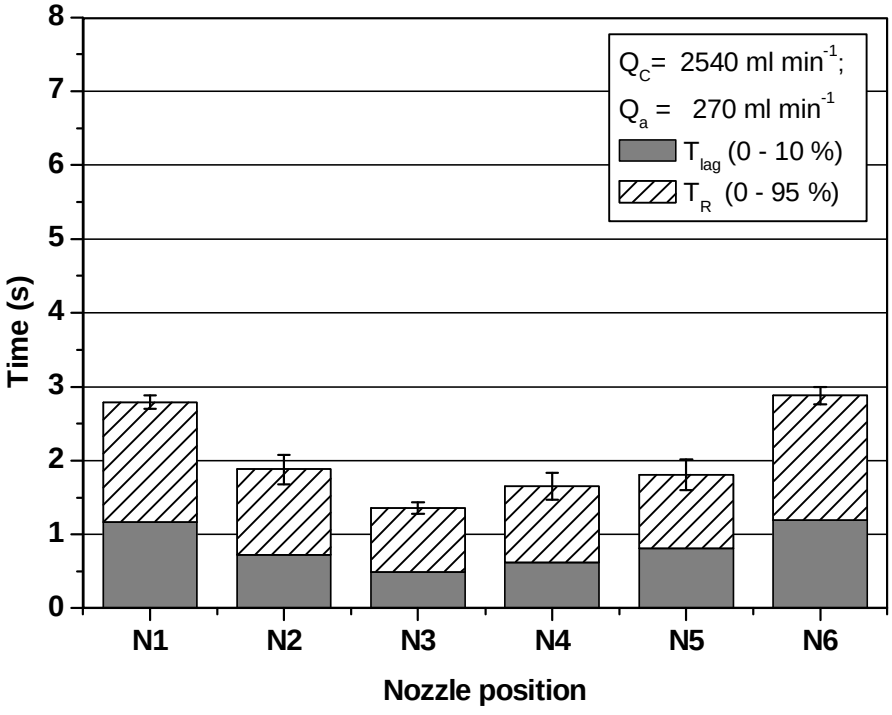

Figure 5. 76: Lag and response times measured at different nozzle positions (boom pipe ID = 6.0 mm)

5.4.1.3 Effect of Carrier Flow Rate

The effect of the carrier flow rate on the lag and response time in combination with variation of the pipe diameter has already been outlined in chapter 5.4.1.1. The influence of the carrier flow rate is more or less related to the concentration of the monitored solution. Figure 5.28 summarises the average lag and response times measured at the outer nozzles 1 and 6 of the 8-8-6-6 mm boom configuration. At different combinations of nozzles and system pressures (1.0 and 3.0 bar), the carrier flow rate Q_c ranged from 340 to 1970 ml min^{-1}. The tracer flow rates Q_a were maintained constant at 385 and 525 ml min^{-1}.

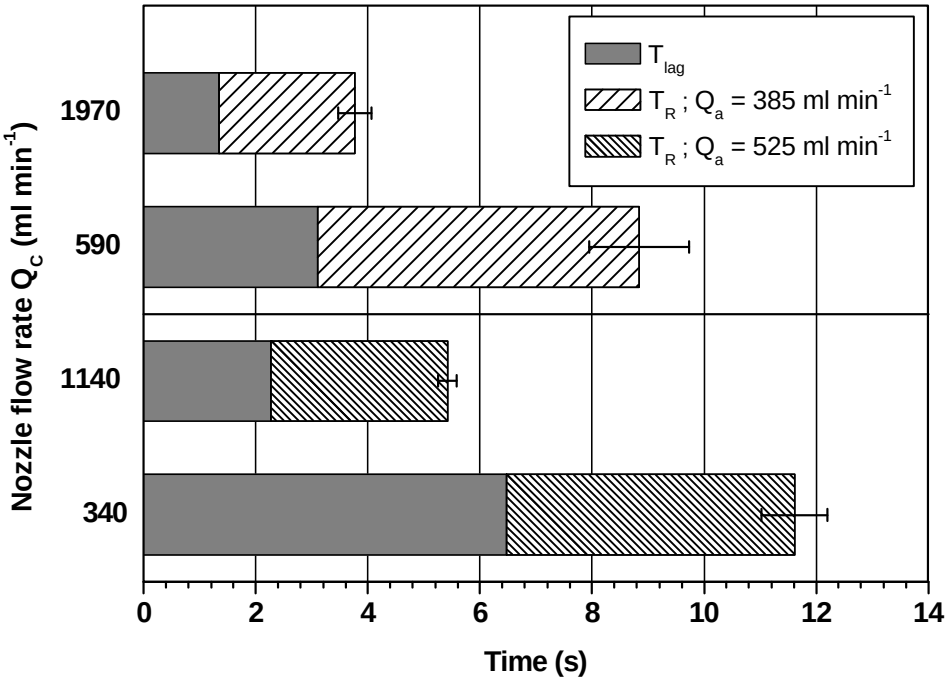

Figure 5. 77: Lag and response times for different carrier flow rates

In general, it can be concluded that the increase in the carrier (nozzle) flow rate reduced the lag and the response time. The shortest times were obtained in both measurements at the greatest carrier flow rate. The lag time of 1.35 s obtained with a low-concentration solution (constant tracer flow rate Q_a = 385 ml min^{-1}, carrier flow rate Q_c = 1970 ml min^{-1}) was nearly twice as short as the one obtained with a solution with a higher concentration (Q_c = 590 ml min^{-1}) where the minimum T_{lag} was 3.10 s. The maximum standard deviation was 0.89 s.

Similar results were obtained for the injection of the tracer at a constant flow rate of 525 ml min^{-1}. The longest lag time measured was 6.48 s at the minimum carrier flow rate of 340 ml min^{-1}. The maximum deviation was 0.59 s. The results from the corresponding measurements are shown in appendix in table 9.9.

5.4.1.4 Effect of Tracer Flow Rate

The effect of the tracer flow rate on the lag and response time is not negligible. However, the results show no significant differences between measured times. The average lag and response times obtained at a constant carrier flow rate of 1970 ml min^{-1} and at different tracer flow rates are summarized in figure 5.29. The tracer flow rate varied from 60 to 385 ml min^{-1}. In figure 5.30 the rise and fall times measured under the same conditions as the response times are compared.

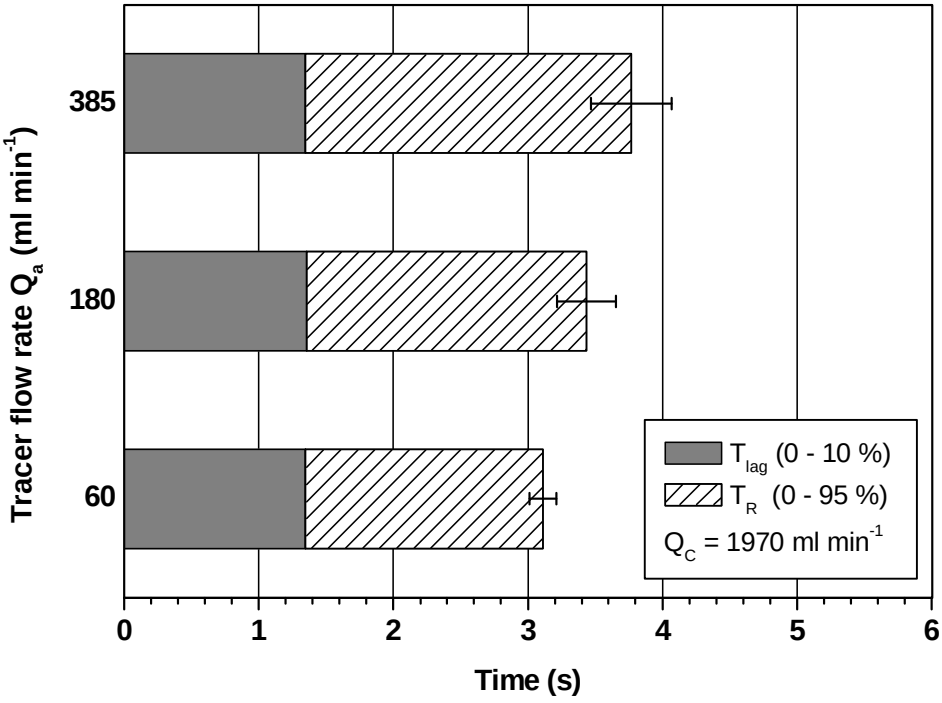

Figure 5. 78 Lag and response times for different tracer flow rates

Figure 5.29 indicates that the decreasing tracer flow rate Q_a reduced the response time slightly. The minimum response time of 3.35 s was obtained at the lowest tracer flow rate of 60 ml min^{-1}, while the longest response time 3.93 s was measured at the highest tracer concentration Q_a = 385 ml min^{-1}. The maximum standard deviation was 0.30 s. The average lag times were in the range from 1.35 to 1.36 s.

In figure 5.30 the rise and fall times at different tracer flow rates are summarized. The effect of the flow rate on the rise time is more evident here. It is possible to conclude that low concentration solutions reach their required concentration faster than higher concentration solutions. The minimum rise time of 1.22 s as well as the minimum fall time of 0.67 s was obtained at the minimum tracer flow rate of 60 ml min^{-1}. The results from the corresponding measurements are shown in appendix in table 9.10.

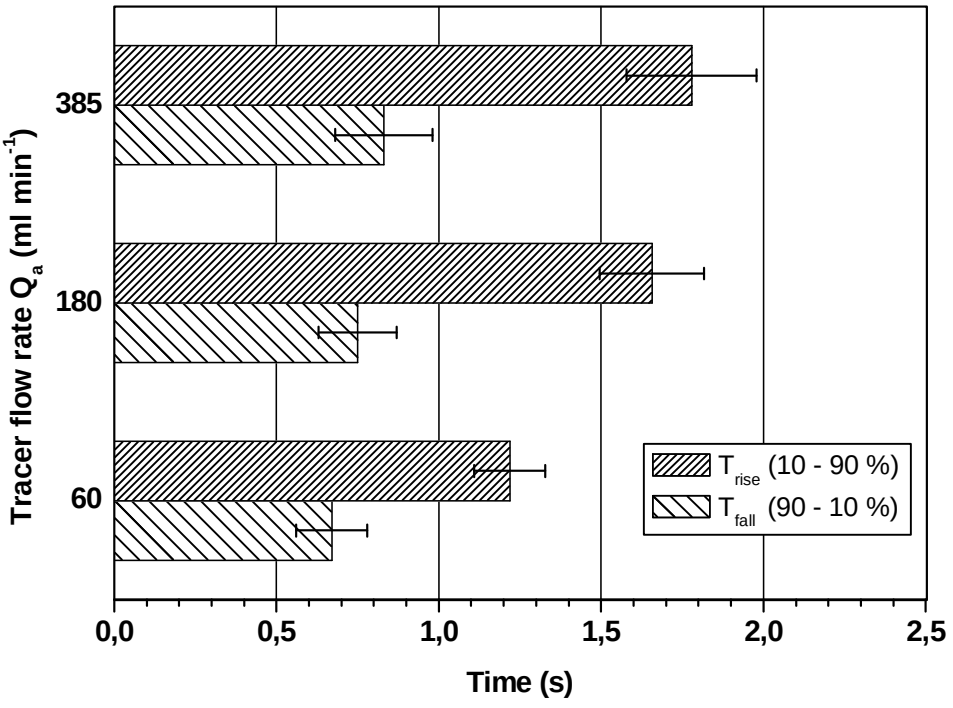

Figure 5. 79: Rise and fall times for different tracer flow rates

5.4.1.5 Effect of Viscosity

The lag and response times for three simulated pesticides (water and two aqueous glycerine solutions with viscosities of 109 and 219 mPa s) are summarized in figures 5.31 and 5.32. The results from the corresponding measurements are shown in appendix in table 9.1. The tracer flow rate Q_a was maintained constant at 60 and 180 ml min^{-1}. The carrier flow rate through the end nozzles Q_c was maintained constant at 1970 ml min^{-1}.

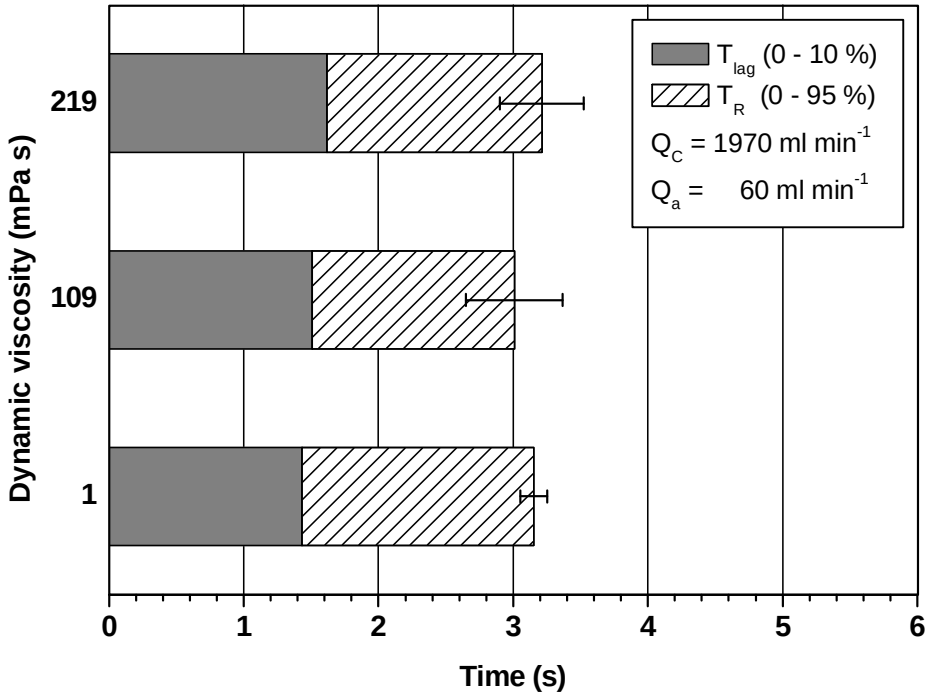

Figure 5. 80: Effect of viscosity on response time; Q_a = 60 ml min^{-1}

The lag times and the response times measured for the viscous tracers were similar to those obtained for water. At both tracer flow rates, the lag time values tented to increase slightly as the viscosity of the tracer increased. The longest lag time of 1.62 s was obtained for the tracer with a viscosity of 219 mPa s. A comparison of the response time statistics for the three tracers using a one-way ANOVA and Tukey's test at p = 0.05 indicates that under the fixed operating conditions the different viscosities did not lead to significant differences between the response times. At Q_a = 60 ml min^{-1}, the response times ranged from 3.01 to 3.21 s with a maximum standard deviation of 0.36 s. At Q_a = 180 ml min^{-1} and for the tracers with viscosities of 1 and 109 mPa s (see Fig. 5.32), the response times were 3.63 and 3.70 s respectively. The maximum standard deviation was 0.37 s.

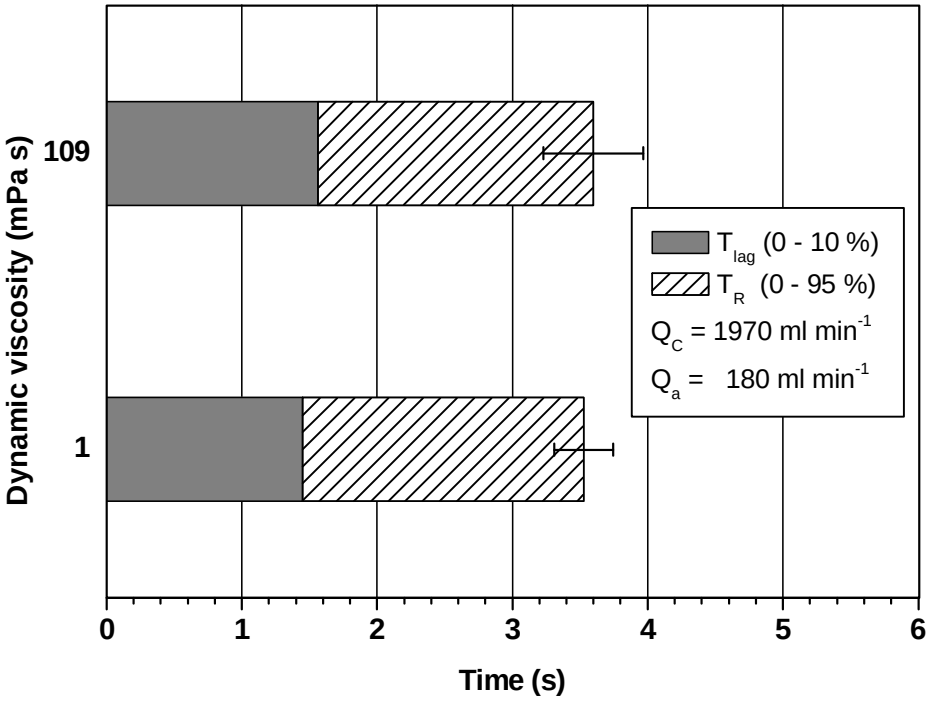

Figure 5. 81: Effect of viscosity on lag and response time; Q_a = 180 ml min^{-1}

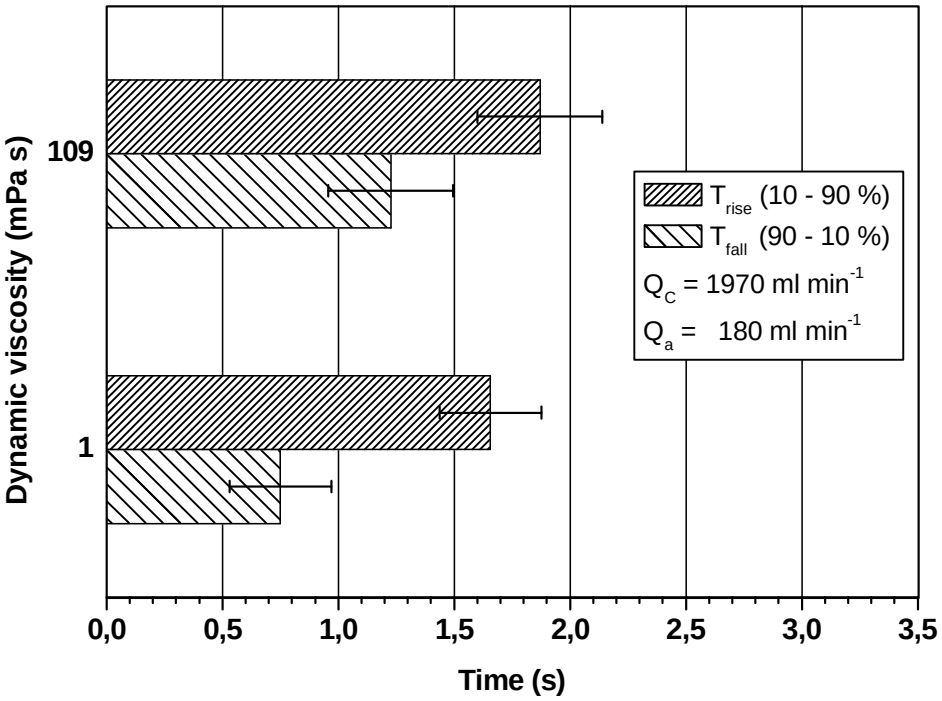

Figure 5. 82: Rise and fall times for water and aqueous glycerine solution (109 mPa s); Q_a = 180 ml min^{-1}

The rise and fall times for water and the aqueous glycerine solution with a viscosity of 109 mPa s at Q_a = 180 ml min^{-1} are shown in figure 5.33. Apart from a discrepancy between the rise and fall times, there was a significant difference between the fall times obtained for both tracers. The average fall time for water was 0.75 s, whereas for the tracer with a viscosity of 109 mPa s it was about 1.23 s, with a standard deviation of 0.27 s.

5.4.2 Response Times of Nozzle Injection Systems

In the following chapters the response times of both direct nozzle injection systems are presented. The results are arranged in the form of a comparison of the two chemical pumps (gear pump and diaphragm pump) used for tracer delivery. The effects studied in these response time measurements were similar to those of the boom injection system.

5.4.2.1 Response Times of Injection into a Set of Nozzles

5.4.2.1.1 Effect of Metering Orifice Size

For direct injection into a set of six nozzles, the effect of the size of the metering orifice on the response was studied using rise and fall times. The values of T_{rise} (10 - 90 %) and T_{fall} (90 - 10 %) were obtained from measurements with three different metering orifices (sizes 4916-08, 10 and 12). The carrier flow rate was maintained constant at 340 and 1970 ml min^{-1}, while the tracer flow rate was set to 10 and 45 ml min^{-1}, depending on the metering orifice being tested. The average rise and fall times measured at the outer nozzles (N1, N6) for three different orifice sizes and at Q_a = 45 ml min^{-1} are compared in figures 5.34 and 5.35. In figure 5.34 the results for Q_c = 1970 ml min^{-1} in combination with the diaphragm pump are shown. There were no significant differences between the resulting rise times, which ranged from 0.82 to 0.92 s. The maximum standard deviation was 0.13 s. When size 10 and 12 orifices were used, the fall times measured by closing the valve were almost twice as short as the rise times measured by opening. However, this effect was absent when the smallest orifice (size 8) was used. In this case, the fall time was approximately 1.20 s, which is about 0.29 s longer than the rise time. This discrepancy was caused by the relatively high differential pressure (5.0 bar) across the orifice. Because of the small orifice size, the pressure in the tracer supply hoses during injection was great. After closing of the control valve there was residual (accumulated) pressure, which could not be controlled, in the dead volume space.

A similar effect is evident in figure 5.35, where the fall time is longer for the size 10 and 12 orifices, too. This was mainly due to the high concentration of the spray solution and the small carrier flow rate of Q_c = 340 ml min^{-1}.

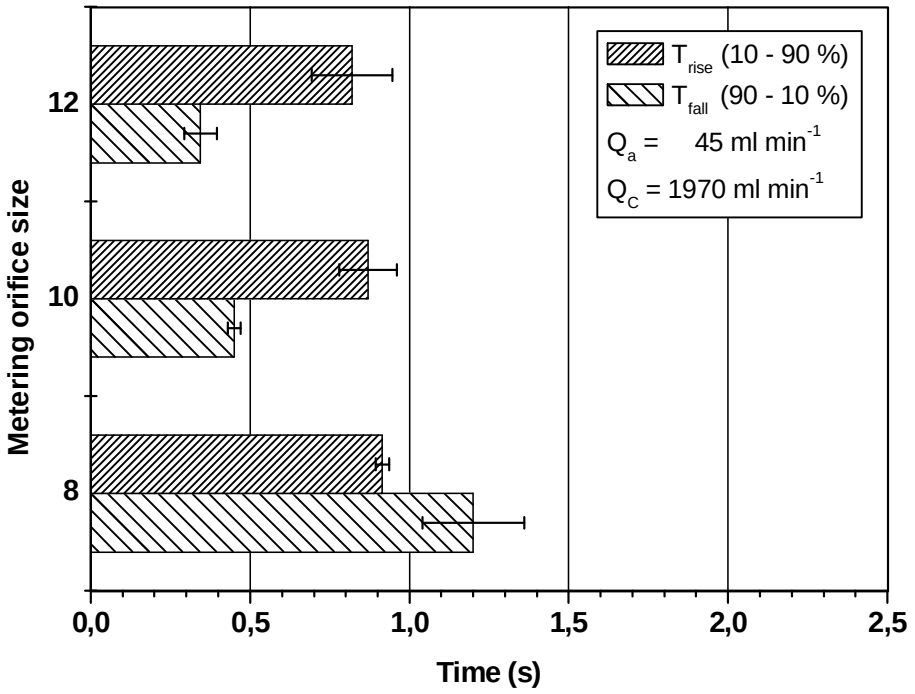

Figure 5. 83: Rise and fall times for different metering orifice sizes; Q_c = 1970 ml min^{-1}

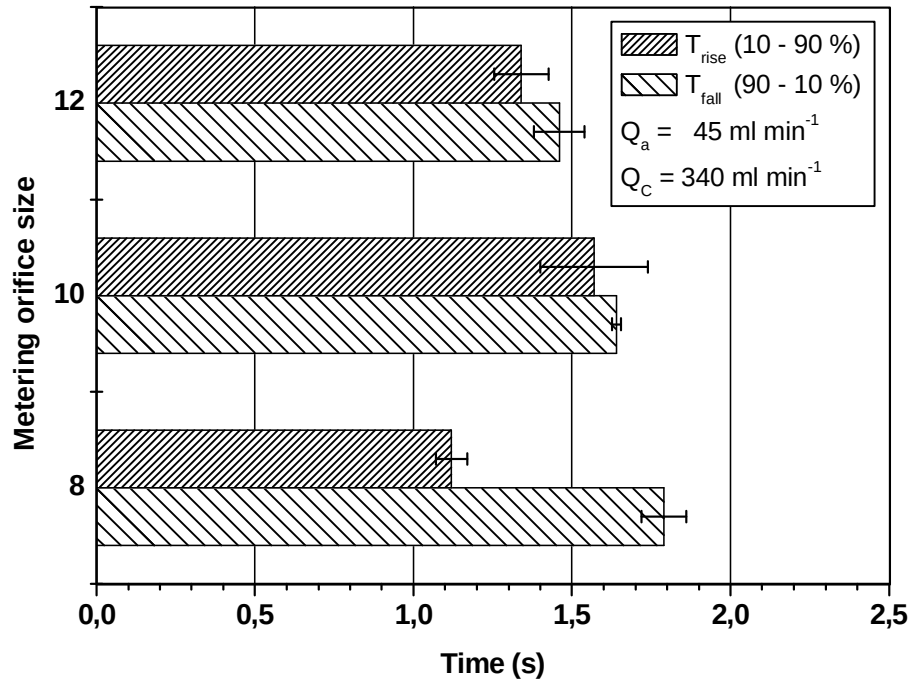

Figure 5. 84: Rise and fall times for different metering orifice sizes; Q_c = 340 ml min^{-1}

5.4.2.1.2 Effect of Tracer Rail Length

For the injection system with injection into a set of six nozzles, the effect of the rail length on the lag and response time was studied at three nozzle locations (N1, N3 and N5). The lag and response times were measured for carrier flow rates of Q_c = 1140 and 1970 ml min^{-1}. The tracer flow rate Q_a was maintained constant at 10 and 30 ml min^{-1}. These two tracer flow rates were supplied by both pumps tested. The average lag and response times obtained for the diaphragm pump at two carrier flow rates and two tracer flow rates of Q_a = 10 and 30 ml min^{-1} respectively are shown in figures 5.36 and 5.37. The response times are much longer than the lag times because of the short distance between the injection point and the conductivity sensor (nozzle). The lag times obtained for each tracer concentration at the different nozzle positions were not significantly different from each other. However, they seem to be longer at the outer nozzles (N1 and N5).

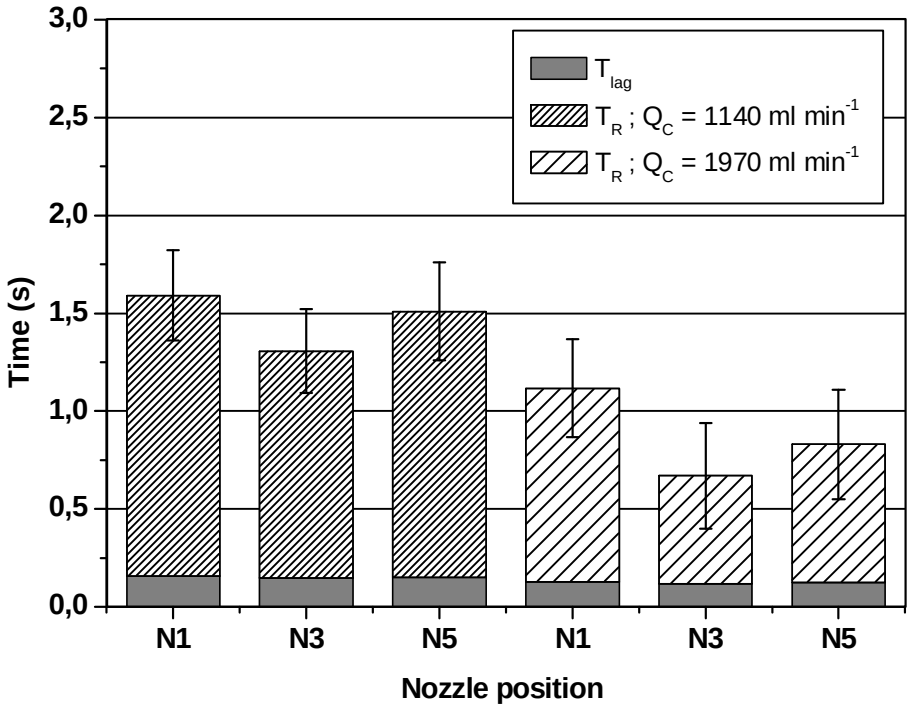

Figure 5. 85: Lag and response times measured at different nozzle positions; diaphragm pump, Q_a = 10 ml min^{-1}

The minimum lag time of 0.12 s was measured at nozzle N3 at Q_a = 10 ml min^{-1} and at a carrier flow rate of 1970 ml min^{-1}. The maximum lag time at Q_a = 30 ml min^{-1} and at a carrier flow rate of 1140 ml min^{-1} was 0.17 s.

In contrast to the lag time, the response time increased significantly with the distance from the centre of the boom (not from the injection position). This discrepancy was mostly caused by the distance between the control valve and the injection points. The minimum response time of 0.67 s was obtained at the middle nozzle N3 at a carrier flow rate of 1970 ml min^{-1} and a tracer flow rate of 10 ml min^{-1}. The response time measured for the last nozzle (N1) was approximately 1.12 s. The maximum standard deviation was 0.28 s.

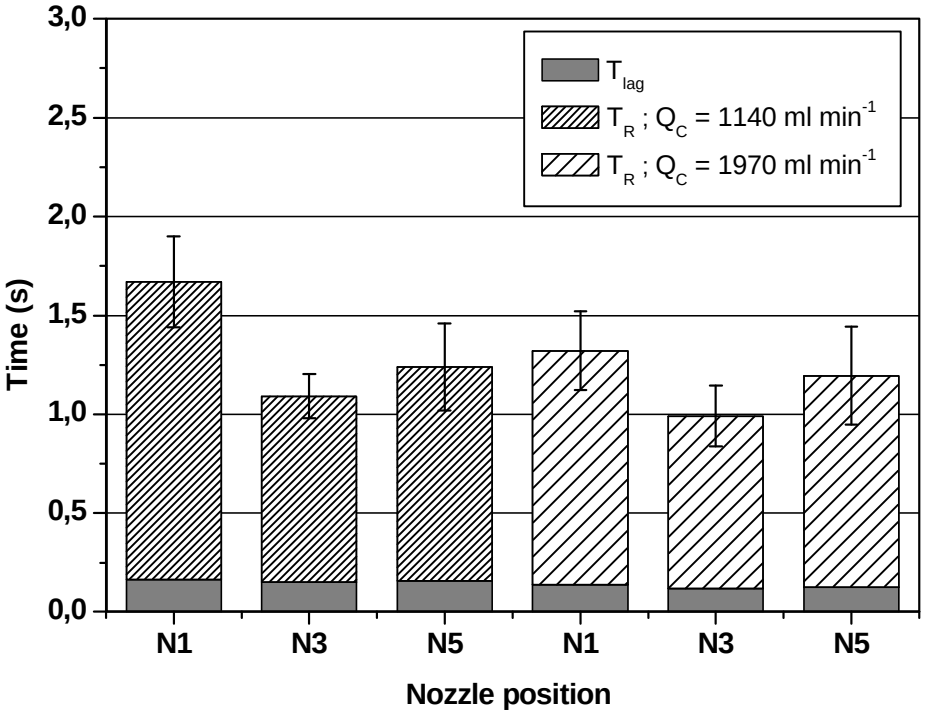

Figure 5. 86: Lag and response times measured at different nozzle positions; diaphragm pump, Q_a = 30 ml min^{-1}

The lag and response times obtained for the gear pump at a constant carrier flow rate of 1970 ml min^{-1} are shown in figure 5.38. The measurement conditions were same as in the measurement with the diaphragm pump. The resulting response times were approximately 0.43 s larger than with the diaphragm pump providing the tracer supply. The minimum response time measured at the outer nozzle N1 was 1.37 s at Q_a = 10 ml min^{-1}. The maximum standard deviation was 0.23 s.

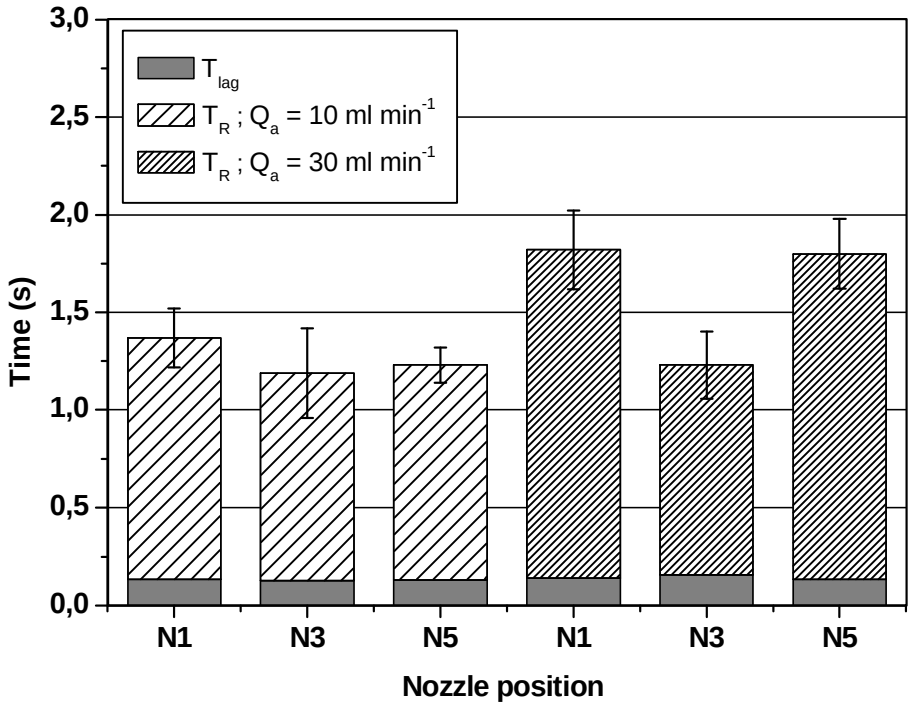

Figure 5. 87: Lag and response times measured at different nozzle positions; gear pump, Q_c = 1970 ml min^{-1}

5.4.2.1.3 Effect of Carrier Flow Rate

The effect of the carrier flow rate on the lag and response time was measured at the outer nozzles N1 and N6. Figure 5.39 summarizes the average lag and response times obtained with the diaphragm pump being used. The carrier flow rate Q_c varied from 340 to 1970 ml min^{-1} while the tracer flow rate Q_a was maintained at a constant level of 10 ml min^{-1}. The graph validates the fact that an increased nozzle flow rate greatly reduced the lag and response time. The longest lag time of 0.33 s was obtained at the minimum carrier flow rate of 340 ml min^{-1}. The minimum lag time of 0.13 s was measured at the maximum carrier flow rate of 1970 ml min^{-1}. The minimum response time of 1.12 s was also obtained at the maximum carrier flow rate with the largest standard deviation being 0.24 s.

Figure 5.40 compares average lag and response times at different carrier flow rates for the tracer delivery gear pump. The carrier flow rate also varied from 340 to 1970 ml min^{-1}. Additionally, the response times were measured at the maximum carrier flow rate of 2540 ml min^{-1} with the aim to obtain the minimal mixture solution concentration of 81.3 ppm of NaCl. The minimum response time of 0.79 s was obtained for this concentration.

The maximum response time with the gear pump being used was 2.28 s; it was measured at the minimal carrier flow rate of 340 ml min^{-1} with a maximum standard error of 0.49 s.

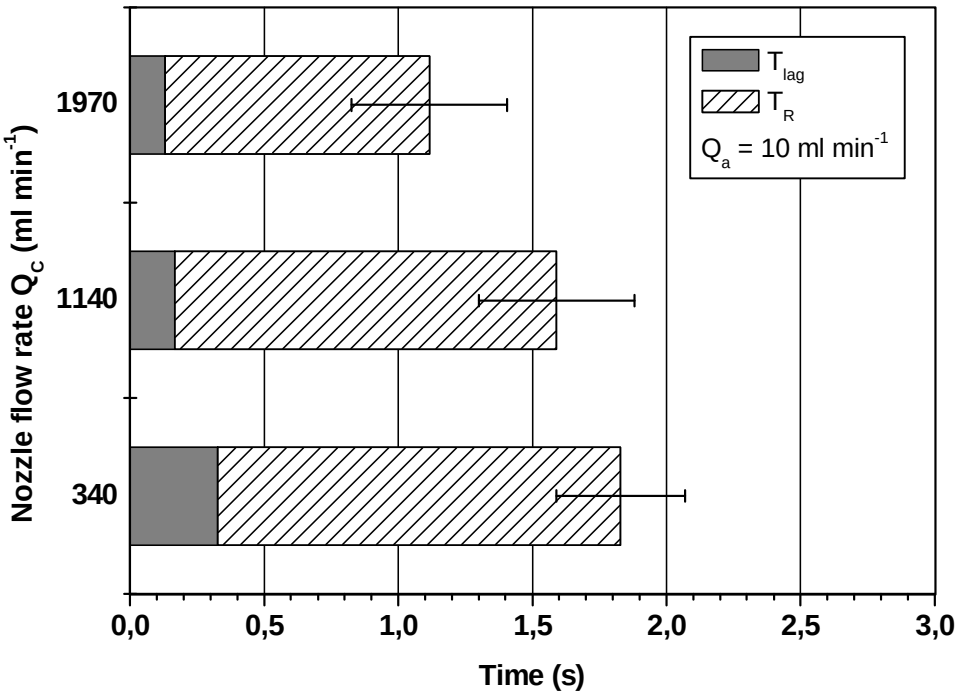

Figure 5. 88: Lag and response times at different carrier flow rates; diaphragm pump

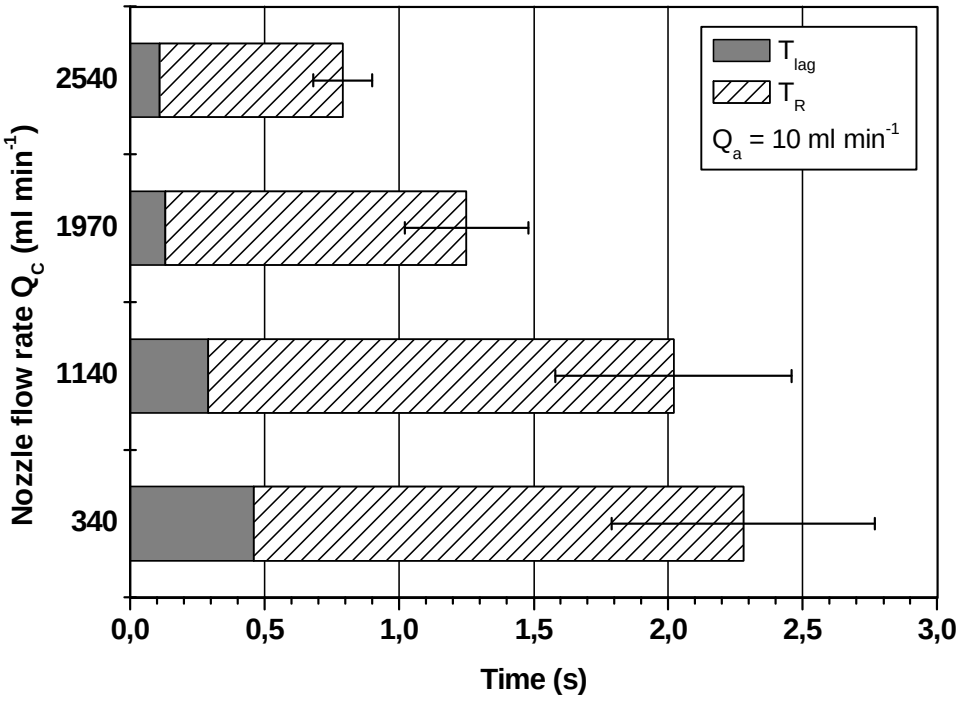

Figure 5. 89: Lag and response times at different carrier flow rates; gear pump

5.4.2.1.4 Effect of Tracer Flow Rate

Figures 5.41 and 5.42 compare average lag and response times obtained from different tracer flow rates measurements. The times were measured at the outer nozzles N1 and N6 of the nozzle injection systems using the diaphragm and the gear pump, respectively. A constant carrier flow rate was maintained at 1140 and 1970 ml min^{-1}. The tracer flow rate was set to 10, 30 and 50 ml min^{-1} so that the spray solution concentration ranged from 101 to 840 ppm of NaCl. The lag times were not significantly affected by the different solution concentrations (tracer flow rates) in the range used for the measurements.

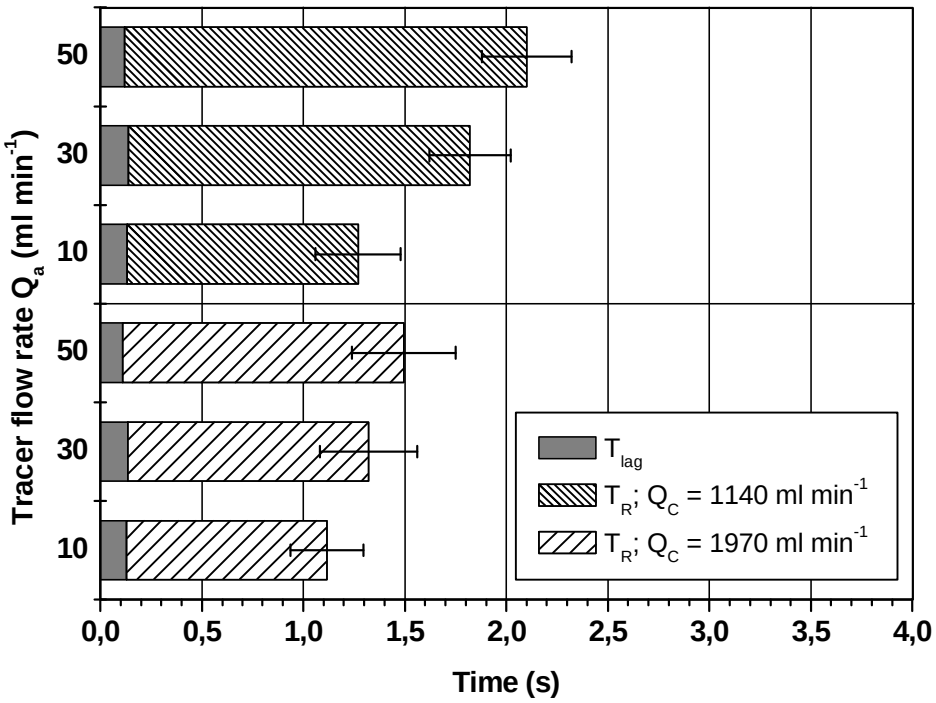

Figure 5. 90: Lag and response times at different tracer flow rates; diaphragm pump

The T_{lag} values were on average 0.12 s for the system using the diaphragm pump and 0.16 s for the system with the gear pump. The minimum and maximum response times obtained for the diaphragm pump were 1.12 and 2.10 s at the minimal and maximal spray solution concentrations, respectively. The resulting response times for the system using the gear pump were on average 0.52 s longer than for the system with the diaphragm pump. The maximum standard error was about 0.25 s.

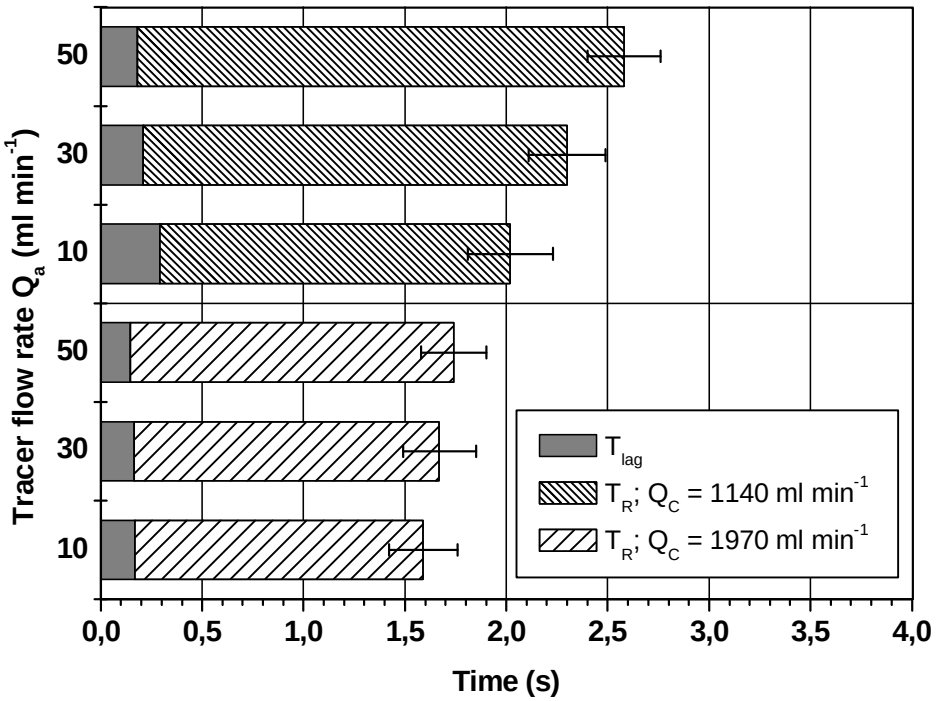

Figure 5. 91: Lag and response times for different tracer flow rates; gear pump

5.4.2.1.5 Effect of Viscosity

The lag and response times for a range of viscous aqueous glycerine solutions are summarized in figures 5.39 and 5.40. The times were measured the and at the outer nozzles (N1 and N6). The tests were performed for the injection system using the gear pump only. The tracer flow rate Q_a was maintained constant at 10 and 30 ml min^{-1} by a CP 4916-10 metering orifice. The carrier flow rate through the end nozzles Q_c was maintained constant at 1970 ml min^{-1} for both tracer concentrations. The longest lag time of 1.73 s was obtained for the tracer with a viscosity of 219 mPa s and at Q_a = 30 ml min^{-1}. The response times at Q_a = 10 ml min^{-1} ranged from 0.95 to 1.10 s with the largest standard deviation being 0.23 s. At Q_a = 30 ml min^{-1} and at tracer viscosities of 1 and 109 mPa s, the response times were 1.66 and 1.73 s respectively. The maximum standard deviation was 0.28 s.

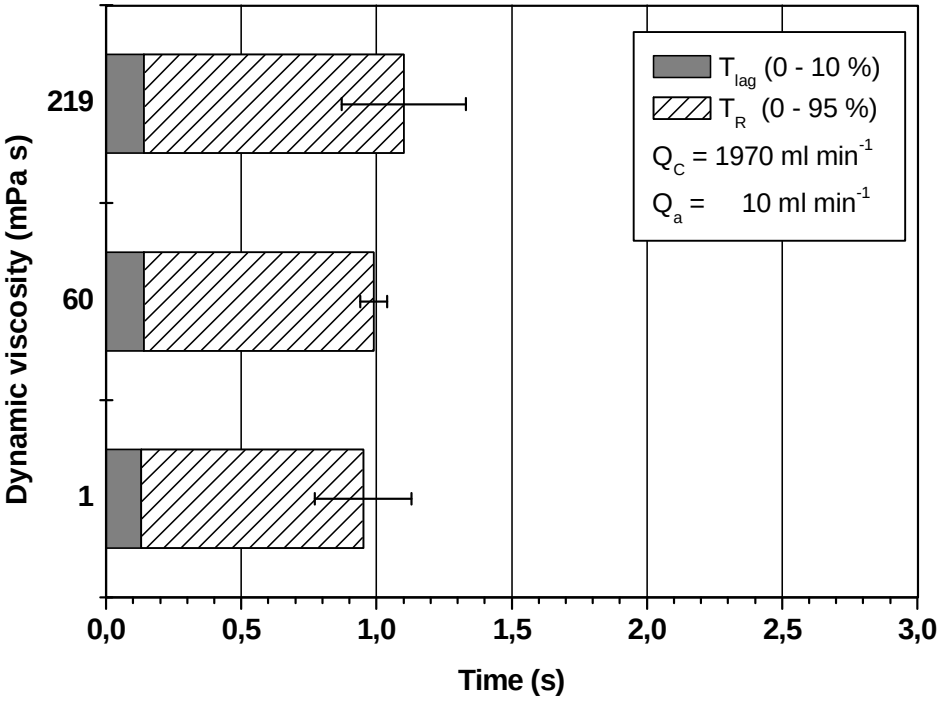

Figure 5. 92: Effect of viscosity on lag and response time; Q_a = 10 ml min^{-1}

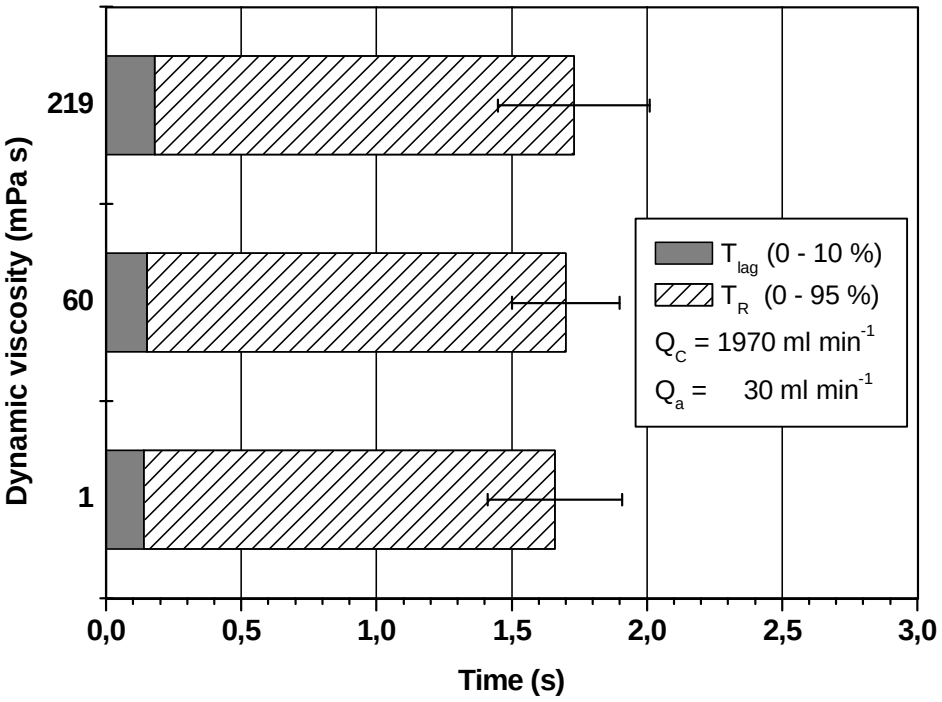

Figure 5. 93: Effect of viscosity on lag and response time; Q_a = 30 ml min^{-1}

5.4.2.2 Response Times of Injection into Individual Nozzles

5.4.2.2.1 Effect of Carrier Flow Rate

The effect of the carrier flow rate on the lag and response time for the system with direct injection into individual nozzles is shown in figures 5.45 and 5.46. Figure 5.45 summarizes the average lag and response times obtained for the configuration with the diaphragm pump. The carrier flow rate Q_c ranged from 340 to 1970 ml min^{-1} while the tracer flow rate Q_a was maintained at a constant level of 10 ml min^{-1}. In this system, moreover, an increased nozzle flow rate greatly reduced the lag and response time. The shortest lag time of 0.08 s was measured at the maximum carrier flow rate of 1970 ml min^{-1}. The longest lag time of 0.12 s was obtained at the minimum carrier flow rate of 340 ml min^{-1}. The shortest response time of 0.27 s was obtained at the maximum carrier flow rate of 1970 ml min^{-1} with a maximum standard deviation of 0.08 s.

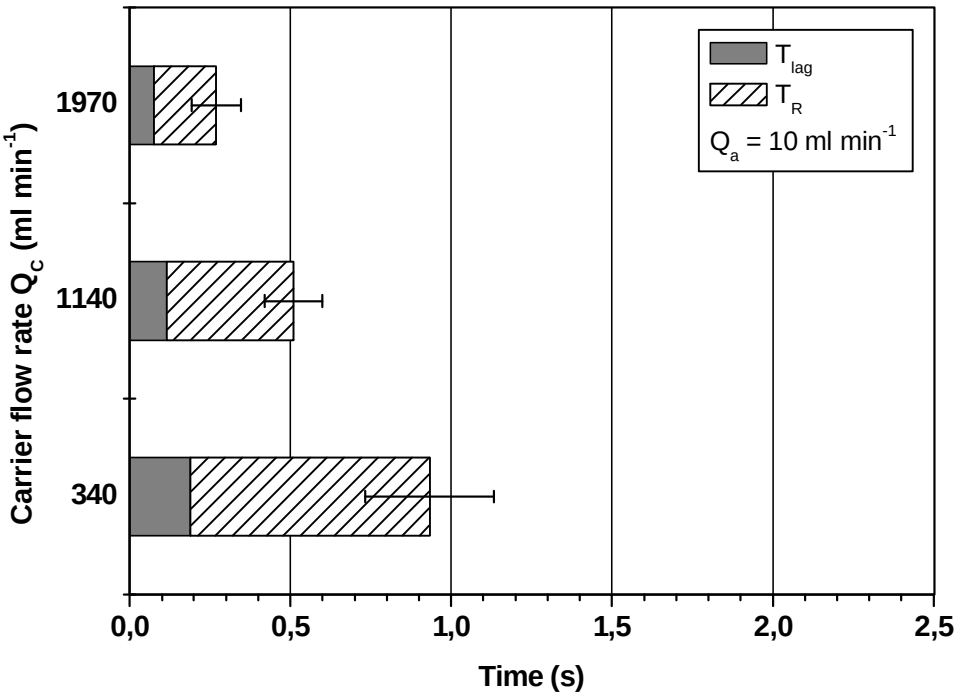

Figure 5. 94: Lag and response times at different carrier flow rates; diaphragm pump

Very short times were also obtained for the system using the gear pump. Figure 5.46 compares average lag and response times at different carrier flow rates for the system using the gear pump for tracer delivery. The carrier flow rates ranged from 340 to 2540 ml min^{-1}.

The minimum response time obtained at the maximum carrier flow rate was 0.32 s with a maximum standard deviation of 0.10 s. For the system using the gear pump, a maximum response time of 0.98 s was measured at the minimal carrier flow rate of 340 ml min^{-1} with a maximum standard deviation of 0.14 s.

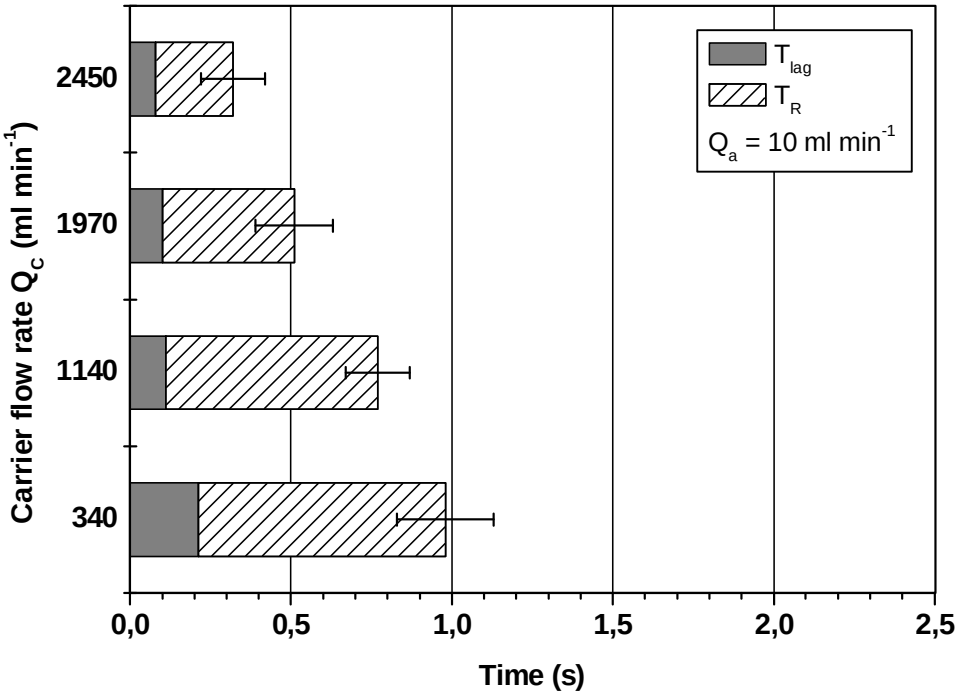

Figure 5. 95: Lag and response times for different carrier flow rates; gear pump

5.4.2.2.2 Effect of Tracer Flow Rate

In figures 5.47 and 5.48 the average lag and response times at different tracer flow rates are compared for the nozzle injection systems with the diaphragm pump and the gear pump, respectively. The carrier flow rate was maintained at 1140 and 1910 ml min^{-1}. The tracer flow rates were set to 10, 30 and 50 ml min^{-1}. The lag times were not significantly affected by the different tracer flow rates in the range used in the measurements. The T_{lag} values ranged from 0.08 to 0.13 s for the system using the diaphragm pump and from 0.10 to 0.13 s for the system using the gear pump. The minimum and maximum response times obtained for the system using the diaphragm pump were 0.27 and 0.94 s at the minimal and maximal tracer flow rate (concentration), respectively. The response times for the system using the gear pump were on average 0.35 s longer than for the system with the diaphragm pump. The maximum standard error was about 0.14 s.

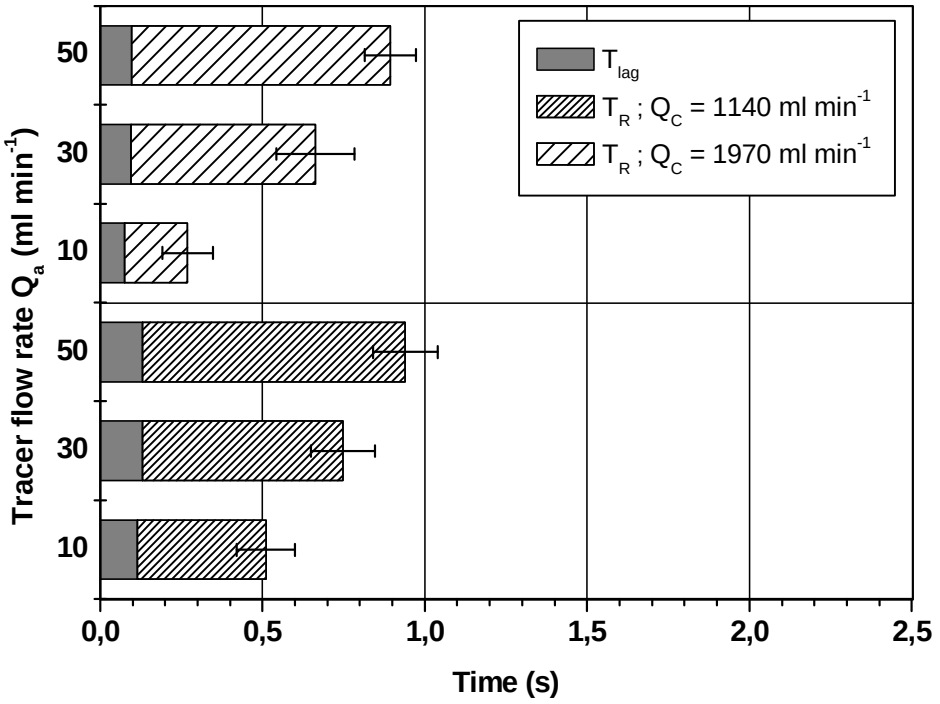

Figure 5. 96: Lag and response times at different tracer flow rates; diaphragm pump

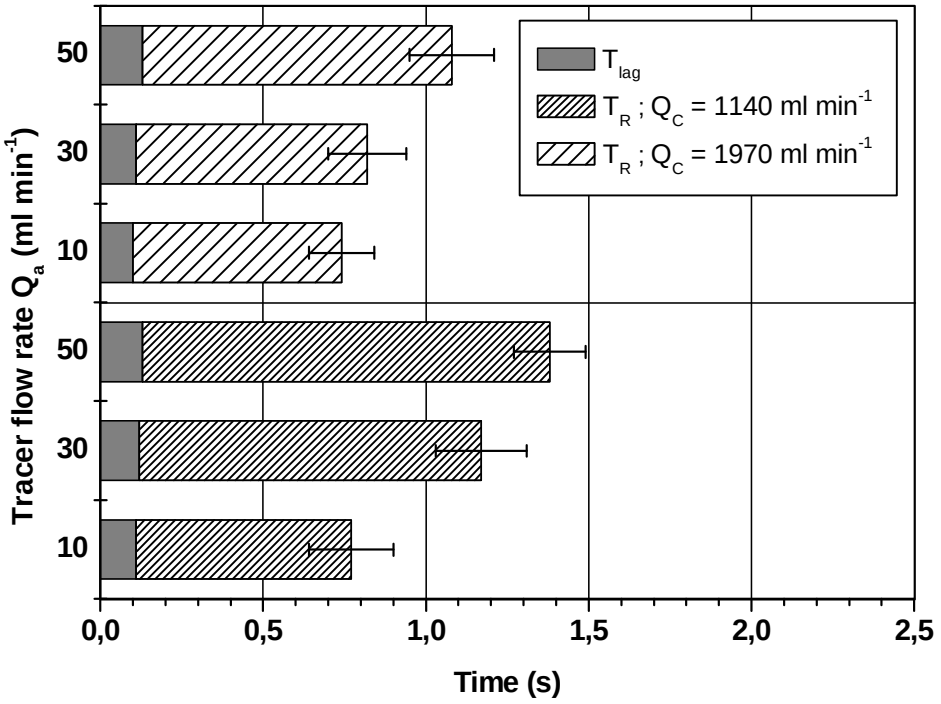

Figure 5. 97: Lag and response times at different tracer flow rates; gear pump

5.4.2.2.3 Effect of Viscosity

Figure 5.49 compares the average response times for water and aqueous glycerine solutions with viscosities of 60 and 219 mPa s. The times were measured for the injection system using the gear pump only. The response times measured for these fluids were similar to those obtained with water at a nozzle flow rate of 1970 ml min^{-1}. The tracer flow rate Q_a was maintained constant at 10 and 30 ml min^{-1}. A comparison of the response time statistics for the three tracers indicates that under fixed working conditions the viscosities did not make a significant difference in the lag and response time. The longest lag time of 0.16 s was obtained for the tracer with a viscosity of 219 mPa s at a tracer flow rate of 30 ml min^{-1}. The response times ranged from 0.74 to 1.27 s at a tracer flow rate of Q_a = 10 ml min^{-1}. The largest deviation found was 0.15 s. At Q_a = 30 ml min^{-1} the measured response times were in a range from 1.04 and 1.57 s. The maximum standard deviation was 0.17 s.

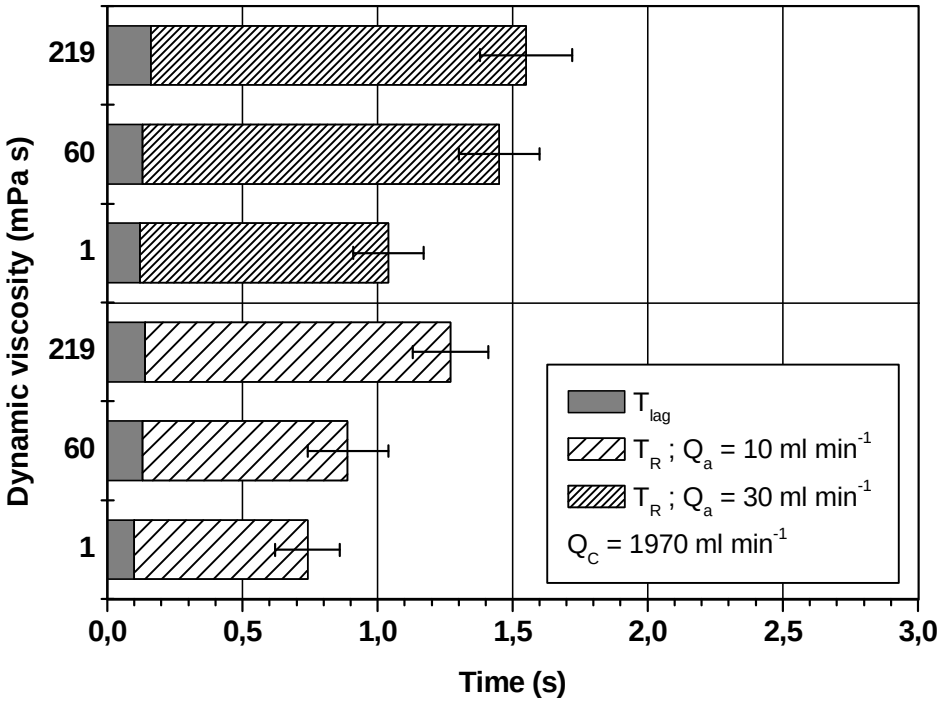

Figure 5. 98 Effect of viscosity on lag and response time; gear pump

6. Discussion

6.1 Evaluation of Flow Regulation Components

The flow regulation components - delivering pumps, metering orifices and proportional valve - showed good accuracy for controlling the flow rate while injecting both water and viscous solutions. The system with injection into a set of nozzles had inaccurate distribution if the metering orifices were not properly sized. However, this negative feature was present only when solutions with higher viscosities ($\eta \sim$ 219 mPa s) were injected by means of the gear pump. One possible reason for the poor distribution was an undersized pump. The flow was too low to create the sufficient pressure for even distribution. When the proportional valve was open the pump was not able to change the flow rate quickly. This issue was not observed when the diaphragm pump was used for tracer delivery. The response of the pump to the pressure drop in the system after opening the valve was adequate for building up the required pressure. The main problem with the two-piston diaphragm pump was flow discontinuity due to pulsations.

The proportional valve operated properly within its specified range of flow rates and viscosities. The calibration curves obtained for water and solutions with different viscosities (see Fig. 5.7) show a rapid drop in flow rate after injection of highly viscous solutions. Therefore, the valve must be specially calibrated for a specific range of viscosity classes. This may cause problems controlling the valve in practical applications.

When the proportional valve was used for tracer control in the system with injection into individual nozzles, a metering orifice had to be used to reduce the tracer flow rate. The proportional valve alone was too large to produce the required solution concentration. There is a risk of blockage when using a small valve orifice.

The metering orifices used in the system with injection into six nozzles fulfilled their expected function of metering and distributing tracer equally into all nozzles. The average variation coefficient of the lateral flow rate distribution for small orifices (CP 4916-08, -10 and -12) was under 10 %. Only when orifices with a larger diameter (CP 4910-16 and -20) were used for metering viscous solutions did the variation of the flow rate along the boom section exceed 20 %, as is clearly shown in figure 5.14.

This unacceptable non-uniformity was caused by the above-mentioned weak performance of the gear pump in delivering the tracer into the outermost nozzles. The orifice metering system was only intended for laboratory experiments to carry out the response time measurements. Metering orifices would hardly be used in practice due to the danger of blockages and due to their very limited flow rate ranges evident in the obtained calibration curves. Metering orifices need to be sized specifically for different chemicals and injection rates in order to ensure the uniformity of flow rates among individual nozzles. An advantage of using metering orifices is that they can easily be coupled with a common nozzle body, thus allowing injection of multiple products at the same time as shown in figure 6.1.

All three systems described above share the general problem of unstable carrier pressure, which influences the metering accuracy and hence the target concentration. Therefore, a system must be developed (special pressure relief valve, check valve or mixing chamber) to ensure that the chemicals are injected into the carrier flow at a constant differential pressure, independent of the actual carrier pressure. This improvement would enable very accurate open loop control of the flow rate without the need to use a flow meter, which would be very complicated under present conditions. The capillary flow meter developed and described in this dissertation was used only for the calibration tests.

Figure 6. 2: Metering orifice injection system – a nozzle body with two points of injection

6.2 Evaluation of Chemical Concentration Measurement Methods

The results from the static and dynamic calibration tests showed good accuracy of all three measurement devices and proved the viability of these methods. The mean and standard deviation of the output voltages from five iterations were determined for each system pressure and mixture concentration. There were significant functional relations between mixture concentration and output signal (value) for each of these methods.

There were some fluctuations in mixture concentration during the calibration tests due to pulsations in the carrier (water) line caused by the pump. These pulsations should be eliminated using a suitable hydraulic accumulator. Moreover, the quality of the active ingredient had to be as uniform as possible, which was a problem especially with the salt solution used in the tests because there was a likelihood of the physical-chemical properties changing from batch to batch.

The in-line measuring cells used in the conductivity and light transmittance method can be installed in any place throughout the length of the spray boom. Thus, they can be used to determine time lag as well as mixture uniformity in online measurements.

The applied methods can be evaluated by comparing their advantages and disadvantages. The conductivity method is an accurate and easily available method. The measuring cell has a simple design with a very small dead volume which caused a static error in the response time measurements. The next advantage of this method is the easy preparation of the basic tracer solution and the ready availability of the active ingredient (NaCl). A main disadvantage is that the mixture temperature has an influence on the outgoing voltage signal U_C. If the temperature of the mixture varies during measuring with a conductance sensor, the temperature variations must be compensated. It is important that the quality of the active ingredient is always the same. For these reasons it is necessary to check the calibrated values before each measurement, even if the sensor was designed for on-line measurements of relative response time parameters. Similar calibration procedure must be done also for the light transmittance method.

The light transmittance method is a relatively accurate method. However, the design of the required sensor is more complicated than the construction of the conductivity sensor. The measuring cell has a larger dead volume than the conductivity sensor because of the sight glass plates which necessitates an appropriate housing. A possible way of reducing the dead volume of the sensor is by using a glass pipe instead of sight glass plates. This would also solve the problem of waterproofing the sight glasses, which requires careful preparation of the cell before each set of measurements. Preparing the basic solution is also more complicated because of the issue with the weighing of the active ingredients. Another disadvantage of this method lies in a certain distortion of the photodiode output voltage U_D. This can occur when, for example, if there are small air bubbles in the nozzle supply lines adhering to the sight glass surface.

The great potential of this method lies in monitoring the concentration of mixtures with more than one tracer. By using more LEDs with different light intensities, it is possible to measure the concentrations of different color tracers with an appropriate absorption spectrum. This method would then allow good evaluation of the injection and mixing process by injecting diverse products with a suitable injection system.

One advantage of the light transmittance method is that it can also be used for measuring mixture uniformity. However, in such measurements an inverse test procedure has to be used. Instead of coloring a carrier, a pre-colored carrier is chemically decolorized.

A CCD camera-based imaging system was tested only under static conditions. For on-line measurements of mixture concentrations it will be necessary to use a high speed camera synchronized with a Nd:YAG laser. A camera system thus equipped provides high quality, sharp images which can be used for further analysis. The system also allows capturing images of sprays exited the nozzle. This can be helpful in studying the effect of different nozzle types on mixture uniformity. The camera system expresses density (IOD levels, GLT and ROD) as purely relative values, reflecting only a ratio of incident illumination to maximum system response.

In addition to changing with any alteration in the lighting conditions, the relative IOD values are affected by any nonlinearities in the components of the measuring chain. For these reasons, a camera-based imaging system requires external calibration if stable and replicable density measurements are to be obtained.

Taking into account all advantages and disadvantages of the methods described above, the conductivity method appears to be the most suitable method for on-line measurements of mixture concentrations and hence of the response time parameters of the proposed direct injection systems.

6.3 Evaluation of Direct Injection Systems

The main criterion for the evaluation of the tested technical variants of the direct injection system was a short response time before a required concentration of tracer in the outermost nozzles is reached. From a theoretical analysis and from measurements it is clear that the shortest time can be achieved with the point of injection positioned as close to the nozzles as possible. This technical solution was successfully used in the nozzle injection system with injection into the individual nozzles. However, from the point of view of site-specific application this design with a high spatial resolution is not suitable for all methods of herbicide application. Under certain conditions, e.g. off-line application, application with low spatial resolution, or high application rates, it will be preferable to use the boom injection system or the nozzle injection system with injection into a set of nozzles. The choice of the most suitable system will depend strongly on the relevant field situation and on the weed recognition technique used. The three metering systems, the resulting response times and the investigated effects will be discussed in the following chapters.

6.3.1 Evaluation of Boom Injection System

In comparison with currently available direct injection systems with a central point of injection, the boom injection system is a significant improvement in terms of site-specific and variable-rate application. However, there are still some issues related to the transport lag time and the response time. The transport lag time correlates to the distance lag of moving systems such as field sprayers, i.e. the distance a sprayer travels before a concentration change reaches the outermost nozzle.

With the transport lag and response time values in figure 5.24, a sprayer traveling at 8 km h^{-1} would experience a distance lag of 7.1 m and 12.8 m respectively, using XR 8005 nozzles and a 12.7 mm boom pipe inner diameter. In variable rate application, such distance lags would result in significant application rate errors. The transport lag in boom injection sprayers can be controlled to some extent by controlling the sprayers' plumbing, the carrier flow rates and the vehicle's forward speed. The effect of the pipe diameter on lag time was studied with different boom configurations. When the spray solution flowed through a boom pipe with ID = 12.7 mm, the time required before the nozzle was reached was approximately double the time required with a boom pipe width of ID = 6.0 mm, as shown in figures 5.23 and 5.24.

A technique called 'position compensation' can be used to compensate the remaining transport lag. This technique requires that the controller changes the desired application rate long enough before it is actually required so that the change in concentration at the nozzles is realized by the time the sprayer arrives at the desired field location. However, in boom injection systems the transport lag is shortest at the centre of the boom section and longest at the ends of the boom section. This effect was first calculated and then proven by the measurements of lag and response times at each nozzle position as shown in figure 5.25. The estimated values were almost identical with those obtained from the measurements. The resulting lag times for two boom pipe configurations (6.0 and 12.7 mm) at the maximal tested nozzle flow rate Q_c = 2540 ml min^{-1} in figures 5.26 and 5.27 show that the difference between the lag times measured at the centre of the boom section and at the outermost nozzles was approximately 2.0 s for the 12.7 mm boom configuration. For the 6.0 mm boom pipe diameter the difference between these two positions was approximately 0.5 s. It is possible to conclude from these facts that non-sprayed areas or areas sprayed with the wrong application rates can be significantly reduced by using the right plumbing configuration.

The effects of other parameters such as carrier flow and tracer flow rate on lag and response times were studied. Carrier flow rate was found to have a great influence on the lag time. It can be concluded that increases in carrier (nozzle) flow rate reduce lag time and response time. In figure 5.28 it is evident that the lag time and the response time measured for the same one boom pipe diameter configuration were reduced by half, regardless of the solution concentration tested.

The results of the measurements with different tracer flow rates show that there is no significant effect of the tracer flow rate on the lag and response time. This can be interpreted to mean that during injection the lag time was the largest component of the complete response time. During this transportation period the tracer and the carrier are mixed well so that it is impossible to recognize any significant differences when measuring solutions with different concentrations. The influence of the tracer flow rate on the response time of the boom injection system is much smaller than the influence of the carrier flow rate.

The effect of the tracer flow rate on the rise and fall times is evident in figure 5.30. Solutions with low concentrations reach the required concentration faster than solutions with higher concentrations. A great discrepancy between rise and fall times was caused mainly by the dynamic behavior of the metering system during opening and closing of the proportional valve.

Moreover, the effect of viscous solutions on lag and response times was not as strong as expected. There were no significant differences between the times obtained for water and for aqueous glycerine solutions. A possible reason for this was the low concentration of the tracer in the carrier and turbulences in the boom pipe, which led to a high level of dilution of the glycerine solutions.

6.3.2 Evaluation of Nozzle Injection Systems

The two nozzle injection systems promised a huge reduction in response time. This hypothesis was validated by the measurements. As the nozzle injection system with injection into a set of nozzles offers a good compromise between the boom injection and the injection into individual nozzles, there is no doubt that the system with injection into individual nozzles is the most suitable choice for accurate and purposeful variable-rate herbicide application in real time. This system is the only one with which the required response time of the whole application system $T_{RS} \leq 0.45$ s can be reached.

6.3.2.1 Evaluation of Injection into a Set of Nozzles

In this metering system the influences of the studied effects were similar to those investigated for the boom injection system. The obtained lag and response times were generally shorter then those for the boom injection system. The main problem with this system was a delay in the transportation of the tracer through the nozzle supply rail between the proportional valve and the point of injection. This effect was caused by the dynamics of the whole injection system including the pump, the control valve and the tracer supply lines (friction losses). After opening the proportional valve, the small gear pump used for tracer delivery did not compensate the pressure drop in the dead volume space between the control valve and the metering orifices rapidly enough. For this reason a diaphragm pump with greater performance was used for the tracer delivery. Measurements were performed for both pumps with the aim of comparing their performance and the corresponding effects on response time.

The influence of the length of the tracer supply rail on response time was studied at different nozzle positions, namely at the centre nozzles and at the ends of the boom section. Similarly to the boom injection system, unequal response times along the boom section was also found in this nozzle injection system. However, the difference between the response times measured at the central nozzles and at the outermost nozzles was smaller than in the boom injection system. The maximum difference was approximately 0.5 s. There were no significant differences between the lag times measured at the different positions (see Fig. 5.36 and 5.37). The average lag time was 0.15 s for all measurements, which does not exceed the maximum standard deviation of 0.28 s obtained during these measurements. When comparing the two delivery pumps used in these measurements, the system with the diaphragm pump reached the required concentration 0.25 s faster on average than the system with the gear pump.

The effects of metering orifice size on rise and fall times are discussed in chapter 5.4.2.1.1. For the practical use of this system it is important to avoid the risk of foreign particles blocking the metering orifices. This can be achieved by using suitable strainers or suitably dimensioned metering orifices. The findings obtained from the measurements suggest that it is best to use orifices larger than size CP 4916-08. On the other hand, when bigger orifice sizes are used for metering liquids with low viscosities, such as water, flow rates under 20 ml min^{-1} per one nozzle cannot be reached.

The effect of the flow rate of the carrier on lag and response times is closely related to the concentration of the mixture solution. From measurements with different pumps (see Fig. 5.39 and 5.40) it is clear that an increased nozzle flow rate greatly reduced lag and response times. When injecting tracer at a constant rate of 10 ml min^{-1} with the diaphragm pump, the longest lag time of 0.33 s was obtained at the minimum carrier flow rate of 340 ml min^{-1}. The minimum lag time of 0.13 s was measured at the maximum carrier flow rate of 1970 ml min^{-1}. The minimum response time of 1.12 s was also obtained at the maximum carrier flow rate. Similar effects were observed when injecting tracer at various flow rates into a constant carrier flow.

At a decreased tracer concentration in the carrier flow, the response time was reduced, while the lag times were not significantly affected by the different solution concentrations in the range used in the measurements. Unlike in the boom injection system, the proportion of lag time to the response time is very small. The main part of the response time is used for building up the required concentration. The use of diaphragm check valves in the nozzle bodies supported the mixing process. However, to achieve adequate mixing and to ensure a uniform concentration in all nozzles along the boom, it is necessary to use additional, static mixers.

In analogy to the boom injection system, the lag times and the response times measured for the viscous tracers were similar to those obtained for water. For both concentrations tested (see Fig. 5.43 and 5.44), the lag time values tended to increase slightly as the viscosity of the tracer increased. A comparison of the response time statistics for the three tracers with a one-way ANOVA and a Tukey's test at $p = 0.05$ indicates that under fixed operating conditions there were no significant differences between the different viscosities in terms of response time.

6.3.2.2 Evaluation of Injection into Individual Nozzles

As mentioned before, the system with injection into individual nozzles has the shortest response times of all systems tested. The distance to be covered by the tracer between the control valve and the nozzle is minimized. The effects of different carrier and tracer flow rates investigated for this system were identical with those investigated for the system with injection into a set of nozzles. The same time dependencies on flow rates (concentrations) were observed. In this system, moreover, increased nozzle flow rates greatly reduced lag and response times. The shortest response times were obtained for the system with a diaphragm pump and a constant tracer flow rate of Q_a = 10 ml min^{-1}. Depending on the nozzle used (carrier flow rate), the response times were in a range from 0.27 to 0.94 s. The average lag time was 0.1 s.

The response times measured for aqueous glycerine solutions with viscosities of 60 and 219 mPa s were similar to those obtained with water at a nozzle flow rate of 1970 ml min^{-1}. At both tracer flow rates, the lag and response time values tended to increase slightly as the viscosity of the tracer increased. This effect was probably due to low pump performance. However, a comparison of the response time statistics for the three tracers indicates that under fixed working conditions there was no significant difference in terms of lag and response times between the different viscosities. The results from this measurement could be distorted by the fact that no mixer was used to obtain adequate mixture homogeneity in the nozzle body. It can be concluded that the viscosity of used glycerine solutions had little influence on lag time.

The time required for the transient response to reach 95 % of full concentration averaged 0.55 s with a maximum standard error of 0.14 s. Depending on the sprayer velocity in the field, this translates into a spatial error band. However, if the efficiency threshold is less than 95 %, then the error time is smaller. For instance, if the efficiency threshold (concentration of chemical for satisfactory weed control) was 50 %, the error time would be 0.30 s, which would meet the design criteria. In others words, it is possible to work with controlled opening of the proportional valve (valve timing). The steepest profile of the transient curve (shortest rise time) is obtained while the valve is being open to full open position. During this period it is possible immediately to decrease the flow rate to the required level by throttling the valve.

7. Conclusion

The laboratory test bench and instrumentation proved means for measuring the response time characteristics of different variants of a direct injection system. All components used to control the tracer and carrier flow rate, such as pumps, valves and metering orifices, were calibrated before they were used in experimental measurements. A differential pressure flow meter for monitoring rapid changes in the flow rate of the injection metering system was designed and assembled. Three different injection systems - one boom injection system and two nozzle injection systems with different systems for controlling the chemical flow rate - were developed and tested.

In assessing the effect of herbicide viscosity on response time, the range of viscosities of the most widely used herbicide products, tap water (~1 mPa s) and three aqueous glycerine solutions with concentrations of 80 % (60.1 mPa s), 85 % (109 mPa s) and 90 % (219 mPa s) were selected for tests as substitute liquids. However, the response times of all three injection systems were not significantly affected by the different viscosities of the simulated herbicides.

A conductivity method and an optical method based on spectrophotometry were developed for on-line measurements of mixture concentrations. The results of static and dynamic calibration tests showed the good accuracy of both measurement devices and proved the practicability of these methods. There were significant functional relations between mixture concentration and output signal for each of these methods. The in-line measuring cells used in the conductivity and light transmittance method can be installed in any place throughout the length of spray booms. Thus, they can be easily used for determining lag and response time and mixture uniformity on-line.

The conductivity method appears as the most suitable method for on-line measurements of mixture concentrations and hence of the response time parameters of the proposed direct injection systems. However, the temperature of the mixture has an influence on the outgoing voltage U_c. If the temperature of the mixture varies during measuring with the conductance sensor, temperature differences must be compensated.

The results from the series of measurements of the response time parameters under different testing conditions indicate that the response times of the boom injection system do not meet the requirements of on-line herbicide application. The boom pipe diameter greatly influenced the spray flow lag time at the end of spray boom. Even with reduced pipe diameters the required lag time was not obtained. The shortest lag time obtained for the most suitable combination of hose diameters (8.0-8.0-6.0-6.0 mm) was approximately 2.79 s at the highest nozzle flow rate of 2540 ml min^{-1}.

Moreover, the flow rate of the carrier had a great influence on the reduction of the lag and response times of this system. The response times measured for each boom pipe diameter configuration were reduced by half. These results were independent of the solution concentration tested.

In the experiments performed with the nozzle injection systems, the carrier and tracer flow rates, as well as the injection points were varied. The effect of the carrier and tracer flow rates on the lag and response times is closely related to the concentration of the mixture solution. The lower the concentration of the tracer in the carrier flow, the shorter was the response time. In the case of injection into a set of six nozzles on one boom section using a proportional valve and metering orifices, the response time was between 0.79 and 2.25 s, depending on the concentration and the tracer delivery pump used.

Under optimal conditions, the response time can be reduced to less than 0.30 s if the tracer is injected directly into individual nozzles. These results indicate that it is possible to design a sprayer with a nozzle injection system in which the flow of the chemicals is controlled individually for each nozzle by means of a proportional valve. At the regular operation speed of field sprayers (8.0 km/h ~ 2.2 m/s), herbicide application rate can be adjusted in a distance of less than 1.0 m. However, the system lag time required for on-line application can only be obtained at nozzle flow rates higher than 1970 ml min^{-1}. For practical applications this has to be reduced. With evolving computer technology, it will be possible to reduce the time necessary for image processing, which will produce greater time reserves for successful online application.

8. References

ANONYMOUS: Pflanzenschutzmittel-Verzeichnis Teil 1, Ackerbau – Wiesen und Weiden - Hopfenbau- Nichtkulturland. Bundesamt für Verbraucherschutz und Lebensmittelsicherheit, 2003

ANTUNIASSI, U.R., MILLER P.C.H. and M.E.R. PAICE: Dynamic and Steady-State Dose Responses of some Chemical Injection Metering Systems. BCPC Conference – Weeds, Symposium Proceedings No. 7D-I, 1997

AMSDEN, R.C. and E.S.E. SOUTHCOMBE: Formulation and the machine. The agricultural Engineering 32 (2), 1977, p. 38-40

ATKINS, P.W.: Physikalische Chemie. 3. Ausgabe, Wiley/VCH, Weinheim, 2002

AUDSLEY, E.: Operational research of patch spraying. Crop Protection 12, 1993, p.111-119

AUTHOR'S COLLECTIVE: Precision Farming im Pflanzenschutz am Beispiel Unkrautbekämpfung. KTBL – Schrift 402, 2001

BACKES, M., SCHUMACHER, D. and L. PLÜMER: The sampling problem in weed control – are currently applied sampling strategies adequate for site-specific weed control? Proceedings of 5th ECPA Conferece, Upsalla, Sveden, 2005, p. 155-160

BBA, BIOLOGISCHE BUNDESANSTALT für LAND- und FORSTWIRTSCHAFT: Richtlinien für die Prüfung von Pflanzenschutzmitteln und Pflanzenschutzgeräten. Teil VII. BBA Braunschweig, 2002

BBA, BIOLOGISCHE BUNDESANSTALT für LAND- und FORSTWIRTSCHAFT: Pflanzenschutzmittelverzeichnis Teil VI. Annerkannte Pflanzenschutzgeräte, 52. Auflage, BBA Braunschweig, 2005

BENNET, K. A. and R. B. BROWN: Direct nozzle injection and precise metering for variable rate herbicide application. ASAE Paper 97-1046, 1997

BENNET, K. and R. BROWN: Towards a real time, intelligent precision sprayer. Agri-food Research in Ontario, Winter ´98-´99, 1998

BRDLICKA, R.: Grundlagen der physikalischen Chemie. VEB Deutscher Verlag der Wissenschaften, Berlin, 1982

BROWN, R. B., STECKLER, J. P. G. A. and G. W. ANDERSON: Remote sensing for identification of weeds in no-till corn. Transactions of the ASAE 37(1), 1994, p. 297-302

BÖTTGER H. and H.-R. LANGER: Neue Technik zur variablen Spritzmitteldosierung. Landtechnik 58 (3), 2003, p. 142-143

BÜRKERT: Product information – Proportional Valves. Bürkert GmbH, 2002

CARDINNA, J., SPARROW D.H. and E.L. MC COY: Analysis of spatial distribution of common lambsquarters (Chenopodium album) in non-till soybean (glacine max). Weed science 43, 1995, p. 258-268

CHI, L., KUSHWAHA, R. L. and F. W. BIGSBY: Chemical flow rate control for an injection type sprayer. Transactions of ASAE Vol. 5 (3), 1989, p. 339-343

CHO, H. K., MARLEY, S. J. and J. L. BACKER: Injection metering of spray concentrates. ASAE Paper No. MCR 85-138, 1985

COCHRAN, D.L., THREADGILL, E.D. and S.E. LAW: Physical properties of three oils and oil-insecticide formulation used in agriculture. Transaction of the ASAE, 30, 1987, p. 1338-1342

CHRISTENSEN, S., WALTER A. M. and T. HEISEL: The patch treatment of weeds in cereals. Proceedings of Brighton Crop Protection Conference - Weeds, 1999, p. 591-600

DARR, M.J.: Development and evaluation of controller area network based autonomous vehicle. Thesis, Lexington, Kentucky, 2004

FELBER, U.R.: Closed transfer systems for small volume refillable containers. A.N.P.P. – B.C.P.C. – Second International Symposium on Pesticide Application Techniques, Strasbourg, 1993

FELTON, W. L. and K. R. MCCLOY: Spot spraying. Agricultural Engineering 11, 1992, p. 9-11

FROST, A. R.: A pesticide metering system for use on agricultural spraying machines. Journal of Agriculture Engineering Research 46, 1990, p. 55-70

GANZELMEIER, H.: Innovative techniques and methods fort the saving of plant protection products. Yearbook of Agriculture Engineering 16, VDMA Landtechnik, VDI, KTBL, 2004

GATE, S. R. and S. C. PHATAK: A compressed air direct injection pesticide sprayer. Applied Engineering in Agriculture, Vol. 7 (2), 1991

GATE, S. R. and C. D. PERRY: Ground speed control of pesticide application rates in a compressed air direct injection sprayer. Transactions of ASAE. 37 (1), 1994, p. 33-38

GEBHARDT, M. R., KLIETHERMES, A. R. and C. E. GOERING: Metering Concentrated Pesticides. Transactions of ASAE, Vol. 27 (1), 1984, p. 18-23

GERHARDS, R.: Verfahren zur Teilschlagspezifischen Unkrautkontrolle. Habilitation Bonn, 1997

GERHARDS, R. and M. SÖKEFELD: Sensor Systems for Automatic Weed Detection. Proceedings of the BCPC Conference – Weeds, 2001, p. 827-834

GERHARDS, R., SÖKEFELD, M., NABOUT, A., THERBURG, R.-D., KROHMANN, P., TIMMERMANN, C. and W. KÜHBAUCH: Online weed control using digital image analysis. Zeitschrift für Pflanzenkrankheiten und Pflanzenschutz, Sonderheft XVIII, 2002, p. 421-427

GERHARDS, R. and S. CHRISTENSEN: Real-time weed detection, decision making and patch spraying in maize, sugar beet, winter wheat and winter barley. Weed Research 43, 2003, p. 385-392

GILES, D.K. and J.A. COMINO: Droplet size and spray pattern characteristic of an electronic flow controller for spray nozzles. Journal of Agricultural Engineering Research, 47, 1990, p. 249-267

GILES, D.K., DOWNEY, D., SLAUGHTER, D.C., BREWIS-ACUNA, J.C. and W.T. LANINI: Herbicide micro-dosing for weed control in field-grown processing tomatoes. Applied Engineering in Agriculture, Vol. 20(6), 2004, p. 735-745

GILLIS, K.P., GILES, D.K., SLAUGHTER, D.C., DOWNEY, D. and C. GLIVER: Development of a machine vision controlled roadside herbicide applicator. ASAE Paper No. 02-1026, 2002

GUYOUN, E., HULIN, J.-P., PETIT, L. and C.D. MITESCU.: Physical Hydrodynamics. Oxford. 2001

GUSTAV HEESS: Product specification – Glycerol 99%, Ph. Eur. 4.00. GUSTAV HESS GmbH, 2002

GÖHLICH, H.: Entwicklungsaufgaben in der Pflanzenschutztechnik. Landtechnische Forschung 18, 1970, p. 95-99

HOCK, B., FEDTKE, C. and R.R. SCHMIDT: Herbizide, Entwicklung, Anwendung, Wirkungen, Nebenwirkungen. Georg Thieme Verlag, Stuttgart, 1995

HOFSTEE, J.W. and D. GOENSEE: Simulation of a controller area network-based tractor-implement data bus according to ISO 11783. Journal of Agriculture Engineering Research, 73, 1999, p.383-394

HOLLSTEIN, A. and R. H. BILLER: Weiterentwicklung eines optoelektronischen Sensorsystems zur gezielten Unkrautkontrolle. Agrartechnische Forschung 4, 1998, p. 11-17

HUGHES, K.L. and A.R. FROST: A review of agricultural spray metering. Journal of Agriculture Engineering Research Vol. 32, 1985, p. 197-207

IMAGING RESEARCH: Densitometry. Internet page - http://www.imagingresearch.com/applications/densitometry.asp, Imaging Research Inc., 2007

KIFFERLE G. and W. STAHLI: Spritz- und Sprühverfahren in Pflanzenschutz und Flüssigdünnung bei Flächenkulturen. Books on Demand GmbH, Norderstedt, Germany, 2001

KOO, Y.M., YOUNG, S.C. and D.K. KUHLMAN: Flow characteristic of injected concentrates in spray booms. ASAE Paper No. 87-16202, 1987

KOO, Y. M. and D.K. KUHLMAN: A variable flow nozzle with consistent spray performance. Transactions of ASAE, Vol. 36 (3), 1993, p. 685-690

KRIZ, R.: Strojirenska prirucka 4, Mechanika tekutin – Termomechanika – Tekutinove mechanismy - Kineticke mechanismy. Scientia, Praha,1994

KUHLMAN, D.K., TENEYCK, D. and G.H. LARSON: Direct metering of pesticides concentrations. Pesticide Formulations and Application Systems, Vol. 5 ASTM STP 915, 1986

LANDERS, A.: Direct injection sprayers – a method of reducing environmental pollution. Proceedings ANPPBCPC second international symposium on pesticide application techniques, Strasbourg, France, 1993, p. 305-312

LANDERS, A.: A compressed air direct injection crop sprayer. Aspects of Applied Biology 48, 1997

LANDERS, A.: The theory and constituent parts of a direct injection sprayer. In: Proc. National Association of Agricultural Contractors - Direct Injection Spraying Seminar. Silsoe Research Institute, Wrest Park, Silsoe, Bedford, 1998

LECHLER, GmbH: Offenlegungsschrift DE 13 53 789 A1, Deutsches Patent- und Markenamt, 2005

LETTNER, J., HANK, K. and P. WAGENER.: Ökonomische Potenziale der teilflächenspezifischen Unkrautbekämpfung, Weihenstephan, 2001

LINDTNER, G.: Geschwindigkeitsabhängige Direkteinspeisung von Pflanzenbehandlungsmitteln (GDE). Landtechnik 3, 1985

LUTMAN, P.J.W. and L.J. REW: Spatially selective weed control in arable crops – where are we now? Proceedings of Brighton Crop Protection Conference - Weeds, 1997, p. 637-640

LUTMAN, P.J.W., PERRY, N. H., HULL, R.I.C., MILLER, P.C.H., WHEELER, H.C. and R.O. HALE: Developing a weed patch spraying system for use in arable crops. HGCA Project Report No. 291, 2002

MARSHALL, E.J.P.: Field-scales estimates of grass weed populations in arable land. Weed Research 28, 1998, p. 191-198

MICRON SPRAYERS: Product information. Micron Sprayers Ltd., 2002

MID-WEST TECHNOLOGY: Product information - TASC injection control system 6600. MID-WEST Technology Inc., 2005

MILLER, M. S. and D. B. SMITH: A direct nozzle injection controlled rate spray boom. Transactions of ASAE 35(3), 1992, p.781-785

MILLER, P.C.H., PAICE, M.E.R. and A.D. GANDERTON: Methods of controlling sprayer output for spatially variable herbicide application. Proceedings Brighton Crop Protection Conference on Precision Agriculture – Weeds, 1997, p. 641-644

MILLER, P.C.H.: Patch spraying: future role of electronics in limiting pesticide use. Pest Management Science 59, 2003, p. 566-574

MILLER, P.C.H.: Plant protection and plant cultivation. Yearbook of Agriculture Engineering 15, VDMA Landtechnik, VDI, KTBL, 2003

MOTZIGEMBA, M., ROTH, N., BOTHE, D., WARNECKE, H.-J., PRÜSS, J., WIELAGE, K. and B. WEIGAND: The Effect of Non-Newtonian Flow Behaviour on Binary Droplet Collisions: VOF-simulation and experimental analysis. In: Lozano (Eds.) Proceedings ILASS – Europe, 2002

MORTENSEN, D. A., JOHNSON G. A. and J. L. YOUNG: Weed distribution in agricultural fields. In: Robert P. and R.H. Rust (Eds.): Soil specific crop management, Agronomy society of America, 1993, p. 113-124

MORTENSEN, D. A. and J. A. DIELEMAN: Why weed patches persist: dynamics of edges and density. In: R.W. MEDD and J.E. PRATLEY (Eds.): Proceedings of Precision Weed Management in Crops and Pasture, Wagga Wagga, Australia, 1998, p. 14-19

MSR DOSIERTECHNIK: Product information – Agroinject. MSR Dosiertechnik GmbH, 2004

NIEBUHR, J. and G. LINDNER: Physikalische Messtechnik mit Sensoren. R. Oldenbourg, Verlag Wien,1994

NORDMEYER, H and P. NIEMANN: Möglichkeiten der gezielten Teilflächenbehandlung mit Herbiziden auf der Grundlage von Unkrautverteilung und Bodenvariabilität. Zeitschrift für Pflanzenkrankheiten und Pflanzeschutz, Sonderheft XIII, 1992, p. 539-547

NORDMEYER, H., HÄUSLER, A. und P. NIEMANN: Weed mapping as a tool for patchy weed control. In: Brown, H., et al. (Eds.): Proceedings of the Second International Weed Control Congress, Volume I, Copenhagen, 1996, p. 119-124

NORDMEYER, H. and P. NIEMANN: Patchy weed control in agricultural practice. Proceedings of Brighton Crop Protection Conference - Weeds, 1997, p. 649-650

NTECH INDUSTRIES: Product information – Weedseeker. NTech Industries Inc. 2005

OEBEL, H., GERHARDS, R., BECKERS, G., DICKE, D., SÖKEFELD, M., LOCK, R., NABOUT, A. and R.-D. THERBURG: Teilschlagspezifische Unkrautbekämpfung durch raumbezogene Bildverarbeitung im Offline (und Online)-Verfahren (TURBO) – erste Erfahrungen aus der Praxis. Zeitschrift für Pflanzenkrankheiten und Pflanzenschutz, Sonderheft XIX, 2004, p. 459-465

OEBEL, H. and R. GERHARDS: Kameragesteuerte Unkrautbekämpfung – eine Verfahrenstechnik für die Praxis. Zeitschrift für Pflanzenkranheiten und Pflanzenschutz Journal of Plant dieses and Protection, Sonderheft XX, 2006

PACIGA, A.: Projektovanie a prevadzka cerpacej techniky. Alfa, Bratislava, 1990

PAICE, M.E.R., MILLER, P.C.H and J.D. BODLE: An Experimental Sprayer for the Spatially Selective Application of Herbicides. Agriculture Engineering Research, 60, 1995, p. 107-116

PAICE, M.E.R., MILLER, P.C.H and A.G. LANE: The response characteristics of a patch spraying system based on injection metering. Aspects of Applied Biology, 48, 1997, p. 41-48

PAICE, M. E. R., MILLER, P.C.H. and W. DAY: Control requirements for spatially selective herbicide sprayers. Computer and Electronics in Agriculture 14, 2001, p. 163-177

PECK, D.R. and L.O. ROTH: Field sprayer induction system development and evaluation. ASAE Papers No. 75-1541.St. Joseph, MI. ASAE, 1975

PEISL, S. and M. ESTLER: Direkteinspeisung von Pflanzenschutzmitteln – Ein Systemvergleich. Landtechnik 47 (3), 1992

PEISL, S. and M. ESTLER: Direkteinspeisung von Pflanzenschutzmitteln – Beobachtungen im praktischen Einsatz. Landtechnik (48) 4 – 93, 1993

PERKOW, W. and H. PLOSS: Wirkungssubstanzen der Pflanzenschutz- und Schädlings-bekämpfungsmittel, Teil 3. Parey Buch Verlag, Berlin, 2004

PESSINA, D., GUERRETTI, M. and D. FACCHINETTI: Test of a “dual” field sprayer with distribution valves driver mechanically and by computer. EuAgEng papers 02-PM-013, 2002

QIU, W., WATKINS, G.A., SOBOLIK, C.J. and S.A. SHEARER: A feasibility study of direct injection for variable-rate herbicide application. Transactions of ASAE 41(2), 1998, p. 291-299

RAVEN INDUSTRIES: Technical Documentation SCS 700. Raven Industries Inc. 2004

ROCKWELL, A. D. and P. D. AYERS: A variable rate, direct nozzle injection field sprayer. Transactions of ASAE 12(5), 1996, p.531-538

SCHMIDT, M.: Direkteinspeisung von Flüssigen Pflanzenbehandlungsmitteln. Dissertation, Berlin, 1983

SCHMITT-OTT, M.: Systeme zur fahrgeschwindigkeitsabhängigen Dosierung von Pflanzenschutzmitteln. Grundlagen der Landtechnik, 24 (2), 1974, p. 61-63

SCHWIEDOP U.: Oral communication. Bayer CropScience A.G., Germany, 2002

SARKER, M.K.U.: Measurement of Droplet Spectra and Spray Drift from Flat-Fan Hydraulic Nozzles and Development of Semi-Empirical Models Using Dimensional Analysis. PhD. Thesis, Cranfield University, UK, 1997

SUMNER, H. R., SUMNER, P. E. and B. G. MULLIMIX: Injection pump frequency effect on sprayer uniformity. Applied Engineering in Agriculture 16(5), 2000, p. 465-470

STAFFORD, J. and P.C.H. MILLER: Spatially selective application of herbicide to cereal crops. Elsevier Science Publishers B.V., 1993

STREETER, V. L.: Handbook of Fluid Dynamics, McGraw-Hill, London, 1961

STONE, M.L., GILES, D.K. and K.J. DIEBALL: Distributed network system for control of spray droplet size and application rate for precision chemical application. ASAE Paper No. 98-1018. St. Joseph, MI: ASAE, 1999

SUDDUTH, K.A., BORGELT, S.C. and J. HOU: Performance of a Chemical Injection Sprayer System. Applied Engineering in Agriculture, Vol. 11 (3), 1995, p. 3434-348

SUI, R., J.A. THOMASON, J.L. WILLERS, F.P. LEE and R. WANG: Variable-Rate Spray System Dynamic Evaluation. ASAE Meeting presentation, Paper: 031128, 2003

SÖKEFELD, M., GERHARDS and W. KÜHBAUCH: Einsatz der Bildvearbeitung zur teilschlagspezifischen Unkrautkontrolle. Sensorsysteme im Precision Farming Tagnung, Rostock, 1999

TIAN, L., REID, J.F. and J.W. HUMMEL: Development of precision sprayer for site specific weed management. Transactions of ASAE 42 (4), 1999, p. 893-900

TOMKINS, F. D., HOWARD, K. D., MOTE, C. R. and R. S. FREELAND: Boom flow characteristic with direct chemical injection. Transactions of ASAE 33(3), 1990, p.737-743

TOMLIN, C.D.S.: The Pesticide Manual, 13th Edition. BCPC, 2003

ULRYCH, E.: Hydromechanika. Ceska Zemedelska Univerzita v Praze. Prague, 2001

VIDRINE, C.G., GOERING, C.E., DAY, C.L., GEBHARDT, M.R. and D.B. SMITH: A constant pesticide application rate sprayer model. Transaction of the ASAE Vol. 18 (2), 1975, p. 439-443

VDI 2225, BLATT 3: Konstruktionsmethodik - Technisch-wirtschaftliches Konstruieren - Technisch-wirtschaftliche Bewertung. VDI-Gesellschaft Entwicklung Konstruktion Vertrieb, 1998

VDI/VDE 2173: Strömungstechnische Kenngrößen von Stellventilen und deren Bestimmung. VDI/VDE-Gesellschaft Mess- und Automatisierungstechnik, 1962

VRINDTS, E.: Automatic recognition of weeds with optical techniques as a basis for site-specific spraying. Dissertation, Leuven, 2000

WALLINGA, J., GROENEVELD, R.M.V. and L.A.P. LOTZ: Measures that describes the spatial patterns at different levels of resolution and their application for patch spraying of weeds. Weed research 38, 1998, p. 351- 359

WANG, N., ZHANG N., DOWELL F. E., SUN Y. and D.E. PETERSON: Design of optical weed sensor using plant spectral characteristics. Transactions of ASAE, Vol. 44 (2), 2001, p.409-419

WARTENBERG, G.: Teilflächenspezifischer Herbizideinsatz. Landtechnik 51 (4), 1996, p. 196-197.

WAY, T.R., VON BERGAEN, K., GRISSO, R.D. and L.L. BASHFORD: Simulation of chemical application accuracy for injection sprayers. Transaction of the ASAE 35(4), 1992, p. 1141-1149

WOMAC, A. R., VALCORE, D. L. and R. A. MAYNARD II: Variable – concentration direct injection from fixed-ratio diluent-driven pump. Transactions of ASAE Vol. 45 (6), 2002, p.1721-1728

WOZNIAK, G.: Zerstäubungstechnik – Prinzipien, Verfahren, Geräte. VDI Buch Springer, 2003

ZHU, H., OZKAN, H. E., FOX, R. D., BRAZEE, R. D. and R. C. DERKSEN: Mixture uniformity in supply lines and spray patterns of a laboratory injection sprayer. Transactions of ASAE Vol. 14 (3), 1998, p. 223-230

ZHU, H., OZKAN, H.E., FOX, R.D., BRAZEE, R.D. and R.C. DERKSEN: Reducing Metering Lag and Nonuniformity for Injection Sprayers Applying Highly Viscous Fluids. ASAE paper No. 97- 1044, 1997

9. Appendices

Table 9. 13: Physical properties of common herbicide products - overview

Active Ingredient	Product Name (Producer)	Formulation Group	Dose Rate A_a [l ha^{-1}]	Density ρ [g cm^{-3}]	Dynamic Viscosity η [mPa s]
Aclonifen	Bandur (Bayer)	SC	1.0 – 4.0	1.46	n.d.
Atrazin – not allowed in the EU	Gesaprim 600 (Syngenta)	SC	1.5 – 3.0	0.9 – 1.23	400 – 700
Bentazone	Basagran (BASF)	SL	2.0	1.2	7.8
Bifenox, Ioxynil, Mecoprop-P	Foxtrill Super (FCS)	SC	2.0	1.31	267
Bromoxymil	Bromotril 250 (FCA)	SC	2.0	1.160	2850
Chloridazon	Pyradex FL (BASF)	DC	5.0 – 6.0	1.14 –1.20	38
Clomazone	Command 36 (FMC Corp.)	CS	0.15 –0.25	1.16	143 – 412
Clopyralid	Lontrel 300 (Dow AgroScience)	SL	0.25 – 0.40	1.16	n.d.
Clethodim	Select Max (Vallent)	EC	0.75 –1.0	0.92	4.76
Cycloxydin	Focus Ultra (BASF)	EC	2.5 – 5.0	0.93	4.7
Dicamba	Banvel 480 (Syngenta)	SL	0.1 – 0.6	1.16 – 1.20	9.81
Diflufenican, Flurtamone	Bacara (Bayer)	SC	1.0	1,113	26
Ethofumesat	Ethosat 500 (FCS)	SC	0.6 – 2.0	1.13	772
Ethofumesat, Phenmedipham	Betanal Expert (Bayer)	EC	1.080	1.080	105 – 150
Flurenol	Starane Dow AgriScience	EC	0.3 – 1.0	1.1	n.d.
Flurochloridone	Racer (FCS)	CS	3.0	0.96 – 1.25	1196
Glufosinate – ammonium	Basta (Bayer)	SC	2.5 – 5.0	1.11	63 - 73
Glyphosat	Roundup Ultra (Monsanto)	SC	3.0 – 5.0	1.17	65
Isoproturon, Ioxynil, Diflufenican	Azur (Bayer)	SC	2.5	1.15	69

Linuron	Afalon 450 (Bayer)	SC	1.0 – 2.0	1.14 –1.24	0.5
MCPA	U 46 M Fluid (BASF)	SC	1.5	1.12	15.5
Mecoprop-P, Diflufenican	Loredo (Bayer)	SC	1.5 – 2.0	1.27	44
Mesotrione	Calistto 480 SC (Syngenta)	SC	0.2 – 0.3	1.19	2700
Metamitron	Goltix Top (AGM)	SC	1.5 – 3.0	1.21	600 – 1200
Metazachlor	Butisan 400	SC	1.5 – 2.0	1.09 – 1.15	< 150
Metolachlor	Dual Gold (Syngenta)	EC	5.0	1.1	128
Nicosulfuron	Milagro (Syngenta)	SC	1.0	0.96	170 – 190
Paraquat	Gramoxone (Syngenta)	SC	2.0 – 3.0	1.08	81.8
Pendimethalin	Stomp SC (BASF)	SC	2.5 – 5.0	1.11	n.d.
Pendimethalin, Flufenacet	Malibu (BASF)	EC	2.0 – 3.0	1.06	11.7
Phenmediphan	Asket 470 (Bayer)	SC	0.65	1.15	146 – 215
Phenmedipham, Ethofumesat	Powertwin plus (FCS)	SC	0.8 – 2.5	1.11	114
Prometryn	Gesagard 500 (Syngenta)	SC	1.0 – 3.0	1.12	400 – 800
Terbuthilazin, Bentazon	Artett (BASF)	SC	3.5 – 5.0	1.11	103
Terbuthilazin, S-metolachlor	Gardoprim Plus Gold 500 (Syngenta)	SC	4.0	1.08	130 – 719
Topramezone	Clio (BASF)	SC	0.15	1.13	65.7
Adjuvant	FCS Rapsöl	L	0.3 – 0.5	0.92	57

Source: HOCK et al.1995; ANONYMOUS, 2003; TOMLIN, 2003; PERKOW and PLOSS 2004; Material Safety Data Sheets

Table 9. 14: Technical specifications of used sensors

Sensor	Type	Manufa-cturer	Output Signal	Operation Voltage	Working range	Accuracy	Notice
Flow meter - Carrier	38410-EM-05-1/2	Spraying Systems Co.	4000 Imp/L	11 - 14 VDC	1 - 20 l min^{-1}	±1 %	Mounted vertically No moving parts
Wheel flow meter - Tracer	FCH- PP	B.I.O-TECH GmbH	2350 Imp/L	5 - 24 VDC	0.03 - 5 l min^{-1}	±0.5 % (repeatabili-ty of frequency response); ±2 %	Nozzle: 1.7 mm; Viscosity range: 1 - 400 cST; System pressure max. 16 bar
Differential pressure flow meter - Tracer	DDS 332 (Diff.)	SIKA Dr. Seibert & Kühn GmbH & Co.	0-10 V	18 – 33 VDC	0 - 300 mbar	±0.5 % lin.	System pressure max. 600 mbar (one side), 25 bar (static)
Pressure transmitter - Carrier	PTMv (Abs.)	Armaturen-bau GmbH	0-10 V	13 - 28 VDC	0 - 25 bar	±0.5 %	½"
Pressure transmitter - Tracer	RÜCO - P-20 DMU (Abs.)	Paul Rüster & Co. GmbH	0-5 V	12 - 32 VDC	0 - 10 bar	±0.5 % lin.; ±1.5 % abs.	¼"
Pocket Digital Thermometer	CheckTemp 1	Hanna Instruments	-	1.5 VDC	-50 - +150 °C	Resolution 0.1 °C ±0.3 °	

Table 9. 15: Technical specifications of components used in the wet system

Component	Type	Manufacturer	Operation Voltage	Flow capacity	Notice
Carrier Pump	AR 120 bp	Annovi-Reverberi	-	169 l min^{-1}	Max. pressure 15 bar
Tracer pump 1	P- Series PDS. 38PPPV1	Tuthill Co.	12 VDC	1.26 l min^{-1}	Max. pressure 9 bar
Tracer pump 2	AR 202 SP VRI	Annovi-Reverberi	-	max. 19.9 l min^{-1}	Max. pressure 20 bar
Pressure relief valve - Carrier	UCM	Annovi-Reverberi	-	160 l min^{-1}	System pressure max. 20 bar
Pressure relief valve – Tracer pump 1	NIRO	ZUWA Pumpe GmbH	-	20 l min^{-1}	System pressure max. 15 bar
Pressure relief valve – Tracer pump 2	VR 20 S	Annovi-Reverberi	-	25 l min^{-1}	System pressure max. 20 bar
Electric pressure regulating valve - Carrier	2/2 way, AA 344 AE -2RL	Spraying Systems Co.	12 VDC	102 l min^{-1}	Setting time 12 s; System pressure max. 20 bar;
PWM valve - Tracer	2/2 way prop. NC; 6022-00,8	Bürkert GmbH	24 VDC	0.3 l min^{-1}	Integrated electronic control - input signal 0 - 10 V; System pressure max. 8 bar; Power consumption 8 W; Setting time < 50ms
Strainer - Carrier	AA122-PP	Spraying Systems Co.	-	45 l min^{-1}	50 mash screen; System pressure max. 10 bar; ½" pipe connection
Strainer - Tracer	AA124A - PP	Spraying Systems Co.	-	129 l min^{-1}	50 mash screen; System pressure max. 5 bar; ½" pipe connection
Cooling Thermostat	Ecoline RE 204	Lauda GmbH & Co.	230 VAC	17 l min^{-1}	Working temperature range -10 °C ... 200 °C; Temperature control ± 0,01 °C

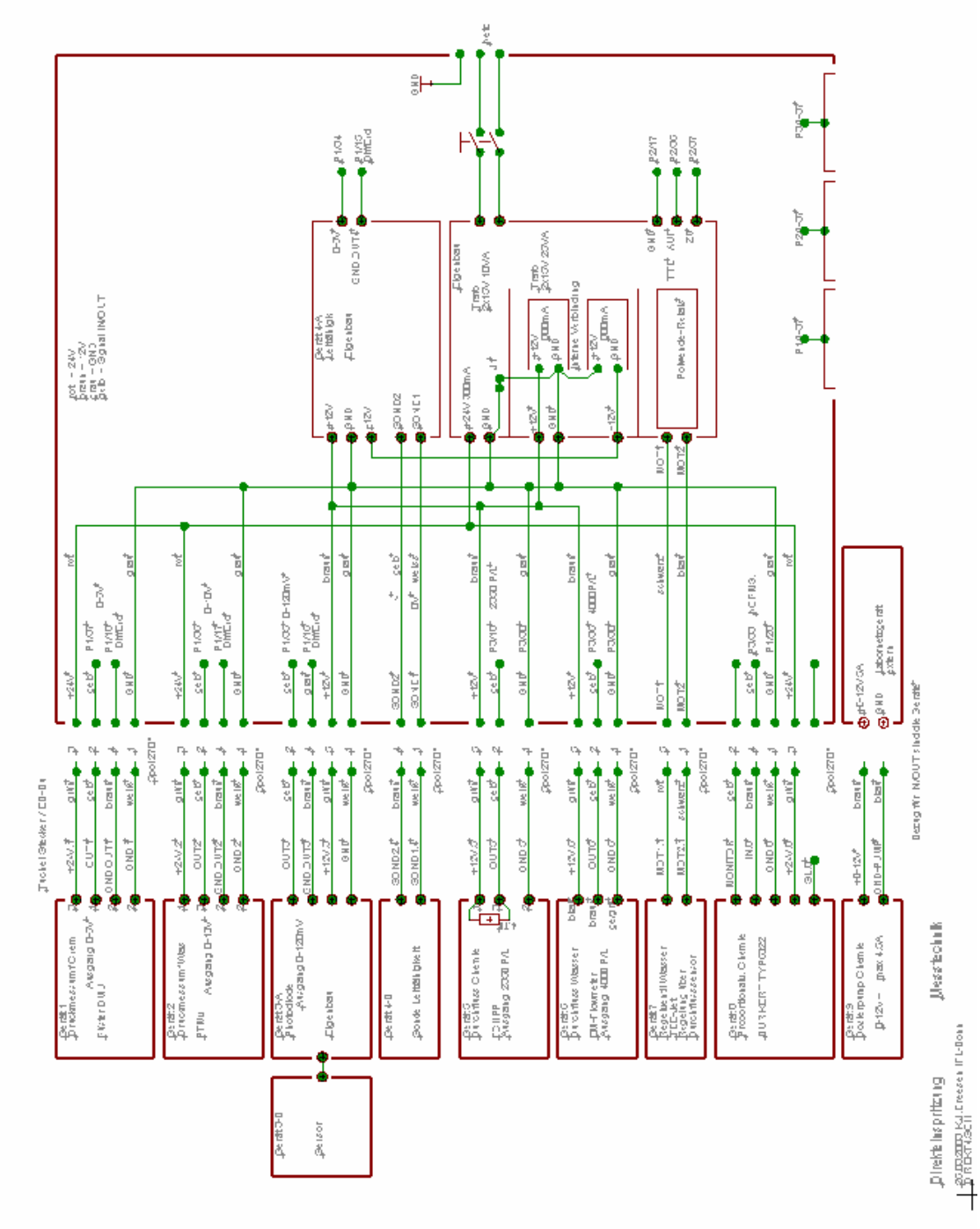

Figure 9. 9: Electrical circuit of the measurement box

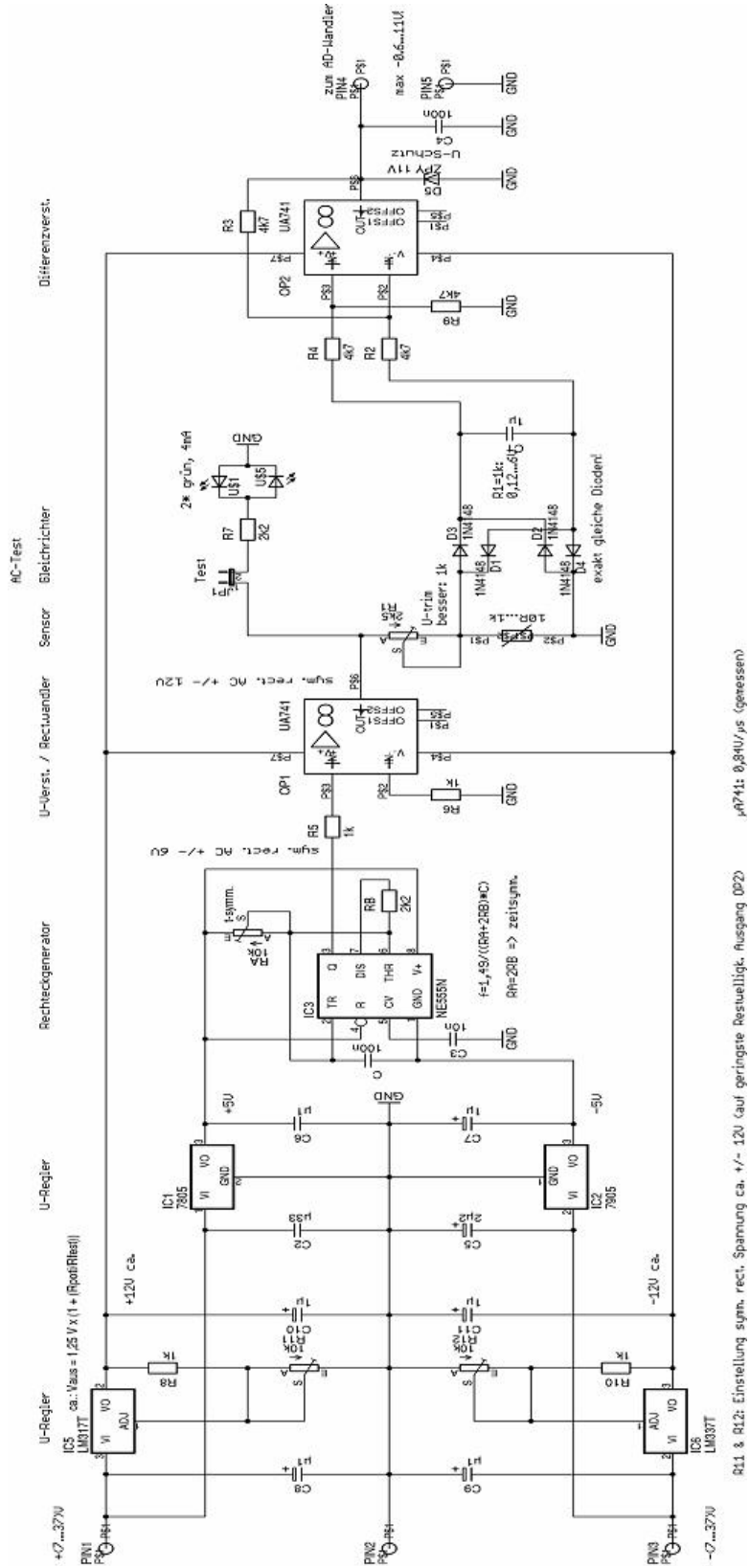

Figure 9. 10: Electrical circuit of the conductivity sensor

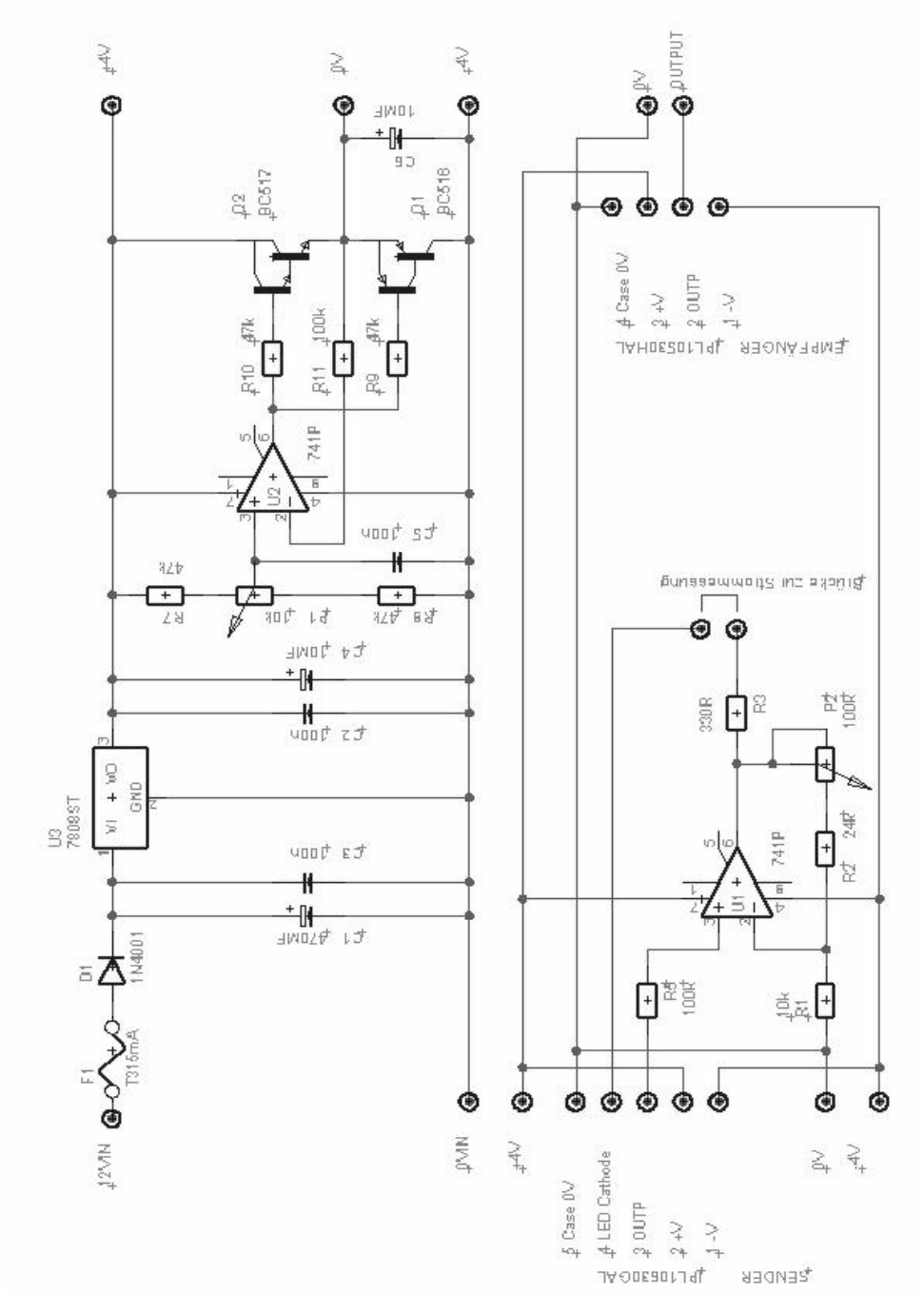

Figure 9. 11: Electrical circuit of the light transmittance sensor

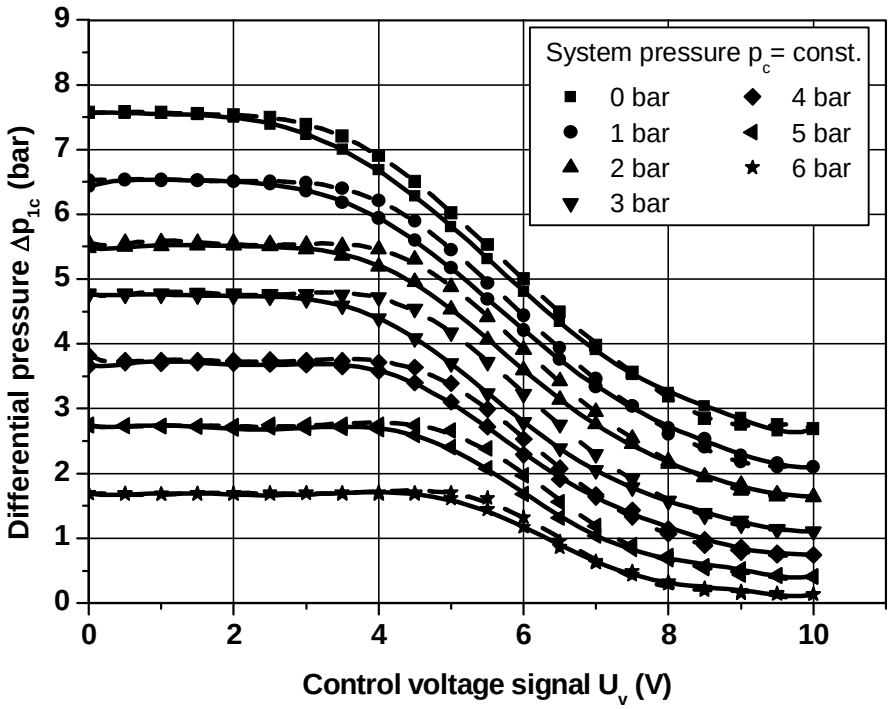

Figure 9. 12: Course of differential pressure p_{1c} (measured at constant system pressure p_c)

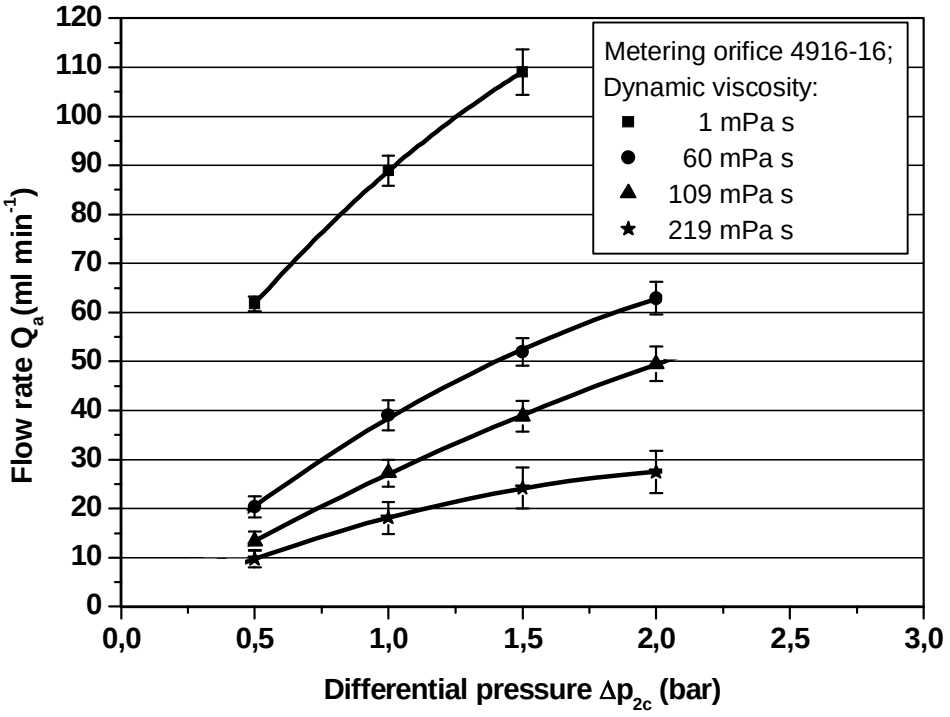

Figure 9. 13: CP4916-16 orifice plate performance across a range of differential pressures and dynamic viscosities

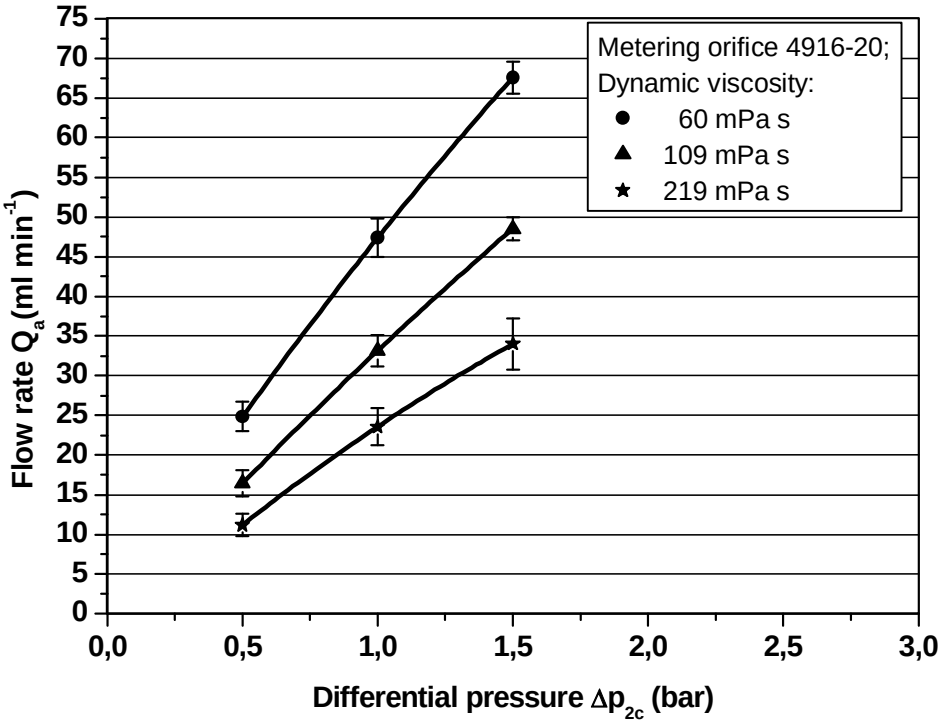

Figure 9. 14: CP4916-20 orifice plate performance across a range of differential pressures and dynamic viscosities

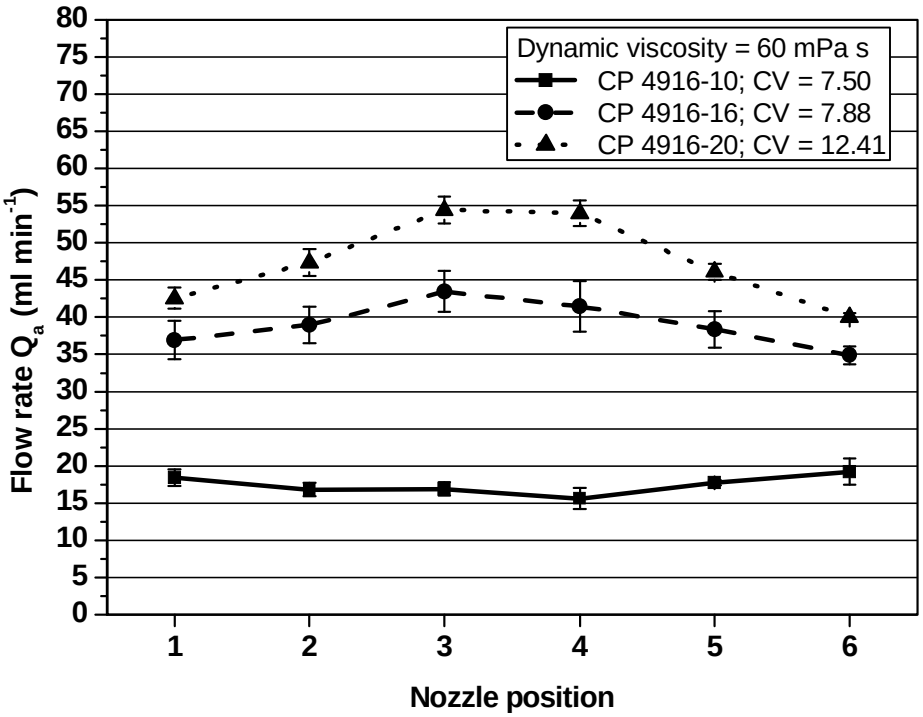

Figure 9. 15: Boom performance for set of six orifice plates; measured for aqueous glycerine solution (60 mPa s) at Δp_{2C} =1bar

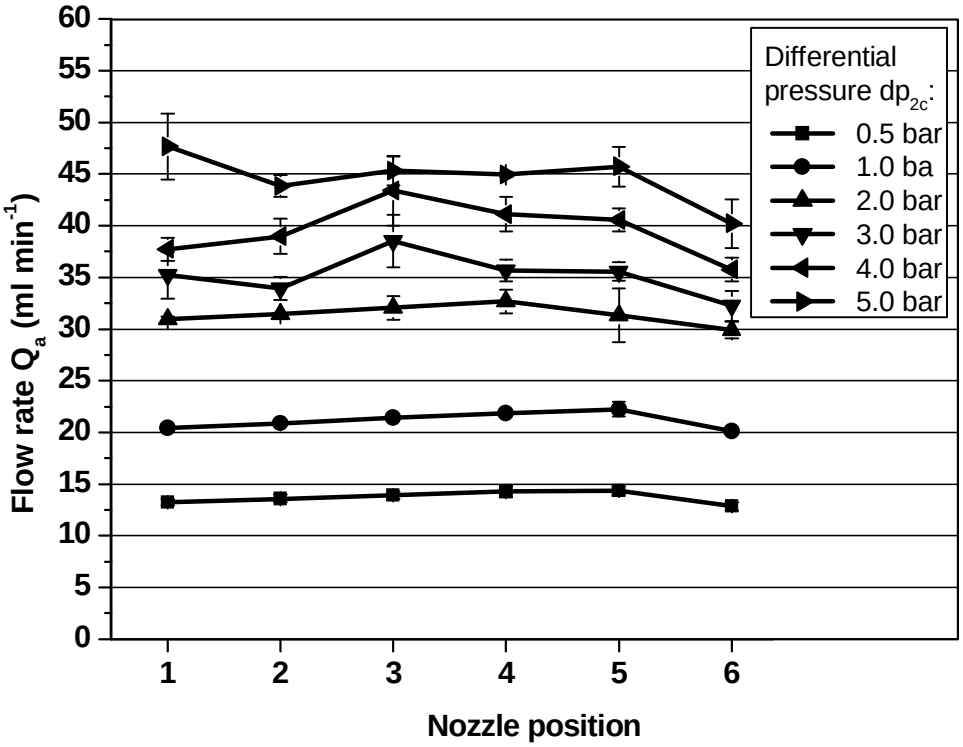

Figure 9. 16: Boom performance for set of six C4916-10 orifice plates across a range of differential pressures Δp_{2C}; measured for water

Table 9. 16: Nominal and calibrated nozzle flow rates for 8-8-6-6 mm boom plumbing configuration

Nozzle size	System pressure (bar)	Nominal flow rate (ml min^{-1})	Nozzle position						CV
			1	2	3	4	5	6	%
XR 80015	1	340	343,0	349,9	347,1	346,0	347,7	347,1	0,65
		SD	1,9	2,3	1,8	4,1	2,2	2,3	
	3	590	593,9	607,1	602,6	598,1	603,7	600,2	0,77
		SD	3,3	6,6	4,0	4,6	4,2	4,4	
	5	760	761,5	772,4	773,2	766,3	771,6	770,5	0,59
		SD	2,6	2,8	3,1	4,3	2,8	6,0	
XR 8005	1	1140	1100,5	1114,3	1112,6	1114,2	1108,8	1086,8	0,98
		SD	12,0	12,7	11,2	12,3	35,1	10,6	
	3	1970	1912,0	1937,6	1930,8	1931,5	1923,0	1895,2	0,82
		SD	8,5	9,8	8,6	5,3	8,7	8,6	
	5	2540	2464,3	2499,3	2515,9	2521,1	2483,4	2455,0	1,09
		SD	13,4	16,4	13,6	9,8	10,3	13,3	

Table 9. 17: Nominal and calibrated nozzle flow rates for 8-8-8-8 mm boom plumbing configuration

Nozzle size	System pressure (bar)	Nominal flow rate (ml min^{-1})	Nozzle position						CV
			1	2	3	4	5	6	%
XR 80015	1	340	346,0	350,3	349,1	344,0	349,9	347,1	0,71
		SD	3,8	1,1	2,4	1,9	4,0	2,2	
	3	590	598,1	608,0	603,8	609,4	605,1	603,0	0,66
		SD	6,6	5,0	6,4	47,7	5,7	7,2	
	5	760	762,4	775,3	771,6	765,6	773,9	773,6	0,67
		SD	5,3	6,1	5,4	4,0	4,2	6,4	
XR 8005	1	1140	1112,9	1120,0	1103,5	1097,4	1119,5	1100,5	0,89
		SD	7,4	5,5	7,5	10,0	19,6	9,6	
	3	1970	1936,2	1956,0	1918,4	1915,6	1939,1	1924,9	0,78
		SD	10,5	8,1	9,6	10,4	9,9	3,3	
	5	2540	2483,1	2522,5	2485,5	2488,4	2487,3	2479,3	0,63
		SD	6,6	10,8	7,1	9,3	12,5	8,1	

Table 9. 18: Nominal and calibrated nozzle flow rates for 12.7-12.7-12.7-12.7 mm boom plumbing configuration

	System pressure (bar)	Nominal flow rate (ml min^{-1})	Nozzle position						CV
			1	2	3	4	5	6	%
XR 80015	1	340	344.5	351.7	349.6	345.2	348.7	350.0	0.81
		SD	0.7	1.3	0.7	1.7	1.5	1.9	
	3	590	595.5	604.4	603.5	597.9	602.8	605.2	0.65
		SD	2.2	2.7	4.6	3.1	3.3	3.6	
	5	760	766.6	778.7	779.4	769.5	776.1	776.9	0.68
		SD	4.6	3.8	8.7	3.8	4.1	3.1	
XR 8005	1	1140	1138.5	1145.7	1121.2	1121.5	1133.1	1124.2	0.89
		SD	6.0	7.2	7.0	10.0	9.1	3.7	
	3	1970	1969.7	1982.1	1947.6	1960.9	1963.6	1952.9	0.63
		SD	7.9	4.9	10.8	13.0	13.6	10.8	
	5	2540	2502.9	2521.3	2488.6	2489.4	2499.3	2484.8	0.54
		SD	12.6	12.5	14.0	17.0	9.3	12.9	

Table 9. 19: Measured and theoretically estimated relationships between lag time (y) and the distance from the boom centre (x)

Q_c (ml min^{-1})	**Functions obtained from the lag time measurements**	**Estimated functions**
340	$y = 2.09\ 10^{-6}\ x^2 + 8.06\ 10^{-4}\ x + 2.330$	$y = 1.61\ 10^{-6}\ x^2 + 0.00148\ x + 2.180$
1140	$y = 7.80\ 10^{-7}\ x^2 + 9.0\ 10^{-5}\ x + 0.848$	$y = 5.02\ 10^{-7}\ x^2 + 4.58\ 10^{-4}\ x + 0.650$
1970	$y = 5.40\ 10^{-7}\ x^2 - 9.0\ 10^{-5}\ x + 0.624$	$y = 2.92\ 10^{-7}\ x^2 + 2.60\ 10^{-4}\ x + 0.376$

Table 9. 20: Lag and response times for different boom pipe diameters; Q_a = 385 ml min^{-1}

Carrier flow rate Qw (ml min^{-1})	**Boom pipe diameter (mm)**	**T_{lag} (s)**	**T_R (s)**	**SD**
590.0	6.0	3.10	8.84	0.89
	8.0	4.63	9.36	0.62
	12.0	9.04	15.58	0.69
1970.0	6.0	1.51	3.93	0.30
	8.0	1.75	4.17	0.26
	12.0	3.39	5.48	0.35

Table 9. 21: Lag and response times for different carrier flow rates; boom pipe ID = 6 .0 mm

Carrier flow rate Q_w (ml min^{-1})	**Tracer flow rate Q_a (ml min^{-1})**	**T_{lag} (s)**	**T_R (s)**	**SD**
590.0	385.00	3.10	8.84	0.89
1970.0		1.51	3.93	0.30
340.0	525.00	6.48	11.61	0.59
1140.0		2.27	5.42	0.17

Table 9. 22: Response time parameters times for different tracer flow rates; Q_c = 1970 l min^{-1}; boom pipe ID = 6 .0 mm

Tracer flow rate Q_a (ml min^{-1})	**T_{lag} (s)**	**T_R (s)**	**T_{rise} (s)**	**T_{fall} (s)**	**SD**
60.0	1.59	3.35	1.22	0.67	0.11
180.0	1.55	3.63	1.66	0.75	0.22
385.0	1.51	3.93	1.78	0.83	0.30

Table 9. 23: Lag and response times for different tracer viscosities; boom pipe ID = 6 .0 mm

Tracer flow rate Q_a (ml min^{-1})	Dynamic viscosity (mPa s)	T_{lag} (s)	T_R (s)	SD
60.0	1.0	1.63	3.35	0.10
	109.0	1.71	3.21	0.36
	219.0	1.82	3.41	0.31
180.0	1.0	1.55	3.63	0.22
	109.0	1.67	3.70	0.37
	219.0	n.a	n.a	n.a

Curriculum Vitae

Name: Peter Hlobeň

Date of Birth: 12. June 1978 in Prague

Education and qualifications

11/2001 – 12/2006	Reinische Friedrich-Wilhelms-Universität Bonn, Germany Institute of Agriculture Engineering PhD study in DFG Research Training Group 722 Topic of the doctoral thesis: "Study on the Response Time of Direct Injection Systems for variable rate application of Herbicides"
08/2000 – 03/2001	Polytechnic School, Kotka, Finland Erasmus programme, International Marketing
10/1996 – 06/2001	Czech University of Agriculture, Prague, CZ Technical Department Graduate Study in Mechanical engineering and business with machinery Topic of the graduate thesis: "Design of Add-Ins file MS Excel for investment decision making in construction machinery and technology"
09/1992 – 05/1996	Mechanical Engineering High School, Prague, CZ.

Work experience

04/2005 – 06/2006	Internship, Product engineer – Field sprayers John Deere Horst, Horst, NL
01/1999 – 12/2000	Internship, Administrative work TNT International Express, Prague CZ
04/1995 – 04/1996	Internship, Product engineer - Rail vehicles KIMAZA, Prague, CZ